RECENT ADVANCES IN PHARMACEUTICAL SCIENCES

VOL. V

Editors

Diego Muñoz-Torrero, M. Pilar Vinardell, Javier Palazón

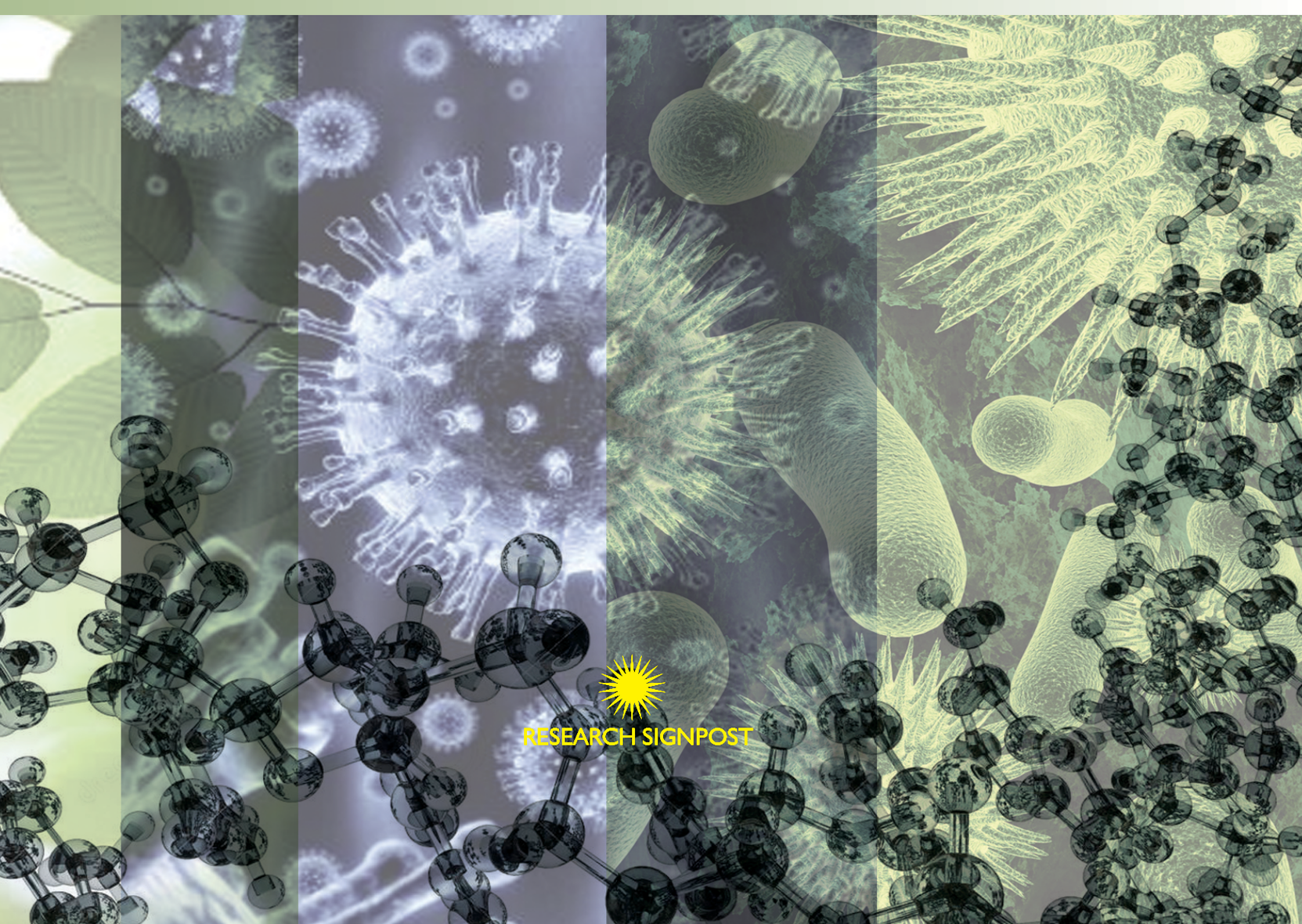

Recent Advances in Pharmaceutical Sciences V

Editors

Diego Muñoz-Torrero
M. Pilar Vinardell
Javier Palazón

Facultat de Farmacia, Universitat de Barcelona,
Av. Joan XXIII, 27-31, 08028-Barcelona, Spain

Research Signpost, T.C. 37/661 (2), Fort P.O., Trivandrum-695 023
Kerala, India

Published by Research Signpost

Research Signpost
T.C. 37/661(2), Fort P.O.,
Trivandrum-695 023, Kerala, India

E-mail IDs: admin@rsflash.com
signpost99@gmail.com; rsignpost@gmail.com

Websites: http://www.ressign.com
http://www.trnres.com
http://www.signpostejournals.com
http://www.signpostebooks.com

ISBN: 978-81-308-0561-0

Preface

This E-book is the fifth volume of a series that compiles contributions from different areas of the multidisciplinary field of Pharmaceutical Sciences. The E-book consists of 11 chapters that cover the areas of organic chemistry, health and environmental management, plant physiology, food science, toxicology, botany, parasitology, physiology, biochemistry and molecular biology, microbiology, and pharmacology.

The key role of sphingolipids in the regulation of a number of cellular functions has boosted important research endeavors towards the development of analogs thereof and their use for shedding light on their biological and biophysical mechanisms. Chapter 1 describes the design and synthesis of particular classes of sphingolipid analogs, namely ceramidase inhibitors, of potential interest in the treatment of chemoresistant forms of prostate cancer, and sphingolipid-based fluorogenic probes with specific applications in structural and cell biology. Chapter 2 deals with the assessment of the human health risk resulting from exposition to groundwater contaminated by chlorinated hydrocarbons using the so-called Risk Based Corrective Action (RBCA) model, a useful tool developed by the American Society of Testing and Materials (ASTM) for determining the amount and urgency of necessary actions for a polluted site regarding human health. *In vitro* culture techniques using plant cell and organ cultures are promising tools for the production of valuable plant secondary metabolites, with important roles in plant defense and as a source of phytochemicals for human health and nutrition. Chapter 3 describes different *in vitro* culture techniques and reports the development of two biotechnological systems for improving the production of two high-value compounds such as the anticancer diterpene alkaloid taxol in cell suspension cultures of *Taxus* spp and ginsenoside in hairy root cultures of *Panax ginseng.* Dietary and physical activity strategies have been reported to be useful for improving the social, cognitive and academic performance of children and adolescents with Attention Deficit and Hyperactive Disorder (ADHD), the most common neurobehavioral disorder of childhood. In Chapter 4, the role of diet and physical activity in the management of ADHD are critically discussed. Chapter 5 reviews the applicability of the zebrafish embryo model in some relevant areas of human toxicology as developmental

toxicity, cardiovascular toxicity and neurotoxicity, as an alternative model to the laborious and costly traditional *in vivo* mammalian screening approaches. Recent molecular phylogenetic studies have shown that the radiation of the genus *Cheirolophus* in the Macaronesian archipielagos was an extraordinarily recent and rapid process, with its diversification in the Canary Islands being among the top ten explosive plant radiations in this oceanic archipelago. In Chapter 6, the main potential patterns and processes involved in the explosive diversification of *Cheirolophus* in the Canary Islands and Madeira are reviewed. Chapter 7 summarizes the ultrastructural knowledge on spermiogenesis and on the spermatozoon in cyclophyllidean cestodes, as a widely accepted valuable tool for the elucidation of the phylogenetic relationships in the Platyhelminthes. This chapter describes the pattern of spermiogenesis and the type of sperm cell for each family of cyclophyllideans and provides new spermatological data on some species of the Anoplocephalidae and the Taeniidae cyclophyllidean families. Intestinal and bronchoalveolar mucosae contribute to homeostasis by preventing the entrance of biological and chemical agents that could alter the stability of the system. Chapter 8 reviews the main effects of dietary supplementation with spray-dried plasma (SDP), a complex mixture of biologically active functional components, on mouse models of acute intestinal and lung inflammation, highlighting the contribution of an SDP-induced increase of regulatory T cell response and enhanced release of anti-inflammatory cytokines. Chapter 9 provides an overview of the current knowledge about the nutritional regulation of alanine aminotransferase expression in fish and its potential use as a biotechnological target for enhancing carbohydrate catabolism for energy purposes, and preserving dietary amino acids for growth, with the aim of sparing protein and improving the sustainability of aquaculture. In Chapter 10, the production of oxylipins, a class of differently hydroxylated fatty acids, by *Pseudomonas aeruginosa* 42A2 grown in submerged culture with oleic or linoleic acid is reported, as well as their potential applications as lubricants or fungicides against phytopathogenic fungal strains. Finally, chapter 11 summarizes novel insights into the crosstalk between heart chronic low-grade inflammatory processes and metabolic disturbances that are involved in the pathogenesis of diabetic cardiomyopathy.

We hope that this E-book may be of interest for a broad readership, not only for those working in the field of pharmaceutical sciences, but also for medical, biological and chemical science researchers.

Dr. Diego Muñoz-Torrero
Dr. M. Pilar Vinardell
Dr. Javier Palazón

Contents

Research Signpost
37/661 (2), Fort P.O.
Trivandrum-695 023
Kerala, India

Recent Advances in Pharmaceutical Sciences V, 2015: 1-12 ISBN: 978-81-308-0561-0
Editors: Diego Muñoz-Torrero, M. Pilar Vinardell and Javier Palazón

1. Chemical approaches to sphingolipid research

Antonio Delgado[1], Josefina Casas[2], José Luis Abad[2] and Gemma Fabriàs[2]

[1]University of Barcelona (UB); Faculty of Pharmacy; Department of Pharmacology and Medicinal Chemistry; Unit of Pharmaceutical Chemistry (Associated Unit to CSIC); Avga. Joan XXIII s/n, E-08028 Barcelona, Spain; [2]Research Unit on BioActive Molecules; Department of Biomedicinal Chemistry; Institute for Advanced Chemistry of Catalonia (IQAC-CSIC), Jordi Girona 18-26; E-08034 Barcelona, Spain

Abstract. Sphingolipids are an important group of biomolecules that play important roles in the regulation of many cell functions. Many efforts have been made in recent years to design analogs suitable for a better understanding of the biological and biophysical roles of sphingolipids. In this review, some of the most relevant contributions in the field from our group are collected. In particular, this review deals with the development of new sphingolipid analogs as acid ceramidase inhibitors, and the design of fluorogenic probes to screen enzyme activities and to the study of biophysical properties.

Introduction

Sphingolipids (SLs) represent an important group of natural products that play crucial roles in cell survival and regulation [1]. Chemically, SLs in

Correspondence/Reprint request: Dr. Antonio Delgado, Department of Pharmacology and Medicinal Chemistry; Unit of Pharmaceutical Chemistry (Associated Unit to CSIC); Avga. Joan XXIII s/n, E-08028 Barcelona, Spain
E-mail: antonio.delgado@ub.edu

mammals contain a lipophilic 2-amino-1,3-diol backbone of eighteen carbon atoms, as found in sphingosine (So). Acylation of the 2-amino group with fatty acids affords ceramides (Cer), responsible for grow inhibition and apoptotis. The so-called complex SLs arise from functionalization at the primary hydroxyl group of Cer. In this case, glucosylation leads to glucosyl ceramide (GlcCer), the precursor of higher glycosphingolipids (GSLs), which play important roles in cell-cell recognition events at the outer membrane [2]. Esterification with phosphorylcholine leads to sphingomyelin (SM), while both Cer and Sph can be also phosphorylated in cells to the corresponding phosphate esters, ceramide-1-phosphate (CerP) [3] and sphingosine-1-phosphate (S1P) [4], which are important as second messengers and also in cell regulation as proliferative agents (Fig. 1).

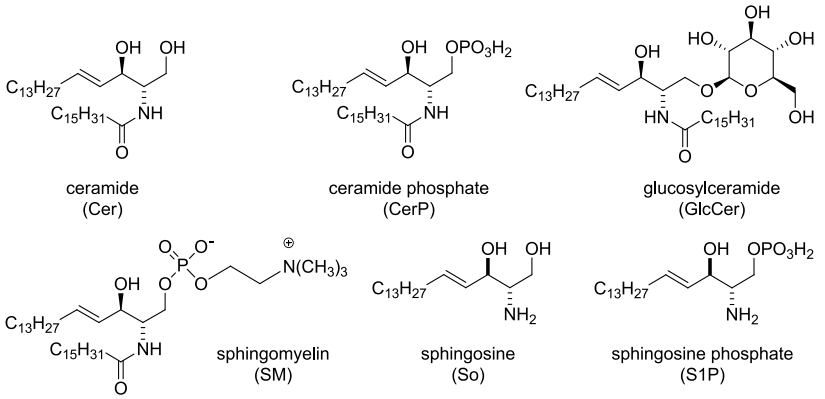

Figure 1. Some of the most representative sphingolipids in mammals.

The effective control of the cellular functions requires a delicate balance of SL levels, which is regulated by finely tuned complex metabolic pathways with the help of specific enzymes However, the enzymatic processes by themselves are not enough to understand this intricate scenario, whose operability depends on the cellular compartmentalization of the different pathways involved (Fig. 2) [1]. This cellular organization is especially relevant for signaling events mediated by SL that are often spatially separated in particular organelle. Since the subcellular distribution of lipids is not uniform [5], local changes in lipid concentrations can be responsible for diverse downstream effects.

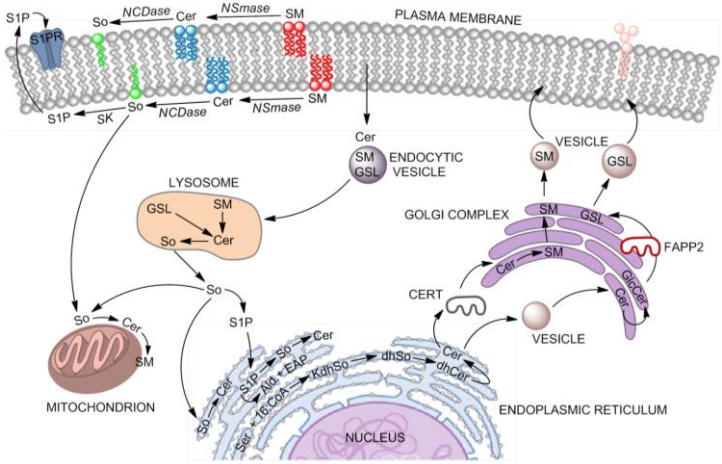

Figure 2. Metabolic pathways and compartmentalization in sphingolipid biosynthesis. (CERT: ceramide transporter protein; dhCer: dihydroceramide; dhKSo: ketosphingosine; dhSo: dihydrosphingosine; GSL: glycosphingolipids; NCDase: neutral ceramidase; NSmase: neutral sphingomyelinase; SK: sphingosine kinase; FAPP2: GlcCer transfer protein).

The fact that the expression of SL metabolizing enzymes is deregulated in many diseases has boosted the design of SL biosynthesis modulators as a rational approach to define new targets and new small molecule chemical entities with potential therapeutic applications [6].

In recent years, the interest on the biophysical properties of SLs, in particular So, Cer and their phosphorylated derivatives, has emerged as a major field of research. In this context, So is known to increase membrane permeability, while Cer increase lipid chain order, induce "flip-flop" motion of lipids and segregate laterally into rigid domains, among other effects [7]. Interestingly, it is the ability of these SL to aggregate into microdomains what accounts for the formation of high local concentrations of secondary messengers that are ultimately responsible for the triggering of some cellular effects.

1. Sphingolipid analogs as enzyme inhibitors

Abnormal SLs metabolism is known to occur in some diseases, such as certain sphingolipidoses [6], cancer [8], diabetes [9], and aterosclerosis [10]. The cellular contents of the various SLs species are controlled by enzymes

involved in their metabolic pathways. In this context, the search for potent and selective inhibitors of SL metabolizing enzymes offers new insights for the discovery of alternative therapeutic agents. Our interest in SL enzymes as potential targets led us to investigate on ceramidases, a type of amidohydrolases that catalyze the cleavage of Cer into So and fatty acids. According to their optimal pH, ceramidases fall into three groups, acidic (aCDase), neutral (NCDase) and alkaline ceramidases (alkCDase). While aCDase is ubiquitously expressed, NCDase is highly expressed in the small intestine along the brush border, where it is involved in the catabolism of dietary sphingolipids thus regulating the levels of bioactive sphingolipid metabolites in the intestinal tract. On the other side, alkaline ceramidases are expressed in the endoplasmic reticulum, where three different types have been identified, based on their localization and the encoding genes [11].

The role of CDases in human disease is well documented. In general, increased CDase activity leads to reduced levels of ceramides and increased amounts of S1P, which results in increased resistance to cytotoxic signals. This situation is often found in cancer progression and resistance to treatments. On the other hand, a decrease of ceramidase activity provokes cell death. A number of reports point to important roles of ceramidases, mainly aCDase, in the initiation and progression of cancer, and the response of tumours to therapy [12]. Overexpression of aCDase is found in several cancer cell lines and cancer tissues [13], which appears to contribute to decreasing the levels of Cer and increasing those of S1P, thereby resulting in resistance to cell death and enhancement of cell proliferation. In most cases, aCDase inhibition induces apoptosis. Multiple reports confirm the relationship between aCDase activity and radio- or chemotherapy resistance, as well as the interest of aCDase inhibitors as anticancer drugs, either alone or in combination with other therapies [11]. The research in this field has led to implicate an over-expression of acid ceramidase (aCDase) in metastatic prostate cancer [14]. Many tumor types express high levels of acid ceramidase (aCDase). Specifically, the expression levels of aCDase in prostate cancer have been reported to be elevated relative to normal prostate tissue [15]. With these considerations in mind, a rational design of an aCDase inhibitor was undertaken. Taking into account that aCDase is a cysteine hydrolase, a small family of Cer analogs modified at the amide linkage with thiol reactive functions was generated and tested. These compounds were inspired in reported cysteine protease inhibitors [16] and included two β-haloamides and several α,β–unsaturated amides as Michael acceptors, as shown in Fig. 3.

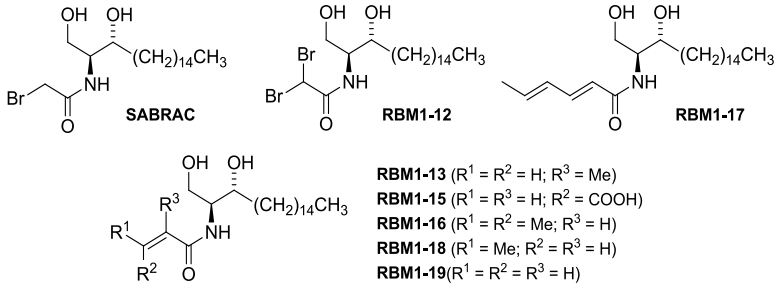

Figure 3. New acid ceramidase inhibitors.

The best inhibitors in intact cells were compounds **RBM1-12**, **RBM1-13**, **RBM1-18** and **SABRAC**, with percentages of inhibition ranging from 50 to 70%. Compounds **RBM1-12**, **RBM1-13**, and **SABRAC** were selected for further studies and were shown to be selective aCDase inhibitors in light of their lack of activity on NCDase, the enzyme that hydrolyses Cer in the cell membrane. *In vitro* dose-response determinations showed that **SABRAC** was the best inhibitor, with an IC_{50} value of 52 nM, followed by **RBM1-12** (IC_{50} = 0.53 μM) and **RBM1-13**, which exhibited the lowest potency (IC_{50} = 11.2 μM). Furthermore, in the presence of **SABRAC** and **RBM1-12**, the enzyme activity showed an exponential decay *versus* incubation time at two protein concentrations, this indicating an irreversible type of inhibition. The above observations confirmed aCDase as a therapeutic target in advanced and chemoresistant forms of prostate cancer and suggested that our new potent and specific inhibitors could act by counteracting critical growth properties of these highly aggressive tumor cells.

2. Sphingolipid analogs as fluorogenic probes

The perception that SL metabolism is composed of a highly intricate, interrelated system of enzymes, whose relative activities determine the intracellular concentration of SLs and, ultimately, the cell fate, has boosted the development of methods to monitor SL enzyme activity. In this context, the use of fluorogenic substrates (substrates that give rise to a fluorescent readout subsequent to a particular enzymatic reaction) represents a breakthrough in the design of probes suitable for determining enzyme activities. Guided by these interests, our group has been working actively in the development of new fluorogenic probes for the development of HTS methods for the screening of several SL metabolizing enzymes. With our focus on aCDase, the fluorogenic coumarinic substrates **RBM14** (Fig. 4)

were designed. After the enzymatic hydrolytic amide cleavage of the above substrates, oxidation of the resulting vicinal amino diol renders an intermediate aldehyde AL (Fig. 4), whose subsequent β-elimination under basic conditions liberates the fluorescent reporter (Fig. 4) [17,18]. Interestingly, the specificity of the substrates towards ceramidases could be modulated by choosing an appropriate acyl chain length. Thus, for aCDase, the highest rate of hydrolysis was observed for the probe with a dodecanoyl group (**RBM14-12**). The recombinant human neutral ceramidase preferred the hexadecanoyl derivative (**RBM14-16**), while the tetradecanoylamide (**RBM14-14**) was preferentially hydrolyzed by lysates of neutral ceramidase-null mouse embryonic fibroblasts at pH 8.5 in the presence of Ca^{+2}. It is worth mentioning that this fluorogenic method is currently used for the diagnosis of Farber disease, a rare disease characterized by the deficiency of aCDase [18].

The *in situ* generation of umbelliferone as a fluorescent reporter to monitor SL enzyme activity was also been applied for the development of a HTS protocol for sphingosine-1-phosphate lyase (SPL). This enzyme plays an important role in cellular functions linked to tumor progression and immunosuppression [19]. It catalyzes the retroaldol cleavage of long chain base phosphates into phosphoethanolamine and a fatty aldehyde (Fig. 5). Since both saturated and unsaturated, as well as truncated base phosphates are transformed by SPL and the reaction is highly stereoselective for the d-*erythro* isomer [20], we reasoned that compound **RBM13** contained the required structural features to behave as a suitable SPL substrate.

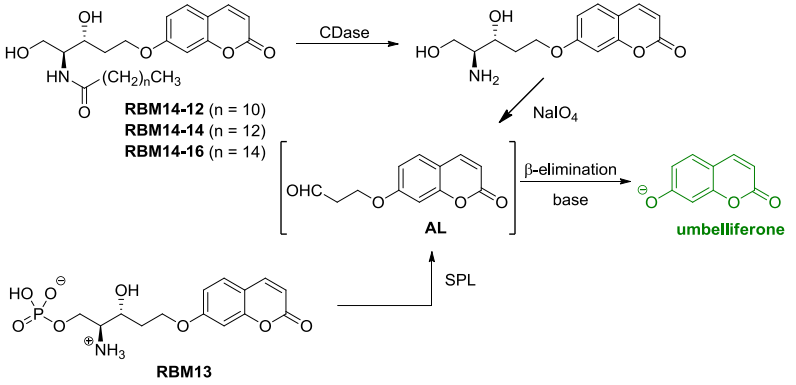

Figure 4. Fluorogenic coumarinic fluorogenic probes to determine CDase and SPL activities.

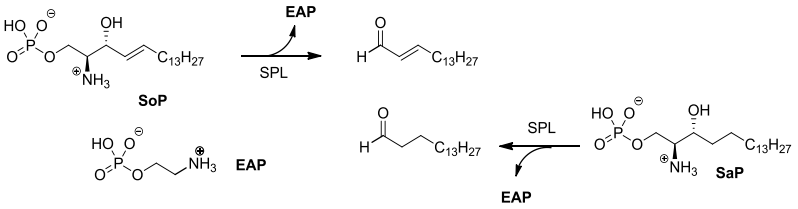

Figure 5. Retroaldol reaction catalyzed by SPL.

Upon enzymatic cleavage, aldehyde AL (Fig. 4) is first produced to render the fluorescent umbelliferone reporter after β-elimination under alkaline conditions [21]. In our optimized protocol, the assay can be performed in microtiter wells, and can be easily adapted to HTS formats.

The above substrates were inspired in the pioneering works by Reymond and co-workers for the development of a fluorogenic assay for hydrolytic enzymes [22].

The synthesis of the above probes can be carried out starting from Garner's aldehyde, following the approach indicated in Fig. 6. The common intermediate **B**, obtained from acidic hydrolysis of **A**, arising, in turn, from Garner's aldehyde in five synthetic steps [17], was selectively phosphorylated at the primary hydroxyl group, to give **C**, and further deprotected in a one-pot two-step process to the required amino phosphate **RBM13**. Alternatively, Boc removal from intermediate B, followed by standard *N*-acylation afforded the required **RBM14** probes.

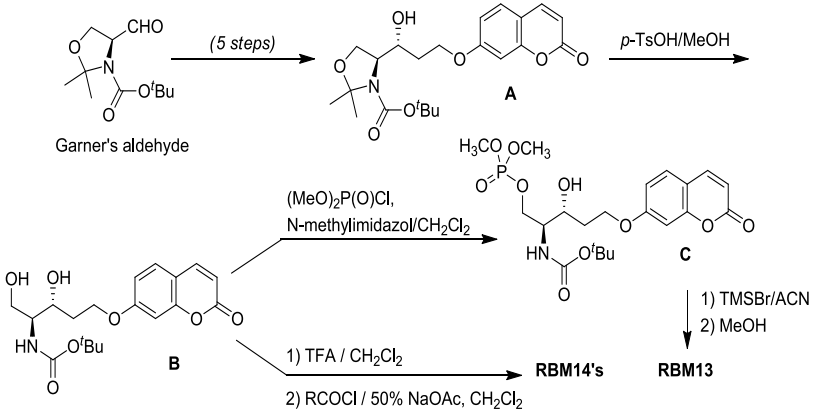

Figure 6. Synthesis of the fluorogenic coumarinic probes **RBM13** and **RBM14**.

3. Azidosphingolipids as probes to study membrane organization

The use of synthetic lipid probes for biophysical applications is a well-recognized strategy in lipid research [23]. In particular, the use of fluorescent tags is useful for the visualization of the membrane architecture and the study of its dynamic properties. The suitability of the substrate is determined by its ability to afford a fast and sensitive detection and also to behave similarly as its untagged counterpart. These two requirements are somehow contradictory when large aromatic fluorescent moieties are used. Because natural membrane lipids do not have such bulky fluorescent tags, dramatic effects on the properties of the resulting probes can be expected, especially as far as trafficking, sorting and/or domain formation is concerned [24]. Ideally, a suitable probe should be structurally similar to its natural counterpart and allow an efficient *in situ* chemoselective functionalization with a suitable fluorescent reagent in a natural environment. These requirements can be envisaged by a judicious use of bioorthogonal chemical reporter strategies, a technique that has become common place for the labelling of biomolecules [25,26]. Based on these premises, and aiming to widen the scope of our research, we undertook the synthesis of the α- and ω-azido probes **RBM2-79** and **RBM 2-77** shown in Fig. 7. As sphingolipid analogs, these probes are amenable to incorporation into natural or artificial membranes. In addition, due to the presence of the terminal azido group, the possibility of a bioorthogonal alkyne-azide cycloaddition "click" reaction with the fluorogenic tag **D** [27] was considered.

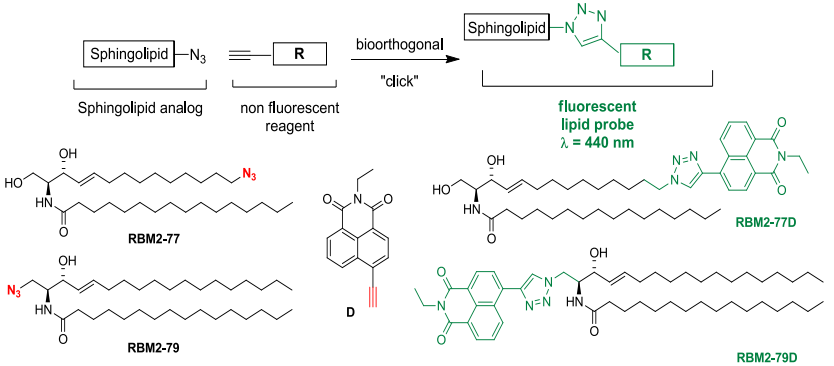

Figure 7. Design of bioorthogonal "click" reactions with azido sphingolipid probes **RBM2-77** and **RBM2-79**. Doble enlace en triazol

In this context, the recent advances in the development of bioorthogonal reactions have boosted their applications in chemical biology [28]. In particular, those involving the Cu(I)-catalyzed Huisgen [3+2] cycloadditions of terminal alkynes with azides [29] (CuAAC, the paradigm of "click chemistry" [30]) have become attractive to researchers due to their simplicity and high reactivity. In order to avoid the potential toxicity of Cu(I) salts, several modifications have been developed to reduce Cu(I) concentration, as the use of water-soluble Cu(I) ligands [31,32] or Cu(I)-chelating azides [33].

In our case, the probes shown in Fig. 7 have been designed to mimic the behaviour of natural ceramides in artificial membranes [34]. Membrane ceramides are important metabolic signals [35,36] that are known to separate laterally to give rise to gel-like ceramide-enriched domains [37–39]. Because of their structural similarity, our probes **RBM2-77** and **RBM2-79** were able to orient in lipid bilayers in parallel with the phospholipids, and eventually to give rise to domains similarly to natural ceramides. Gratifyingly, our *in situ* synthetic method allowed the observation of ceramide domains in living cells.

Click reactions required the use of an *in situ* generated Cu^{+} catalyst by ascorbate promoted reduction of a Cu^{2+} salt. The photoactivation of the probes was checked by microscopy experiments using giant unilamellar vesicles (GUVs) of ePC:**1** and ePC:**2** (10 mol% of clickable probe in both cases). When GUVs were treated with the labeling solution, a clear fluorescence intensity was collected in both cases between 450-500 nm, which was attributed to the formation of the corresponding fluorescent click cycloadducts shown in Fig. 7. This fluorescence was not observed when GUVs were incubated under control conditions (in the absence of the Cu^{2+} salt catalyst precursor) after 3h incubation. These results constitute a proof of principle that fluorescent ceramide derivatives may be formed within lipid membranes starting from minimally modified non-fluorescent azido sphingolipids. This technique can be extended to the study of ceramide-enriched domains by fluorescent confocal microscopy and also to the study of the so-called ceramide platforms [40]. Finally, despite Cu^{2+} may be toxic to cells, localization of ceramide-rich domains in cell membranes can be performed on fixed cell preparations. In any, case, the use of Cu-free click chemistry protocols [41] is also considered as a natural evolution of this technique.

The above probes were synthesized following standard protocols, as exemplified for **RBM2-77** in Fig. 8. Thus, the cross methathesis [42,43] of 11-bromo-1-undecene with vinyl alcohol **E**, obtained from Garner's aldehyde following a reported protocol [44], afforded bromide **F** in moderate

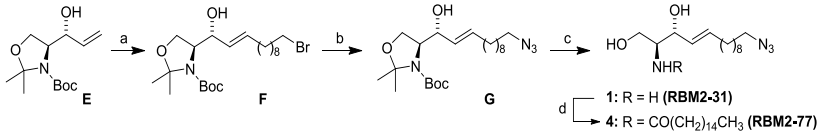

Figure 8. Synthesis of probe **RBM2-77**; a: 11-bromo-1-undecene, Grubb's 2nd generation, CH_2Cl_2, 45 ºC, 59%; b: NaN_3, DMF, 80 ºC (93%); c: $ClCOCH_3$, MeOH, rt, 1h (84%); d: $C_{15}H_{31}COOH$, EDC. HOBt, Et_3N, CH_2Cl_2, 65%.

yield and excellent *E*-selectivity. Reaction of **F** with excess NaN_3 in DMF at 80 ºC, followed by the simultaneous deprotection of the oxazolidine and *N*-Boc groups of intermediate azide **G** under acidic conditions, afforded **RBM2-31** in excellent yield. Acylation with palmitic acid, using EDC/HOBt as coupling system, afforded probe **RBM2-77**.

4. Conclusions

In this review we have tried to show the potential of the chemical modifications of sphingolipids by means of a selection of some of our recent results in this area. Thus, the biochemical functions of natural sphingolipids can be efficiently modulated by the judicious design of analogs addressed at interfering with specific enzymes of key sphingolipid metabolic pathways. In this account, this approach has been illustrated with the design of a new family of aCDase inhibitors, which have also allowed the identification of this enzyme as a therapeutic target in chemoresistant forms of prostate cancer. In a conceptually different approach, chemical modifications of sphingolipids have also been used to design chemical probes with specific applications in structural and cell biology. This is the case of the fluorogenic probes **RBM13** and **RBM14**, designed to develop HTS protocols to monitor the activity profiles of SPL and CDases, respectively. In a related context, the azido sphingolipids **RBM2-77** and **RBM2-79** have found applications in structural biology for their ability to visualize the membrane organization of natural ceramides after a biorthogonal click reaction with a suitable fluorogenic reporter.

Acknowledgements

The authors are grateful to the Spanish Council for Scientific Research (CSIC, Grant 200580F0211), Generalitat de Catalunya (Grant 2009SGR-1072) and the Ministerio de Ciencia e Innovación", Spain (Projects SAF2011-22444 and CTQ2014-54743-R).

References

1. Hannun, Y. A. , Obeid, L. M. 2008, *Nat. Rev. Mol. Cell Biol.*, 9, 139.
2. Sillence, D. J. 2007, *Int. Rev. Cytol.*, 262, 151.
3. Gomez-Munoz, A. 2006, *Biochim. Biophys. Acta*, 1758, 2049.
4. Spiegel, S., Milstien, S. 2002, *J. Biol. Chem.*, 277, 25851.
5. Lev, S., 2010, *Nat. Rev. Mol. Cell Biol.*, 11, 739.
6. Kolter, T., 2011, *Chem. Phys. Lipids*, 164, 590.
7. Goñi, F. M., Sot, J., Alonso, A. 2014, *Biochem. Soc. Trans.*, 42, 1401.
8. Ryland, L. K. , Fox, T. E., Liu, X., Loughran, T. P., Kester, M. 2011, *Cancer Biol. Ther.*, 11, 138.
9. Hla, T. , Dannenberg, A. J. 2012, *Cell Metab.*, 16, 420.
10. Bismuth, J. , Lin, P., Yao, Q. , Chen, C. 2008, *Atherosclerosis*, 196, 497.
11. Fabrias, G., Bedia, C. , Casas, J., Abad, J. L., Delgado, A. 2011, *Anticancer Agents Med. Chem.*, 11, 830.
12. Liu, X., Elojeimy, S., Turner, L. S., Mahdy, A. E. M., Zeidan, Y. H., Bielawska, A., Bielawski, J., Dong, J.-Y., El-Zawahry, A. M., Guo, G. W., Hannun, Y. A., Holman, D. H., Rubinchik, S., Szulc, Z., Keane, T. E., Tavassoli, M., Norris, J. S. 2008, *Front. Biosci.*, 13, 2293.
13. Elojeimy, S. , Liu, X., McKillop, J. C., El-Zawahry, A. M., Holman, D. H., Cheng, J. Y., Meacham, W. D., Mahdy, A. E. M., Saad, A. F., Turner, L. S., Cheng, J., A Day, T., Dong, J. Y., Bielawska, A., Hannun, Y. A., Norris, J. S. 2007, *Mol. Ther.*, 15, 1259.
14. Camacho, L., Meca-Cortés, O., Abad, J. L., García, S., Rubio, N., Díaz, A., Celiá-Terrassa, T., Cingolani, F., Bermudo, R., Fernández, P. L., Blanco, J., Delgado, A., Casas, J., Fabriàs, G., Thomson, T. M. 2013, *J. Lipid Res.*,
15. 54, 1207.
16. Seelan, R. S., Qian, C., Yokomizo, A., Bostwick, D. G., Smith, D. I., Liu, W. 2000, *Genes Chromosom. Cancer*, 29, 137.
17. Otto, H. H., Schirmeister, T. 1997, *Chem. Rev.*, 97, 133.
18. Bedia, C., Casas, J., Garcia, V., Levade, T., Fabrias, G. 2007, *ChemBioChem*,
19. 8, 642.
20. Bedia, C., Camacho, L., Abad, J. L., Fabrias, G., Levade, T. 2010, *J. Lipid Res.*, 51, 3542.
21. Bourquin, F., Riezman, H., Capitani, G., Grutter, M. G. 2010, *Structure*,
22. 18, 1054.
23. van Veldhoven, P. P., Mannaerts, G. P. 1993, *Adv. Lipid Res.*, 26, 69.
24. Bedia, C., Camacho, L., Casas, J., Abad, J. L., Delgado, A., Van Veldhoven, P. R., Fabrias, G. 2009, *ChemBioChem*, 10, 820.
25. Wahler, D., Badalassi, F., Crotti, P., Reymond, J. L. 2001, *Angew. Chem. Int. Ed. Engl.*, 40, 4457.
26. Loura, L. M., Ramalho, J. P. 2011, *Molecules*, 16, 5437.
27. Maier, O., Oberle, V., Hoekstra, D. 2002, *Chem. Phys. Lipids*, 116, 3.
28. Neef, A. B., Schultz, C. 2009, *Angew. Chem. Int. Ed. Engl.*, 48, 1498.
29. Lim, R. K. V., Lin, Q. 2010, *Chem. Commun.*, 46, 1589.

30. Sawa, M., Hsu, T. L., Itoh, T., Sugiyama, M., Hanson, S. R., Vogt, P. K., Wong, C. H. 2006, *Proc. Natl. Acad. Sci. U. S. A.*, 103, 12371.
31. Lang, K., Chin, J. W. 2014, *ACS Chem. Biol.*, 9, 16.
32. Rostovtsev, V. V., Green, L. G., Fokin, V. V., Sharpless, K. B. 2002, *Angew. Chem. Int. Ed. Eng.*, 41, 2596.
33. Kolb, H. C., Finn, M. G., Sharpless, K. B. 2001, *Angew. Chem. Int. Ed. Engl.*, 40, 2004.
34. Hong, V., Steinmetz, N. F., Manchester, M., Finn, M. G. 2010, *Bioconjug. Chem.*, 21, 1912.
35. Besanceney-Webler, C., Jiang, H., Zheng, T., Feng, L., Soriano del Amo, D., Wang, W., Klivansky, L. M., Marlow, F. L., Liu, Y., Wu, P. 2011, *Angew. Chem. Int. Ed. Engl.*, 50, 8051.
36. Kuang, G.-C., Michaels, H. A., Simmons, J. T., Clark, R. J., Zhu, L. 2010, *J. Org. Chem.*, 75, 6540.
37. Garrido, M., Abad, J. L., Alonso, A., Goni, F. M., Delgado, A., Montes, L.-R. 2012, *J. Chem. Biol.*, 5, 119.
38. Stancevic, B., Kolesnick, R. 2010, *FEBS Lett.*, 584, 1728.
39. Gulbins, E., Kolesnick, R. 2003, *Oncogene*, 22, 7070.
40. Kooijman, E., Sot, J., Montes, R., Alonso, A., Gericke, A., De Kruijff, B., Kumar, S., Goñi, F. M. 2008, *Biophys. J.*, 94, 4320.
41. Goñi, F. M., Alonso, A. 2009, *Chem. Phys. Lipids*, 160, S2.
42. de Almeida, R. F., Loura, L. M., Prieto, M. 2009, *Chem. Phys. Lipids*, 157, 61.
43. Cremesti, A. E., Goñi, F. M., Kolesnick, R. 2002, *FEBS Lett.*, 531, 47.
44. Mizukami, S., Hori, Y., Kikuchi, K. 2014, *Acc. Chem. Res.*, 47, 247.
45. Chatterjee, A. K., Choi, T. L., Sanders, D. P., Grubbs, R. H. 2003, *J. Am. Chem. Soc.*, 125, 11360.
46. Peters, C., Billich, A., Ghobrial, M., Hogenauer, K., Ullrich, T., Nussbaumer, P. 2007, *J. Org. Chem.*, 72, 1842.
47. Herold, P. 1988, *Helv. Chim. Acta.*, 71, 354.

Research Signpost
37/661 (2), Fort P.O.
Trivandrum-695 023
Kerala, India

Recent Advances in Pharmaceutical Sciences V, 2015: 13-31 ISBN: 978-81-308-0561-0
Editors: Diego Muñoz-Torrero, M. Pilar Vinardell and Javier Palazón

2. Detailed human risk assessment arising from groundwater contaminated by chlorinated hydrocarbons (DNAPLs)

Célia Baratier[1] and Amparo Cortés[2]
[1]*Biohealth & Computing, Erasmus Mundus Master Program,*
[2]*Department of Natural Product, Plant Biology and Soil Science, Faculty of Pharmacy.*
Universitat de Barcelona. 08028 Barcelona, Spain

Abstract. Human health risk assessment is the basis for groundwater contamination and remediation goals definitions. Chlorinated solvents have a high toxicity for humans, even at low concentrations, and are important soil and groundwater pollutants. The main objective of this work is to assess the human health risk derived of exposition to a contaminated groundwater using a commercial Risk Analysis model (RBCA) and taking into consideration different exposure factors. A case study was used. Some risk differences were observed using specific exposure factors in different countries, which were explained by differences in life style.

Introduction

Chlorinated solvents are a type of DNAPLs (Denser-than-water Non Aqueous-Phase Liquids) that include: Tetrachloroethene (PCE), 1,1,1

Correspondence/Reprint request: Dra. Amparo Cortés, Department of Natural Products, Plant Biology and Soil Science, Universitat de Barcelona, Avda. Joan XXIII, s/n, 08028 Barcelona, Spain. E-mail: acortes@ub.edu

Tricloroethane (111TCA), 1,1,2 Tricloroethane (112TCA), 1,2 Dichloroethane (DCA), Chloroethane (CA), Trichloroethene (TCE), cis-1,2-Dichloroethene (c-DCE), trans-1,2-Dichloroethene (t-DCE), Vinylchoride (VC), Carbon tetrachloride (CT), Chloroform (CF), Dichloromethane (DCM), and Chloromethane (CM).

They have been produced and utilised widely since the beginning of the 20th century. The typical uses were: dry cleaning (mostly tetrachloroethene), metal degreasing, pharmaceutical production, and pesticide formulation [1]; they were also used in the rubber industry and as coating products [2]. Their importance as soil and groundwater contaminants was not recognised until the 1980s.

Thereby since 1970, chlorinated solvents have been less and less used in order to preserve the environment. They are now under control by REACH (European Regulation on Restriction, Evaluation, and Authorization of Chemicals) [3].

These solvents have a high toxicity, even at low concentrations [1]. The major target organ of these compounds is central nervous system; other targets are skin and mucus membranes, heart, eyes, lung, liver, and kidneys. An acute toxicity can be observed on these organs that results in: ravage of the central nervous system (depression, reversible mood, and behavioural changes, impairment of coordination,…). PCE can cause irritation of the upper

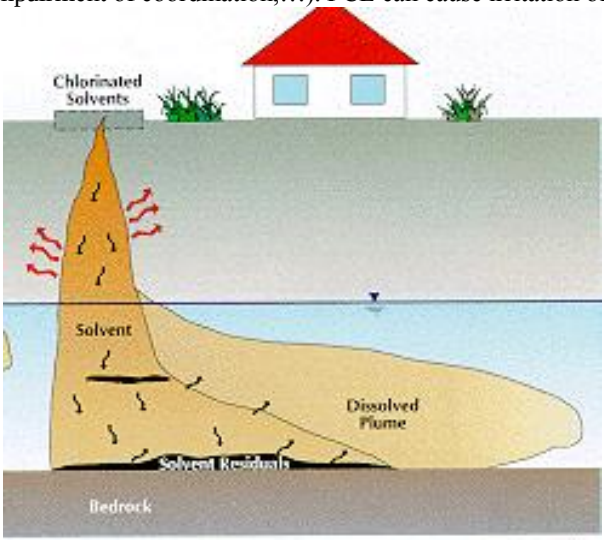

Figure 1. Fate of chlorinated solvents in the media.

respiratory tract and eyes, kidney dysfunction, headache, sleepiness and unconsciousness. The liver toxicity is particularly due to carbon tetrachloride. Heart excitability or irritation of the nose and throat are consequences of TCE exposition. High concentrations of TCE have caused numbness and facial pain, unconsciousness, irregular heartbeat, and death. CF causes depression, rapid and irregular heartbeat, as well as liver and kidney damage [4]. A chronic toxicity has all been stated on all the targets organs, as well as a potential carcinogen effect [2]. VC is admitted to produce angiosarcoma [5]; indeed, IARC (International Agency for Research on Cancer) classifies: VC in the group 1, carcinogenic to humans, [6]; TCE, in group 2A, probably carcinogen to humans; PCE, CT, CF and DCM in group 2B, possibly carcinogen to humans, and TCA in group 3, unclassifiable by its carcinogenicity to humans [7,8].

There may be a natural attenuation of such a contaminants by physical (volatilization), chemical (dilution, absorption, dispersion) and biological processes (biodegradation). The above mentioned processes contribute to the diminution of risk for the human health [4].

Some microorganisms as *Dehalococoides* spp. are able to use chlorinated solvent as electron acceptors during the dehalorespiration and dechlorinate them. Sometimes, biotransformation of the initial compounds produces other compounds more toxic or more persistent at the media [4].

The first exposed people are usually the workers in the industries but, due to the dispersion in groundwaters, the population can be also exposed during long time through the consumption of drinking water, representing an important public health issue locally.

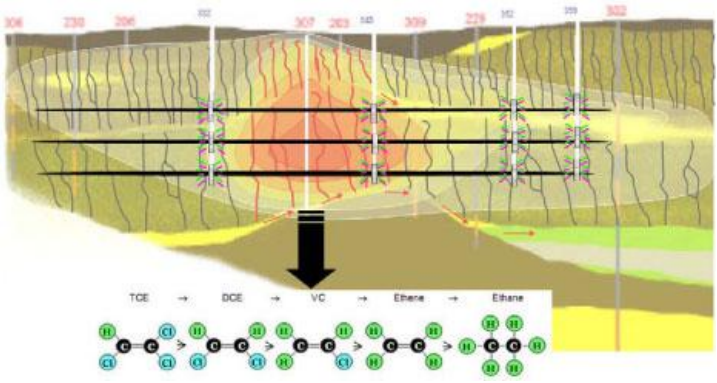

(Source: Danish Environmental Project No. 1295, 2009) [9]
Figure 2. Natural attenuation of chlorinated solvents at the media.

RBCA (Risk Based Corrective Action) is a tool developed by the American Society of Testing and Materials (ASTM) for determining the amount and urgency of necessary actions for a polluted site regarding human health [10]. This model is used to identify exposure pathways and receptors at a site, determine the level and urgency of response required, determine the level of surveillance appropriate for a site, and incorporate risk analysis into all phases of the corrective action process [11]. RBCA combines contaminant transport models and risk assessment tools to calculate baseline risk levels and derive risk-based clean-up standards for a full array of soil, groundwater, surface water, and air exposure pathways. Environmental site managers, regulatory authorities, and consultants around the world have increasingly turned to Risk-Based Corrective Action (RBCA) for the management of contaminated soil and groundwater [12].

Table 1. Main exposure related parameters.

	Water	Soil	Air
RBCA			
Dermal contact	– Dermal slope factor (Sf_{der}) – Dermal reference dose (RfD_{oral}) – Permeability constant (K_p)	– Dermal slope factor (Sf_{der}) – Dermal reference dose (RfD_{der}) – Absorption coefficient	– Dermal slope factor (Sf_{der}) – Dermal reference dose (RfD_{der})
Inhalation	– Inhalation slope factor (Sf_{inh}) – Inhalation reference dose (RfD_{inh}) – Henry's law constant (K_H) – Vapor pressure (P_{vap})	– Inhalation slope factor (Sf_{inh}) – Inhalation reference dose (RfD_{inh}) – Henry's law constant – Vapor pressure (P_{vap})	– Inhalation slope factor (Sf_{inh}) – Inhalation reference concentration (RfD_{inh}) – Threshold limit value (time weighted average); TLV–TWA – Vapor pressure (P_{vap})
Ingestion	– Oral slope factor (Sf_{oral}) – Oral reference dose (RfD_{oral}) – Fish bioconcentration factor – Beef transfer coefficient – Gastrointestinal absorption coefficient (GI) – Soil-to-plant wet uptake factor (BV_{wet}) – Octanol/water partition coefficient ($\log K_{ow}$) – Milk transfer coefficient	– Oral slope factor (Sf_{oral}) – Oral reference dose (RfD_{oral}) – Beef transfer coefficient – Gastrointestinal absorption coefficient (GI) – Soil-to-plant wet uptake factor (BV_{wet}) – Octanol/water partition coefficient ($\log K_{ow}$) – Milk transfer coefficient	

The main objective of this work is to assess the human risk of contaminated groundwater by chlorinated hydrocarbons using the RBCA model that is widely regarded as a useful one for specific scenarios. Site-specific consideration allows for attenuation process to be taken into account along the pathway from the source of groundwater pollution. Secondary objectives are: to verify the correct toxicological and exposure values to be used to fit the model, to establish different exposure scenarios, and to identify data gaps.

1. Study area

The pollution episode studied was detected in 1996 at an industrial plant inside a chemical complex, but it is not well known when the episode started.

Two chlorinated methanes were associated with the episode: carbon tetrachloride (CT) and chloroform (CF), stored independently at the site. Repeated leaks and spills are responsible for the current situation. The area is located at a small sedimentary basin. Characterization studies, monitoring, and control of groundwater's quality began in 1996. 196 m^2 of the soil were then affected by contamination of CT, CF, DCM, 1,1,1,2 PCA, 1,1,2,2 PCA, 1,1,1 TCA 1,1,2 TCA, PCE, TCE, 1,1 DCE, tDCE, and cDCE, from 0.5 to 6 m of depth.

Concerning the water, the polluted plume is supposed to be 4 m thick and big of 2 m. Concentrations recorded at the groundwater, ranged between 15 and 22,600 μg/L for CF, and between the detection limit and 86 μg/L for CT [13]. Six samples were taken from a well for analysis; every sample was analysed by triplicate. The methodology used for chlorinated solvent characterization has been gas chromatography because, being sensible, specific and applicable, it is the most performing method, with a detection limit of 0,01-0,1 μg L^{-1}[14,15].

2. Exposure assessment

The following equation has been used to model the exposure rate (E):

$$E = (CR \times EF \times ED) / (BW \times AT) \quad [1]$$

Which depends on the entrance via (ingestion, inhalation, dermal contact) rate (CR), the exposure frequency (EF), the exposure duration (ED), the body weight (BW), and the average time of exposure (AT).

Due to the presence of an operating industrial plant at the polluted area, the first receptors are regular and temporary workers. Exposure point primarily for on-site workers involved in excavation, digging, and other activities that turn over the soil or that are in touch with groundwater. Workers can be exposed principally by inhalation of the compounds in the outdoor air, but national legislations use to oblige also to take into account: accidental ingestion of contaminants in soil, and inhalation of contaminated dust in air.

No residents are present at the affected area, but to take into consideration population that could be exposed outside the area (residents and visitors who dig holes for planting trees, installing swimming pools, or other uses) it has been considered that the residential population can be exposed 500 m far from the area (Point of Exposure 1, POE1) and 1,000 m far from the characterised area (POE 2); if contaminated groundwater is being supplied as drinking water, then the residents may be exposed via ingestion, inhalation (from volatilization during shower), and dermal contact (when taking a shower/bath).

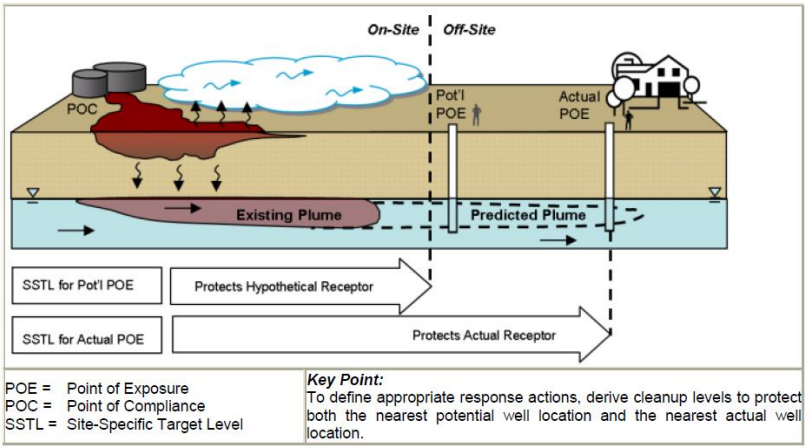

Figure 3. Points of exposure (POE) considered at the modelisation.

3. Toxicity assessment

For non-carcinogenic compounds, the RfD is the used reference, which is an estimate (with uncertainty spanning perhaps an order of magnitude) of the daily exposure to the human population, including sensitive subgroups, that is likely to be without an appreciable risk of deleterious effects during the lifetime. The RfD is generally expressed in units of milligrams per kilogram of body weight per day (mg/kg/day). The RfD is determined for all routes of exposure by using the following equation:

$$RfD = NOAEL / (UF \times MF) \quad [2]$$

RfD is usually derived from an experimentally determined "no-observed-adverse-effect level (NOAEL) which is the experimentally determined dose at which there was no statistically or biologically significant indication of toxic effects of concern. Uncertainty Factors (UF) and Modifying Factors (MF) are used, based on a professional judgment [16].

For the carcinogenic exposure this is done by quantifying how the number of cancers observed in exposed animals or humans increases with the dose. Typically, it is assumed that the dose-response curve for cancer has no threshold (i.e., there is no dose other than zero that does not increase the risk of cancer), arising from the origin and increasing linearly until high doses are reached. Thus, the most convenient descriptor of cancer potency is

the slope of the dose-response curve at low doses (where the slope is still linear). This is referred as the Slope Factor (SF), which is expressed as risk of cancer per unit dose.

4. Individual risk analysis

For the non-carcinogenic compounds it's represented by the Hazard Ratio (HR):

$$HR = E / RDf \quad [3]$$

If HR is higher than 1, they is a risk because the exposure dose is higher than the exposure dose without significant effect.

For the carcinogenic compounds which don't have threshold, the following equation is used:

$$R = E \times SF \quad [4]$$

Where:
R = Risk, a unitless probability (e.g., 2×10^{-5}) of an individual developing cancer;
E = chronic daily intake averaged over 70 years (mg/kg-day);
SF = slope factor, expressed in (mg/kg-day).

The most widely used value of acceptable risk is 10^{-5}, what means that one new case of cancer due to this compounds exposure every 100,000 people is accepted.

5. Cumulative risk analysis

The risk commonly used for the case by case risk assessment is the cumulative risk, which takes into account all the compounds together. The cumulative risk for carcinogens (sum of risk for all chemicals and all complete exposure pathways) must not exceed $1x10^{-4}$ or $1x10^{-5}$, according different legislations.

For non-carcinogenic compounds, the site-wide hazard index, which is the sum of hazard quotients for all chemicals and all complete exposure pathways, must not exceed 1.0.

6. Pollutant transfer and degradation

Pollutant transfer and degradation contribute to contaminants depletion, which results in less risk. Risk analysis considers a constant concentration value for the contaminant/s throughout the entire exposure period, which is a very conservative assumption.

Cross media transfer factors: To take in account the transfer of pollution between media, as for example, volatilisation of chlorinated solvent from the groundwater to the outside air, the used model applies the following equations:

Groundwater Volatilization Equation

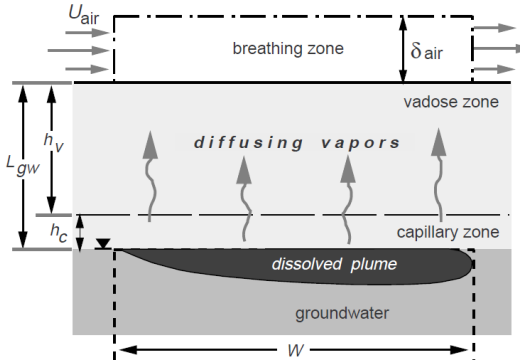

$$VF_{wamb}\left[\frac{\left(\frac{mg}{m^3}-air\right)}{\frac{mg}{L}-H2O)}\right]=\frac{H}{1+\left[\frac{U_{air}\delta_{air}\,L_{GW}}{WD_{ws}^{eff}}\right]}\times 10^3$$

Definitionfor Cross-Media Transfer equation			
d	Lower depth of surfacial soil zone (cm)	P_e	Particulate emissionrate (g/cm²-s)
d_s	Thickness of affected subsurface soils	U_{air}	Wind speed above ground surface in ambient mixing zone (cm/s)
D^{air}	Diffusion coefficient in air (cm²/s)	V_{gw}	Groundwater Darcy velocity (cm/s)
D^{wat}	Diffusion coefficient in water (cm2/s)	W	Width of source area parallel to wind, or groundwaterflow direction (cm)
ER	Enclosed-space air exchange rate (L/s)	δ_{air}	Ambient air mixingzone height (cm
f_{oc}	Fraction of organic carbon in soil (g C/g soil)	δ_{gw}	Groundwater mixingzone height (cm
H	Henry's law constant (cm³-H_2O)/(cm³-air)	Θ_{acrack}	Areal fraction of cracks in foundations/walls (cm²-cracks/cm²-total area)
h_{cap}	Thickness of capillary fringe (cm)	Θ_{acap}	Volumetric air content in capillary fringe soils (cm³-air/cm³-soil)
h_v	Thickness of vadose zone (cm)	Θ_{avadz}	Volumetric air content in vadose zone soils (cm3-air/cm3-soil)
I	Infiltration rate of water through soil (cm/year)	Θ_{as}	Volumetric air content in foundation/wall cracks (cm3-air/cm3-volume)
K_{oc}	Carbon-water sorption coefficient (g-H_2O/g C)	Θ_T	Total soil porosity (cm³-pore-space/cm³-soil)
K_s	Soil-water sportion coefficent (g-H_2O/g-soil)	Θ_{wcap}	Volumetric water content in capillary fringe soils (cm³-H_2O)/(cm³-soil)
L_B	Enclosed-space volume/Infiltration area ratio (cm)	Θ_{wcrack}	Volumetric water content in foundation / wall cracks (cm³-H_2O)/(cm³-total volume)
L_{crack}	Enclosed space foundation or wall thickness (cm)	Θ_{wvs}	Volumetric water content in vadose zone soils (cm³-H_2O)/(cm³-soil)
L_{GW}	Depth to groundwater = h_{cap}+h_v (cm)	ρ_b	Soil bulk density (g-soil/cm³-soil)
L_s	Depth to subsurface soil source (cm)	T	Averaging time for vapourflux (s)

$$D_{ws}^{eff}\left[\frac{cm^2}{s}\right]=\left(h_{cap}+h_v\right)\left[\frac{h_{cap}}{D_{cap}^{eff}}+\frac{h_v}{D_s^{eff}}\right]^{-1}$$

D_{ws}^{eff}

$$D_{cap}^{eff}\left[\frac{cm^2}{s}\right]=D^{air}\frac{\theta_{acap}^{2.33}}{\theta_T^2}+\left[\frac{D^{wat}}{H}\right]\left[\frac{\theta_{wcap}^{2.33}}{\theta_T^2}\right]^{1}$$

D_{cap}^{eff}

$$D_s^{eff}\left[\frac{cm^2}{s}\right]=D^{air}\frac{\theta_{as}^{2.33}}{\theta_T^2}+\left[\frac{D^{wat}}{H}\right]\left[\frac{\theta_{ws}^{2.33}}{\theta_T^2}\right]^{1}$$

D_s^{eff}

(Source: GSI, 1996) [17]

Lateral Groundwater transport equation

To account for attenuation of affected groundwater concentrations between the source and the receptors, this model considers a partially or completely penetrating vertical plane source, perpendicular to groundwater flow, to simulate the release of organics from the mixing zone to the moving groundwater.

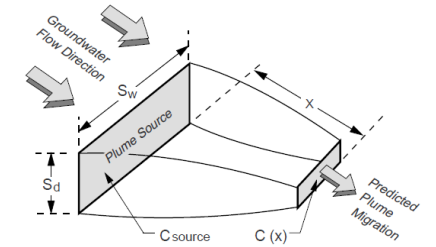

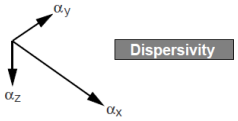

Lateral Groundwater Dilution Attenuation Factor

LT-1a: Solute Transport with First-Order Decay:

$$\frac{C(x)_i}{Csi} = \exp\left(\frac{x}{2\alpha_x}\left[1-\sqrt{1+\frac{4\lambda_i\alpha_x R_i}{v}}\right]\right)\operatorname{erf}\left(\frac{S_w}{4\sqrt{\alpha_y x}}\right)\operatorname{erf}\left(\frac{S_d}{4\sqrt{\alpha_z x}}\right)$$

Where $v = \frac{Ki}{\theta_e}$

LT-1b: Solute Transport with Biodegradation by Electron-Acceptor Superposition Method

$$C(x)_i = \left[(C_{si} + BC_i)\operatorname{erf}\left(\frac{S_w}{4\sqrt{\alpha_y x}}\right)\operatorname{erf}\left(\frac{S_d}{4\sqrt{\alpha_z x}}\right)\right] - BC_i$$

Where $BC_i = BC_T \times \frac{C_{ri}}{\Sigma C_{ri}}$ and $BC_T = \Sigma\frac{C(ea)_n}{UF_n}$

[Note: for Equations LT-1a and LT-1b, NAF= Csi/C(x)i]

Definitions for lateral transport equations			
C(x)i	Concentration of constituent i at distance x downstream of source (mg/L) or (mg/m³)	K	Hydraulic conductivity cm/day)
C_{ri}	Concentration of constituent i in source zone (mg/L) or (mg/m³)	β_i	Constituent retardation factor
B_{ri}	Biodegradation capacity available for constituent in total biodegradation capacity of all electron acceptors in groundwater	I	Hydraulic Gradient (cm/cm)
BCT		S_w	Source Width (cm)
C(ea)n	Concentration of electron acceptor n in groundwater	S_d	Source Depth (cm)
U_{En}	Utilization factor for electron acceptor n (i.e. mass ratio of electron acceptor to hydrocarbon consumed in biodegradation reaction	δ_{az}	Ambient air mixing zone height (cm)
x	Distance downgradient of source (cm)	Q	Air volumetric flow rate through mixing zone (cm³/s)
α_x	Longitudinal groundwater dispersivity (cm	U_{air}	Wind Speed (cm/sec)
α_y	Transverse groundwater dispersivity (cm)	y	lateral distance from source zone (cm)
α_z	Vertical groundwater dispersivity (cm)	z	Height of breathing Zone (assumed equal to δ_{az}) (cm)
θ_e	Effective soil porosity	A	Cross sectional area of air emissions source (cm²)
λ_i	First-Order Degradation Rate (day-1) for constituent i	L	Length of air emissions source (cm) parallel to wind direction
v	groundwater seepage velocity (cm/day)		

Source: GSI, 1996 [17].

The general experience is that these substances may be, under different environmental conditions, adaptively degraded.

The estimated half-lives for chlorinated solvents should therefore be considered, being in accordance with "the realistic worst-case concept", in order to establish the realistic exposition level.

Table 2. Half life of chlorinated solvents in groundwaters.

COMPOUNDS	Half time life (days)			
	CAS	Model value	Min	Max
CT	56-23-5	360 [a]	7 [b]	360[b]
CF	67-66-3	1800 [a]	1825 [b]	
CM	74-87-3	546 [c]	14 [b]	56 [b]
DCM	75-09-2	56 [a]	14 [b]	56 [b]
PCE	127-18-4	720 [a]	360 [b]	720 [b]
TCE	79-01-6	1653 [a]	321 [b]	1653 [b]
tDCE	156-60-5	2880 [a]	2880 [a]	
cDCE	156-59-2	2875 [c]	2880 [a]	
VC	75-01-4	2880 [a]	56 [b]	2850 [b]
1,1,1 TCA	71-55-6	730 [a]	140 [b]	546 [b]
1,1,2 TCA	79-00-5	730 [c]	136 [b]	730 [b]
1,2DCA	107-06-2	360 [a]	100 [b]	360 [b]
CA	75-00-3	56 [a]	14 [b]	56 [b]

a: Data from the RBCA model

b: Data bank of environmental properties of chemicals (EnviChem), 2013 [18].

7. Data used to fit the model

Physicochemical parameters and toxicological data of contaminants

The verification of the properties' data in the model is important for the validity of the results. The variability in parameter values may have a significant effect on the predicted contaminant's behavior and ultimately on the estimated human exposure. So, it has been decided to take into account the maximum and the minimum values, and to make the average of the different values found in bibliography to have a complete extent.

From different data bases, such as Reaxys, and IRIS [16,19], or toxicological reviews of the EPA [20,21], we built a data base with maximum, minimum and average values for: Solubility, Vapor pressure, Henry's constant, Partition Coefficient octanol/water, Coefficient Koc, and Coefficient of diffusion in air and in water (see Table 3).

Table 3. Physicochemical parameters of contaminants.

		Chloromethane				Chloroethene					Chloroethane			
Propriety		CT	CF	CM	DCM	PCE	TCE	tDCE	cDCE	VC	1,1,1 TCA	1,1,2 TCA	1,2DCA	CA
CAS		56-23-5	67-66-3	74-87-3	75-09-2	127-18-4	79-01-6	156-60-5	156-59-2	75-01-4	71-55-6	79-00-5	107-06-2	75-00-3
Molecular weight		153,8	119,38	50,49	84,9	165,8	131,4	96,94	96,94	62,5	133,4	133,4	98,96	64,51
Solubility (mg/L)	Max	805 [a]	7920 [a]	7250 [a]	15400 [a]	200 [a]	1198 [e]	6300 [e]	4930 [a]	2760 [a]	1330 [a]	4420 [a]	8700 [e]	20000 [a]
	Average	799	4360	6025	14200	175,5	1149	6300	4215	2180	1232,5	4410	8700	12870
	Min	793 [e]	800 [e]	4800 [e]	13000 [d]	151 [e]	1100 [a]	6300 [a]	3500 [e]	1600 [e]	1135 [e]	4400 [e]	8700 [a]	5740 [e]
Vapour pressure P ·C (mmHg) (20-25C)	Max	115,25 [e]	198 [a]	4310 [c]	455 [a]	18,4 [a]	9000 [e]	395 [e]	202,52 [e]	2800 [a]	124 [a]	25,2 [a]	81,3 [a]	1400 [e]
	Average	113,625	196,09	4037,5	442,2	18,2384	4536	373,5	188,758	2730	122,5	24,1	80,025	1300
	Min	112 [a]	194,18 [e]	3765 [a]	429,4 [d]	18,077 [e]	72 [a]	352 [a]	175 [a]	2660 [e]	121 [e]	23 [e]	78,75 [e]	1200 [a]
H	Max	1,25 [d]	0,15 [a]	1,44 [a]	0,09[a]	0,8 [e]	0,43[a]	0,39 [a]	0,19 [a]	3,49 [a]	0,75 [e]	0,038[a]	0,05 [a]	0,21 [a]
	Average	1,223608	0,148581	0,899661	0,09041915	0,782444	0,4250855	0,1983233	0,09519035	2,30094	0,732502	0,03767731	0,0466548	0,1106535
	Min	1,197 [a]	0,1446 [e]	0,361 [c]	0,0898 [d]	0,765[a]	0,422 [d]	0,0067 [e]	0,0029 [e]	1,11 [d]	0,715 [a]	0,0374 [d]	0,0401 [d]	0,0093 [e]
Log Koc	Max	2,27 [a]	1,67 [a]	0,778 [a]	1,25[d]	2,19 [a]	2,22 [d]	1,72 [d]	1,55 [d]	1,27 [d]	2,04 [a]	1,7 [d]	1,5 [e]	1,25 [a]
	Average	2,155	1,635	0,739	1,16	2,19016585	2,095	1,71	1,506199	1,16	2,03	1,7	1,37	1,25
	Min	2,04 [e]	1,6 [d]	0,7 [c]	1,07 [a]	2,19	1,97 [a]	1,7 [a]	1,46 [a]	1,04 [a]	2,02 [b]	1,7 [a]	1,24 [a]	1,25 [e]
Log Kow	Max	2,73 [d]	1,97 [e]	1,0865 [a]	1,34 [a]	2,965 [a]	2,71 [d]	2,07 [a]	1,86 [e]	1,62 [a]	2,77[a]	2,05 [e]	1,83 [a]	1,578 [a]
	Average	2,58605	1,7455	0,99825	1,29525	2,8177	2,59155	2,065	1,86	1,56165	2,6246	2,03105	1,6508	1,4888
	Min	2,4421 [a]	1,521 [a]	0,91 [c]	1,25 [d]	2,67 [d]	2,47 [a]	2,06 [e]	1,86 [a]	1,5 [d]	2,48 [e]	2,01 [a]	1,47 [d]	1,4 [e]
Coeficient Diffusion Air (cm2/s)		0,078 [a]	0,104 [a]	0,126 [a]	0,101 [a]	0,072 [a]	0,079 [a]	0,0707 [a]	0,0735 [a]	0,106 [a]	0,078 a	0,0792 [a]	0,104 [a]	0,15 [a]
Coeficient Diffusion water (cm2/s)		0,0000088 [a]	0,00001 [a]	0,0000065 [a]	0,0000117 [a]	0,0000082 [a]	0,0000091 [a]	0,0000119 [a]	0,0000113 [a]	0,000123 [a]	0,0000088 [a]	0,0000088 [a]	0,0000091 [a]	0,0000118 [a]

a : Data base from RBCA model

b: US-EPA. Toxicological review of 1,1,1-Trichloroethane (CAS No. 71-55-6) In Support of Summary Information on the Integrated Risk Information System (IRIS). Aug 2007.

c: US-EPA. Toxicological review of methyl chloride (CAS No. 74-87-3) In Support of Summary Information on the Integrated Risk Information System (IRIS). June 2001.

d: US- EPA, Integrated Risk Information System, review, 2010.

e: Elsevier. Reaxys. 2013. Elsevier Information Systems GmbH.

The same process has been accomplished to collect the toxicological data from IRIS [16] and other reviews or articles [22]. Concerning the toxicological properties, Reference Dose (RfD) and Reference Concentration (RfC) for different routes of entry has been used to determine the potential of a toxic effect. Slope factors (SF) and Unit risks level (URL) have been used to determine the development of excess number of cancers in receptors [23].

Exposure parameters

The exposure factors change according to the social behavior, which is different from one place to another, from one gender to the other, or according to the age. For example, children have usually hand-to-mouth activities; at the adolescence, they stop this behavior but they are still in contact with higher amounts of soils (through playing football or other games) than adults [24]. So it is interesting to differentiate the risk evaluation for each subpopulation group. Indeed, males and females (as children/adults) do not have the same food needs or body weights.

Exposure parameters for different countries have been checked. Concerning quantity of food ingested, exposure time, the maximum available values or the 95th percentile have been chosen, in order to have the worst scenarios. If the specific exposure parameter was not available, the default value of the RBCA model has been used.

Groundwater parameters

A minimum of three wells in the aquifer have been necessary for triangulation of water levels and to indicate groundwater flow direction. Other parameters are shown in Table 5.1.

Air parameters

It has been also needed to characterize air parameters, the dimension of the zone, and also the dispersion taxes (see Table 5.2).

Table 4. Toxicological parameters.

		Toxicological parameters																	
		RfD TDSI oral (mg/kg/day)			RdE TDSI derma (mg/kg/day)			RfC TCA inhalation equivalent (mg/m3)			Oral Slope factor equivalent			Derma Slope factor equivalent			Unit risk factor equivalent for inhalation (µg/m3)		
		Max	Average	Min	Max	Av	Min	Max	Average	Min	Max	Average	Min	Max	Av	Min	Max	Average	Min
Chloromethane	CT	4 E-3 [b]	2,35 E-3	7 E-4 [a]	4 E-3 [b]	2,35 E-3	7 E-4 [a]	0,1 [b]	5,10E-02	2 E-3 [g]	0,13 [a]	0,1	7 E-2 [b]	0,13 [a]	0,1	7 E-2 [b]	3 E-6 [b]	9,0E-06	1,5 E-5 [c]
	CF	1 E-2 [b]	1 E-2	1 E-2 [a]	1 E-2 [b]	1 E-2	1 E-2 [a]	Not establish by EPA			3,1 E-2 [g]	1,85 E-2	6,1E-3 [c]	3,1 E-2 [g]	1,85 E-2	6,1E-3 [c]	2,3 E-6 [c]	1,4E-05	5,3E-6 [i]
	CM	-		-	-		-	9 E-2 [b]	9 E-2	9 E-2 [g]	1,3 E-2 [a]			1,3 E-2 [a]			1,8 E-6 [h]		1,8 E-6 [g]
	DCM	6 E-2 [a]	3,3 E-2	6 E-3 [b]	6 E-2 [a]	3,3 E-2	6 E-3 [a]	3 [g]	1,53	0,6 [b]	7,5 E-3 [c]	4,75 E-3	2 E-3 [a]	7,5 E-3 [c]	4,75 E-3	2 E-3 [a]	4,7E-7[c]	2,4E-07	1 E-8 [b]
Chloroethene	PCE	1 E-2 [a]	8 E-3	6 E-3 [b]	1 E-2 [a]	8 E-3	6 E-3 [b]	0,27 [g]	0,155	4 E-2 [b]	0,54 [a]	0,27	1,5E-3[b]	0,54 [a]	0,27	1,5E-3[b]	1,9 E-7 [b]	3,9E-07	5,8E-7 [c]
	TCE	6 E-3 [a]	3,19 E-3	3,7 E-4 [b]	6 E-3 [a]	3,19 E-3	3,7 E-4 [b]	1,9E-3 [b]			4,6 E-2 [b]	2,4 E-2	2,1 E-3[g]	4,6 E-2 [b]	2,4 E-2	2,1 E-3[g]	4,1E-6 [b]	1,7E-06	1,7E-6 [c]
	DCE	2 E-2 [b]	2 E-2	2 E-2 [a]	2 E-2 [b]	2 E-2	2 E-2 [a]	In discussion [b]		0,793 [g]	-		-	-		-	-		-
	cDCE	1E-2 [a]	6 E-3	2 E-3 [b]	1E-2 [a]	6 E-3	2 E-3 [b]			0,793 [g]	-		-	-		-	-		-
	VC	3 E-3 [b]	3 E-3	3 E-3 [a]	3 E-3 [b]	3 E-3	3 E-3 [a]	0,1 [b]	0,1	0,1 [g]	1,9 [c]	1,33	7,5E-1 [b]	1,9 [c]	1,33	7,5E-1 [b]	8,4E-6 [c]	4,4E-05	4,4E-6 [b]
Chloroethane	1,1,1 TCA	2 [a]	1,1	0,2 [g]	2 [a]	1,1	0,2 [g]	1 [d]	1	1 [g]	-		-	-		-	-		-
	1,1,2 TCA	4 E-3 [b]	4 E-3	4 E-3 [a]	4 E-3 [b]	4 E-3	4 E-3 [a]	Not establish by EPA			5,7E-2 [b]	5,7E-2	5,7E-2 [c]	5,7E-2 [b]	5,7E-2	5,7E-2 [g]	1,6E-5 [b]	1,6E-5	1,6E-5 [i]
	1,2DCA	-		-	-		-	2,42 [g]			9,1E-2 [b]	9,1E-2	9,1E-2 [g]	9,1E-2 [b]	9,1E-2	9,1E-2 [g]	2,6E-5 [b]	2,6E-5	2,6E-5 [g]
	CA	0,4 [g]	0,4	0,4 [a]	0,4 [g]	0,4	0,4 [a]	10 [b]	10	10 [g]	-		-	-		-	-		-

a: Data from the model

b: US-EPA, Integrated Risk Information System (IRIS) data bases 2010.

c: US-EPA, Technical Factsheet on: CARBON TETRACHLORIDE.

d: US-EPA,. Part 2: Development of pathway-specific soil screening level in Soil screening guidance: technical background 2nd Ed, EPA, Washington DC, 1996, pp 9-62.

e: Department of Environmental Toxicology University of California Davis. Final draft report: Intermedia Transfer Factors for Contaminants Found at Hazardous Waste Sites TETRACHLOROETHYLENE (PCE) Risk Science Program (RSP), California, 1994, 44pp.

f: US-EPA, Toxicological review of cis-1,2-DICHLOROETHYLENE and trans-1,2-DICHLOROETHYLENE, EPA/635/R-09/006F, In Support of Summary Information on the Integrated Risk Information System (IRIS), 2010, 174 pp.

g: NHDES (New Hampshire Department of Environmental Service), Risk Characterization and Management Policy (Section 7.4(4)),Revision 2013, 55 pp.

h: NJDEP (New Jersey Department of Environmental Protection), Toxicity Factors for Methyl chloride (chloromethane), 2008, 2pp.

i: California EPA, Consolidated table of OEHHA/ARB app roved risk assessment health values, 2012, 15pp.

j: Environnement Canada, Santé Canada. Ébauche d'évaluation préalable pour le Défi concernant le chloromethane, Numéro de registre du Chemical Abstracts Service 74-87-3. 2009. 58 pp

k: PRTR No of Japan: 95, Summary of Initial Risk Assessment Report Chloroform, R0032. 6pp

l: PRTR No of Japan:145, Summary of Initial Risk Assessment Report Dichloromethane; methylene dichloride, R0054. 6pp.

m: PRTR No of Japan:74, Summary of Initial Risk Assessment Report Chloroethane, R0036, 6pp.

n: OECD SIDS (Screening Information Dataset), VINYL CHLORIDE, Initial Assessment Report for SIAM 13. United Nation Environment Program (UNEP) PUBLICATIONS, Bern, 2001, 244pp.

o: OECD SIDS (Screening Information Dataset), 1,2-DICHLOROETHANE, Initial Assessment Report for 14th SIAM. United Nation Environment Program (UNEP) PUBLICATIONS, Paris, 2002, 203 pp.

p: US-EPA, Technical Factsheet on: TRICHLOROETHYLENE.

q: GSI Environemental Inc, GSI Chemical properties Database, 2010.

r: Department of Environmental Toxicology University of California Davis, Final draft report Intermedia Transfer Factors for Contaminants Found at Hazardous Waste Sites TRICHLOROETHYLENE (TCE) Risk Science Program (RSP), California, 1994, 46 pp. ALL THESE REFERENCES MUST BE AT THE FINAL REFERENCE LIST. HERE, ONLY NAMES AND YEARS MUST APPEAR.

Table 5.1. Water parameters to fit the RBCA model.

Water-Bearing Unit		
Hydrogeology		
Groundwater Darcy velocity (cm/d)	8,5	
Groundwater seepage velocity (cm/d)	22	
Hydraulic conductivity (cm/d)	854	
Hydraulic gradient	0,0021	
Effective porosity	0,11-0,23	
Sorption	Max	Min
Fraction organic carbon-saturated zone	0,000059	0,000011
Groundwater pH	6,15	
Groundwater source zone		
Groundwater plume width at source (m)	2,5	
Plume (mixing zone) thickness at source(m)	18,5	
Groundwater dispersion	outside 1	outside 2
Distance to GW receptors (m)	500	1000
Longitudinal dispersivity (m)	50	100
transversal dispersivity (m)	16,5	33
vertical dispersivity (m)	2,5	5

Table 5.2. Air parameters to fit the RBCA model.

Dispersion in Air	**Off-site1**	**Off-site2**
Distance to offsite air receptor (m)	500	1000
Horizontal dispersive (m)	47,72333	91,62205
Vertical dispersive (m)	31,04168	59,02011
Air source zone		
Air mixing zone height (m)	2	
ambient air velocity in mixing zone (m/s)	2,25	
Particulate emission		
Particulate emission factor (kg/m^3)	6,9E-12	
Areal particulate emission flux (g/cm^2/s)	6,9E-14	

8. Results

Thanks to the risk analyses applied according exposure parameters considerations made in different countries, we have had a large view of different scenarios, with different exposure parameters for the potential on site receptors.

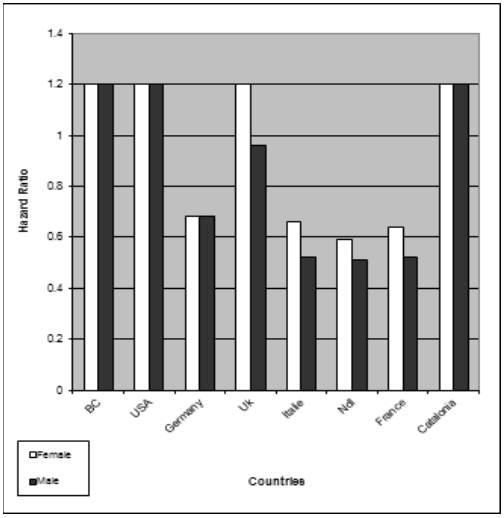

Figure 4. Hazard Ratio from the exposition of males and females working at the polluted area and exposed to polluted groundwater according to exposition default values applied at each country.

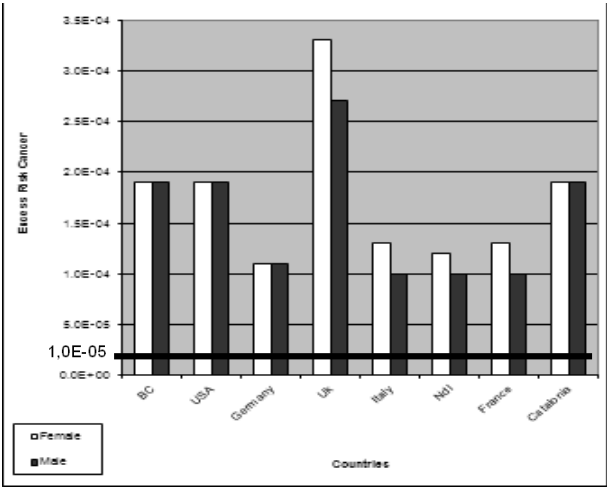

Figure 5. Excess risk of cancer from the exposition of males and females working at the polluted area and exposed to polluted groundwater according to exposition default values applied at each country.

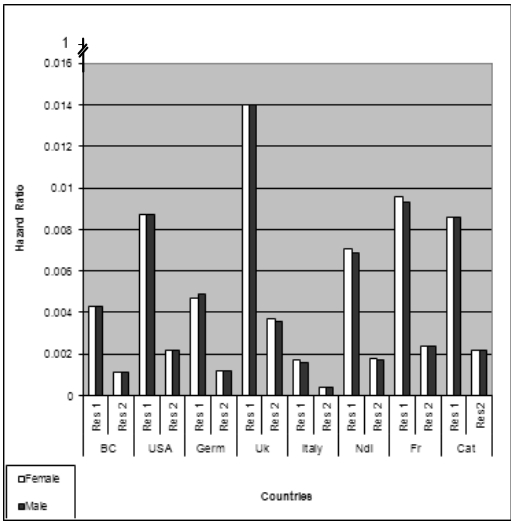

Figure 6. Hazard risk from the exposition of males and females living at the polluted areas and exposed to the polluted groundwater according the exposition default values applied at each country.

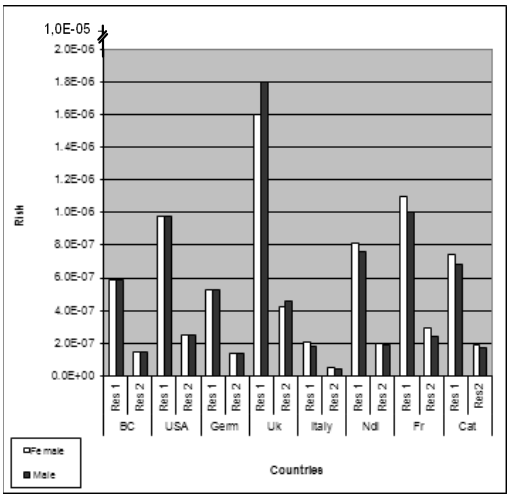

Figure 7. Excess risk of cancer from the exposition of males and females living at the polluted areas and exposed to the polluted groundwater according the exposition default values applied at each country.

The variation of the calculated risk between female and male depends on the exposure parameters which can differ from one gender to another, when considering specific exposure parameters (body weight, dairy products ingestion,…). The parameter which changes the most is the body weight. For example, for Catalonian female body weight is statistically 55 kg, whereas for male is 70 kg; or, 70 and 83.2 kg respectively in UK. Indeed, as female have a lower body weight than male and that body weight is on the denominator of the excess risk equation, a lower body weight increase the risk. Vegetable uptake or skin surface are also changing between male and female. Indeed, the UK exposure factors, for the consummation of water polluted for the receptor residential the risk is higher for men than for women. This can be explained by differences in the water uptake for man (3.17 L) and woman (2.27 L), so male is more exposed and that means a higher risk.

Conclusion

This work was focused on the value of the real exposure time and exposure parameters in a particular industrial region and on contamination of chlorinated solvent DNAPL's, but it can be extrapolated to different scenarios. Differences in human exposure factors data, including anthropometric and sociocultural data (e.g., body weights, skin-surface areas, and life expectancy), behavioural data (e.g., non-dietary ingestion rates, activity/time use patterns, and consumer product use), factors that may be influenced by the physiological needs of the body, metabolic activity, and health and weight status (e.g., water and food intake, and inhalation rates), and other factors (e.g., building characteristics) can lead to variations in calculated risk.

Acknowledgements

This work was made possible by an Erasmus Mundus Master Scholarship received by Celia Baratier. The authors are grateful to the Biohealth & Computing EM Master Program Coordinator and to Jofre Herrero and Diana Puigserver for analytical assistance.

References

1. Kueper, B.H., Wealthall, G.P., Smith, J.W.N., Leharne, S.A., Lerner, D.N. 2003. Environment Agency, Bristol. 65.
2. Viala, A. 1998, Cachan, pp 241.

3. REACH. 2006, (EC) No 1907/2006.
4. Cortés, A., Puigserver, D., Carmona, J.M., Viladevall, M. 2011, Research Signpost, Kerala. 223
5. Nriagu, J.O. 2011, Elsevier, 301.
6. IARC. 2008, *IARC Monogr Eval Carcinog Risks Hum*, Lyon, vol 97.
7. IARC. 1995, IARC *Monogr Eval Carcinog* Risks Hum, Lyon, vol 63.
8. InVS, 2009, Paris, 31.
9. Miljøstyrelsen, DK. 2009. *Delrapport II.*
10. DOE. 1998, DOE/EH-413-9815. Washington, D.C, 14.
11. DEQ. http://www.michigan.gov/deq/0,1607,7-135-3311_4109_4215-17592--,00.html [Last consultation 17th June 2013].
12. GCI http://www.gsi-net.com/en/software/rbca-for-chemical-releases-v25.html . [Last consultation 17th June 2013].
13. INERCO. 2008, División de Medio Ambiente [Document with restrictive access].
14. US-EPA. 1996, Method 8260B, 86.
15. US-EPA. 1999, Washington DC.
16. US-EPA. 2010, IRIS Databases.
17. GSI. 1996, NGWA Petroleum Hydrocarbons Conference, Houston.
18. Data bank of environmental properties of chemicals (EnviChem) http://wwwp.ymparisto.fi/scripts/Kemrek/Kemrek.asp?Method=MAKECHEMSEARCHFORM [last consultation 31th of July 2013]
19. Reaxys. 2013, Elsevier Information Systems GmbH.
20. US-EPA. 2007, In Support of Summary Information on the Integrated Risk Information System (IRIS).
21. US-EPA. 2001, In Support of Summary Information on the Integrated Risk Information System (IRIS). .
22. US- EPA. 2010, Integrated Risk Information System, review.
23. RAIS. Tutorial. http://rais.ornl.gov/tutorials/tutorial.html. [Last consultation 17th June 2013].
24. US-EPA. 2005, EPA/630/P-03/003F, Washington DC.
25. US-EPA, Technical Factsheet http://www.epa.gov/ogwdw/pdfs/factsheets/voc/tech/carbonte.pdf [Last consultation 17th June 2013].
26. US-EPA. 1996, EPA Document Number: EPA/540/R-95/128, Washington DC, pp 9-62.
27. DET. 1994, Risk Science Program (RSP), California, 44.
28. US-EPA. 2010, EPA/635/R-09/006F, 174.
29. NHDES. 2013, Section 7.4(4), Revision, 55.
30. NJDEP. 2008. http://www.state.nj.us/dep/standards/pdf/74-87-3-tox.pdf
31. CALIFORNIA EPA. http://www.arb.ca.gov/toxics/healthval/contable.pdf
32. ENVIRONNEMENT CANADA.2009, https://www.ec.gc.ca/ese-ees/
33. E-PRTR. 95. http://prtr.ec.europa.eu/pgLibraryPollutants.aspx
34. E-PRTR 145, http://prtr.ec.europa.eu/pgLibraryPollutants.aspx
35. E-PRTR 74, http://prtr.ec.europa.eu/pgLibraryPollutants.aspx

36. OECD SIDS, DOW, http://msdssearch.dow.com/PublishedLiteratureDOWCOM/dh_090a/0901b8038090a252.pdf?filepath=productsafety/pdfs/noreg/233-00271.pdf&fromPage=GetDoc
37. OECD SIDS http://www.inchem.org/documents/sids/sids/DICHLOROETH.pdf
38. US-EPA, http://www.epa.gov/ogwdw/pdfs/factsheets/voc/tech/trichlor.pdf
39. GSI Environemental Inc. 2010, GSI Chemical properties Database.

Research Signpost
37/661 (2), Fort P.O.
Trivandrum-695 023
Kerala, India

Recent Advances in Pharmaceutical Sciences V, 2015: 33-49 ISBN: 978-81-308-0561-0
Editors: Diego Muñoz-Torrero, M. Pilar Vinardell and Javier Palazón

3. Plant cell and organ cultures as a source of phytochemicals

Mercedes Bonfill, Rosa M Cusidó, Liliana Lalaleo and Javier Palazón
[1]*Department of Plant Physiology, Faculty of Pharmacy, Barcelona University,Avda Joan XXIII s/n, Barcelona, Spain*

Abstract. Plant cell and organ cultures constitute a promising platform for the production of numerous valuable secondary compounds. Currently, *in vitro* culture techniques involve both empirical and rational approaches as suitable strategies to condition high metabolite production and establish competitive plant cell-based bioprocesses. In this context, we have developed hairy root cultures of *Panax ginseng*, and engineered hairy root cultures of *Duboisia*, *Datura metel* and *Hyoscyamus* spp and plant cell cultures of *Centella asiatica* and *Taxus* spp. This chapter describes our work on the development of two different biotechnological systems to improve taxol production in cell suspension cultures of *Taxus* spp and ginsenoside production in hairy root cultures of *Panax ginseng*.

Introduction

Plant secondary metabolites play an important role in plant defense and constitute a source of phytochemicals for human health and nutrition. The three main groups of plant secondary metabolites (alkaloids, polyphenols

Correspondence/Reprint request: Dr. Mercedes Bonfill, Department of Plant Physiology, Faculty of Pharmacy, Barcelona University, Avda Joan XXIII s/n, Barcelona, Spain. E-mail: mbonfill@ub.edu

and terpenes) include a wide range of compounds with high added value. Some of them can be synthesized chemically, but due to their highly complex structures most are extracted from the plant. However, sometimes even extraction from the plant is not feasible, due to low production levels, and the risk of endangering the species.

In vitro culture techniques using plant cell and organ cultures are promising tools for the production of numerous valuable secondary compounds. Empirical approaches have long been employed for the development and optimization of plant cell-based bioprocesses, focusing on input (cell line, medium, culture parameters, bioreactors, process operations, etc.) and output factors (cell growth, nutrient uptake, productivity, yield, etc.). In addition, a rational approach, taking into account the molecular and cellular basis of metabolic pathways and their regulation, is currently being used. The successful biotechnological production of phytochemicals with high added value, such as the anticancer compound taxol, shows that plant cell and organ cultures can constitute an alternative to the culture of the whole plant for the production of secondary metabolites with biological activity [1].

The biotechnological production of plant secondary metabolites has several advantages over the culture of the whole plant in the field, including:

- The desired product can be harvested anywhere in the world, maintaining strict control of production and quality.
- It is not necessary to use herbicides and pesticides.
- Climate or ecological problems are avoided.
- Growth cycles are of weeks rather than years.

Our research is based on plant *in vitro* culture and genetic and metabolic engineering techniques with the aim of increasing the production of high-value phytochemicals and obtaining plant stem cells for cosmetic uses (Fig. 1). Working with plant *in vitro* cultures, we are interested in the selection of highly productive genotypes and the micropropagation of aromatic and medicinal plants in order to maintain the most productive ones and, in cases of endangered plants, to help preserve the species. Plant micropropagation also represents the best way to obtain virus-free plants to meet phytosanitary requirements for plant import-export. Another goal is using plant cells and hairy root cultures for the production of phytochemicals.

Another field of our research involves the application of genetic and metabolic engineering techniques to improve the production of target secondary metabolites. In this case, it is necessary to understand the relevant biosynthetic pathways and to know which enzymes catalyze the sequence of

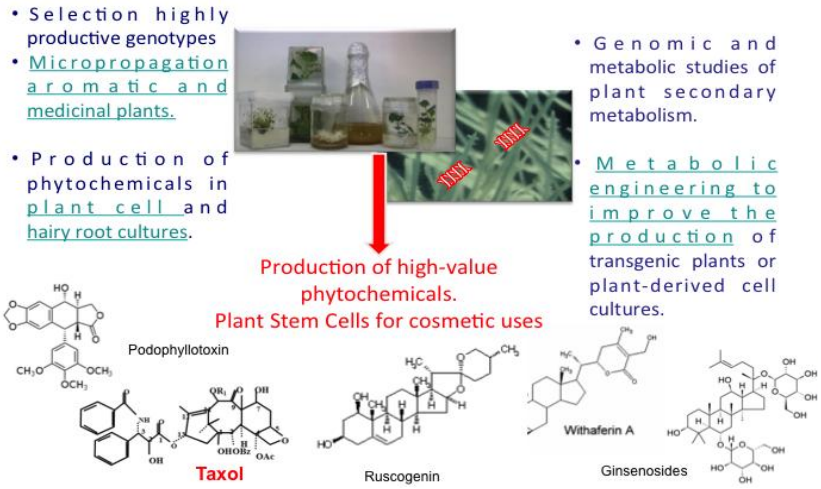

Figure 1. Plant *in vitro* culture and genetic and metabolic engineering techniques as the basis of Plant Biotechnology.

reactions, especially the slow steps, and the genes encoding these enzymes. Using the aforementioned techniques, the plant secondary pathways are studied to detect the flux-limiting steps and improve production.

In this chapter, we will describe the different *in vitro* techniques being used in our laboratory, with relevant examples of the plant species we have studied. Finally, we will describe our work on the development of a biotechnological system to increase taxol and taxane production using *Taxus baccata* and *T. media* cell suspension cultures and ginsenoside production in hairy root cultures of *Panax ginseng*.

1. Plant *in vitro* cultures

Micropropagation of aromatic and medicinal plants

Micropropagation is a way of obtaining a large number of plants *in vitro* in an asexual manner, ensuring that they are genetically and phenotypically identical to the original plant. It consists of the culture of variably sized plant pieces using a suitable culture medium. In this field, our group has developed specific protocols to micropropagate *Lavandula dentata* [2], *Ruscus aculeatus* [3], etc. Recently our work has focused on the micropropagation of *Centella asiatica* using synthetic seeds and obtaining several virus-free varieties of *Vitis vinifera* plants for exportation (Fig. 2).

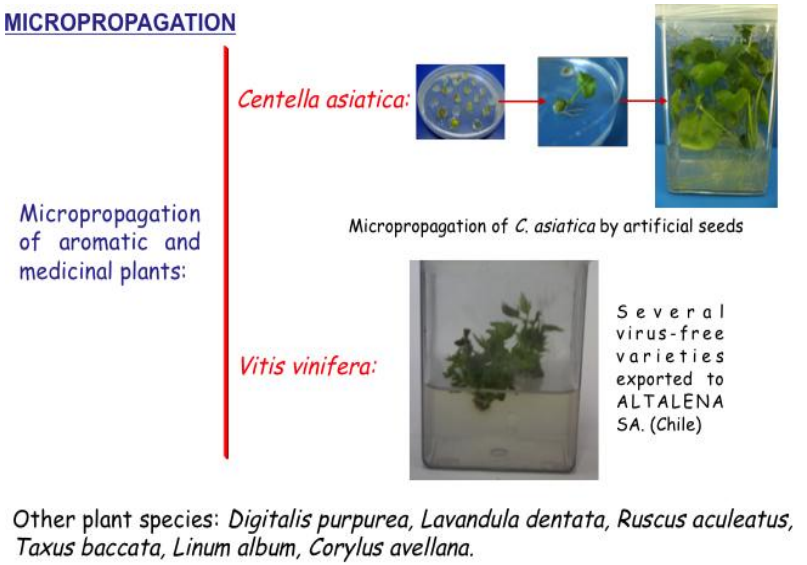

Figure 2. Our Background in Micropropagation.

Plant cell factories and stem cells

Plant cell factories constitute a biotechnological platform for the production of phytochemicals. In this way, cell cultures, also known as plant stem cells, can be utilized as cell suspensions or immobilized cells. Plant stem cells have an unlimited capacity for growth and an ability to produce identical new plants. By means of *in vitro* culture techniques, we are able to obtain plant stem cells with the same biosynthetic capacity as the whole plant. To establish a cell suspension culture that can act as a plant cell factory, it is first necessary to obtain a high callus biomass.

The methodology employed (Fig. 3) involves the following steps: selection of highly productive genotypes of the target plant; induction of calli from the best explant to obtain callus biomass; disintegration of calli by shaking in a liquid medium to obtain cell suspension cultures; optimization of the culture conditions by assaying several basic media, plant growth regulators (PGRs), sugar supplements, addition of elicitors, precursors, etc. to improve the production; and finally, scale-up to bioreactor level. Sometimes immobilization in alginate beads may be necessary to improve the biotechnological production [4].

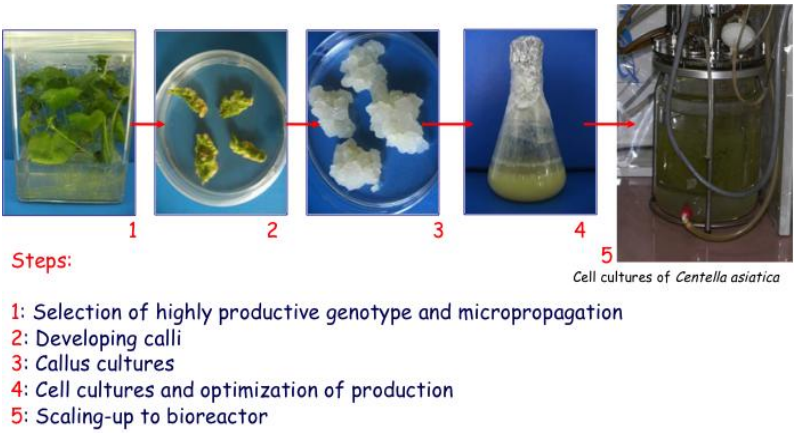

Figure 3. Plant cell factories: methodology

Regarding the development of plant biofactories, our group is working on centelloside production in cell suspension cultures of *Centella asiatica* [5]. We are also working on ruscogenin production in *Ruscus aculeatus* and podophyllotoxin production in *Linum album*, but our main research line is focused on the biotechnological production of taxol and taxanes in cell suspension cultures of *Taxus baccata* and *T.media* [6, 7]. We have previously developed cell cultures for the production of digoxin, digitoxin, tobacco alkaloids and galphimines.

We have also recently obtained plant stem cells of *Vitis vinifera* and *Centella asiatica* for cosmetic uses. *C.asiatica* was traditionally used in Ayurveda medicine and due to its dermatological applications, its stem cells are currently an important target for cosmetic purposes in Europe.

Plant biotransformations

Another cell culture application is biotransformation. In this context, we have established a single protocol for extracting α-amyrin from copal resin, which is then added as a substrate to cell suspension cultures of *C. asiatica* for its bioconversion into compounds with high added value, such as centellosides [8]. The results have demonstrated that cell lines are capable of biotransforming a compound with low biological activity but that is abundant in nature, such as amyrin, into other compounds widely used for their pharmacological properties, such as the centellosides (Fig. 4).

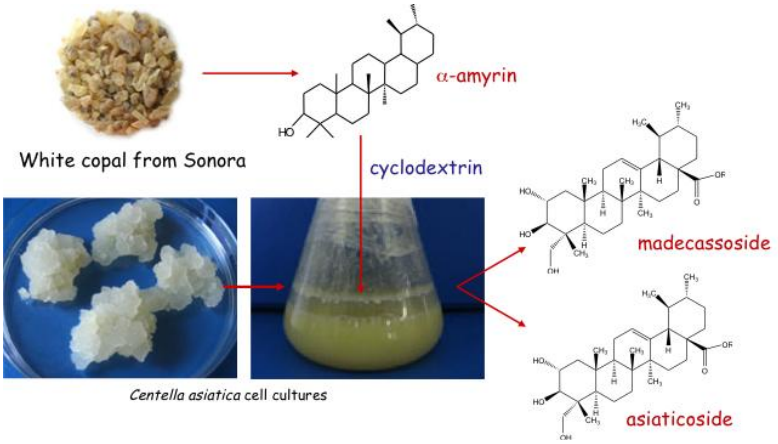

Figure 4. Biotransformation of the substrate α-amyrin into centellosides.

Hairy root cultures

Sometimes the production of plant secondary metabolites requires organized cultures such as roots or aerial shoots. In this context, our group uses the *Agrobacterium rhizogenes* system to genetically transform plant cells and develop hairy root cultures. *A.rhizogenes* is a bacterium that infects plants in nature, transferring a part of its plasmidic DNA, the Transfer-DNA or T-DNA, to the plant cell. The infected plant then develops large roots called hairy roots. Biotechnological processes based on hairy root cultures show a very high biomass production and a metabolic profile similar to the root of the whole plant.

This methodology (Fig. 5) is based on obtaining hairy root lines after infection with *A.rhizogenes*, the isolation and selection of the most productive root lines, optimization of culture conditions for maximum production and eventual scale-up to bioreactors. The scaling up of these cultures is very difficult because bioreactors are generally designed for the culture of microorganisms and need to be specially adapted for the culture of transformed roots.

Our group has worked with hairy root cultures for the production of ajmalicine in *Catharanthus roseus* [9], ginsenosides in *Panax ginseng* [10], tropane alkaloids in *Datura metel*, *Duboisia* sp and *Hyoscyamus* sp. [11,12], withanolides in *Withania coagulans* [13] and lately we have also been working on transformed root cultures of *Linum album* for the production of podophyllotoxin and methoxypodophyllotoxin [14].

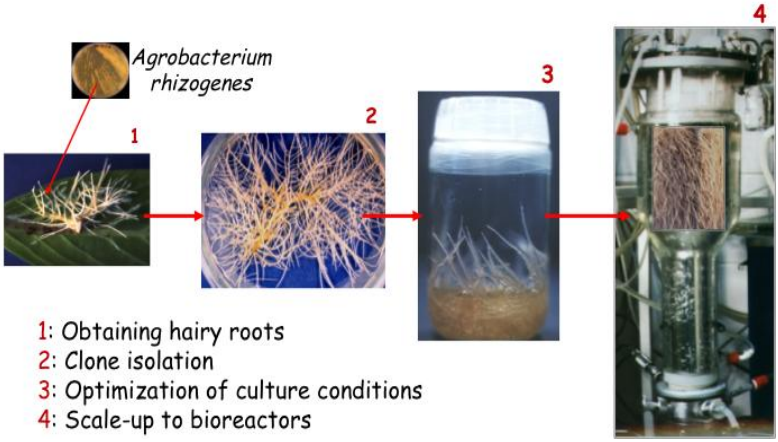

Figure 5. Hairy root cultures of *Catharanthus roseus* scaled up to airlift bioreactor level.

2. Genetic and metabolic engineering techniques

To improve the biotechnological production of a secondary metabolite, it is necessary to understand the relevant biosynthetic pathways. It is also necessary to know which enzymes catalyze the sequence of reactions, especially the slow steps, and the genes encoding these enzymes. Using genetic and metabolic engineering techniques, we can study the plant secondary pathways to detect the flux-limiting steps in the biosynthesis of phytochemicals and use engineering techniques to design plants and cell cultures with improved production.

We have used metabolic engineering techniques to improve the production of scopolamine in the species *Datura metel*, *Hyoscyamus muticus* and a *Duboisia* hybrid. The first step was to obtain hairy root cultures of the aforementioned species and then select the most productive ones to be scaled up to bioreactor level (Fig. 6).

The second step was the overexpression, both separately and together, of the genes encoding the enzymes putrescine methyltransferase (PMT), which constitutes the first committed step in the scopolamine biosynthesis, and hyoscyamine 6-β-hydroxylase (H6H), which transforms hyoscyamine into scopolamine [15]. The best results were obtained by overexpressing both genes together in transformed roots of *H. muticus* (Fig. 7).

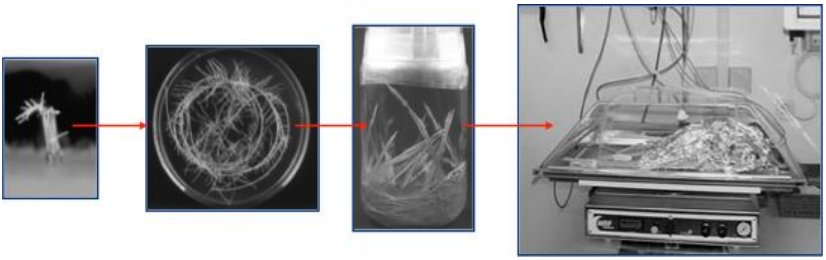

Figure 6. 1st step: Obtaining hairy root cultures of a *Duboisia* hybrid and scaling up to wave bioreactor level.

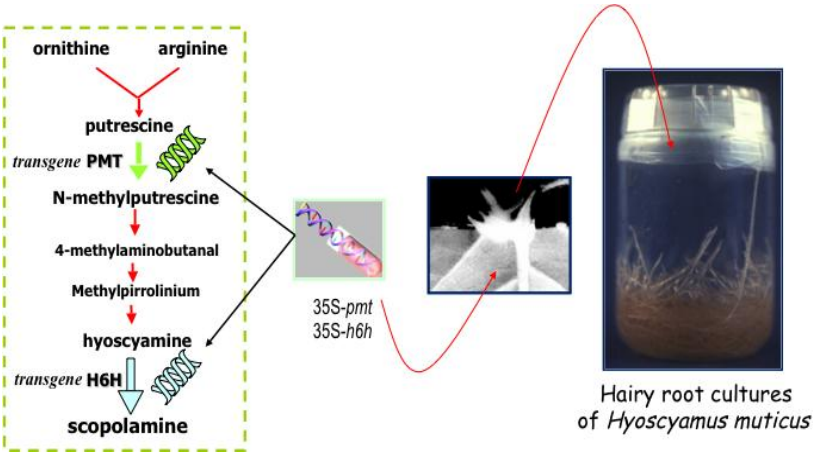

Figure 7. 2nd step: Overexpression of putrescine methyltransferase and hyoscyamine 6-β-hydroxylase.

Thirdly, since scopolamine is an alkaloid of greater commercial interest than the more naturally abundant hyoscyamine, we developed a biotechnological system to biotransform exogenous hyoscyamine into scopolamine based on tobacco transformed roots carrying the hyoscyamine 6-β-hydroxylase gene of *H. muticus* (Fig. 8).

In addition, with the aim of scaling up the system and avoiding the problems of root cultures in bioreactors, we dedifferentiated the roots and established cell suspensions that were also able to biotransform hyoscyamine into scopolamine at a bioreactor level [16].

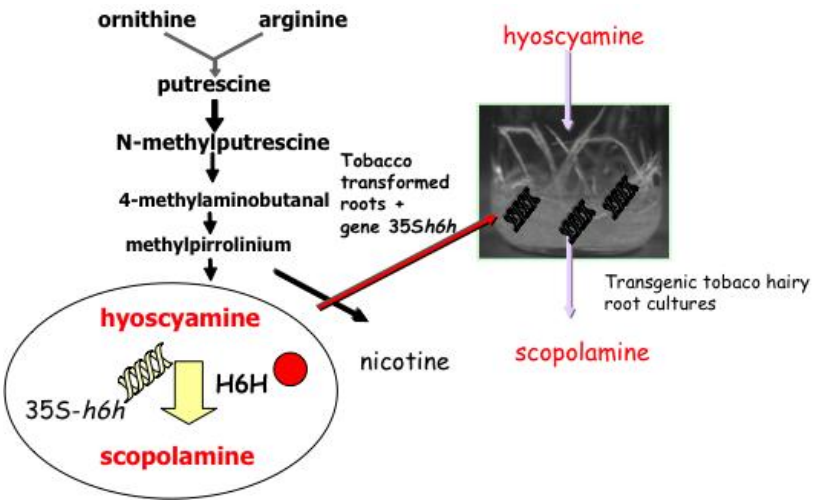

Figure 8. 3rd step: Biotransformation of hyoscyamine into scopolamine in tobacco hairy root cultures.

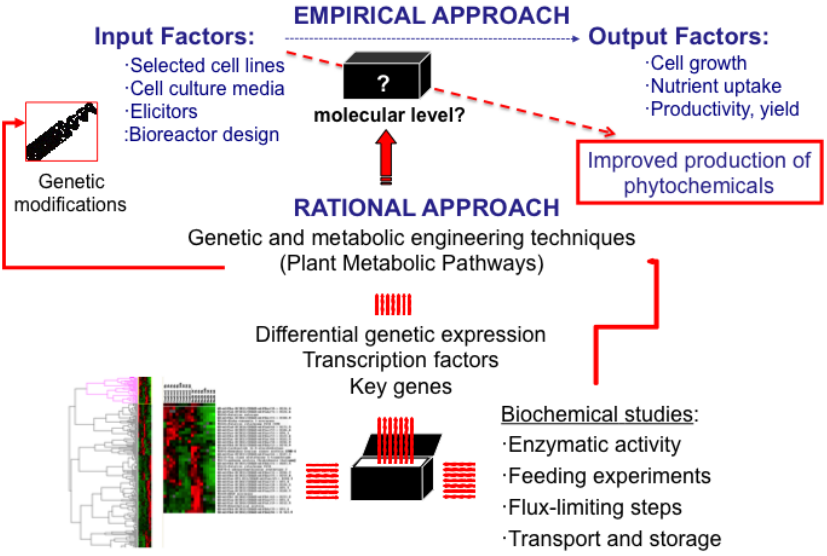

Figure 9. Improving secondary metabolite production using empirical and rational approaches.

To sum up, to improve secondary metabolite production using *in vitro* cultures one can consider two principal approaches (Fig. 9). An empirical strategy involves the modification of input factors, such as the selection of more productive cell lines, optimizing culture media, the use of elicitor treatments, bioreactor design, etc. However, this does not provide information about what is happening in the producer cells at the molecular level. By taking a rational approach based on genetic and metabolic engineering techniques, we can study how the input factors change the metabolic and transcriptomic profile of the target cell cultures.

3. Improving taxol and taxane production in cell suspension cultures of *Taxus* sp.

For some time now, one aspect of our research work has been focused on taxol production using cell cultures of different *Taxus* species. Taxol, a diterpene alkaloid with a very complex chemical structure, is one of the most effective anticancer drugs ever developed. It presents a unique mode of action on the microtubular cell system by inhibiting cell proliferation at the G2 phase of the cell cycle, thus blocking mitosis.

The natural source of taxol is the inner bark of several *Taxus* species. The disadvantages of this source are that taxol accumulates at a very low concentration (0.02% of dry weight), its extraction involves the destruction of yew trees and is very expensive. Moreover, the endangered status of several *Taxus* species excludes this method of obtaining taxol. For these reasons, alternative sources of taxol have been assayed, including its preparation by total synthesis, but this process is not commercially viable. Another possibility is producing taxol semisynthetically from more abundant taxanes, for example, via the conversion of baccatin III found in *Taxus* needles, but the cost and difficulty of the extraction and purification process of these precursors are also very high. An alternative consists of cultivating *Taxus* trees in the field. In fact, in Yunnan province in China, there are conventional *Taxus* crops for the production of taxol, but a harvest can only be obtained after several years and the extraction remains very expensive [17]. Therefore, the most promising approach to a sustainable commercial production of taxol, or other compounds synthesized by plants in similarly small quantities, is provided by plant cell cultures.

In order to obtain cell suspensions, first on a small scale and then at bioreactor level, it is necessary to establish fast-growing callus cultures from which the cell suspensions are derived. *Taxus* callus cultures were obtained from young stems of 3-4-year-old yew trees cultured in optimum conditions.

Figure 10 shows the whole process until the establishment of a small-scale cell suspension culture.

To develop a biotechnological system for a high taxol production, it is necessary to optimize the culture conditions by assaying several basic media, plant growth regulators, sugar supplements etc., which requires knowledge of the growth curves of the system. A growth curve represents the biomass production (growth) in relation to the time of culture, and appears as a sigmoid curve with 3 characteristic phases: 1) A lag phase in which the biomass does not increase, when cells are preparing all the machinery for the cell division that will start in the exponential phase. 2) An exponential phase in which cells are dividing continuously by mitosis. All the processes related with mitosis, which are part of the plant's primary metabolism, are now taking place inside the cells, including DNA duplication, and RNA and protein synthesis. In these conditions secondary metabolism is inhibited. 3) A stationary phase in which the biomass of the system remains constant and the number of cells that divide by mitosis is almost equal to the number of dying cells. In these conditions, the cells can accumulate precursors for the biosynthesis of phytochemicals and the machinery of plant secondary metabolism begins to work.

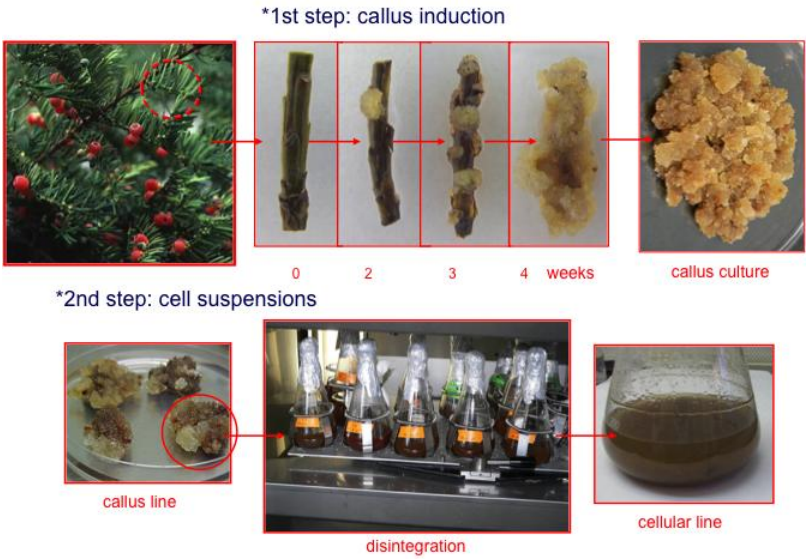

Figure 10. Establishment of *Taxus* cell suspension cultures.

Once the growth curve of a culture is established, we know how long each phase is and when the stationary phase begins, which is the moment for adding precursors, elicitors, permeabilizing agents etc. to improve the production. Knowledge of the growth curve is particularly useful in a two-stage culture, that is, when a separate medium is required to enhance growth and another to increase production. In this case, during the exponential phase the cells are cultured in the growth medium and then transferred to the production medium at the start of the stationary phase.

A two-stage culture system was established for taxol production. Plant cells were first cultured in a medium optimised for their growth, which was then replaced by a production medium that mainly stimulates the biosynthesis of secondary metabolites. This system has an added advantage of permitting the addition of biosynthetic precursors and elicitors in the production medium.

In summary, taxol and baccatin III production was clearly enhanced by the transfer of cells from the growth to the production medium containing the elicitor methyl jasmonate (MeJA) [18]. After optimizing the culture conditions, we scaled up the culture in a stirred bioreactor where the production improved 2.4-fold for taxol and 9-fold for baccatin III.

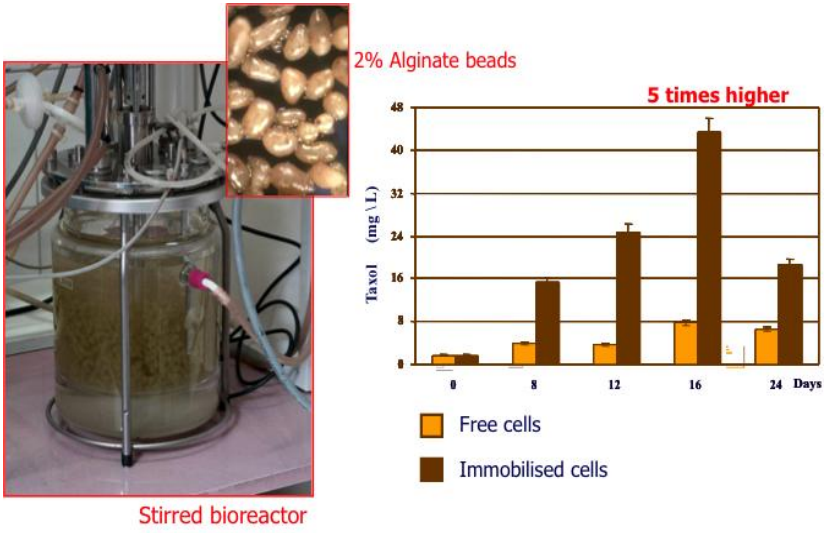

Figure 11. Taxol production in immobilized cell cultures of *Taxus baccata* in a stirred bioreactor.

We continued our study on the improvement of taxol and related taxane production by establishing immobilized cell cultures, first on a small scale and then at bioreactor level. Numerous studies have reported that immobilization of plant cell suspensions enhances the production of valuable plant metabolites. Taxol production clearly improved when cell suspensions were immobilised in 2% alginate beads and cultured in a stirred bioreactor, using the optimum medium for the biosynthesis of taxol. When the taxol production was at its highest, on day 16, its levels were more than 5-fold higher than those obtained by the same cell line growing freely in the same conditions (Fig. 11). The novelty of this work was to demonstrate that immobilization strongly constrains the physiology of *T. baccata* cells and substantially enhances taxane production in bioreactor cultures [4].

4. Ginsenoside production in hairy root cultures of *Panax ginseng*

Ginsenosides are triterpenes with a great variety of properties, being used as tonics, analgesics, antipyretics, stress-beaters, etc.

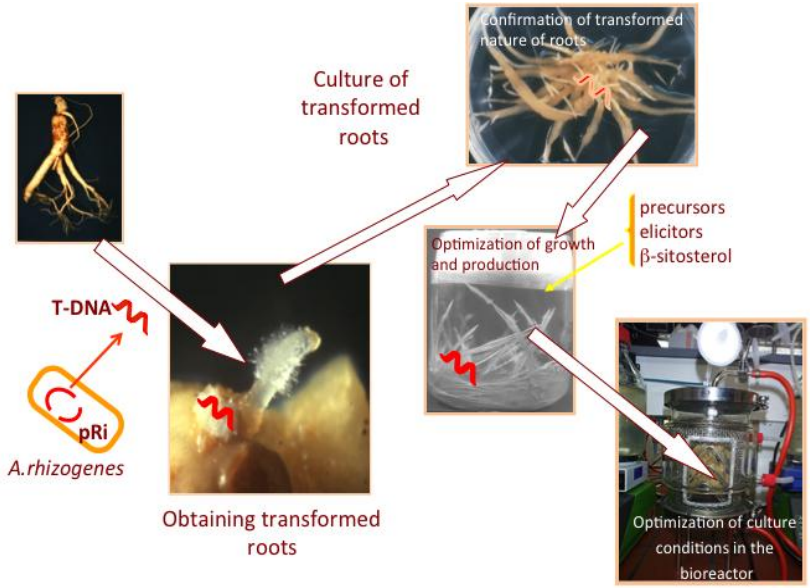

Figure 12. Improving ginsenoside production in hairy root cultures of *Panax ginseng.*

Hairy root cultures were obtained using the following protocol. After infection of the rhizome with *A. rhizogenes*, we obtained hairy roots that were cultured in a solid growth medium and their transformed nature was confirmed. The transformed roots were then transferred to a liquid medium to optimize growth and production, using elicitors, precursors and beta-sitosterol. Finally, we scaled up the culture by assaying different types of bioreactors, optimizing the culture conditions. A two-stage system was not used in this case. Figure 12 summarizes the whole process.

After the infection of the rizome with *A. rhizogenes* we obtained roots with 3 types of morphology: 50% had a typical hairy root morphology (HR-M), 35% a callus morphology (C-M) and 15% a thin morphology (T-M) [19]. The transformed nature of each type of root was confirmed by amplifying the *rol C* gene. The highest growth in solid medium was displayed by C-M roots, although the total ginsenoside content was higher in T-M roots, albeit lower than in the plant rhizome.

After transferring the roots from the solid to the liquid medium to optimize the growth and production, the best growth was achieved by the C-M roots, followed by the HR-M roots, as occurred in the solid medium. It should be emphasized that all the roots grew better in liquid medium.

Regarding the ginsenoside production, the best results were obtained with HR-M roots in liquid medium, in contrast with the solid medium where the best production was obtained with T-M roots.

We then optimized the culture conditions by assaying several elicitors (chitosan, methyl jasmonate, vanadyl sulfate), precursors (mevalonic acid, squalene, farnesol) and beta-sitosterol (which bioregulates the synthesis of ginsenosides). The best result was obtained with MeJA, which increased the production of ginsenosides in all the root types [20]. The precursors and beta-sitosterol did not yield any significant results. Compared with a 4-year-old *Panax ginseng* plant rhizome, the ginsenoside production of a transformed HR-M root grown in liquid medium with MeJA for 4 weeks was almost 2-fold higher.

Finally, we optimized the process at a bioreactor level. We first selected the most productive hairy root line (HR-M), which was cultured in the liquid medium optimized on a small scale in 3 types of bioreactors: airlift, spray and wave. After 28 days of culture without changing the medium, the best growth was obtained in the wave bioreactor, but the best ginsenoside production was achieved in the spray bioreactor. However, if we determine the productivity, that is, the ginsenoside production per liter and per day, the best results were obtained with the wave bioreactor in the same culture conditions: after 28 days without changing the media. This confirms that the

productivity of a culture does not only depend on the accumulation of the target compound but also on its growth capacity.

In summary, after 28 days of culture without changing the media, we obtained the best production in a spray bioreactor but the best productivity in a wave bioreactor. Optimum growth was also obtained in the wave bioreactor.

We next determined the biomass and ginsenoside production in 2 bioreactors (spray and wave) after 28 days of culture but this time changing the culture medium at day 15. In these conditions, the biomass production increased in both bioreactors, and was therefore higher in the wave bioreactor. Regarding the ginsenoside production, the results again showed more production in the spray bioreactor, but when we determined the productivity, the roots in the wave bioreactor were the most productive, as before.

Finally, we cultured the roots (HR-M) in the two bioreactors (spray and wave) but now for 56 days and changing the medium every 15 days [21]. The highest productivity of the roots was again achieved in the wave bioreactor, being almost 2-fold higher than in the small flasks (Fig. 13).

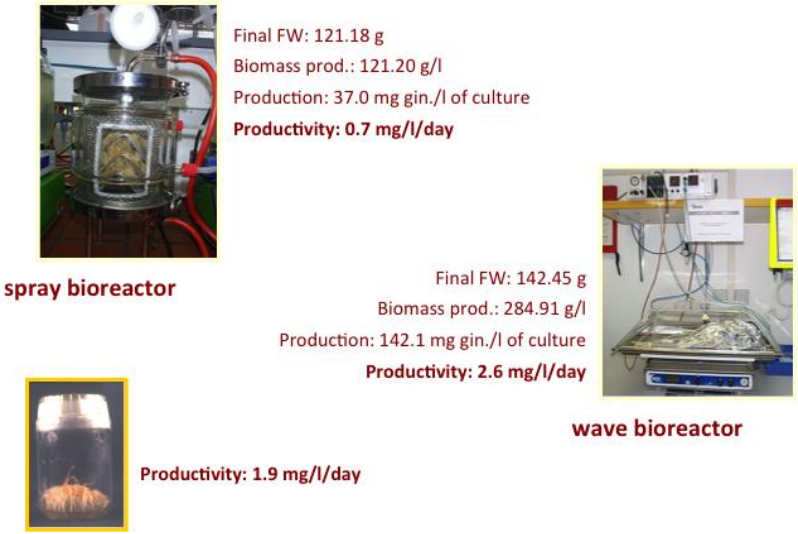

Figure 13. Ginsenoside productivity of typical hairy roots (HR-M) grown in small flasks, spray and wave bioreactors on a 56-day culture with change of media every 15 days.

5. Conclusion

We have established two biotechnological systems (cell suspension cultures of *Taxus* sp. and hairy roots of *Panax ginseng*) to improve the production of two high-value target compounds (taxol and ginsenosides) using an empirical approach that considers input and output factors (Fig. 9). Taxol production was improved employing a two-stage culture system, elicitation with MeJA, immobilization in alginate beds and scaling up in a stirred bioreactor. Ginsenoside production was improved using selected hairy root lines of three different morphologies, elicitation with MeJA, changing the medium during the culture, assaying three bioreactor designs and taking into account production and productivity. These results can be improved in future studies taking a rational approach.

Acknowledgements

Work in the Plant Physiology Laboratory (University of Barcelona) was financially supported by the Spanish MINECO (BIO2011-29856-C01; BIO2014-51861-R) and the Generalitat de Catalunya (2009SGR1217; 2014 SGR 215). The authors are very grateful to Dr. Hiroko Murata from the Setsunan University, Osaka, Japan, for supplying *Panax ginseng* rhizomes.

References

1. Malik, S., Cusido, R.M., Mirjalili, M.H., Moyano, E., Palazón, J., Bonfill, M. 2011, *Process Biochem*., 46, 23.
2. Sudriá, C., Piñol, M.T., Palazón, J., Cusidó, R.M., Vila, R., Morales, C., Bonfill, M., Cañigueral, S. 1999, *Plant Cell Tiss. Org*., 58, 177.
3. Moyano E., Montero, M., Bonfill, M., Cusidó, R.M., Palazón, J., Piñol, M.T. 2006, *Biol. Plantarum*, 50, 441.
4. Bentebibel, S., Moyano, E., Palazón, J., Cusidó, R.M., Bonfill, M., Eibl, R., Piñol, M.T. 2005, *Biotechnol. Bioeng*., 89, 647.
5. Bonfill, M., Mangas, S., Moyano, E., Cusido, R.M., Palazon, J. 2011, *PCTOC: J. Biotechnol*., 104, 61.
6. Cusido, R.M., Onrubia, M., Sabater-Jara, A.B., Moyano, E., Bonfill, M., Goossens, A., Pedreño, M.A., Palazon, J. 2014, *Biotechnol. Adv*., 32, 1157.
7. Syklowska-Baranek, K., Pilarek, M., Bonfill, M., Kafel, K., Pietrosiuk, A. 2015, *PCTOC: J. Biotechnol*., 120, 1051.
8. Hernandez-Vazquez, L., Bonfill, M., Moyano, E., Cusido, R.M., Navarro-Ocaña, A., Palazón, J. 2010, *Biotechnol. Lett*., 32, 315.
9. Palazón, J., Cusidó, R.M., Gonzalo, J., Bonfill, M., Morales, C., Piñol, M.T. 1998, *J. Plant Physiol*., 153, 712.

10. Mallol, A., Cusidó, R.M., Palazón, J., Bonfill, M., Morales, C., Piñol, M.T. 2001, *Phytochemistry*, 57, 365.
11. Cusidó, R.M., Palazón, J., Piñol, M.T., Bonfill, M., Morales, C. 1999, *Planta Med*., 65, 144.
12. Zhang, L., Ding, R., Yourong, C.H., Bonfill, M., Moyano, E., Oksman-Caldentey, K.J., Xu, T., , Y., Wang, Z., Zhang, H., Kai, G., Liao, Z., Sun, X., Tang, K. 2004, *PNAS*, 101, 6786.
13. Mirjalili, M.H., Fakhr-Tabatabaei, S.M., Bonfill, M., Alizadeh, H., Cusidó, R.M., Ghassempour, A., Palazón, J. 2009, *Eng. Life Sci*., 9, 197.
14. Chashmi, N.A., Sharifi, M., Yousefzadi, M., Behmanesh, M., Rezadoost, H., Cardillo, A., Palazón, J. 2013, *J. Med. Chem. Res*., 22, 745.
15. Palazón, J., Moyano, E., Cusidó, R.M., Bonfill, M., Oksman-Caldentey, K.M., Piñol, M.T. 2003, *Plant Sci.*, 165, 1289.
16. Moyano, E., Palazón, J., Bonfill, M., Osuna, L., Cusidó, R.M., Oksman-Caldentey, K.M., Piñol, M.T. 2007, *J. Plant Physiol*., 164, 521.
17. Malik, S., Cusido, R.M., Mirjalili, M.H., Moyano, E., Palazón, J., Bonfill, M. 2011, *Process Biochem.*, 46, 23.
18. Bonfill, M., Bentebibel, S., Moyano, E., Palazón, J., Cusidó, R.M., Eibl, R., Piñol, M.T. 2007, *Biol. Plantarum*, 51, 647.
19. Mallol, A., Cusidó, R.M., Palazón, J., Bonfill, M., Morales, C., Piñol, M.T. 2001, *Phytochemistry*, 57, 365.
20. Palazón, J., Cusidó, R.M., Bonfill, M., Mallol, A,. Morales, C., Piñol, M.T. 2003, *Plant Physiol. Bioch*., 41, 1019.
21. Palazón, J., Mallol, A., Eibl, R., Lettenbauer, C., Cusidó, R.M., Piñol, M.T. 2003, *Planta Med*., 69, 344.

Research Signpost
37/661 (2), Fort P.O.
Trivandrum-695 023
Kerala, India

Recent Advances in Pharmaceutical Sciences V, 2015: 51-64 ISBN: 978-81-308-0561-0
Editors: Diego Muñoz-Torrero, M. Pilar Vinardell and Javier Palazón

4. The role of diet and physical activity in children and adolescents with ADHD

María Izquierdo-Pulido[1,2], Alejandra Ríos[1], Andreu Farran-Codina[1] and José Ángel Alda[3]

[1]Department of Nutrition and Food Science, School of Pharmacy, Universitat de Barcelona, Barcelona, Spain; 2CIBER Fisiopatología de la Obesidad y la Nutrición (CIBEROBN), Spain; 3Department of Mental Health and Psychiatry, Hospital Sant Joan de Déu, Barcelona, Spain

Abstract. ADHD (Attention Deficit and Hyperactive Disorder) is the most common neurobehavioral disorder of childhood, presenting with pervasive and impairing symptoms of inattention, hyperactivity, impulsivity, or a combination. There is scientific evidence that some dietary and physical activity strategies may be useful to improve the symptoms of ADHD and benefit the social, cognitive and academic performance of children and adolescents with ADHD. The purpose of our study was to review the scientific literature on the role of diet and physical activity in ADHD symptomatology up to date.

Introduction

Attention deficit and hyperactivity disorder (ADHD) is one of the most common psychiatric disorders in early childhood and adolescence with a prevalence rate exceeding 5% [1]. Some of the most common symptoms

Correspondence/Reprint request: Dr. Maria Izquierdo-Pulido, Department of Nutrition and Food Science, School of Pharmacy, University of Barcelona, Av. Joan XXIII s/n 08028 Barcelona, Spain
E-mail: maria_izquierdo@ub.edu

associated with ADHD are hyperactivity, attention deficit, cognitive deficit and poor impulse control [2]. The etiology of ADHD is still unknown, although there are several factors which may have a certain influence in the symptomatology, including diet and physical activity [2].

The research aimed to study the association between diet and ADHD has been growing in the last decades. Thus, children and adolescents with ADHD seem to have lower levels of certain nutrients such as: iron [3], zinc [4,5], and omega 3 [6,7], among others. In some cases, the supplementation with these nutrients, especially with omega 3 [6], has showed to improve the ADHD symptomatology. The most significant research done in this field is summarized in Table 1.

Table 1. Relevant scientific evidence of deficiency or supplementation in essential nutrients observed in ADHD children and adolescents.

Study	Nutrients	Study design	Main Findings
Colter *et al.*[8]	Omega 3-Omega 6	Case-control	Children with ADHD have lower omega 3 and 6 plasma levels than healthy children.
Transler *et al.* [9]		Placebo-controlled studies	A daily supplementation (for 4 months) with a mixture of omega-3 and 6 decreased frequency and severity of symptoms.
Bloch and Qawasmi [6]		Systematic review and meta-analysis	Supplementation was statistically significant beneficial for children with ADHD. EPA's effect was bigger than DHA' effect.
Gillies *et al.* [7]		Systematic review	A combination of omega-3 and -6 is not statistically significant in the treatment of ADHD.
Widenhorn-Müller *et al.* [10]		Randomized placebo-controlled intervention trial	Supplementation improves working memory function in ADHD children.
Konofal *et al.* [11]	Iron	Case- control	Serum ferritin levels were lower in children with ADHD than controls. Lower ferritin levels were correlated with more severe ADHD symptoms.
Konofal *et al.* [3]		Double-blind, placebo-controlled, randomized trial	Supplementation (80 mg/day) appeared to improve ADHD symptoms in children with low serum ferritin levels.
Oner *et al.* [12]		Cross-sectional	Hyperactivity was significantly associated with ferritin levels but not with cognitive measures.
Donfrancesco *et al.* [13]		Case-control	No significant relationship between serum ferritin levels and ADHD.
Bilici *et al.* [4]	Zinc	Placebo-controlled double-blind study	Supplementation was significantly better to placebo in reducing symptoms of hyperactivity, impulsivity and impaired socialization in patients with ADHD.
Akhondzadeh *et al.* [5]		Double blind and randomized trial	Supplementation might be beneficial in the treatment of children with ADHD
Arnold et al.[14]		Placebo-controlled double-blind	Zinc supplementation alone (8 weeks) did not improve inattention, but when combined with pharmacological treatment, the optimal dose of the drug was reduced by 37%.
Kozielec and Starobrat-Hermelin [15]	Magnesium	Case-control	95% of ADHD children showed deficiency in magnesium comparing to controls. After 6 months of Mg supplementation (200 mg/day) hyperactivity was reduced.
Mousain-Bosc et al.[16]		Placebo-controlled double-blind	Mg supplementation (100 mg/day) combined with vitamin B6 for 6 months improved symptomatology
Huss et al.[17]		Observational study	Hyperactivity and inattention of most of patients was reduced after supplementation for 12 weeks with a combination of omega-3 and 6, magnesium and zinc.

Other studies suggest that diets rich in sugars and artificial colorings increase the hyperactivity of children [18–22]; however, those findings are still inconsistent and more data are needed. Research about the associations of different dietary patterns and ADHD has also been conducted [22–25]. This approach is really interesting since it assesses the influence of the whole diet.

Besides the potential benefits that a healthy dietary pattern may have on neurocognitive, behavioral and physical growth, it has also been suggested that physical activity might have a positive impact in behavior, neurocognitive function, motor skills, and school performance of children and adolescents with ADHD [26–29], as it will be discussed further.

Although the pathophysiology of ADHD has been not fully demonstrated, there is an important hypothesized mechanism of deregulated dopamine in the prefrontal cortex (PFC). The PFC has the function to regulate behavior, inhibit inappropriate emotions, impulses and habits [30]. Several studies indicate that patients with ADHD present anatomic abnormalities or neurochemical brain dysfunction [31]. Stimulant medications (such as methylphenidate and amphetamines) are used to treat the majority of the symptoms of children with ADHD, but not all the patients have a good response to them and some parents have the concern about the side effects of these drugs in the growth, nervous and cardiovascular system of their children [32]. There is an important need to develop other interventions that do not have repercussion in the health and wellness of the children. Thus, it has been proposed that the combination of diet and physical activity could help children and adolescents with ADHD to improve the symptomatology and their whole quality of life. The aim of this chapter is to review the scientific literature regarding the possible benefits of different dietary approaches and physical activity for symptom management for children and adolescents with ADHD.

1. Role of the whole diet on ADHD: healthy patterns *versus* restrictive elimination diets?

1.1. Dietary patterns and ADHD

As mentioned above, several studies have analyzed the beneficial or detrimental effects of specific single nutrients on ADHD symptomology [33]. Moreover, associations between dietary patterns and ADHD have been recently examined in several cross-sectional studies (Table 2). This new approach is of great interest since nutrients are nearly always consumed together, and they are highly interrelated in the food matrix. Therefore, the

study of dietary patterns is really useful for understanding much better the role of diet in ADHD. Assessing the whole diet instead of the effects of a single nutrient on the relation between diet and ADHD may contribute even more to understand this complex relationship.

The majority of studies on diet and ADHD conclude that ADHD patients have a tendency to have a poor quality diet, which could cause certain nutrient deficiencies. Those deficiencies might affect the neurocognitive, behavioral and physical development at this important stage of life. Indeed, Park *et al.* [35] found that higher intakes of sweetened desserts, fried food, and salt were associated with more learning, attention, and behavioral problems. On the other side, a balanced diet, regular meals, and a high intake of dairy products and vegetables were associated with less learning, attention, and behavioral problems.

Table 2. Summary of the main studies on the influence of the diet on children and adolescents with attention-deficit and hyperactive disorder (ADHD).

Reference	Design	N; age	Country	Main Findings
Howard *et al.* [24]	Cross-sectional study	115; 14y follow-up	Australia	A Western-style diet[a] may be associated with ADHD.
Azadbakht & Esmaillzadeh [23]	Cross-sectional study	375; 6-11y	Iran	Significant independent associations between the sweet[b] and fast food[c] dietary patterns and the prevalence of ADHD.
van Egmond-Fröhlich *et al.* [34]	Cross-sectional study	9,428; 6-17y	Germany	Poor nutrition quality and high-energy intake appear to be independently associated with ADHD symptoms.
Park *et al.* [35]	Cross-sectional study	986; 8-11y	Korea	High intake of sweetened desserts, fried food, and salt is associated with more learning, attention, and behavioral problems, whereas a balanced diet, regular meals, high intake of dairy products and vegetables is associated with fewer problems.
Woo *et al.* [25]	Case-Control study	192; 7-12y	Korea	The traditional-healthy Korean[d] dietary pattern was associated with lower odds having ADHD
Liu *et al.* [36]	Cross-sectional study	417; 6-11y	China	Positive correlation between diet intake (processed meat, salty snacks) and hyperactivity index. Children's diet pattern is an important environmental impact factor for ADHD.
Ghanizadeh and Haddad [37]	Randomized controlled clinical trial	106; 5-14y	Iran	Encouraging the children with ADHD to increase their intake of recommended diet markedly improves their attention.

[a]High in total fat, saturated fat, refined sugar, and sodium; [b]High in ice cream, refined grains sweet desserts, sugar, and soft drinks; [c]High in processed meat, commercially produced fruit juices, pizza, snacks, sauces and soft drinks; [d]High intake of kimchi, grains, and bonefish, and low intake of fast-food and beverages.

The “unhealthy” dietary patterns identified in the different studies (such as “Western”, “fast food” or “sweet” patterns) were generally high in total fat, saturated fat, refined sugars, and sodium. The relationship observed between higher scores for the “unhealthy” dietary pattern and an increased odds for ADHD supports the hypothesis that highly processed and energy-dense foods are linked with ADHD symptomatology [24,34,35].

Howard *et al.* [24] suggested that children eating a “Western” diet, high in fried food, sweetened desserts and unbalanced, are also likely to have micronutrient and/or PUFA deficiencies. Iron, zinc or magnesium deficiencies and lower circulating levels of omega-3, higher levels of omega-6, and a lower omega-3 *versus* omega-6 ratio has been reported in children and adolescents with ADHD [8]. An inadequate micronutrient intake, coming from an unbalanced dietary pattern, could result in suboptimal brain function in children and adolescents [23]. Futhermore, Van Egmond-Fröhlich *et al.* [34] pointed out that ADHD symptoms might be associated with poor food selection rather than overeating in terms of volume.

“Unhealthy” or “junk foods” besides being usually high in fat and sugars may be rich also in artificial food colorings and preservatives, which could negatively affect ADHD symptoms [38]. It has been suggested, as it will be discussed below, that certain food additives may lead to hyperactivity or changes in neurotransmitter function [21]. An interesting point is that the relationship observed between poor dietary choices and ADHD may be bidirectional [24]. The results observed could be explained, especially for adolescents, by the tendency of them to experience emotional distress to crave fat-rich snack foods as a self-soothing strategy. Therefore, the results found could be more reflective of adolescent dietary preferences and cravings rather than nutritional factors alone. Also, it has been observed that a healthy diet is related to better family functioning [39] and given that families of children and adolescents with ADHD are more likely to face parenting challenges, it is possible that the relationship between a “unhealthy” dietary pattern and ADHD diagnosis is mediated by poor family functioning [24].

Despite the fact that conclusions of these studies are challenging, we cannot justify that a poor dietary choice is the responsible for ADHD. The idea that dietary factors are the exclusive and sufficient explanation for childhood behavioral problems may place a barrier in the way of access to appropriate evidence-based assessment and treatment – so placing the child at unnecessary risk [40]. Further studies are necessary to understand the role that the dietary pattern has in this disorder and to know which dietary approaches can benefit the ADHD symptomatology.

1.2. Restrictive dietary treatments for ADHD

There are mainly two dietary treatments for ADHD, which have been tested in repeated, randomized controlled trials: the artificial food colors elimination (AFCE) and the restricted elimination diets (RED).

1.2.1. Artificial food colorants elimination (AFCE)

The research within artificial food colorants and other additives began in the 1970s. Dr. Benjamin Feingold proposed a new diet called the "Kaiser Permanente diet" also known as the "K-P diet" or the Feingold diet. It was hypothesized that the hyperactivity and learning problems observed in certain schoolchildren were due to the ingestion of certain foods and food additives [41].

The K-P diet removed all foods containing artificial food colors and flavorings and certain preservatives and also food which naturally contain salicylates (Table 3). It was very popular during the 70s and 80s, although it received repeated criticism because solid scientific studies demonstrating its efficacy were very scarce [41] and subsequently support from professionals waned. The "K-P diet" is not longer used, but some of the recommendations, including the elimination of artificial colors, are still being applied. Indeed, two recent meta-analyses carried out concluded that artificial food colorants have small, but statistically significant adverse effect on ADHD symptoms in some children [38,42], even though the conclusions were based on studies of limited quality, as the authors themselves pointed out.

Table 3. Dietary guidelines of the "Kaiser Permanente diet".

- To avoid all food, medications, and cosmetic which may contain artificial colors and flavors.
- To avoid all food that may contain preservatives such BHA, BHT, TBHQ and sodium benzoate[a]
- To avoid foods that naturally contain salicylates: almonds, apples, peaches, apricots, nectarines, cherries, grapes, raisins, oranges, plums, tomatoes, cucumber, coffee and tea.

[a] Those preservatives were later added to the list. Abbreviations: BHA, buttylated hydroxyanisole; BHT, butylated hydroxytoluene; TBHQ, tertiary butylhydroquinone.

In the same direction, Stevenson *et al.* [43] concluded that the artificial food color elimination is a potentially valuable treatment for ADHD but its effect size remains uncertain, as does the type of child for whom it is likely to be efficacious. The authors added the urgent need for studies using more redefined methodologies with blind evaluation to unselected samples of children with ADHD and also the concern that some studies of food colorings and additives were undertaken some time ago, so the findings could be no clear as diet and food products have changed markedly.

The possible mechanisms by which the food colorants and other additives may trigger symptoms are not well understood [44]. Therefore, the controversy about the hypothesis that certain food colorants and additives mainly may cause hyperactivity and inattention in children both ADHD diagnosed or without this disorder is still open. Some authors strongly affirm that these additives do not cause ADHD [2,45], relaying in the fact that the symptomatology of ADHD is different from those induced by artificial coloring [21,44]. The last ones have been associated with more irritability and insomnia than restlessness and inattention.

In 2007, a study funded by the Food Safety Agency (FSA) from UK and conducted by McCann *et al.* [21] had a high impact on the public opinion. The authors provided statistically evidence on the relationship between the consumption of certain mixtures of artificial food colorings (tartrazine, quinoline yellow, sunset yellow, azorubine, cochineal red and allura red) and an artificial preservative (sodium benzoate) and the increase of the hyperactivity in children of 3 years and also in children from 8 to 9 years. In view of these results, the FSA recommended to parents with hyperactive children to consider limiting the intake of these colorants and preservatives. The study, however, has certain methodology weaknesses, as the authors themselves recognized in their publication. The changes observed in the hyperactivity children were very small relative to the inter-individual variation, while the changes in behavior were not evident in all the studied children. Furthermore, it was not possible to extrapolate the study findings to each single additive, which was in the mixture assayed. Moreover, information about the possible biological mechanisms was not provided.

While neither the EFSA (European Food Safety Agency) nor the European Commission have issued any cautious recommendation, nowadays, in the European Union, is required on the food packaging the following warning *"This product may have adverse effect on activity and attention in children"* when sunset yellow (E110), quinoline yellow (E104), azorubine/carmoisine (E122), allura red AC (E129), tartrazine (E102) and cochineal natural red (E124) are employed in foods and beverages.

There is a consensus in the scientific community about the need for more studies on the association between artificial colorings and hyperactivity and ADHD. It is required some caution before advising a complete restriction of foods containing these colorings. The imposition of a diet completely free of artificial colorings should not be done until a reliable methodology is developed to identify which colorant or colorants may be responsible, and who is really sensitive to these compounds, given the inter-individual variation observed.

1.2.2. Restricted elimination diets (RED) or few foods diets

A restricted elimination diet (also called oligoantigenic) removes most foods that may have antigenic or allergenic potential, such as milk and dairy products, eggs, nuts and some fruits, among others. It is thought that ADHD may be, in some children, a hypersensitivity reaction to certain foods [41,45,46]. Therefore, according to this allergic hypothesis, there would be foods that induce high levels of IgG, leading to a relapse in ADHD child behavior, while the intake of those that does not induce IgG or very low levels of them, would not cause a recurrence in ADHD symptoms [32,47]. While interesting the hypothesis, it has not yet been fully demonstrated. Pelsser *et al.* [45] carried out a study about restricted elimination diets with uncertain results. They did conclude that the children who responded to the dietary intervention, independently of whether IgG levels were high or low, showed a decrease of 20.8 points on the ADHD rating scale (ADHD Rating Scale) and 11.6 points on the Conners Scale (Conner's Score). However, the determination of IgG levels was not useful, since the levels of IgG and symptoms of ADHD were totally independent.

More recently a meta-analysis on ADHD, restriction diet and food color additives has been published [42], concluding that a restriction diet benefits some children with ADHD since it reduces ADHD symptoms; however, the authors themselves strongly recommended a renewed investigation of diet and ADHD. From a practical point of view, the restricted elimination diets are very difficult to follow, both for ADHD patients and for the families. Moreover, children and adolescents who are prescribed to follow a different diet than their friends may influence in their behavior, creating unnecessary stress situations [19,20].

To summarize, restricted elimination diets may be beneficial, but large-scale studies are needed, using blind assessment, and including assessment of long-term outcome. On the other hand, artificial food color elimination is a potentially valuable treatment but its effect size remains uncertain, as does the type of child for whom it is likely to be efficacious. Three recommendations have been suggested for the design of future studies: 1) To

have a sample of children with ADHD who have not been selected on the basis of previous responses to food constituents, 2) To include observations of the children´s behavior by a reporter who is truly blind as to dietary treatment, and 3) to control for nonspecific treatment effects [38,43].

2. The role of physical activity on ADHD

It is well established that physical activity (PA) has positive effects on mental health in both clinical and nonclinical populations. In the last decade, several studies have been addressed to study the potential benefits of exercise in children diagnosed with ADHD. The evidence suggests that physical exercise may have benefits in behavioral, neurocognitive, and scholastic performance [27,47,48] and in inhibitory control [47,49]. The etiology of ADHD and the putative mechanisms by which PA impacts cognitive performance suggest that PA might be particularly beneficial for ADHD individuals [27].

Pontifex *et al.* [48] concluded that moderately intense aerobic exercise might have positive implications for aspects of neurocognitive function and inhibitory control in children with ADHD, improving their school performance (Fig. 1). The children could better focus and were less distracted after a quick workout. Moreover, it seems that this type of exercise produces enhancements in reading and in mathematics [49]. This is interesting because children with ADHD have usually more learning problems in these two areas. On the other hand, moderate exercise sessions in ADHD's children have led to improvements in behavior and attention, but no relationship with academic performance has been found [50].

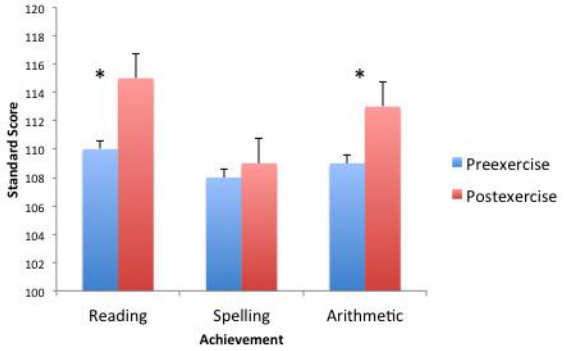

Figure 1. Mean (+SE) standard score for each session on each of the three academic performance tests done. Bars with * are statistically different (adapted from [48]).

Other authors have investigated if the beneficial effects of short moderate PA are also helpful when exercise is carried out for longer periods of time. Thus, Verret *et al.* [50] demonstrated that, in addition to producing improvements in strength and motor skills, exercise showed a positive influence on the behavior and attention of ADHD's children. Also, the work done by Smith *et al.* [47] suggested that after 26 min of continuous moderate-to-vigorous physical activity daily over eight school weeks offered benefits to motor, cognitive, social, and behavioral functioning in young people exhibiting ADHD symptoms. Both authors [47,48] pointed out that the benefits of PA would act on the inhibitory control and the executive function. ADHD appears to have a strong impact on executive function, where processes related to learning and behavior are altered. Although it is not clear which elements are regulated by the executive function, it is believed to be related to cognitive processes such as memory, emotional control, activation, arousal, effort, organization and planning tasks [51].

On the other hand, the majority of exercise and cognition research has primarily focused on aerobic exercise but it is also important to consider forms of coordinative exercise, which includes exercises involving motor coordination and cognitive training. Yu-Kai Chang *et al.* [52] demonstrated that an aquatic exercise intervention, which involves both aerobic and coordinative exercises, influences positively on the restraint inhibition component of behavioral inhibition in children with ADHD.

Research aimed to investigate the influence of PA in children with ADHD under drug therapy, such as methylphenidate, has also been carried out [53], demonstrating that the PA had a positive impact in ADHD symptomatology when medication was present, too. It was found that besides improving strength and motor skills, PA positively influences behavior and cognitive function such as attention in children under medication. Although there is limited research about how drugs affect the motor skills and physical lifestyle of children with ADHD, most of the studies agree that motor skills are improved as a result of PA [50]. In order to add support to those outcomes, future research should include greater executive functions assessment. Moreover, follow-up and additive effects of others therapies should be explored.

Children with ADHD might have lower participation in sport activities, because of their mood liability, disciplinary problems, poor self-esteem, anxiety and inattention. However, research evidence has showed that ADHD children who participated in three or more sports present fewer anxiety or depression symptoms than did those who participated in fewer than three sports. Another aspect worth to comment is the positive influence that PA has showed also in aerobic function, flexibility and cardiovascular fitness,

since children with ADHD have lower levels of them compared with typically developed children. Thus, when compared only between ADHD children the ADHD training group demonstrated more favorable levels of aerobic function and flexibility than the ADHD no training group after the PA intervention [54].

All these findings related to PA and improvement in ADHD symptomatology would support the hypothesis that the pathophysiology of ADHD is related with inadequate levels of certain neurotransmitters [55] such as serotonin, dopamine, and noradrenaline. PA increased the levels of these three neurotransmitters in the prefrontal cortex, which seems to be crucial for the attention and inhibitory control [51]. Individuals with ADHD might have neurochemical and neuroanatomical anomalies in this brain region, which could lead to neurotransmitter deficits and originating some of the cognitive problems related to the ADHD.

As a summary, the research done up to now seems to support the fact that physical exercise could establish itself as an adjunct treatment for people with ADHD [28,47,48,50]. It is recommended that clinicians, parents and teachers work together monitoring the participation of these children in physical and sports activities to help them improve their motor skills performance (Fig. 2).

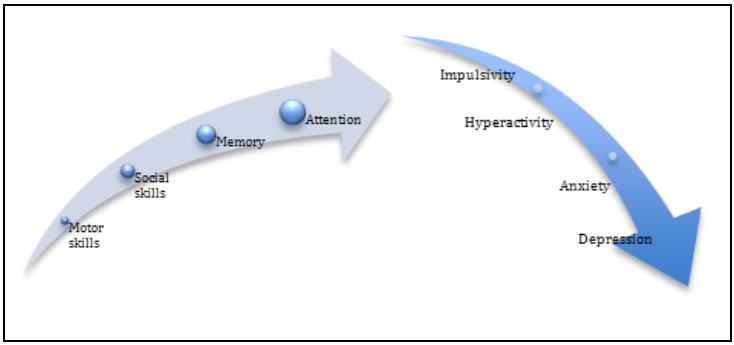

Figure 2. Effects of exercise on ADHD children behavior.

3. Conclusions

The cause of ADHD is multifactorial, with a certain influence of the environmental factors, such as diet and physical activity. The multimodal treatment is recommended by principal clinical practice guidelines for ADHD and includes psychological, psycoeducational and pharmacologic

treatment. Nevertheless, the review of the published scientific evidence indicated that several dietary strategies and physical activity might also help to improve the quality of life of children and adolescents with ADHD. The main recommendation is to educate families and children: 1) to have healthy eating habits with a balanced diet, avoiding excessive consumption of saturated fats and simple sugars, foods with artificial colorants, a good consumption of fish, nuts and seeds, all of them rich in omega 3 and 2) to introduce into the routine of children and adolescents daily physical activity, adapted to their preferences and needs.

Acknowledgements

This work was supported by the *Instituto de Salud Carlos III* from the *Ministerio de Economía y Competitividad* from Spain (PI11/2009). Alejandra Rios was supported by a scholarship from the *Consejo Nacional de Ciencia y Tecnología*, *CONACYT* from Mexico.

References

1. Cortese, S., Angriman, M., Lecendreux, M. 2012. *Expert Rev. Neurother.*, 12, 1227.
2. Biederman, J., Faraone, S.V. 2005. *Lancet*, 366, 237.
3. Konofal, E., Lecendreux, M., Deron, J., Marchand, M., Cortese, S., Zaïm, M., Mouren, M. C., Arnulf, I. 2008. *Pediatr. Neurol.*, 38, 20.
4. Bilici, M., Yildirim, F., Kandil, S., Bekaroğlu, M., Yildirmiş, S, Değer, O., Ulgen, M., Yildiran, A., Aksu, H. 2004. *Prog. Neuropsychopharmacol. Biol. Psychiatry*, 28, 181.
5. Akhondzadeh, S., Mohammadi, M., Khademi, M. 2004. *BMC Psych.*, 6, 1.
6. Bloch, M. H., Qawasmi, A. 2011. *J. Am. Acad. Child Adolesc. Psychiatry*, 50, 991.
7. Gillies, D., Taylor, F., Gray, C., O'Brien, L., D'Abrew, N. 2012. *Cochrane Database Syst. Rev.*, 12, CD006726.
8. Colter, A. L., Cutler, C., Meckling, K. A. 2008. *Nutr. J.*, 7, 8.
9. Transler, C., Eilander, A., Mitchell, S., van de Meer, N. 2010. *J. Atten. Disord.*, 14, 232.
10. Widenhorn-Müller, K., Schwanda, S., Scholz, E., Spitzer, M., Bode, H. 2014. *Prostaglandins Leukot. Essent. Fat. Acids*, 91, 49.
11. Konofal, E., Lecendreux, M., Arnulf, I., Mouren, M.-C. 2004. *Arch. Pediatr. Adolesc. Med.*, 158, 1113.
12. Oner, O., Oner, P., Bozkurt, O. H., Odabas, E., Keser, N., Karadag, H., Kizilgün, M. 2010. *Child Psychiatry Hum. Dev.*, 41, 441.
13. Donfrancesco, R., Parisi, P., Vanacore, N., Martines, F., Sargentini, V., Cortese, S. 2013. *J. Atten. Disord.*, 17, 347.

14. Arnold, L. E., Disilvestro, R. A., Bozzolo, D., Bozzolo, H., Crowl, L., Fernandez, S., Ramadan, Y., Thompson, S., Mo, X., Abedl-Rasoul, M., Joseph, E. 2011. *J. Child Adolesc. Psychopharmacol.*, 21, 1.
15. Kozielec, T., Starobrat-Hermelin, B. 1997. *Magnes. Res.*, 10, 143.
16. Mousain-Bosc, M., Roche, M., Rapin, J., Bali, J.-P. 2004. *J. Am. Coll. Nutr.*, 23, 545S.
17. Huss, M., Völp, A., Stauss-Grabo, M. 2010. *Lipids Health Dis.*, 9, 105 .
18. Schab, D. W., Trinh, N.-H. T. 2004. *J. Dev. Behav. Pediatr.*, 25, 423.
19. Stevens, L. J., Burgess, J. R., Stochelski, M. A., Kuczek, T. 2014. *Clin. Pediatr.*, 53, 133.
20. Kanarek, R. B. 2011. *Nutr. Rev.*, 69, 385.
21. McCann, D., Barret, A., Cooper, A., Crumpler, D., Dalen, L., Grimshaw, K., Kitchin, E., Lok, K., Porteous, L., Prince, E., Sonuga-Barke, E., Warner, J. O., Stevenson, J. 2007. *Lancet*, 370, 1560.
22. Blunden, S. L., Milte, C. M., Sinn, N. 2011. *J. Child Health Care*, 15, 14.
23. Azadbakht, L., Esmaillzadeh, A. 2012. *Nutrition*, 28, 242.
24. Howard, A. L., Robinson, M., Smith, G. J., Ambrosini, G. L., Piek, J. P., Oddy, W. H. 2011. *J. Atten. Disord.*, 15, 403.
25. Woo, H. D., Kim, D. W., Hong, Y.-S., Kim, Y.-M., Seo, J.-H., Choe, B. M., Park, J. H., Kang, J.-W., Yoo, J.-H., Chueh, H. W., Lee, J. H., Kwak, M. J., Kim, J. 2014. *Nutrients*, 6, 1539.
26. Grassmann, V., Alves, M. V., Santos-Galduróz, R. F., Galduróz, J. C. F. *J. Atten. Disord.*, 2014, 1087054714526041.
27. Gapin, J. I., Labban, J. D., Etnier, J. L. 2011. *Prev. Med. (Baltim).*, 52, S70.
28. Wigal, S. B., Emmerson, N., Gehricke, J.-G., Galassetti, P. 2013. *J. Atten. Disord.*, 17, 279.
29. Berwid, O. G., Halperin, J. M. 2012. *Curr. Psychiatry Rep.*, 14, 543.
30. Arnsten, A. F. T. 2009. *CNS Drugs*, 23, 33.
31. Faraone, S. V, Biederman, J. 1998. *Biol. Psychiatry*, 44, 951.
32. National Institute of Mental Health. Attention Deficit Hyperactivity Disorder (ADHD) Publication. at <http://www.nimh.nih.gov/health/publications/attention-deficit-hyperactivity-disorder/adhd_booklet_cl508.pdf>
33. Heilskov Rytter, M. J., Borup Andersen, L. B., Houmann, T., Bilenberg, N., Hvolby, A., Mølgaard, C. 2014. *Nord. J. Psychiatry*, 69, 1.
34. Van Egmond-Fröhlich, A. W. A, Weghuber, D., de Zwaan, M. 2012. *PLoS One*, 7, e4978.
35. Park, S., Cho, S.-C., Hong, Y.-C., Oh, S-Y., Kim, J.-W., Shin, M.-S., Kim, B.-N., Yoo, H.-J., Cho, Y.-H., Bhang, S.-Y. 2012. *Psychiatry Res.*, 198, 468.
36. Liu, J., He, P., Li, L., Shen, T., Wu, M., Hu, J., Zhuang, Y., Yin, J., He, G. *2014. Wei Sheng Yan Jiu*, 43, 235.
37. Ghanizadeh, A., Haddad, B. 2015. *Ann. Gen. Psychiatry*, 14, 1.
38. Sonuga-Barke, E. J., Brandeis, D., Cortese, S., Daley, D., Ferrin, M., Holtmann, M., Stevenson, J., Danckaerts, M., van der Oord, S., Döpfner, M., Dittmann, R. W., Simonoff, E., Zuddas, A., Banaschewski, T., Buitelaar, J., Coghill, D., Hollis,

C., Konofal, E., Lecendreux, M., Wong, I. C., Sergeant, J. European ADHD Guidelines Group. 2013. *Am. J. Psychiatry*, 170, 275.
39. Ambrosini, G. L., Oddy, W. H., Robinson, M., O´Sullivan, T. A., Hands, B. P., de Klerk, N. H., Silburn, S. R., Zubrick, S. R., Kendall, G. E., Stanley, F. J., Beilin, L. J. 2009. *Public Health Nutr.*, 12, 1807.
40. Sonuga-Barke, E. J. S. 2015. *J. Child Psychol. Psychiatry*, 56, 497.
41. Stevens, L. J., Kuczek, T., Burgess, J. R., Hurt, E., Arnold, L. E. 2011. *Clin. Pediatr.*, 50, 279.
42. Nigg, J. T., Lewis, K., Edinger, T., Falk, M. 2012. *J. Am. Acad. Child Adolesc. Psychiatry*, 51, 86.
43. Stevenson, J., Buitelaar, J., Cortese, S., Ferrin, M., Konofal, E., Lecendreux, M., Simonoff, E., Wong, I. C., Sonuga-Barke, E. 2014. *J. Child Psychol. Psychiatry.*, 55, 416.
44. Rowe, K.S., Rowe, K. J. 1994. *J. Pediatr.*, 125, 691.
45. Pelsser, L. M., Frankena, K., Toorman, J., Savelkoul, H. F., Dubois, A. E., Pereira, R. R., Haagen, T. A., Rommelse, N. N., Buitelaar, J. K. 2011. *Lancet*, 377, 494.
46. Millichap, J. G., Yee, M. M. 2012. *Pediatrics*, 129, 330.
47. Smith, A. L., Hoza, B., Linnea, K., McQuade, J. D., Tomb, M., Vaughn, A. J., Shoulberg, E. K., Hook, H. 2013. *J. Atten. Disord.*, 17, 70.
48. Pontifex, M. B., Saliba, B. J., Raine, L. B., Picchietti, D. L., Hillman, C. H. 2013. *J. Pediatr.*, 162, 543.
49. Hillman, C. H., Pontifex, M. B., Castelli, D. M., Khan, N. A., Raine, L. B., Scudder, M. R., Drollette, E. S., Moore, R. D., Wu, C. T., Kamijo, K. 2014. *Pediatrics*, 134, e1063.
50. Verret, C., Guay, M.-C., Berthiaume, C., Gardiner, P. & Béliveau, L 2012. *J. Atten. Disord.*, 16, 71.
51. Carriedo, A. 2014. *J. Sport Heal. Res.*, 6, 47.
52. Chang, Y.-K., Liu, S., Yu, H.-H., Lee, Y.-H. 2012. *Arch. Clin. Neuropsychol.*, 27, 225.
53. Verret, C., Gardiner, P., Béliveau, L. 2010. *Adapt. Phys. Activ. Q.*, 27, 337.
54. Pan, C.-Y., Chang, Y.-K., Tsai, C.-L., Chu, C.-H., Cheng, Y.-W., Sung, M.-C. 2014. *J. Atten. Disord.*,1087054714533192.
55. Volkow, N. D., Wang, G.-J., Newcorn, J. H., Kollins, S. H., Wigal, T. L., Telang, F., Fowler, J. S., Goldstein, R. Z., Klein, N., Logan, J., Wong, C., Swanson, J. M. 2011. *Mol. Psychiatry* 16, 1147.

Research Signpost
37/661 (2), Fort P.O.
Trivandrum-695 023
Kerala, India

Recent Advances in Pharmaceutical Sciences V, 2015: 65-83 ISBN: 978-81-308-0561-0
Editors: Diego Muñoz-Torrero, M. Pilar Vinardell and Javier Palazón

5. Zebrafish as a model for developmental toxicity assessment

Elisabet Teixidó, Ester Piqué, Núria Boix, Joan M Llobet and Jesús Gómez-Catalán
Toxicology Unit, GRET-CERETOX, Faculty of Pharmacy, University of Barcelona 08028 Barcelona, Spain

Abstract. The zebrafish embryo has emerged as promising alternative model for traditional in vivo developmental toxicological screening due to their advantageous characteristics as their small size and transparency. In this paper, we reviewed the applicability of the zebrafish embryo model in some relevant areas to human toxicology as developmental toxicity, cardiovascular toxicity and neurotoxicity (behavioral assessment). Despite the promising results, further optimization and testing of more substances as well as a harmonized methodology is needed to streamline the methods and make the assay conducive to medium-throughput.

Introduction

The potential toxicity of a chemical has traditionally been carried out through in vivo mammalian screening approaches. Traditional guideline methods are laborious, costly, require large number of animals and attract increasingly ethical concerns [1]. Moreover, animal testing will increase

Correspondence/Reprint request: Dr. Elisabet Teixidó, Toxicology Unit, Faculty of Pharmacy, University of Barcelona, Av. Joan XXIII s/n, 08028 Barcelona, Spain E-mail: elisabet.teixido@gmail.com

dramatically over next decade as a consequence of implementation of EU initiative for the Registration, Evaluation and Authorization of Chemicals, REACH [2]. Reproductive and developmental toxicity studies will use by far the most animals and resources within REACH (61% of animals and 54% of resources). Thus, the use of alternative methods in hazard assessment is encouraged and animal experiments should only be used as a last resort [3]. In addition to the REACH initiatives, it has been estimated that out of 10,000 new drug entities that a pharmaceutical may start with, only one or two are finally approved by the European Medicines Agency (EMA) at an estimated cost of €1,172 million [4]. A large proportion of this cost is due to animal testing. The use of alternative methods at multiple stages in the drug discovery process would potentially reduce the attrition rate and costs by reducing the use of mammals and unnecessary clinical trials. The use of screening assays before clinical phases to select the best candidates is also one strategy to identify potential new active pharmaceuticals ingredients.

Fish have been used for years to assess the ecotoxicity of xenobiotics, but during the last years assays using embryonic stages of the zebrafish (*Danio rerio*) have attracted the attention of toxicologists due to their several advantages. In particular, in compliance with international animal welfare regulations, the fish embryo provides an ethically acceptable small-scale analysis system with complexity of a complete organism [5-7]

Most advanced and promising in the field of human hazard prediction is the use of the zebrafish embryo test (ZFET) to screen for developmental disorders as an indicator of teratogenic effects. Modifications of the ZFET protocol allow the use of this model also for the detection of specific organ toxicity such as cardiotoxicity, neurotoxicity, hepatotoxicity or nephrotoxicity [8].

In the following sections, the applications of the zebrafish embryo test in toxicology are reviewed as a screening level tool and as a system to predict mammalian developmental toxicity. Considering the current research activity on this topic, and based in our own research experience, we have selected some examples of the use of the zebrafish embryo model in toxicology. Additionally, we have included some of our last results in the field.

1. The zebrafish embryo as a model organism

Zebrafish is a tropical freshwater teleost fish native to the rivers of India and South Asia [9]. Adult fishes are simple and inexpensive to raise and maintain. One pair of adults routinely lays hundreds of fertilized eggs in a single cross. Large-scale breeding chambers allow the efficient and reliable generation of thousands of embryos each day (Fig. 1).

Figure 1. Custom made breeding chamber. A grid is located in the bottom in order to avoid predation of the eggs by the parent fishes. Plastic plants and marbles can be placed in the tank in order to stimulate the spawning. The shape of the tank, as a funnel on the bottom, allows simple release of the newly spawned eggs.

The development of zebrafish is very similar to the embryogenesis in higher vertebrates, but, unlike mammals, the zebrafish egg develops outside the mother. Moreover, the embryos themselves are transparent during the first few days of their lives allowing an easy visualization of internal organ-tissues that facilitates developmental and organ toxicity studies. Also its development is very fast and has been well characterized, including morphological, biochemical and physiological information at all stages of early development [10].

During the first 24 hours after fertilization, all major organs are formed and within 3 days the fish hatches. After 3-4 months zebrafish are sexually mature and can generate new offspring.

Besides this, the small size of the embryo allows the ability of culture large number of zebrafish embryos in small volumes of media facilitating

rapid toxicity testing of compounds, while using a minimal amount of compound [11]. All the above mentioned properties of the zebrafish model represent a reduction on the experimental time and cost.

Zebrafish has been used predominantly in fundamental research (developmental biology and molecular genetics), so a lot of resources are available (genetic tools, mutant lines…) which the community can get the most benefit. In addition, zebrafish shares a high degree of homology with the human genome (about a 70%) [12], as well as structural similarities (about 86% of orthologs of human drug targets) [13]. All these unique advantages make using zebrafish an attractive alternative that also represents an advance towards the aim of reducing and refining animal use in research [14].

2. Zebrafish embryo assays in toxicology

Teratogenesis

The assessment of potential developmental toxicity is an integral part of European (and international) regulation for the risk assessment of pharmaceuticals, industrial chemicals, food additives, biocides and plant protection products. The assessment is performed based on OECD guidelines to allow international harmonization. Particularly, in teratogenesis tests, pregnant laboratories animals of two species, typically rats and rabbits, are exposed to the investigated chemical during the period of major organogenesis and offspring is monitored for endpoints such as death, growth changes, and morphological abnormalities. The use of mammalian models is laborious, time-consuming and results in the suffering of animals.

Ever since the thalidomide tragedy, there has been a presumed need to routinely use two species for developmental toxicity testing. Next to ethical concerns, animal experiments have been also criticized because of the partially weak reliability for the prediction of human teratogenicity [15]. Further problems have arisen due to the new EU cosmetics directive, which excludes any animal testing for cosmetic ingredients. Therefore, there is an increasing demand to develop alternative *in vitro* methods.

Up to date a few alternative approaches have been proposed for teratogenicity testing of chemicals and drugs. These approaches require either cultured cell lines [16], dissociated cells of embryonic buds or the midbrain of rat embryos [17], or the culture of whole embryo rodents [18] and lower vertebrates (e.g. Xenopus and zebrafish)[19].

Results from numerous small-scale pilot studies with zebrafish embryos have been shown to correctly classify mammalian teratogens and non-teratogens with an overall concordance of 72-92% (Table 1). These assays are focused on three manifestations of deviant development: death, malformation and growth retardation [20]. However, they applied different experimental protocols and the number and the variety of assayed substances were limited. Currently there is no consensus about the optimal procedure in some basic features as the specific endpoints and scoring systems to use, the time of exposure and the stage of embryonic/larval development to do the observations. There is an increasing common interest to harmonize zebrafish developmental toxicity assays in order to ensure high concordance with mammalian data and increase cross-laboratory reliability [21].

Table 1. List of the published zebrafish teratogenicity assays with its overall concordance with mammalian data. Exposure was done during different windows of development and the teratogenic potential of chemicals was based on different criteria.

Reference	Chemicals tested	Exposure window (hpf)	Mammalian concordance (%)	Teratogenic potential
Nagel, [22]	41	1 to 48	88	LC_{50}/EC_{50}
Chapin et al., [23] [a]	12	24 to 96	83	LD_{50}/LOAEL
Eimon and Rubinstein, [11] [b]	18	1 to 24/48	72	n/d
Eimon and Rubinstein, [11] [c]	24	4-6 to 120	92	NOAEL/LC_{25}
Brannen et al., [24]	31	4-6 to 120	87	NOAEL/LC_{25}
Selderslaghs et al., [25]	27	2 to 144	81	LC_{50}/EC_{50}
Hermsen et al., [26]	14	1 to 72	n/d	BMC_{GMS}
Van den Bulck et al., [27]	15	4 to 96	75	Teratogenic endpoint and body burden
Gustafson et al., [21] [d]	40	4-6 to 120	85	NOAEL/LC_{25}

Note: a, collaborative pilot study of Phylonix, Inc. with Bristol-Myers Squibb. b, developed by DanioLabs Ltd and evaluated in a pilot study run by Pfizer, Inc. and ECVAM. c, results from Bristol-Myers Squibb group. d, compounds tested in the ring test-2. n/d, not defined. Hours post-fertilization (hpf).

In this regard, our group focused on achieving a better characterization of growth retardation in the zebrafish embryo test [28]. In this study the suitability of a biochemical endpoint, the measurement of acetylcholinesterase activity (AChE), as a marker of developmental delay in zebrafish embryos was explored. The expression of AChE starts early and increases with age along the embryo development. It is an easy, robust and sensitive endpoint that could be liable to automation and higher throughput than morphological endpoints like the measurement of head-trunk angle. Evidently, any substance with some specific action on AChE expression or activity, as AChE inhibitors, could produce results unrelated to developmental age. These substances can be easily discarded by means of an *in vitro* AChE activity assay.

The measurement of AChE activity allowed us to detect substances with a clear effect on developmental delay (valproic acid, methoxyacetic acid and boric acid) at non-teratogenic concentrations, thus increasing the sensitivity of the assay. As figure 2 shows, these substances presented a strong correlation between AChE activity and head-trunk angle with a slope similar to that obtained in normally developmental embryos at different developmental stages. However, our results do not allow concluding about

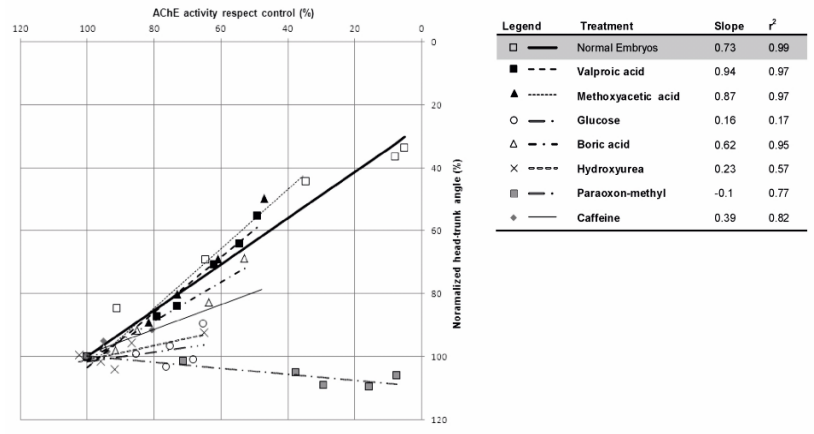

Figure 2. Correlation analysis between AChE activity values versus normalized head-trunk angle values [(180°- head-trunk angle)*100/(180°- control head-trunk angle)] in each compound that produced a significant change in AChE activity. Slope and coefficient of correlation of each simple linear regression. The correlation analysis of the values of normally developed embryos was obtained from the evaluation of the age-dependent AChE activity and head-trunk angle.

the discriminating efficiency of developmental retardation endpoints in the zebrafish assay to predict teratogenic potential in mammals. Probably, for a major part of substance, developmental delay is an unspecific effect unrelated or secondary to teratogenic activity.

Cardiovascular toxicity

Cardiotoxicity is a highly relevant area of toxicity assessment as drug candidates were frequently found to have cardiac adverse effects being a leading cause of drug withdraws [29]. Current available *in vivo* assays such as the Langendott-perfused rabbit heart model are laborious, costly and time-consuming [30]. Moreover, *in vitro* cardiotoxicity screenings such as the patch clam assay focusing on assessing the effects of compounds on potassium, sodium and calcium ion channels are limited by biological simplicity and an inability to detect drug–drug interactions [31]. Due to the limitations of both traditional mammalian models and *in vitro* approaches, researchers are showing increasing interest in zebrafish-based assays to assess cardiovascular safety and toxicity.

The cardiovascular system is the first major system to function within the embryo. Unlike the double circulation in mammals, the fish heart is two-chambered, consisting of an atrium and a ventricle separated by an atrioventricular valve. Zebrafish and mammalian heart exhibit a closed cardiovascular system, but organs and tissues of zebrafish embryos do not depend on the cardiac output for oxygen delivery. Embryos rely on oxygen diffusion through the skin from the swimming medium up to 14 days post-fertilization (dpf) [32]. Therefore, this feature permits embryos with severe cardiovascular defects to survive during the initial phase of embryonic development. By contrast, avian and mammalian embryos would die rapidly in the absence of a functional cardiovascular system.

Effects on cardiovascular system can be visually assessed in living zebrafish using a stereomicroscope and a microscope. Different cardiac and vascular abnormalities from developmental exposure to zebrafish have been reported (Table 2) being edema and heart rate change the most commonly assessed [33].

Several methods have been employed successfully in the larval fish to study heart function, for example, electrocardiogram [34], laser Doppler microscope technique [35] and laser confocal scanning microscopy [36]. However, these tools are labor-intensive, require special instrumentation and are not scalable for high-throughput screening. Therefore, we propose the use of a non-invasive method using simple light microscopy and a fast digital camera. Recent development in digital image analysis tools makes

Table 2. Cardiac and vascular abnormalities reported from developmental exposure to zebrafish (Reviewed by [33]).

Cardiac and vascular abnormalities
Heart function
Tachycardia (increased heart rate)
Bradycardia (slow heart rate)
Arrhythmia
Pericardial edema
Defective heart morphology
Altered heart size
Apoptosis in heart region/pericardial epithelium
Circulatory system
Aberrant vascular patterning in trunk/common cardinal vein
Abnormal/disorganized cranial vessels
Smaller blood vessels
Altered blood flow
Blood accumulation in yolk extension
Hemorrhage
Trunk edema
Hematopoietic system
Altered number of circulating erythrocytes
Abnormal erythrocytes

analysis of cardiovascular function, such as cardiac output, traveling speed of the blood cells, blood cell count, visualization and analysis of blood cells distribution in transparent zebrafish larvae easier [37].

The zebrafish is also used as a preclinical model in order to study drug-induced cardiac arrhythmias such as QT prolongation [38]. Drug-induced prolongation of the QT interval in the electrocardiogram usually results from concentration dependent inhibition of the hERG (the human Ether-à-go-go-Related Gene) potassium channel. Moreover, drugs blocking this potassium current either as an intended pharmacologic effect (eg. antiarrhythmics dofetilide and almokalant) or as an unwanted side-effect (eg. antihistamine drugs, antidepressive drugs and macrolide antibiotics) are potential human teratogens [39].

Numerous groups have screened pharmacologically relevant collections of compounds in zebrafish using bradycardia or/and atrioventricular dissociation as indicators of QT prolongation [30, 40, 41]. These assays were able to detect known QT prolonging drugs that block hERG such as terfenadine or cisapride, as well as compounds that block L-type calcium channels, not affecting the hERG channel.

In our case, we established the methodology for screening cardiovascular drugs using two reference compounds, terfenadine and isoprenaline (Fig. 3 and Fig. 4). Embryos exposed to terfenadine (10 µM) displayed a 2:1 atrioventricular block and bradychardia with a reduced cardiac output. In contrast, isoprenaline exposure increased the heart rate and cardiac output without causing an atrioventricular block.

Cardiovascular performance can also be assessed by recording the blood flow through the dorsal aorta. Scan lines obtained parallel to the flow of blood within the dorsal aorta were used to measure the cellular velocity and other cardiac indices. Figure 5 shows as an example the measured changes in blood flow velocity and diameter of the blood vessel in zebrafish embryos exposed to terfenadine and isoprenaline.

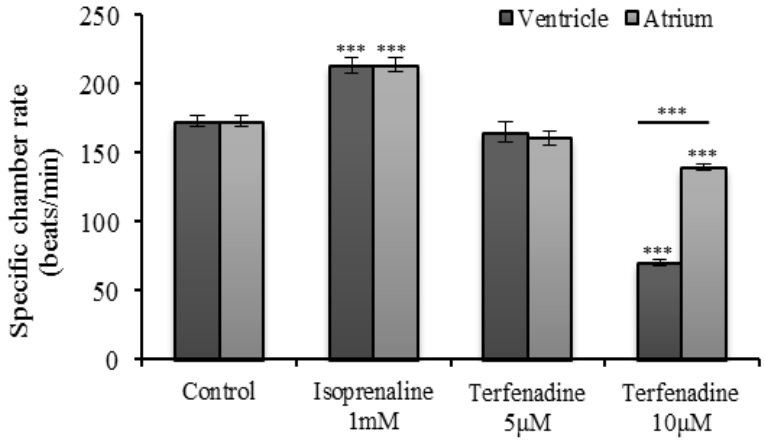

Figure 3. Atrial and ventricular rates of embryos exposed to terfenadine and isoprenaline for 3 h at 72 hpf. Values are mean ± SEM of two independent test (n= 6). Asterisks indicate significant difference at ***p<0.001, t-student test.

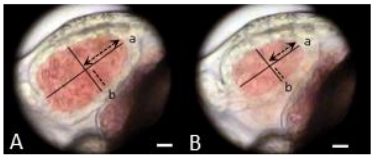

Treatment	Cardiac output (nL/min)
Control	40.2 ± 1.3
Terfenadine 5 µM	38.8 ± 3.6
Terfenadine 10 µM	20.8 ± 1.3***
Isoprenaline 1 mM	64.1 ± 5.3***

Figure 4. Representative end-diastolic (A) and end-systolic (B) images of a heart ventricle of zebrafish larva at 3 dpf. Calculation of ventricle volume during systole and diastole was based on the formula for the volume of a prolate spheroid: $4/3\pi ab^2$ where a represents the major axe radius and b of the minor axe radius of the ventricle image. Cardiac output (nl/min) = Stroke volume (end-diastolic volume – end-systolic volume) x heart rate. (Scale bar= 20µm).Table at the right shows the cardiac output of zebrafish embryos exposed to terfenadine and isoprenaline (n= 6). Asterisks indicate significant difference respect the control group at ***p<0.001, t-student test.

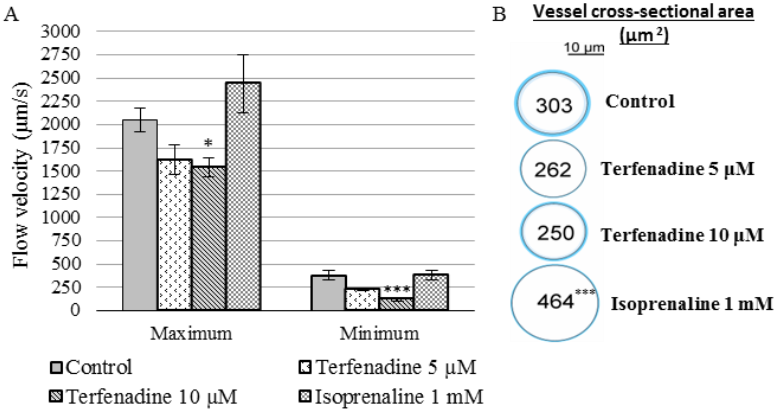

Figure 5. (A) Maximum and minimum blood cell velocity, measured from embryos treated with terfenadine and isoprenaline. Data are presented as mean ± SEM (n=6). (B) Mean vessel cross section represented as a black outline, while the surrounding color shading indicates the standard deviation of the mean. Numerical values indicate the corresponding vessel cross-sectional area (µm2). Asterisks indicate significant difference at *p<0.05 and ***p<0.001, t-student test.

In addition, several transgenic lines with heart tissue and vascular fluorescent reporters have been generated [42, 43] and can be really useful for detecting changes in specific tissues, to visualize cardiomyocytes and vascular endothelium as well as precursor cells.

These tools can contribute to a better understanding of the key cardiotoxic mechanisms in a whole-organism, cost-effective and medium high-throughput manner.

Behavioral assessment of neurotoxic effects

Current in vivo methods for the assessment of developmental neurotoxic compounds [44] are designed to screen for adverse effects of pre and postnatal exposures on the development and function of the nervous system. However, these guidelines are unsuitable for screening large number of chemicals for many reasons including low throughput, high cost, and questions regarding reliability [45]. Therefore, new, reliable, and efficient screening and assessment tools are needed for better identification, prioritization, and evaluation of chemicals with the potential to induce developmental neurotoxicity.

Larval zebrafish nervous system exhibits developmental, structural and pharmacological conservation with the mammalian nervous system [46]. Locomotor patterns that develop early in the larva [47] (see Fig. 6) can be monitored for systematic screening of the genes, pharmaceuticals and environmental toxicants that can influence behavior [48, 49]. Moreover,

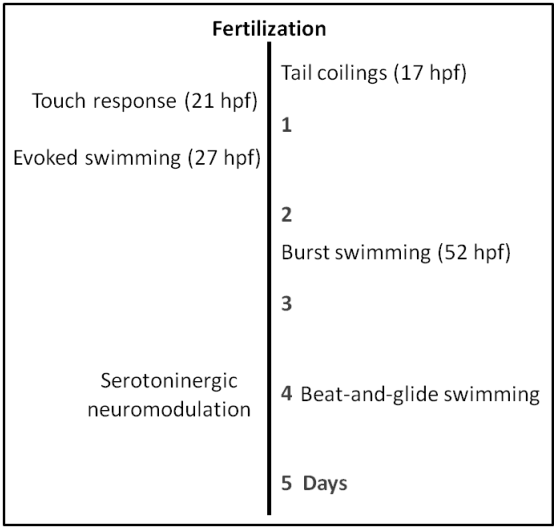

Figure 6. Chronological sequence of appearance of motility patterns during development of the zebrafish.

several studies suggest that zebrafish larvae are sensitive to neuroactive drugs and that their locomotor response is similar to that of mammals [50, 51].

Many assays have been developed in zebrafish larvae by taking advantage of its locomotor repertoire and inherent visual reflexes (Table 3). Among these is the visual motor response test that consists in brief (10-30 min) alternating periods of light and dark and is characterized by low (basal) locomotor activity under light exposure and transient but robust behavioral hyperactivity on sudden transition to dark [52].

Table 3. Different types of behavioral patterns exhibited by zebrafish larvae that can be measured as indicators of toxicant exposure (modified from [53]).

Behavior	Time	Stimulus	Selected chemical (reference)
Coiling	21-25hpf	None	Clorpyrifos [49]
Touch-induced escape response	>26hpf	Touch	Cadmium [55]
Evoked swimming	27hpf until hatching	Touch	Fluoxetine [51]
Photomotor response	30hpf	Light intensity	Neuroactive drugs [56]
Visual motor response	>4dpf	Alternating light-dark periods	Ethanol [50]
Optokinetic response (eye movements)	>73hpf	Moving objects	Ethanol [57]
Optomotor response (Whole-body movements)	>4dpf	Moving objects	Atropin [30]
Startle response	>5dpf	Acoustic	Ethanol [58]
Turning behavior	6-9 dpf	Touch, approaching object, sudden change of light conditions, sound	Clorpyrifos [49]
Prey capture	>5dpf	Prey	Methylmercury [59]

Locomotor activity endpoints included swimming speed, distances swum, time spent in the different sections of the tank, time spent immobile, erratic movements, turning rate, etc. For an accurate, objective, and efficient measurement of these parameters, the use of automated video tracking systems is recommended [53]. In these systems, movement in the vertical plane is usually ignored or minimized by reducing water depth of the vessels [54] and currently, several commercial setups are available on the market (e.g. Viewpoint ZebraLab videotrack system).

Figure 7 shows as example the assessment of locomotor activity of zebrafish after being exposed to increasing concentrations of d-amphetamine. The experimental conditions and data processing implemented in our laboratory permitted to reproduce the effects of d-amphetamine being the results similar to those reported by Irons et al. [50]. Our results demonstrated that d-amphetamine produced an evident biphasic "inverted U" concentration-response pattern with a highly consistent behavioral pattern between light and dark periods. The lowest concentration

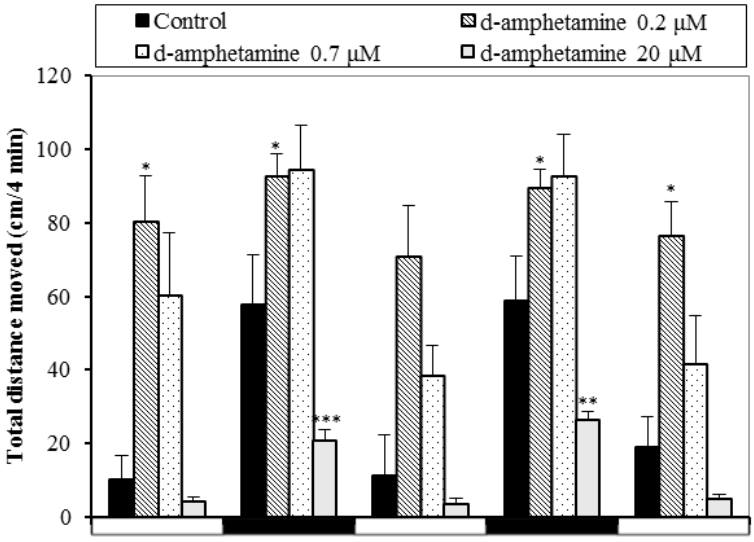

Figure 7. Effects of d-amphetamine on larval locomotion. Values are mean + SEM of the total distance moved in 4 min interval Asterisks indicate significant difference at *p<0.05, **p<0.01 respect control. Black and white bars at the bottom signify dark and light conditions, respectively.

of d-amphetamine produced hyperactivity and the highest concentration tested caused hypoactivity, mainly in dark periods. The effects reflect those found in mammalian models, proving the usefulness of the zebrafish embryo model for neurobehavioral studies. In addition, it is likely that can be used to unveil abnormal nervous system developmental/maturation due to developmental neurotoxicity [50].

There are several conditions which need to be controlled in order to get consistent and reproducible outcomes especially involving locomotor activity (Table 4). For example, MacPhail et al. [60] found that zebrafish larvae are more active in the morning than in the afternoon, so locomotor activity depends on the time of day. It must be noted that, although behavior is the ultimate result of neuronal development and signaling, not all behavioral modifications are of neurological origin. Malformed limbs or other morphological based conditions may be associated with behaviors not apparent in normal individuals. For instance, a reduced visual sensitivity or higher visual threshold could delay the transition in activity when darkness is switched to light [60]. Therefore, if our final objective is to detect neurotoxic effects, embryos with malformations should be not used in the locomotor activity assay [61].

Table 4. Variables that influence larval zebrafish behavior.

Factors that influence zebrafish behavior	Reference
Developmental stage	[61]
Time of day	[60]
Density of rearing zebrafish embryos	[62]
Intensity of light or light conditions	[61]
Lighting conditions during development	[63]
Acclimatization-time before testing	[60]
Containing vessels during test	[61]
Developmental malformations	[61]
Carrier solvents	[64]

Hurdles to the acceptance of zebrafish assays

Despite the promising zebrafish studies described above, there are still significant issues to be addressed before the zebrafish is accepted as a toxicological model.

Absorption, distribution, metabolism and excretion are crucial factors affecting the toxicity of chemicals. Most of the zebrafish assays relay on aqueous exposure and compound uptake predominantly by diffusion through the skin. Compound uptake may be not linear and it is dependent upon a number of physicochemical variables [65]. Internal concentration analysis is therefore needed in order to correlate the toxic phenotype observed with the actual concentration of the compound within the larvae. It is also necessary in order to identify false-negative results attributable to poor compound absorption and to link effect concentrations between mammals and fish embryos [66].

One of the alleged weaknesses of the zebrafish embryo as a model for teratogenicity in mammals is the difference in metabolic activity towards exogenous substances. This is especially relevant in the case of xenobiotics that need bioactivation. Zebrafish embryos and larvae have the ability to perform both phase I (oxidation, n-demethylation, o-demethylation and n-dealkylation) and phase II (sulfation and glucuronidation) metabolism reactions [65]. In particular, zebrafish have a total of 94 CYP genes, distributed among 18 gene families, most of which are direct orthologs of human CYPs. Most of these CYPs are expressed in embryos during various time courses along the first 48 hours after fertilization. Indeed, some maternally-derived CYPs RNA transcripts are present in the unfertilized egg [67]. Some studies have been shown the capacity of zebrafish embryos to metabolize different drugs, some of that known human proteratogenic substances [68-70]. However, differences to mammalian metabolic pathways have been identified. Cisapride, for example, was mainly metabolized to cisapride N-sulfate in zebrafish larvae, which is only a minor metabolite in mammals. Therefore, more extensive studies are required to evaluate the similarities and differences in metabolic pathways between human and zebrafish.

Conclusions

We have shown various examples of the applicability of the zebrafish embryo model in toxicology, focusing on the developmental toxicity evaluation of chemicals. The zebrafish embryo model is still struggling for recognition by regulators and industry as a screening tool in drug development and toxicological testing of chemicals other than water quality assessment. The first steps are promising [13, 71] and demonstrate the reliability of the zebrafish embryo model in human risk assessment. Further systematic testing of toxicologically concerning substances in all applicable areas relevant to humans will definitely provide a significant picture of the

predictive power of the zebrafish embryo assay. However, embryonic development is a very complex biological process so a single *in vitro* test capable of covering this whole process with satisfactory predictivity cannot be expected. An integrated testing approach with different test species should help minimize risk in the animal-human extrapolation [72].

In order to accurately predict and relate chemical impacts across species, it is necessary to have a mechanistic understanding of the effects of pathway perturbation. Recently, the use of the concept of Adverse Outcome pathways (AOPs) provides a framework in which data and knowledge are collected at many levels of biological organization and can be synthesized in a way that is useful to risk assessors and toxicologists that support this activity [73]. All this new developments in hazard assessment will contribute to have a more human-relevant and more predictive alternatives to traditional testing.

Acknowledgments

The work was supported by a Scholarship of the University of Barcelona (APIF).

References

1. Hartung, T., Rovida, C. 2009, *Nature*, 460, 1080.
2. Van der Jagt, K., Munn, S., Torslov, J., de Bruijn, J. 2004, *JRC Publications*, 1.
3. Scialli, A. R., Guikema, A. J. 2012, *Syst. Biol. Reprod. Med.*, 58, 63.
4. Mestre-Ferrandiz, J., Sussex, J., Towse, A. 2012, *Office of Health Economics*, 1.
5. European Union Directive 2010/63/EU. 2010, *Off. J. Eur. Union*., 276, 33.
6. Strähle, U., Scholz, S., Geisler, R., Hollert, H., Rastegar, S., Schumacher, A., Selderslaghs, I., Weiss, C., Witters, H., Braunbeck, T. 2012, *Reprod. Toxicol.*, 33, 128.
7. Embry, M. R., Belanger, S. E., Braunbeck, T. A., Galay-Burgos, M., Halder, M., Hinton, D. E., Léonard, M. A., Lillicrap, A., Norberg-King, T., Whale, G. Graham. 2010, *Aquat. Toxicol.* , 97, 79.
8. Scholz, S. 2013, *Arch. Toxicol.*, 87, 769.
9. Eaton, R., Farley, R. 1974, *Copeia 1974*, 195.
10. Hill, A. J., Teraoka, H., Heideman, W., Peterson, R. E. 2005, *Toxicol. Sci*., 86, 6.
11. Eimon, P. M., Rubinstein, A. L. 2009, *Expert Opin. Drug Metab. Toxicol.*, 5, 393.
12. Howe, K., Clark, M. D., Torroja, C.F., et al. 2013, *Nature*, 496, 498.
13. Gunnarsson, L., Jauhiainen, A., Kristiansson, E., Nerman, O., Larsson, D. G. 2008, *Env. Sci. Technol*., 42, 5807.
14. Yang, L., Ho, N. Y., Alshut, R., Legradi, J., Weiss, C., Reischl, M., Mikut, R., Liebel, U., Müller, F., Strähle, U. 2009, *Reprod. Toxicol*., 28, 245.

15. Bailey, J., Knight, A., Balcombe, J. 2005, *Biogenic Amines*, 19, 97.
16. Seiler, A. E. M., Spielmann, H. 2011, *Nature protocols*, 6, 961.
17. Genschow, E., Spielmann, H., Scholz, G., Seiler, A., Brown, N., Piersma, A., Brady, M., Clemann, N., Huuskonen, H., Paillard, F., Bremer, S., Becker, K. 2002, *Altern. Lab. Anim*., 30, 151.
18. Barenys, M., Flick, B., Boix, N., Almeida, B., Joglar, J., Klug, S., Llobet, J. M. 2012, *Reprod. Toxicol*., 34, 57.
19. Bantle, J. A., Burton, D. T., Dawson, D. A., Dumont, J. N., Finch, R. A., Fort, D. J., Linder, G., et al. 1994, *J. Appl. Toxicol.*, 14, 213.
20. Wilson, J. G. 1977, Handbook of teratology. New York, *NY: Plenum Press*. 1, 47.
21. Gustafson, A. L., Stedman, D. B., Ball, J., Hillegass, J. M., Flood, A., Zhang, C. X., Panzica-Kelly, J., Cao, J., Coburn, A., Enright, B. P., Tornesi, M. B., Hetheridge, M., Augustine-Rauch, K. 2012, *Reprod. Toxicol.*, 33, 155
22. Nagel, R. 2002, *ALTEX Altern zu Tierexperimenten*, 19 Suppl 1, 38.
23. Chapin, R., Augustine-Rauch, K., Beyer, B., Daston, G., Finnell, R., Flynn, T., Hunter, S., Mirkes, P., O'Shea, K. S., Piersma, A., Sandler, D., Vanparys, P., Van Maele-Fabry, G. 2008, Birth Defects Res. B Dev. *Reprod. Toxicol*., 83, 446.
24. Brannen, K. C., Panzica-Kelly, J. M., Danberry, T. L., Augustine-Rauch, K. 2010, Birth Defects Res. B Dev. *Reprod. Toxicol*., 89, 66.
25. Selderslaghs, I. W. T., Blust, R., Witters, H. E. 2012, *Reprod. Toxicol.*, 33, 142.
26. Hermsen, S. B., van den Brandhof, E. J., van der Ven, L. T. M., Piersma, A. H. 2011, *Toxicol. In Vitro*, 25, 745.
27. Van den Bulck, K., Hill, A., Mesens, N., Diekman, H., De Schaepdrijver, L., Lammens, L. 2011, *Reprod. Toxicol*., 32, 213.
28. Teixidó, E., Piqué, E., Gómez-Catalán, J., Llobet, J. M. 2013, *Toxicol. In Vitro*, 27, 469.
29. Peterson, R. T., & Macrae, C. A. 2012, *Annu. Rev. Pharmacol. Toxicol.*, 52, 433.
30. Berghmans, S., Butler, P., Goldsmith, P., Waldron, G., Gardner, I., Golder, Z., Richards, F. M., Kimber, G., Roach, A., Alderton, W., Fleming, A. 2008, *J. Pharmacol. Toxicol. Methods*, 58, 59.
31. Zhu, J.-J., Xu, Y.-Q., He, J.-H., Yu, H.-P., Huang, C.-J., Gao, J.-M., Dong, Q.-X., Xuan, Y.-X., Li, C.-Q. 2014, *J. Appl. Toxicol.*, 34, 139.
32. Rombough, P. 2002, *J. Exp. Biol.*, 205, 1787.
33. Mccollum, C. W., Ducharme, N. A., Bondesson, M., Gustafsson, J. A. 2011, *Birth Defects Res. C Embryo Today*, 93, 67.
34. Forouhar, A. S, Hove, J. R., Calvert, C., Flores, J., Jadvar, H., Gharib, M. 2004, *Conf Proc IEEE Eng. Med. Biol. Soc*., 5, 3615.
35. Schwerte, T., Fritsche, R. 2003, *Comp. Biochem. Physiol. A Mol. Integr. Physiol*., 135, 131.
36. Malone, M. H., Sciaky, N., Stalheim, L., Hahn, K. M., Linney, E., Johnson, G. L. 2007, *BMC Biotechnol.*, 7, 40.
37. Chan, P. K., Lin, C. C., Cheng, S. H. 2009, *BMC Biotechnol.*, 9, 11.
38. Mittelstadt, S. W., Hemenway, C. L., Craig, M. P., Hove, J. R. 2008, *J. Pharmacol. Toxicol. Methods*, 57, 100.

39. Karlsson, M., Danielsson, B. R., Nilsson, M. F., Danielsson, C., Webster, W. S. 2007, *Curr. Pharm. Des.*, 13, 2979.
40. Langheinrich, U., Vacun, G., Wagner, T. 2003, *Toxicol. Appl. Pharmacol*. 193, 370.
41. Milan, D. J., Peterson, T. A., Ruskin, J. N., Peterson, R. T., MacRae, C. A. 2003, *Circulation*, 107, 1355.
42. Poon, K. L., Liebling, M., Kondrychyn, I., Garcia-Lecea, M., Korzh V. 2010, *Dev. Dyn*., 239, 914.
43. Lawson, N., Weinstein, B. 2002, *Dev. Biol*., 248, 307.
44. OECD, 2007. Guideline 426. Developmental Neurotoxicity Study.
45. Bal-Price, A. K., Coecke, S., Costa, L., Crofton, K. M., Fritsche, E., Goldberg, A., Grandjean, P., Lein, P. J., Li, A., Lucchini, R., Mundy, W. R., Padilla, S., Persico, A. M. Seiler, A. E. M., Kreysa, J. 2012, *ALTEX*, 29, 202.
46. Anderson, K. V., Ingham, P. W. 2003, *Nat. Genet.*, 33 Suppl, 285.
47. Brustein, E., Saint-Amant, L., Buss, R. R., Chong, M., McDearmid, J. R., Drapeau, P. 2003, *J. Physiol. Paris*, 97, 77.
48. Kokel, D., Peterson, R.T. 2008, *Briefings Funct. Genomics Proteomics*, 7, 483.
49. Selderslaghs, I. W. T., Hooyberghs, J., De Coen, W., Witters, H. E. 2010, *Neurotoxicol. Teratol*., 32, 460.
50. Irons, T. D., MacPhail, R. C., Hunter, D. L., Padilla, S. 2010, *Neurotoxicol. Teratol*., 32, 84.
51. Airhart, M. J., Lee, D. H., Wilson, T. D., Miller, B. E., Miller, M. N., Skalko, R.G. 2007, *Neurotoxicol. Teratol*., 29, 652.
52. Ali, S., Champagne, D. L., Richardson, M. K. 2012, *Behav. Brain Res.* 228, 272.
53. Ahmad, F., Noldus, L. P. J. J., Tegelenbosch, R. A. J., Richardson, M. K. 2012, *Behaviour*, 149, 1241.
54. Tierney, K. B. 2011, *Biochim. Biophys. Acta Mol. Basis Dis.*, 1812, 381.
55. Hallare, A. V., Schirling, M., Luckenbach, T., Köhler, H. R., Triebskorn, R. 2005, *J. Therm. Biol*., 30, 7.
56. Kokel, D., Bryan, J., Laggner, C., White, R., Cheung, C. Y. J., Mateus, R., Healey, D., Kim, S., Werdich, A. A., Haggarty, S. J., MacRae, C. A., Shoichet, B., Peterson, R.T. 2010, *Nat. Chem. Biol*., 6, 231.
57. Matsui, J. I., Egana, A. L., Sponholtz, T.R., Adolph, A.R., Dowling, J.E. 2006, *Investig, Ophthalmol. Vis. Sci.*, 47, 4589.
58. Carvan, M. J., Loucks, E., Weber, D.N., Williams, F.E. 2004, *Neurotoxicol. Teratol.*, 757.
59. Samson, J., Shenker, J. 2000, *Aquat. Toxicol.*, 48, 343.
60. MacPhail, R. C., Brooks, J., Hunter, D. L., Padnos, B., Irons, T. D., Padilla, S. 2009, *Neurotoxicology*, 30, 52.
61. Padilla, S., Hunter, D. L., Padnos, B., et al. 2011, *Neurotoxicol. Teratol.*, 33, 624.
62. Zellner, D., Padnos, B., Hunter, D .L., et al. 2011, *Neurotoxicol. Teratol.*, 33, 674.
63. Bilotta, J. 2000, *Behav. Brain Res.*, 116, 81.

64. Chen, T. H., Wang, Y. H., Wu, Y. H. 2011, *Aquat. Toxicol.*, 102, 162.
65. Diekmann, H., Hill, A. 2013, *Drug Discov.Today Dis Models*, 10, e31.
66. Knöbel, M., Busser, F. J. M., Rico-rico, A., Kramer, N. I., Hermens, J. L. M., Hafner, C., Tanneberger, K., Schirmer, K., Scholz, S. 2012, *Environ. Sci. Thechnol.*, 46, 9690.
67. Goldstone, J. V, McArthur, A. G., Kubota, A., Zanette, J., Parente, T., Jönsson, M. E., Nelson, D. R., Stegeman, J. J. 2010, *BMC genomics*, 11, 643.
68. Jones, H. S., Panter, G. H., Hutchinson, T. H., Chipman, J. K. 2010, *Zebrafish*, 7, 23.
69. Alderton, W., Berghmans, S., Butler, P., Chassaing, H., Fleming, A., Golder, Z., Richards, F., Gardner, I. 2010, *Xenobiotica*, 40, 547.
70. Weigt, S., Huebler, N., Strecker, R., Braunbeck, T., Broschard, T. H. 2011, *Toxicology*, 281, 25.
71. Padilla, S., Corum, D., Padnos, B., Hunter, D. L., Beam, A., Houck, K., Sipes, N., Kleinstreuer, N., Knudsen, T., Dix, D. J., Reif D. M. 2012, *Reprod. Toxicol.*, 33, 174.
72. Sogorb, M. A., Pamies, D., de Lapuente, J., Estevan, C., Estévez, J., Vilanova, E. 2014, *Toxicology letters*, 230, 356.
73. Ankley, G. T., Bennett, R. S., Erickson, R. J., Hoff, D. J., Hornung, M. W., Johnson, R. D., Mount, D. R., Nichols, J. W., Russom, C. L., Schmieder, P. K., Serrrano, J. A., Tietge, J. E., Villeneuve, D. L. 2010, *Environ.Toxicol.Chem.*, 29, 730.

Research Signpost
37/661 (2), Fort P.O.
Trivandrum-695 023
Kerala, India

Recent Advances in Pharmaceutical Sciences V, 2015: 85-100 ISBN: 978-81-308-0561-0
Editors: Diego Muñoz-Torrero, M. Pilar Vinardell and Javier Palazón

6. Molecular insights into the diversification of *Cheirolophus* (Asteraceae) in Macaronesia

Daniel Vitales[1,2], Jaume Pellicer[3], Joan Vallès[1] and Teresa Garnatje[2]

[1]Laboratori de Botànica – Unitat associada CSIC, Facultat de Farmàcia, Universitat de Barcelona Avinguda Joan XXIII s/n, 08028 Barcelona, Catalonia, Spain; [2]Institut Botànic de Barcelona (IBB-CSIC-ICUB), Passeig del Migdia s/n, Parc de Montjuïc, 08038 Barcelona, Catalonia, Spain [3]Jodrell Laboratory, Royal Botanic Gardens, Kew, Richmond, Surrey, TW9 3AB, United Kingdom

Abstract. The diversification of *Cheirolophus* in Macaronesian archipelagos constitutes a paradigmatic example of radiation on oceanic islands. Phylogenetic and molecular dating analyses indicate an extraordinarily fast process, showing one of the highest speciation rates ever found on plants from oceanic islands. Such radiation has been recently studied employing phylogeographic, population genetic and molecular cytogenetic approaches. Here, the main potential patterns and processes involved in the diversification of the genus in the Canary Islands and Madeira are reviewed and discussed as a whole.

Introduction

The observations of Darwin [1] and Wallace [2] about diversification processes on island biotas meant an outstanding contribution to the origins of

Correspondence/Reprint request: Dr. Daniel Vitales, Laboratori de Botànica – Unitat associada CSIC, Facultat de Farmàcia, Universitat de Barcelona, Avinguda Joan XXIII s/n, 08028 Barcelona, Catalonia, Spain
E-mail: dvitales@ub.edu

modern evolutionary biology. From that moment, island radiations have become the object of numerous studies focusing on plants and animals from archipelagos all over the world [3, 4]. This interest on islands relies in the number of characteristics they possess, which make them attractive to researchers in the field –such as their relative small size, the existence of clear boundaries, the ecological simplicity compared to the continent, and the high diversity they usually harbour– making them natural laboratories where it is easier to observe, test and interpret general evolutionary patterns [5]. In recent times, Macaronesian archipelagos (Azores, Madeira, Canaries, Selvagens and Cape Verde, which constitute, together with a small nearby fraction of the African continent, the Macaronesian biogeographic region) and particularly the Canary Islands have become one of the favorite scenarios for researchers working on plant diversification processes (e.g. [6–9]). In this sense, many of the groups that have shown higher insular endemism levels -and therefore offering better possibilities to analyse island radiation processes- have been targeted (e.g. *Argyranthemum* Webb [10]; *Aeonium* Webb & Berthel. [11]; *Bystropogon* L.Hér. [12]; *Sideritis* L., [13]; *Sonchus* L. alliance [14]; *Echium* L. [15]; *Tolpis* Adans. [16]; *Pericallis* Webb & Berthel., [17]; *Cheirolophus* Cass. [18, 19]).

Among them all, in this review we will focus in the genus *Cheirolophus* Cass., whose diversification in the Canary Islands is considered as one of the top ten explosive plant radiations in this oceanic archipelago [20]. In addition to that, the Macaronesian representatives of this genus feature several typical traits of plants that have been able to diversify on insular environments, such as e.g. increasing woodiness [3], larger inflorescences and both showier flowers and inflorescences [21], reduction in genome size [7, 22] and small population size [23], thus making *Cheirolophus* a perfect model to study radiations on oceanic islands. Until recently, however, comprehensive understanding of the diversification of the genus in Macaronesia was missing. Based in previous phylogenetic reconstructions, it had been hypothesized that the radiation of *Cheirolophus* in the Canary Islands was a considerably fast and recent process [24, 25]. Unfortunately, those early studies lacked of a solid temporal frame, so it was neither possible to estimate speciation rate nor to establish comparisons with other well-known cases of explosive radiations in Macaronesia (e.g. [15]) or in other oceanic archipelagos (e.g. [26]).

Figure 1. Morphological and ecological diversity found on the genus *Cheirolophus* a) *Ch. arbutifolius* (Svent.) G.Kunkel., b) *Ch. burchardii* Susanna, c) *Ch. canariensis* (Willd.) Holub, d) *Ch. crassifolius* (Bertol.) Susanna, e) *Ch. falcisectus* Svent. ex Montelongo & Moraleda, f) *Ch. intybaceus* (Lam.) Dostál, g) *Ch. junonianus* (Svent.) Holub, h, i) Cliffs in Madeira with *Ch. massonianus* (Lowe) A.Hansen & Sunding, j) *Ch. tagananensis* (Svent.) Holub, k) *Ch. teydis* (C.Sm.) G.López, l) *Ch. uliginosus* (Brot.) Dostál. (Images: L. Barres, T. Garnatje, D. Vitales, http://commons.wikimedia.org).

The genus *Cheirolophus* has also been pointed out to represent a paradigmatic example of non-adaptive radiation on islands [4]. Indeed, most of the Macaronesian species of the genus exploit similar ecological niches, showing at the same time mostly inconspicuous morphological

differences. Nevertheless, Macaronesian *Cheirolophus* show as well a few cases of ecological adaptations to particular habitats (e.g. *Ch. teydis* from subalpine zone of Tenerife and La Palma; or *Ch. junonianus* from the southern arid part of La Palma island; see Figure 1). These and other questions that have been found to play an important role on island diversification -such as hybridisation and among population gene flow [10, 11, 17]; colonisation and dispersal patterns among islands [9, 27]; or reproduction biology factors [28, 29]– have been the subject of some recent studies focusing on *Cheirolophus* radiation [18, 19, 25, 30]. In this chapter, we will present different methodological approaches employed to disentangle the evolutionary history of this genus, discussing the results obtained from a holistic perspective.

1. Brief overview of the genus *Cheirolophus*

First of all, we must circumscribe *Cheirolophus* (Asteraceae, Cardueae, Centureineae) within a taxonomic and phylogenetic context. The genus was first described by Cassini [31] based on the segregation of a group of species formerly included in the genus *Centaurea* L. Afterwards, Boissier [32] included additional species to those previously segregated by Cassini, grouping them all in a new genus, *Ptosimopappus* Boiss., which comprised species from sections *Cheirolophus* Cass. and *Microlophus* (Cass.) DC., that had been described within the genus *Centaurea*. Moreover, this author proposed the inclusion of *Centaurea arguta* Nees and *Centaurea uliginosa* Brot. to this new genus, describing as well some new species such as *Ptosimopappus bracteatus* Boiss. and *Ptosimopappus arboreus* Boiss. [33].

These taxonomic reorganisations have been in some cases conflicting. In fact, while authors like Pomel [34], Holub [35], Dostál [36], or Bremer [37] continued considering *Cheirolophus* as an independent genus, Dittrich [38] or Talavera [39], among others, preferred maintaining it as a section of *Centaurea*. Nonetheless, the most recent revisions of the Cardueae tribe based on molecular phylogenetic data (e.g.[40, 41]), clearly supported the segregation of *Cheirolophus* as an independent taxonomic entity, revealing the position of the genus as a basal lineage within subtribe Centaureinae.

This genus contains approximately 27-30 species, depending on the authors consulted, distributed along the western Mediterranean basin as far as Malta, and the Macaronesian archipelagos of Madeira and Canary Islands (Figure 2). Some of the species have a wide distribution, such as *Ch. intybaceus* (Lam.) Dostál or and *Ch. sempervirens* Pomel (Fig. 2).

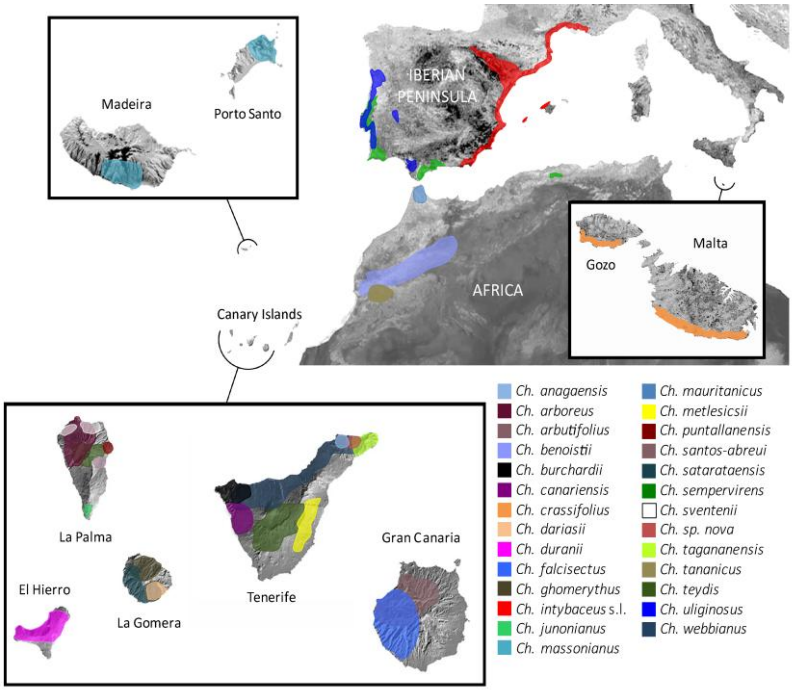

Figure 2. Approximate geographical distribution of the genus *Cheirolophus* on Western Mediterranean, North Africa and Macaronesia.

Others, however, are more restricted geographically, and limited in many cases to very few populations, such as *Ch. duranii* (Burchard) Holub from El Hierro island or *Ch. tagananensis* (Svent.) Holub from Anaga peninsula in the northern part of Tenerife (Fig. 2). Indeed, most of the endemic *Cheirolophus* species from Macaronesia present extremely restricted distributions. To date, 20 species, one subspecies and one variety have been described in the Canarian archipelago [42], plus another species endemic to the islands of Madeira and Porto Santo. The low number of populations as well as the small population size reported for some of these species was a key factor for many of them to be included in different national and international red lists of endangered flora (e.g. Libro Rojo de la Flora Vascular Amenazada de España [43]; or the IUCN Red List [44]).

2. Molecular phylogenetic studies in *Cheirolophus*

The pioneering molecular systematic studies in *Cheirolophus* employed isoenzyme electrophoresis technique to analyse the genetic variability among populations of different species [45, 46]. This methodological approach provided little resolution on the evolutionary relationships among species, but served to propose for the first time a recent origin for the diversification of the Macaronesian members of the genus. Sometime later, a phylogenetic reconstruction based on the internal transcript spacer (ITS) of the nrDNA allowed a taxonomic delimitation of *Cheirolophus*, including the species *Ch. crassifolius* (Bertol.) Susanna and confirming the monophyly of the Macaronesian grade [24]. This question was also readdressed afterwards with a combined approach consisting on genome size data and sequencing of both the ITS and external transcript spacer (ETS) regions [25]. As mentioned above, this study indentified *Ch. crassifolius* as the sister species to the rest of the members and evidenced the existence of two main lineages, the Macaronesian and the Mediterranean clades. Unfortunately, none of these works were able to accurately reconstruct the evolutionary history of *Cheirolophus*, and the interspecific relationships within the Macaronesian group remained particularly unresolved.

A recent reconstruction of the evolutionary history of the genus [18] has, however, provided a relevant contribution to former phylogenetic works. This new study has been based on the analysis of two nrDNA regions (ITS and ETS) as well as four cpDNA regions (*rpl*32-*trn*L, *rpo*B-*trn*D, *rps*16-*trn*K and *trn*S-*trn*C), to analyse the whole specific and virtually all infraspecific diversity within the genus.

The results showed a significant phylogenetic incongruence among nuclear and plastid markers, a pattern usually explained by phenomena like incomplete lineage sorting (ILS), hybridisation or polyploidy, among others [47]. Incongruent position of species within the Mediterranean clade was explained by the slow evolutionary rate of plastid markers, preventing us from tracking accurately the speciation events in this group. A different hypothesis was proposed for the conflicting position of *Ch. massonianus* (Lowe) A.Hansen & Sunding between the plastid and nuclear trees. In this case, the placement of this Madeiran endemic in each phylogenetic reconstruction is so discordant that phenomena related to sharing alleles were discarded. Moreover, *Ch. massonianus* shows an intermediate genome size (though not exclusive) half way between that of the continental and the remaining insular species [25], hence constituting another evidence of potential hybridisation in this species.

Regardless of this incongruence, both markers resulted useful to reconstruct the phylogeny when analysed independently (see Vitales *et al*. [18]). As it had been reported in former studies (e.g. [48]), whereas nuclear DNA provided resolution to the backbone of the phylogeny as well as for generating a temporal frame for the evolutionary history, plastid markers resulted more helpful unravelling the phylogeographic relationships among closely related species. Both datasets supported the monophyly of the genus and the existence of a well-differentiated insular clade. However, as a result of the potential hybridisation involving *Ch. massonianus*, the nuclear tree included the endemic species from Madeira within the insular clade, while the sampling on the plastid tree was restricted to Canarian species. The reconstruction based on ITS and ETS markers also resolved the Mediterranean clade, reflecting morphological and geographical affinities among the species of this group. *Cheirolophus crassifolius*, endemic to Malta and Gozo Islands, appeared in both analyses as an early-diverged lineage, and sister to the rest of the members of the genus. In relation to *Ch. uliginosus*, the only hemicryptophyte representative, this species is also placed in a basal position relative to the diversification of the species within the Mediterranean and the Macaronesian clades - although not entirely resolved- according to both nuclear and plastid datasets.

As already mentioned above, the analysis of the nuclear regions was particularly useful for studying the early stages of the evolutionary history of *Cheirolophus*, as well as to establish a time frame for the phylogeny (Figure 3). The origin of the diversification of the genus was dated to the mid-Miocene period. At that time, the Mediterranean basin still featured tropical climate characteristics, but a progressive aridification starting in the east around 11-9 Ma [49] might had pushed *Cheirolophus* westwards, explaining its current Western Mediterranean and Macaronesian distribution. Concerning the radiation of the genus in Macaronesia, the time-calibrated phylogeny indicated that *Cheirolophus* diversified rapidly, with c. 20 species arising in less than 1.8 Ma, at a rate of 0.34–2.84 species per Ma. Such high speciation rate is only comparable to those exhibited by other island radiations such as Hawaiian *Bidens* L. (0.3–2.3 species Myr^{-1}) or Macaronesian *Echium* (0.4–1.5 species Myr^{-1}), considered as the fastest plant radiations on volcanic islands to date [26]. Indeed, taking into account the area covered by both the Canary Islands and Madeira (8,321 km^2), Macaronesian *Cheirolophus* may well represent the highest per-unit-area rate of diversification (4.09×10^{-5} to 3.41×10^{-4} species Myr^{-1} km^{-2}) observed so far in plants [26, 50, 51].

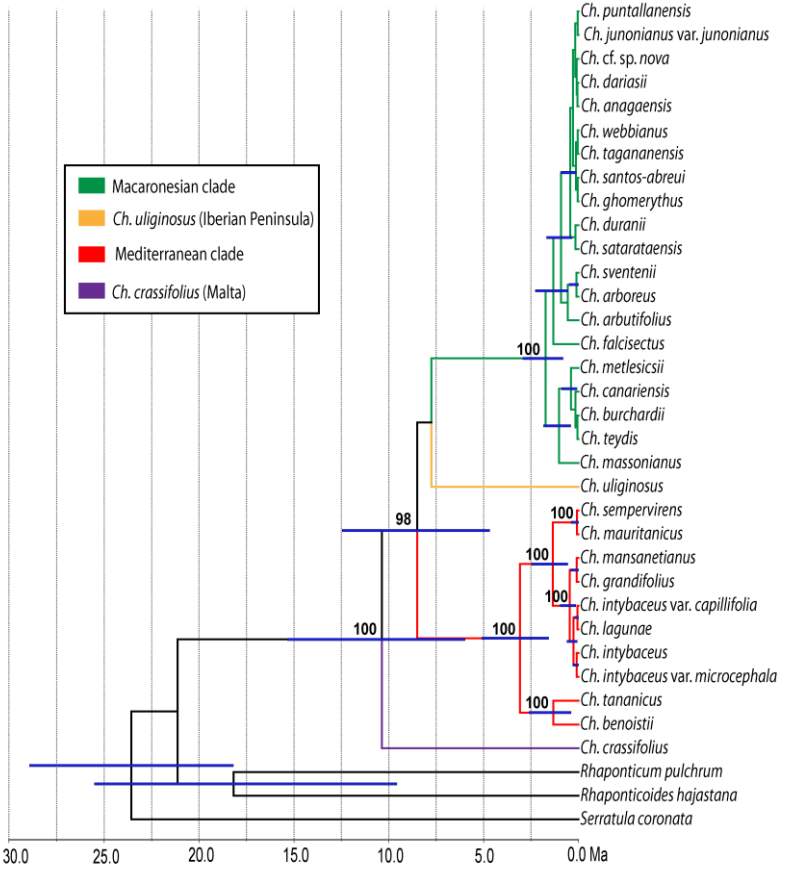

Figure 3. Time-calibrated Bayesian phylogenetic tree inferred from nuclear (ITS and ETS) DNA sequences. Bayesian posterior probabilities (PP) above 95% are indicated above main interesting branches. Blue bars indicate 95% high posterior density intervals (for nodes with posterior probability > 50%) of node ages.

3. Phylogeography of Macaronesian *Cheirolophus*

Having provided strong evidence explaining the radiation process, the question arose as to which mechanisms were underlying such rapid diversification. Another point to further investigate was the role played by the phylogeographic history of Macaronesian *Cheirolophus* in such rapid

diversification. The phylogeographic analyses performed by Vitales *et al*. [18] highlighted Tenerife island as the most likely source area of inter-island dispersal, with a pivoting role in successive colonisations towards the East (from Tenerife to Gran Canaria) and towards the West (from Tenerife to La Gomera and la Palma, on the one hand and towards La Gomera and El Hierro, on the other hand). During this process, the analyses suggested that La Gomera could have been colonised twice. These results are consistent with other phylogeographic studies focusing on the Canary Islands (e.g. [52–54]), which propose that this central island could had served as a major hub for the colonisation of the archipelago. The ancient geological history of this island [55], together with its central position in the archipelago and the high diversity of habitats, probably explains this central phylogeographic role of Tenerife. Moreover, Tenerife harbours the highest genetic diversity for *Cheirolophus* in the archipelago, as observed also in other genera in the Canarian area such as *Bystropogon* [12], *Sideritis* [13] or *Aeonium* [11]. The higher genetic and taxonomic diversity levels found in Tenerife have also been attributed to the complex palaeogeographic history of this island [55]. Successive fragmentation and connexion process among the habitats due to major climatic and geologic events affecting Tenerife during this period may have contributed to the allopatric differentiation among populations.

The largest islands -particularly Tenerife and La Palma- experienced several cases of intra-island diversification, probably driven by genetic isolation, but also due to different processes such as incipient ecological adaptation or introgression events. This model of radiation has been proposed to be common in other plants and animals that diversified -more or less- in the Canary Islands (see Sanmartín *et al*. [9] for a review). Certainly, these typical patterns of colonization, dispersal and differentiation experienced by *Cheirolophus* cannot explain on their own the extraordinarily rapid radiation occurred in Macaronesia, so other intrinsic or extrinsic factors must have contributed to this spectacular process of island diversification.

4. Genomic insights in *Cheirolophus*

Several authors have recently proposed that certain genomic factors such as the genome size [7, 22, 56] or the number of nrDNA loci [57] could be related to the process of diversification on islands. In *Cheirolophus*, this topic has been the subject of different studies [25, 30], addressing genome size, karyological and molecular cytogenetic aspects of some Macaronesian and continental species of the genus.

Cheirolophus is the only genus within the Centaureinae that has radiated in the Canary Islands. Similarly to other closely related genera (*Callicephalus* C.A.Mey, *Myopordon* Boiss., *Oligochaeta* K.Koch, *Rhaponticum* Ludw. and *Centaurea*, see Hidalgo *et al*. [58, 59] for further details), the genus displays the 35S and the 5S nrDNA loci physically separated in the chromosomes. By contrast, while those phylogenetically related genera contain a relatively low number of 35S loci [60], fluorescent *in situ* hybridisation (FISH) analyses in *Cheirolophus* revealed a strikingly high number of chromomycin bands and 35S loci, predominantly located at terminal position. Likewise, a certain trend towards an increasing number of 35S loci in Macaronesian species was observed, preliminarily suggesting that this unusual number of loci appeared during island radiation process. However, other continental species of the genus such as *Ch. benoistii* (Humbert) Holub or *Ch. intybaceus* showed as well a high number of 35S signals, indicating that the abundance of terminal 35S predated the radiation in Macaronesia. Finally, Garnatje *et al*. [30] hypothesised a positive effect of the 35S loci pattern promoting the radiation of *Cheirolophus*.

In a previous study focusing on genome size variation within the genus *Cheirolophus*, Garnatje *et al*. [25] evidenced a significant progressive genome downsizing since early stages of its evolutionary history, and particularly noticeable within the Macaronesian clade. Some evolutionary mechanisms such as homologous recombination and illegitimate recombination (see Leitch and Leitch [61], for a review) have been proposed to be able to affect both genome size and rDNA loci distribution. In *Oligochaeta divaricata* K.Koch (another species included within basal Centaureinae and closely related to *Cheirolophus*), a deep chromosomal restructuring process resulted on a significant loss of DNA associated to an increase of 35S loci and the reorganisation of their position in the chromosomes. It should be noted, however, that terminal 35S positions in *Cheirolophus* were not affected by genome size reduction. In summary, despite that *Cheirolophus* radiation was not associated to changes in chromosome number or ploidy level, the patterns of rDNA loci distribution and the reduction of the DNA content evidence certain capacity for genomic dynamism in the group. Indeed, the association among genomic size changes, nrDNA organisation and cladogenesis has been recently discussed by several authors (e.g. [62, 63]), but the precise putative role played by these mechanisms on *Cheirolophus* radiation will require further investigation.

5. Population genetics study in Macaronesian *Cheirolophus*

As stated earlier, the phylogenetic study of *Cheirolophus* based on nrDNA and cpDNA sequences [18] provided valuable information about the early evolutionary history of the genus. However, the phylogenetic resolution within the Macaronesian lineage was poor due to the rapidity of the diversification process and the limited variability of the employed markers. For that reason, the radiation of *Cheirolophus* in the Canary Islands and Madeira was subsequently investigated using a population genetics approach with AFLP markers [19].

First, this methodology was employed to study the taxonomic delimitation within the Macaronesian species of the genus, a subject that had been already under discussion in earlier studies focusing on *Cheirolophus* evolution [45]. The phylogenetic results obtained from AFLP data provided full support to the current taxonomic species' circumscription. Thus, our results corroborate the distinctiveness of these extraordinarily recently diverged species and support the suitability of classical diagnostic characters employed in the taxonomical delimitation of Macaronesian *Cheirolophus*.

The phylogenetic relationships among the Macaronesian species were not entirely reconstructed with the AFLP data, but the diverse analytical approaches proved useful to better understand the evolutionary history of these insular lineages. The genetic structure of populations showed a significant segregation pattern among western islands (La Palma and El Hierro) and central/eastern islands (La Gomera, Tenerife, Gran Canaria). The important role played by allopatric differentiation became even more evident when considering additional genetic clusters: most of the populations grouped geographically, either among the islands or within the islands. Here again, the genetic structure found in Tenerife populations was particularly interesting, already reported in other plant groups [12], and suggesting a lineage disjunction related to the ancient palaeoislands of Anaga and Teno [64].

Despite the limited population sampling, the study carried out by Vitales *et al*. [19] also suggested a reduced gene flow among the Macaronesian populations. The strong signal of isolation-by-distance, the low within-population heterozygosity and the high values of the fragmentation indexes indicated a limited genetic flow among the populations. These results agreed with the low dispersal capacity of *Cheirolophus* seeds, the geographic isolation of populations and their small size, possibly contributing to their progressive genetic differentiation. In contrast, the phylogeographic pattern observed in this group -including numerous colonisation and recolonisation events, both intra- and inter-island

suggest that Macaronesian *Cheirolophus* showed a considerable ability for sporadic long distance dispersal (see Crawford *et al*. [28] for some hypotheses). In this way, authors such as Ellis *et al*. [65] or Knope *et al*. [26] have proposed that the combination of reduced gene flow and certain ability for long distance dispersal may play an important role on radiation processes experienced by plants.

As mentioned in the introduction section, the Macaronesian *Cheirolophus* have been proposed as an example of non-adaptive radiation on islands [4]. In this regard, the correlation analyses among morphological and genetic distances performed by Vitales *et al*. [19] indicated that there is not a straightforward association among genetic lineages and the ecomorphological traits studied in these species. Clearly, the data and the methods employed in this study are preliminary and somewhat insufficient to discard an essential role of adaptive selection in the radiation of this group. However, these results suggested that ecological adaptation did not drive the initial stages of Macaronesian *Cheirolophus* diversification. The examples of adaptations to specific ecological conditions found in some species (e.g. *Ch. junonianus* from the southern extreme of La Palma, or *Ch teydis* from the subalpine zone of Tenerife and La Palma) seem to correspond with relatively recent and independent processes of ecomorphological differentiation.

Another mechanism potentially playing an important role in the evolutionary history of Macaronesian *Cheirolophus* is introgression [18]. We have already discussed the case of *Ch. massonianus*, putatively experiencing a chloroplast capture process from a continental taxon. In addition, our analyses also suggested some cases of genetic introgression between several species from the Canary Islands. Particularly, some evidences of genetic admixture were found in *Ch. teydis* and *Ch. arboreus* from La Palma, and *Ch. duranii* from El Hierro. In some cases these genetic traces seemed supported by morphological data and/or heteromorphic positions found in the nrDNA regions of these species. That said, one should bear in mind that some of these signals could also be explained by retention of ancestral polymorphisms or incomplete lineage sorting (ILS) phenomena, especially considering the speed of the radiation. Therefore, the relative importance of genetic introgression in the radiation of Macaronesian *Cheirolophus* should be further studied more in detail.

6. Conclusion

Recent molecular phylogenetic studies have shown that the radiation of *Cheirolophus* in Macaronesia was an extraordinarily recent and rapid process.

Phylogeographic analyses indicated that Tenerife Island played an important role in this explosive diversification that, according to our data, could have been driven by allopatric differentiation, incipient ecological adaptation and introgression events. Molecular cytogenetic studies have revealed that *Cheirolophus* has undergone a significant increase in the number of 35S rDNA loci, which started just after the diversification of the genus in the Mediterranean region. This pattern contrasts with the gradual genome downsizing observed during the evolution of the genus, and evidences a certain genomic dynamism in the genus, probably related with the ability to radiate on islands. Finally, a population genetic approach suggested that the combination of poor gene flow capacity and a certain ability for sporadic long-distance colonization could have also played an important role enhancing the explosive diversification of this genus in Macaronesia.

Acknowledgements

The authors acknowledge all researchers involved in previous *Cheirolophus* studies for their substantial contributions and improvements to the knowledge of this group of plants from all perspectives, and all our colleagues who have kindly given their permission to use graphics and captions already published. This work was subsidized by the Spanish Ministry of Science (projects CGL2010-22234-C02-01 and 02/BOS, CGL2013-49097-C2-2-P) and the Generalitat de Catalunya (Ajuts a grups de recerca consolidats, 2009/SGR/439, 2014/SGR/514). Daniel Vitales benefited from a FPU grant from the Spanish Ministry of Education. Jaume Pellicer benefited from a Beatriu de Pinós postdoctoral fellowship with the support of the Secretary for Universities and Research of the Ministry of Economy and Knowledge (Government of Catalonia) and the co-fund of Marie Curie Actions (European Union 7th R&D Framework Programme).

References

1. Darwin, C. 1859, On the Origin of the Species by Means of Natural Selection, Murray, London.
2. Wallace, A.R. 1878, Tropical Nature and Other Assays, McMillan, London.
3. Carlquist, S. 1974, Island Biology, Columbia University Press, New York.
4. Whittaker, R.J., Fernández-Palacios, J-M. 2007, Island Biogeography: Ecology, Evolution and Conservation, Oxford University Press, Oxford.
5. Losos, J.B., Ricklefs, R.E. 2009, *Nature*, 457, 830.
6. Juan, I., Emerson, B., Orom, I., Hewitt, G. 2000, *Trends Ecol. Evol.*, 15, 104.

7. Suda, J., Kyncl, T., Jarolímová, V. 2005, *Plant Syst. Evol.*, 252, 215.
8. Kim, S-C., McGowen, M.R., Lubinsky, P., Barber, J.C., Mort, M.E., Santos-Guerra, A. 2008, *PLoS One*, 3, e2139.
9. Sanmartín, I., van der Mark, P., Ronquist, F. 2008, *J. Biogeogr.*, 35, 428.
10. Francisco-Ortega, J., Jansen, R.K., Santos-Guerra, A. 1996, *Proc. Natl. Acad. Sci. U.S.A.*, 93, 4085.
11. Jorgensen, T.H., Olesen, J.M. 2001, *Perspect. Plant Ecol. Evol. Syst.*, 4, 29.
12. Trusty, J.L., Olmstead, R.G., Santos-Guerra, A., Sá-Fontinha, S., Francisco-Ortega, J. 2005, *Mol. Ecol*., 14, 1177.
13. Barber, J.C., Finch, C.C., Francisco-Ortega, J., Santos-Guerra, A., Jansen, R.K. 2007, *Taxon*, 56, 74.
14. Kim, S.C., Crawford, D.J., Francisco-Ortega, J., Santos-Guerra, A. 1996, *Proc. Natl. Acad. Sci. U.S.A.*, 93, 7743.
15. García-Maroto, F., Mañas-Fernández, A., Garrido-Cárdenas, J.A., Alonso, D.L., Guil-Guerrero, J.L., Guzmán, B., Vargas, P. 2009, *Mol. Phylogenet. Evol.*, 52, 563.
16. Gruenstaeudl, M., Santos-Guerra, A., Jansen, R.K. 2012, *Cladistics*, 1, 1.
17. Jones, K.E., Reyes-Betancort, J.A., Hiscock, S.J., Carine, M.A. 2014, *Am. J. Bot.*, 101, 637.
18. Vitales, D., Garnatje, T., Pellicer, J., Vallès, J., Santos-Guerra, A., Sanmartín, I. 2014, *BMC Evol. Biol.*, 14, 118.
19. Vitales, D., García-Fernández, A., Pellicer, J., Vallès, J., Santos-Guerra, A., Cowan, R.S., Fay, M.F., Hidalgo, O., Garnatje, T. 2014, *PLoS One*, 9, e113207.
20. Fernández-Palacios, J.M. 2008, *J. Biogeogr*., 35, 379.
21. Böhle, U.-R., Hilger, H.H., Martin, W.F. 1996, *Proc. Natl. Acad. Sci. U.S.A.*, 93, 11740.
22. Kapralov, M.V., Filatov, D.A. 2011, *J. Bot.*, 2011, 458684.
23. Caujapé-Castells, J., Tye, A., Crawford, D.J., Santos-Guerra, A., Sakai, A., Beaver, K., Lobin, W., Vincent Florens, F.B., Moura, M., Jardim, R. 2010, *Perspect. Plant Ecol. Evol. Syst.*, 12, 107.
24. Susanna, A., Garnatje, T., Garcia-Jacas, N. 1999, *Plant Syst. Evol.*, 214, 147.
25. Garnatje, T., Garcia, S., Canela, M.Á. 2007, *Plant Syst. Evol.*, 264, 117.
26. Knope, M.L., Morden, C.W., Funk, V.A., Fukami, T. 2012, *J. Biogeogr.*, 39, 1206.
27. Cowie, R.H., Holland, B.S. 2006, *J. Biogeogr.*, 33, 193.
28. Crawford, D.J., Lowrey, T.K., Anderson, G.J., Bernardello, G., Santos-Guerra, A., Stuessy, T.F. 2009, In: Systematics, Evolution, and Biogeography of Compositae, Funk, V.A., Susanna, A., Stuessy, T.F., Bayer, R.J. (Eds.), International Association for Plant Taxonomy, Vienna, 151.
29. Crawford, D.J., Anderson, G.J., Bernardello, G. 2011, In. The biology of islands floras, Bramwell, D., Caujapé-Castells, J. (Eds.), Cambridge University Press, Cambridge, 11.
30. Garnatje, T., Hidalgo, O., Vitales, D., Pellicer, J., Vallès, J., Robin, O., Garcia, S. 2012, *Genome*, 55, 529.

31. Cassini, H. 1817, *Cheirolophus*. In: Dictionnaire des Sciences Naturelles, Cuvier, Paris, 250.
32. Boissier, P.-E. 1839-1845, Voyage Botanique dans le Midi de l'Espagne pendant l'année 1837, Gide et Cie. librairies-éditeurs, Paris.
33. Boissier, P.-E. 1875, *Flora Orientalis*, vol. 3. H. Georg, Geneve-Basel, 1033.
34. Pomel, A.N. 1874, *Bull. Soc. des Sci. Phys. Nat. Climatol. l'Algerie*, 11, 1.
35. Holub, J.L. 1973, *Folia Geobot. Phytotaxon.*, 8, 155.
36. Dostál, J., *Cheirolophus*. In: Flora Europaea, Tutin, T.G., Heywwod, V.H., Burges, N.A., Moore, D.M., Valentine, D.H., Waltets, S.M. (Eds.), Cambridge University Press, Cambridge, 249.
37. Bremer, K. 1994, Asteraceae, Cladistics and Classification, Timber Press, Portland.
38. Dittrich, M. 1968, Botanical Jahrbücher für Systematic Pflanzengeschichte und Pflanzengeographie, 88, 70.
39. Talavera, S. 1987, Asteraceae. In: Flora Vascular de Andalucía Occidental,Valdés, B., Talavera, S., Fernández-Galiano, E. (Eds.), Ketres Editora, Barcelona, 5.
40. Susanna, A., Galbany-Casals, M., Romaschenko, K., Barres, L., Martín, J., Garcia-Jacas, N. 2011, *Ann. Bot.*, 108, 263.
41. Barres, L., Sanmartín, I., Anderson, C.L., Susanna, A., Buerki, S., Galvany-Casals, M., Vilatersana, R. 2013, *Am. J. Bot.*, 100, 867.
42. Bramwell, D., Bramwell, Z. 2010, Wild Flowers of the Canary Islands, Editorial Rueda, Madrid.
43. Bañares, A., Blanca, G., Güemes, J., Moreno, J.C., Ortiz, S. 2010, Atlas y Libro Rojo de la Flora Vascular Amenazada de España. Adenda 2010. Dirección General de Medio Natural y Política Forestal y Sociedad Española de Biología de la Conservación de Plantas, Madrid.
44. IUCN Red List of Threatened Species. Version 2015.1.
45. Garnatje, T.1995, PhD. dissertation, University of Barcelona, Barcelona, Spain.
46. Garnatje, T., Susanna, A., Messeguer, R. 1998, *Plant Syst. Evol.*, 213, 7.
47. Wendel, J.F., Doyle, J.J. 1998, In: Molecular systematics of plants II, Soltis, D.E., Soltis, P.S., Doyle, J.J. (Eds.), Springer, New York, 265.
48. Comes, H.P., Abbott, R.J. 2001, *Evolution*, 55, 1943.
49. Thompson, J.D. 2005, Plant Evolution in the Mediterranean, Oxford University Press, Oxford.
50. Valente, L.M., Savolainen, V., Vargas, P. 2010, *Proc. Biol. Sci.*, 277, 1489.
51. Hughes, C., Eastwood, R. 2006, *Proc. Natl. Acad. Sci. U.S.A.*, 103, 10334.
52. Allan, G.J., Francisco-Ortega, J., Santos-Guerra, A., Boerner, E., Zimmer, E.A. 2004, *Mol. Phylogenet. Evol.*, 32, 123.
53. Goodson, B.E., Santos-Guerra, A., Jansen, R.K. 2006, *Taxon*, 55, 671.
54. Guzmán, B., Vargas, P. 2010, *Perspect. Plant Ecol. Evol. Syst.*, 12, 163.
55. Carracedo, J.C., Badiola, E.R., Guillou, H., Paterne, M., Scaillet, S., Pérez Torrado, F.J., Paris, R., Fra-Paleo, U., Hansen, A. 2007, *Geol. Soc. Am. Bull.*, 119,1027.

56. Suda, J., Kron, P., Husband, B.C., Trávníček, P. 2007, In: Flow Citometry with Plant Cells, Doležel, J., Greilhuber, J., Suda, J. (Eds.), Wiley-VCH Verlag GmbH & Co.,Weinheim.
57. Mandáková, T., Heenan, P.B., Lysak, M.A. 2010, *BMC Evol. Biol.*,10, 367.
58. Hidalgo, O., Garcia-Jacas, N., Garnatje, T., Susanna, A. 2006, *Ann. Bot.*, 97, 705.
59. Hidalgo, O., Garcia-Jacas, N., Garnatje, T., Susanna, A., Siljak-Yakovlev, S. 2007, *Bot. J. Linn. Soc.*, 28, 193.
60. Hidalgo, O., Garcia-Jacas, N., Garnatje, T., Romashchenko, K. 2008, *Taxon*, 57, 769.
61. Leitch, I.J., Leitch, A.R. 2013, In: Plant Genome Diversity Volume 2, Greilhuber, J., Doležel, J., Wendel, J.F. (Eds.), Springer, Vienna, 307.
62. Lim, K.Y., Kovarik, A., Matyasek, R., Chase, M.W., Knapp, S., McCarthy, E., Clarkson, J.J., Leitch, A.R. 2006, *Plant J.*, 48, 907.
63. Mank, J.E., Avise, J.C. 2006, *Proc. Biol. Sci.*, 273, 33.
64. Ancochea, E., Huertas, M.J., Cantagrel, J.M., Coello, J., Fuster, J.M., Arnaud, N., Ibarrola, E. 1999, *J. Volcanol. Geotherm. Res.*, 88, 177.
65. Ellis, A.G., Weis, A.E., Gaut, B.S. 2006, *Evolution*, 60, 39.

Research Signpost
37/661 (2), Fort P.O.
Trivandrum-695 023
Kerala, India

Recent Advances in Pharmaceutical Sciences V, 2015: 101-115 ISBN: 978-81-308-0561-0
Editors: Diego Muñoz-Torrero, M. Pilar Vinardell and Javier Palazón

7. Ultrastructure of spermiogenesis and the spermatozoon in cyclophyllidean cestodes

Jordi Miquel, Jordi Torres and Carlos Feliu
Laboratori de Parasitologia, Departament de Microbiologia i Parasitologia Sanitàries, Facultat de Farmàcia, Universitat de Barcelona, Av. Joan XXIII, sn, 08028 Barcelona, Spain; Institut de Recerca de la Biodiversitat, Facultat de Biologia, Universitat de Barcelona Av. Diagonal, 645, 08028 Barcelona, Spain

Abstract. The usefulness of the ultrastructural characters of spermiogenesis and of the spermatozoon in the interpretation of relationships in the Platyhelminthes has been widely demonstrated. The present paper provides a review and an update on the ultrastructural knowledge on spermiogenesis and on the spermatozoon in cyclophyllidean cestodes. For each family of cyclophyllideans the pattern of spermiogenesis and the type of sperm cell is provided. Moreover, the most interesting characteristics of both spermiogenesis and the spermatozoon are compiled and illustrated for each family. Finally, new spermatological data on some species of the Anoplocephalidae and the Taeniidae are provided.

Introduction

The utility of ultrastructural characters of spermiogenesis and spermatozoa as a valuable tool for the elucidation of phylogenetic relationships in the

Correspondence/Reprint request: Dr. Jordi Miquel, Laboratori de Parasitologia, Departament de Microbiologia i Parasitologia Sanitàries, Facultat de Farmàcia, Universitat de Barcelona, Av. Joan XXIII, sn, 08028 Barcelona, Spain. E-mail: jordimiquel@ub.edu

Platyhelminthes has been widely demonstrated [1-13]. To date, the ultrastructure of spermiogenesis and/or the spermatozoon has been studied in more than 125 species of eucestodes belonging to the orders Bothriocephalidea, Caryophyllidea, Cyclophyllidea, Diphyllidea, Diphyllobothriidea, Haplobothriidea, Lecanicephalidea, Proteocephalidea, Spathebothriidea, Tetrabothriidea, Tetraphyllidea and Trypanorhyncha [14-27].

The Cyclophyllidea is undoubtedly the most extensively studied order, and data on the ultrastructure of spermiogenesis and/or spermatozoa is available for more than 60 species. According to the Global Cestode Database [28], the order Cyclophyllidea is constituted by 14 to 18 families, 380 to 400 genera and more than 3,000 species. To date, there are spermatological data on 12 families of cyclophyllideans, which will be analyzed in the present work. The studied families are Anoplocephalidae, Catenotaeniidae, Davaineidae, Dilepididae, Dipylidiidae, Gryporhynchidae, Hymenolepididae, Mesocestoididae, Metadilepididae, Nematotaeniidae, Paruterinidae and Taeniidae. Thus, the aim of the present chapter is to provide a review and an update concerning the ultrastructural knowledge on spermiogenesis and on the spermatozoon of cyclophyllidean cestodes.

1. Materials and methods

In the present chapter, new and preliminary spermatological results are showed concerning three species, namely *Thysanotaenia congolensis*, *Echinococcus granulosus* and *Echinococcus multilocularis*. Other illustrations refer to original TEM micrographs of previously published studies. These are *Gallegoides arfaai* [29], *Raillietina micracantha* [30], *Molluscotaenia crassiscolex* [31], *Mesocestoides lineatus* [32] and *Taenia taeniaeformis* [33].

Live specimens of *T. congolensis* were isolated from naturally infected black rats (*Rattus rattus*) from Sao Domingos and Orgaos (Cape Verde). Specimens of *E. multilocularis* were obtained from naturally infected red foxes (*Vulpes vulpes*) from La Roche sur Foron (France). Finally, *E. granulosus* were isolated from experimentally infected dogs from Sidi Thabet (Tunisia).

Adult studied tapeworms were immediately rinsed with a 0.9 % NaCl solution. Later, they were fixed in cold (4 °C) 2.5 % glutaraldehyde in a 0.1 M sodium cacodylate buffer at pH 7.4 for a minimum of 2 h, rinsed in 0.1 M sodium cacodylate buffer at pH 7.4, post-fixed in cold (4 °C) 1 % osmium tetroxide with 0.9 % potassium ferricyanide [$K_3Fe(CN)_6$] in the same buffer for 1 h, rinsed in milliQ water, dehydrated in an ethanol series and propylene

oxide, embedded in Spurr's resin and polymerised at 60 °C for 72 h. Ultrathin sections (60–90 nm thick) of mature segments at the level of the *vas efferens* and testes were obtained in a Reichert-Jung Ultracut E ultramicrotome. Sections were placed on copper grids and double-stained with uranyl acetate and lead citrate according to the Reynolds [34] methodology. The grids were examined in a JEOL 1010 transmission electron microscope operated at 80 kV, in the "Centres Científics i Tecnològics" of the University of Barcelona (CCiTUB).

2. Spermiogenesis and the spermatozoa in the Cyclophyllidea

Spermatogenesis in tapeworms is of the rosette type. The primary spermatogonium divides mitotically, forming two secondary spermatogonia. All further divisions occur simultaneously, resulting in a rosette of four tertiary, then eight quaternary spermatogonia and sixteen primary spermatocytes. The first meiotic division forms thirty-two secondary spermatocytes and after the second meiotic division, sixty-four spermatids are formed.

The initial stages of spermiogenesis in all cestodes are similar. They are characterized by the formation of a zone of differentiation delimited by a ring of arched membranes and supported by cortical microtubules, and by a change in the density of the nucleus. The zone of differentiation contains two centrioles and sometimes an intercentriolar body and striated rootlets. A cytoplasmic extension elongates from this zone of differentiation and the two centrioles give rise to one or two flagella. Bâ & Marchand [7] described four types of spermiogenesis in the Cestoda mainly characterized by the formation of one or two flagella and by the presence/absence of flagellar rotation and proximodistal fusion between the flagellum/a and the cytoplasmic extension. All studied cyclophyllideans present spermiogenesis of pattern 3 or 4, except for mesocestoidids [32, 35] (see Table 1).

The spermatozoa of tapeworms are filiform cells, tapered at both extremities and lacking mitochondria. The absence of mitochondria in eucestode spermatozoa is a clear spermatological synapomorphy. Considering diverse characters, Levron *et al.* [13] described seven types of spermatozoa in the eucestodes. These characters include the presence of one or two axonemes, the parallel or spiralled pattern of cortical microtubules and nucleus, and the presence/absence of crested bodies, periaxonemal sheath and intracytoplasmic walls. All cyclophyllideans exhibit spermatozoa of types V, VI or VII, containing only one axoneme, with crested body/ies, twisted cortical microtubules and a nucleus spiralled around the axoneme

(see Table 2). Some characters such as the presence/absence of a periaxonemal sheath surrounding the axoneme and the presence/absence of transverse intracytoplasmic walls connecting the layer of cortical microtubules and the periaxonemal sheath allow differentiating these three types of sperm cells in cyclophyllideans. Mesocestoidids are the unique exception in the model of sperm cells within cyclophyllideans, showing a parallel disposition of cortical microtubules [32, 35] and thus a type IV spermatozoon.

2.1. Family Anoplocephalidae

In the family Anoplocephalidae there are ultrastructural studies on the spermiogenesis and/or the spermatozoon in 16 species belonging to the different subfamilies of anoplocephalids. These are *Anoplocephaloides dentata*, *Aporina delafondi*, *Gallegoides arfaai*, *Moniezia benedenii*, *Moniezia expansa*, *Monoecocestus americanus*, *Mosgovoyia ctenoides*, *Paranoplocephala omphalodes* and *Sudarikovina taterae* (Anoplocephalinae) [29, 36-44], *Inermicapsifer guineensis* and *Inermicapsifer madagascariensis* (Inermicapsiferinae) [45, 46], *Mathevotaenia herpestis* and *Oochoristica agamae* (Linstowiinae) [47, 48], and *Avitellina centripunctata*, *Avitellina lahorea*, *Stilesia globipunctata* and *Thysaniezia ovilla* (Thysanosomatinae) [49-52]. The type of sperm cells varies in this family. Thus, the studied anoplocephalines and also *Thysaniezia* [29, 36, 37, 39, 42-44, 52] exhibit the type V sperm of Levron *et al.* [13], which is mainly characterized by the absence of periaxonemal sheath and intracytoplasmic walls (Fig. 1a). Both *Inermicapsifer* studied species exhibit type VII sperm, characterized by the presence of periaxonemal sheath and intracytoplasmic walls. Moreover, preliminary observations on another inermicapsiferine (*Thysanotaenia congolensis*) show the same type VII sperm cells (Fig. 1d). In the Linstowiinae the spermatozoon is of type VI with periaxonemal sheath but without intracytoplasmic walls. In the subfamily Thysanosomatinae the three studied genera exhibit three different types of male gametes: the above mentioned *Thysaniezia* presents a type V spermatozoon [52], whereas *Stilesia* presents a type VI spermatozoon [51] and *Avitellina* presents a type VII spermatozoon [49].

Crested body or bodies always mark the anterior extremity of the spermatozoon, constituting a constant character in all cyclophyllideans. In this order the number of crested bodies is usually one or two. Most anoplocephalids exhibit one or two crested bodies in the anterior spermatozoon extremity (see Table 2). However, there are two species belonging to the subfamily Anoplocephalinae that exhibit more than two

crested bodies, namely *A. delafondi* [37] with five and *S. taterae* [44] with seven crested bodies.

In inermicapsiferines only scarce data on spermatogenesis of *I. madagascariensis* in known [46], and details on spermiogenesis are not given. For the Anoplocephalinae in which spermiogenesis has been studied [36-38, 40, 42, 44], this process follows the type 4 of Bâ & Marchand [7] characterized by the absence of proximodistal fusion. In the Linstowiinae, pattern 3 spermiogenesis has been described in *M. herpestis* [47]. For the Thysanosomatinae only data on *T. ovilla* are known and spermiogenesis follows the pattern 4 [52].

Table 1. Ultrastructural data on spermiogenesis in cyclophyllideans.

Family and subfamily	**Character**				
	Type*	**SR**	**IB**	**FR**	**PF**
Anoplocephalidae					
Anoplocephalinae	4	-/vsr	-	-	-
Inermicapsiferinae	?	?	?	?	?
Linstowiinae	3	-	-	-	+
Thysanosomatinae	4	-	-	-	-
Catenotaeniidae					
Catenotaeniinae	3	-	-	+ (<90º)	+
Skrjabinotaeniinae	?	?	?	?	?
Davaineidae	3	-	-	-	+
Dilepididae	4	-	-	-	-
Dipylidiidae	3	+/vsr	-	-	+
Gryporhynchidae	4	-	-	-	-
Hymenolepididae	4	-	-	-	-
Mesocestoididae	2	+	+	+ (90º)	+
Metadilepididae	3	vsr	-	-	+
Nematotaeniidae	3	-	-	-	+
Paruterinidae	3	vsr	-	+ (<90º)	+
Taeniidae					
Echinococcinae	3	vsr	?	?	+
Taeniinae	3	-/vsr	-	+ (<90º)/-	+

FR – flagellar rotation, IB – intercentriolar body, PF – proximodistal fusion, SR – striated rootlets, vsr – vestigial striated rootlets, ? – unknown data, +/- – presence/absence of character, * – type according to Bâ & Marchand [7].

During spermiogenesis, some anoplocephalids such as *A. dentata*, *G. arfaai*, *M. expansa* and *M. ctenoides* exhibit thin striated rootlets or spiral rootlets associated to centrioles [36, 38, 40, 42]. In order to increase homogeneity in the designation of the previously described non-typical striated rootlets, the common designation of vestigial striated rootlets was proposed [see 38]. Similar root-like structures, named as thin, filamentous or vestigial striated rootlets, also occur in species from other families (Dipylidiidae, Metadilepididae, Paruterinidae and Taeniidae) [21, 53-58].

2.2. Family Catenotaeniidae

In catenotaeniids only two species were studied, *Catenotaenia pusilla* (Catenotaeniinae) and *Skrjabinotaenia lobata* (Skrjabinotaeniinae) [59, 60]. The spermatozoon has been characterized in both subfamilies and corresponds to the type VI [13]. With respect to spermiogenesis, there is data concerning only *C. pusilla* [59] and it follows the pattern 3 [7]. However, a flagellar rotation of about 45º was observed in this species [59].

Table 2. Ultrastructural data on the spermatozoon in cyclophyllideans.

Family and subfamily	**Character**						
	Type*	**CB**	**CM**	**N**	**PS**	**IW**	**G**
Anoplocephalidae							
Anoplocephalinae	V	2, 5, 7	15-45º	Spi	-	-	+
Inermicapsiferinae	VII	2	45º	Spi	+	+	-
Linstowiinae	VI	1	40º	Spi	+	-	-
Thysanosomatinae	V/VI/VII	1, 2	35-50º	Spi	+/-	+/-	+/-
Catenotaeniidae	VI	2	40º	Spi	+	-	-
Davaineidae	VII	2	45-60º	Spi	+	+	+
Dilepididae	VI	1, 2	30-45º	Spi	+	-	+
Dipylidiidae	VI	1	40º	Spi	+	-	-
Gryporhynchidae	VI	1	45º	Spi	+	-	+
Hymenolepididae	V	6, 8, 9, 10, 12	15-30º	Spi	-	-	+
Mesocestoididae	IV	1	0º	Spi	-	-	+
Metadilepididae	VII	1	30-40º	Spi	+	+	-
Nematotaeniidae	V	1	Spi	Spi	-	-	+
Paruterinidae	VII	1	35-40º	Spi	+	+	+
Taeniidae							
Echinococcinae	VII	1, 2?	Spi	Spi	+	+	-
Taeniinae	VII	1	40-50º	Spi	+	+	-

CB – number of crested bodies, CM – angle of cortical microtubules, G – electron-dense granules, IW – intracytoplasmic walls, N – nucleus, PS – periaxonemal sheath, Spi – spiralled, ? – unknown data, +/- – presence/absence of character, * – type according to Levron *et al.* [13].

2.3. Family Davaineidae

Seven species of davaineids were analysed: *Cotugnia polyacantha*, *Paroniella reynoldsae*, *Raillietina baeri*, *Raillietina carneostrobilata*, *Raillietina micracantha*, *Raillietina tunetensis* and *Raillietina vinagoi* [30, 61-66]. The spermatozoon in this family corresponds to type VII according to Levron *et al* [13] (Fig. 1e). In davaineids, spermiogenesis has been studied only in *R. micracantha* and *R. tunetensis* [30, 65]. In both cases spermiogenesis follows the pattern 3 of Bâ & Marchand [7].

2.4. Family Dilepididae

There are spermatological studies concerning five species of Dilepididae. These are *Anomotaenia quelea*, *Angularella beema*, *Dilepis undula*, *Kowalewskiella glareola* and *Molluscotaenia crassiscolex* [18, 31, 67-69]. The ultrastructural organization of the mature spermatozoon of dilepidids corresponds to the type VI of Levron *et al.* [13] (Fig. 1c). Available data on spermiogenesis concerns only *A. beema* and *M. crassiscolex* [31, 67], corresponding to the pattern 4 of Bâ & Marchand [7].

2.5. Family Dipylidiidae

There are ultrastructural studies on the spermiogenesis and the spermatozoon of *Dipylidium caninum*, *Joyeuxiella echinorhyncoides* and *Joyeuxiella pasqualei* [53, 54, 70, 71]. The ultrastructural organization of their spermatozoa corresponds to the type VI [13]. Spermiogenesis in these species is also well described and follows the pattern 3 [7]. However, striated rootlets are described in these species. In the case of *Joyeuxiella* spp. two well-developed striated rootlets associated to both centrioles were observed [71]. In *D. caninum* there are several thin striated rootlets [53, 54].

2.6. Family Gryporhynchidae

In this family, only *Valipora mutabilis* [72] has been studied. Spermiogenesis follows the pattern 4 of Bâ & Marchand [7] and the mature spermatozoon is of type VI of Levron *et al.* [13].

2.7. Family Hymenolepididae

Numerous species of this family have been the subject of spermatological studies. To our knowledge these are *Cladogynia*

guberiana, *Cladogynia serrata*, *Dicranotaenia coronula*, *Diorchis parvogenitalis*, *Echinocotyle dolosa*, *Hymenolepis diminuta*, *Hymenolepis sulcata*, *Monorcholepis dujardini*, *Rodentolepis fraterna*, *Rodentolepis microstoma*, *Rodentolepis myoxi*, *Rodentolepis nana* and *Rodentolepis straminea* [73-85].

However, most of them consist in incomplete and partial analyses of the spermatozoon. There are consistent studies of the spermatozoon in the case of *C. serrata*, *E. dolosa*, *R. microstoma*, *R. nana* and *R. straminea* [74, 77, 83-85] and the ultrastructural organization of sperm cells for all these species corresponds to the type V [13].

Spermiogenesis is well known for *R. microstoma* and *R. nana* [83, 84], corresponding to the pattern 4 of Bâ & Marchand [7].

In hymenolepidids the high number of crested bodies present in the spermatozoon is particularly interesting (see Table 2). There are six crested bodies in *C. serrata* [74], up to eight in *E. dolosa* and *R. straminea* [77, 85], up to nine in *H. sulcata* and *R. myoxi* [81], up to 10 in *R. fraterna* [81] and 12 in *H. nana* [84].

2.8. Family Mesocestoididae

The spermiogenesis and the ultrastructural organization of the spermatozoon of two mesocestoidids (*Mesocestoides lineatus* and *Mesocestoides litteratus*) have been studied [32, 35].

In contrast with the remaining cyclophyllideans, these species show a parallel arrangement of cortical microtubules in the spermatozoon and thus, the sperm cell is of type IV of Levron *et al.* [13] (Fig. 1b).

With respect to spermiogenesis, the pattern is also particular in comparison with the remaining cyclophyllideans. Mesocestoidids follow the pattern 2 of Bâ & Marchand [7], which is characterized by the formation of a single flagellum that rotates and fuses proximodistally with a cytoplasmic extension. Both species also exhibit a reduced intercentriolar body and well-developed striated rootlets associated to centrioles in the zone of differentiation [32, 35].

Both the parallel arrangement of cortical microtubules in the mature spermatozoon and the pattern 2 of spermiogenesis with their associated characteristics are unique within cyclophyllideans and constitute the plesiomorphic condition of these characters. These ultrastructural results are in agreement with other morphologic and molecular data, confirming the problematic systematics of mesocestoidids [see 32, 35].

2.9. Family Metadilepididae

Only *Skrjabinoporus merops* has been analysed in this family [55]. The spermatozoon is of type VII of Levron *et al.* [13], containing both periaxonemal sheath and intracytoplasmic walls. Spermiogenesis has also been described and follows the pattern 3 of Bâ & Marchand [7]. Additionally, vestigial striated rootlets associated to centrioles were observed [55].

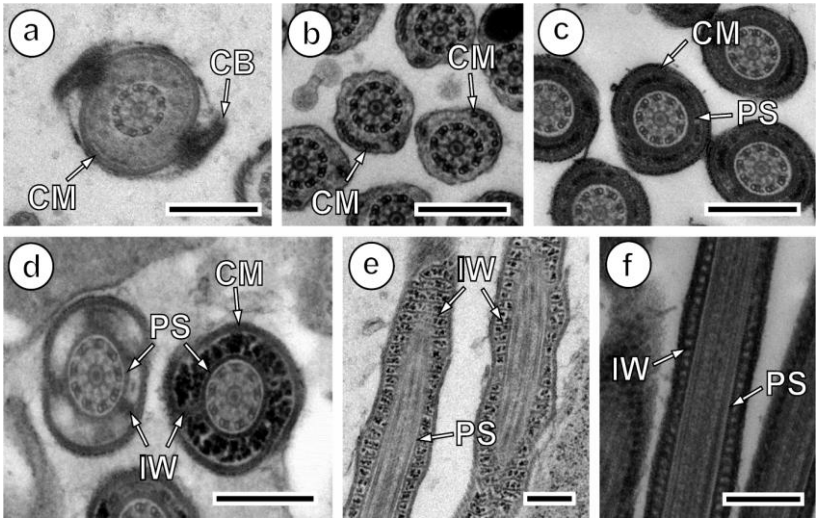

Figure 1. Longitudinal and cross-sections of spermatozoa of a) *Gallegoides arfaai*, b) *Mesocestoides lineatus*, c) *Molluscotaenia crassiscolex*, d) *Thysanotaenia congolensis*, e) *Raillietina micracantha*, and f) *Taenia taeniaeformis*. CB – crested bodies, CM – cortical microtubules, IW – intracytoplasmic walls, PS – periaxonemal sheath. Scale bars = 0.3 μm.

2.10. Family Nematotaeniidae

To date, spermatological data from nematotaeniids are available concerning only *Cylindrotaenia hickmani* and *Nematotaenia chantalae* [86-88]. In *C. hickmani* there are two ultrastructural studies on the cirrus pouch and sperm ducts [86, 87] in which some sections of spermatozoa are shown. As in *N. chantalae* [88], the ultrastructural organization of the spermatozoon seems to be of type V [13]. Concerning spermiogenesis, only data on

N. chantalae exists [88] and this process corresponds to pattern 3 of Bâ & Marchand [7].

2.11. Family Paruterinidae

Three paruterinids were the subject of ultrastructural studies on spermiogenesis and on the mature spermatozoon: *Anonchotaenia globata*, *Notopentorchis* sp. and *Triaenorhina rectangula* [21, 56, 57]. All three paruterinids exhibit a type VII spermatozoon according to the Levron *et al.* models [13] and the pattern 3 spermiogenesis of Bâ & Marchand [7]. As mentioned above, paruterinids present vestigial striated rootlets associated to centrioles. Moreover, a non-parallel development of the free flagellum was described and thus, a flagellar rotation occurs before the proximodistal fusion between flagellum and cytoplasmic extension.

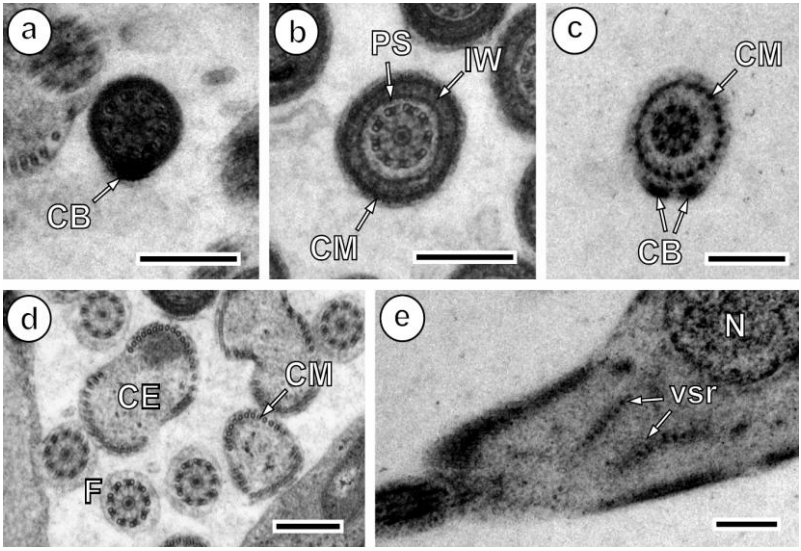

Figure 2. Spermiogenesis and the spermatozoon of *Echinococcus* spp. a) Spermatozoon of *E. granulosus*, b) Spermatozoon of *E. multilocularis*, c and d) Spermatids of *E. granulosus*, and e) Zone of differentiation of *E. multilocularis*. CB – crested bodies, CE – cytoplasmic extension, CM – cortical microtubules, F – flagellum, IW – intracytoplasmic walls, N – nucleus, PS – periaxonemal sheath, vsr – vestigial striated rootlets. Scale bars = 0.3 μm.

2.12. Family Taeniidae

In this family there are spermatological studies on eight species of the genus *Taenia*, namely *T. crassiceps*, *T. hydatigena*, *T. mustelae*, *T. parva*, *T. pisiformis*, *T. saginata*, *T. solium* and *T. taeniaeformis* [27, 33, 58, 89-96], and in two species of the genus *Echinococcus*, namely *E. granulosus* and *E. multilocularis* [97-99]. However, for some of these species, the spermatological data are only partial [89, 90, 93, 94, 96, 97-99].

In the genus *Taenia*, a type VII permatozoon of Levron *et al.* [13] was described (Fig. 1f). Spermiogenesis follows the pattern 3 of Bâ & Marchand [7], although good descriptions are published concerning only two species, *T. parva* and *T. taeniaeformis* [58, 93]. In both species a flagellar rotation was described and in the case of *T. taeniaeformis*, additionally, the presence of vestigial striated rootlets was illustrated [58].

In the genus *Echinococcus* there are some published papers that show scarce results on *E. granulosus* and *E. multilocularis* [97-99]. Nevertheless, new preliminary observations on these two species indicate a pattern 3 spermiogenesis of Bâ & Marchand [7] with the presence of vestigial striated rootlets associated to centrioles in both species (Fig. 2d,e). Concerning the spermatozoon, the presence of both periaxonemal sheath and transverse intracytoplasmic walls characterize the sperm cell as belonging to the type VII of Levron *et al.* [13] (Fig. 2a,b). In the case of *E. multilocularis*, two crested bodies have been observed during spermiogenesis, but this fact is still to be confirmed in the mature spermatozoon (Fig. 2c).

3. Conclusion

The present review highlights the usefulness of spermatological data for the systematics and phylogenetics of cestodes. Indeed, the last decade of ultrastructural research on spermiogenesis and sperm structure provided extensive information. This fact leads to a considerable increase in the existing dataset of characters suitable for the assessment of phylogenetic relationships of cestodes. In the case of Cyclophyllidea, future research should be focused on species belonging to those families lacking spermatological studies (Acoleidae, Amabiliidae, Dioecocestidae and Progynotaeniidae), but also on other families that have been poorly studied.

In cyclophyllideans, both spermiogenesis patterns and sperm models are quite homogeneous, with the exception of anoplocephalids, for which an important variability is observed. In this Order, the suitability of sperm characters is clearly shown in mesocestoidids or in inermicapsiferines. The plesiomorphic characters present during spermiogenesis and in the mature

spermatozoon of *Mesocestoides* are unique within cyclophyllideans and they are also observed in other primitive groups of tapeworms. Thus, these spermatological data support the separation of the Mesocestoididae from the Cyclophyllidea [see 32, 35]. On the other hand, the available data on the spermatozoa of *Inermicapsifer* and *Thysanotaenia* indicate their proximity to davaineids. However, as it is generally accepted, all these spermatological data should be combined with molecular studies to obtain a more robust phylogeny of cestodes [10-12].

Acknowledgements

The authors are grateful to all the personnel of "Centres Científics i Tecnològics" of the University of Barcelona (CCiTUB) for their support in the preparation of studied samples. This work was financially supported by the European Commission Contract KBBE 2010 1.3-01 265862 (PARAVAC) and by Spanish grants from "Ministerio de Educación y Ciencia" (no. CGL2006-04937/BOS), "Ministerio de Ciencia e Innovación" (no. CGL2009-07759), "Ministerio de Economía y Competitividad" (no. CGL2014-52315-P), AECID (no. A1/035356/11) and AGAUR (nos. 1996-SGR-00003, 1998-SGR-00003, 2000-SGR-00032, 2001-SGR-00088, 2005-SGR-00576, 2009-SGR-403, 2014-SGR-1241).

References

1. Euzet, L., Świderski, Z., Mokhtar-Maamouri, F. 1981, *Ann. Parasitol. (Paris)*, 56, 247.
2. Świderski, Z. 1986, *Proc. XI Int. Cong. Electron Microsc.*, 2959.
3. Justine, J.-L. 1991, *Can. J. Zool.*, 69, 1421.
4. Justine, J.-L. 1995, *Mém. Mus. Natn. Hist. Nat.*, 166, 55.
5. Justine, J.-L. 1998, *J. Parasitol.*, 84, 385.
6. Justine, J.-L. 2001, Interrelationships of the Platyhelminthes. Littlewood, D.T.J., Bray, R.A. (Eds.), Taylor and Francis, London, 231.
7. Bâ, C.T., Marchand, B. 1995, *Mém. Mus. Natn. Hist. Nat.*, 166, 87.
8. Hoberg, E.P., Mariaux, J., Justine, J.-L., Brooks, D.R., Weekes, P.J. 1997, *J. Parasitol.*, 83, 1128.
9. Hoberg, E.P., Gardner, S.L., Campbell, R.A. 1999, *Syst. Parasitol.*, 42, 1.
10. Olson, P.D., Littlewood, D.T.J., Bray, R.A., Mariaux, J. 2001, *Mol. Phylogenet. Evol.*, 19, 443.
11. Waeschenbach, A., Webster, B.L., Bray, R.A., Littlewood, D.T.J. 2007, *Mol. Phylogenet. Evol.*, 45, 311.
12. Waeschenbach, A., Webster, B.L., Littlewood, D.T.J. 2012, *Mol. Phylogenet. Evol.*, 63, 874.
13. Levron, C., Miquel, J., Oros, M., Scholz, T. 2010, *Biol. Rev.*, 85, 523.

14. Marigo, A.M. 2011, PhD Thesis, University of Barcelona, http://www.tdx.cat/handle/10803/109219.
15. Bruňanská, M., Kostič, B. 2012, *Parasitol. Res.*, 110, 141.
16. Bruňanská, M., Matey, V., Nebesářová, J. 2012, *Parasitol. Res.*, 111, 1037.
17. Bâ, A., Quilichini, Y., Ndiaye, P.I., Bâ, C.T., Marchand, B. 2012, *J. Parasitol.*, 98, 502.
18. Bâ, A., Ndiaye, P.I., Bâ, C.T., Miquel, J. 2014, *Zool. Anz.*, 253, 119.
19. Ndiaye, P.I., Quilichini, Y., Bâ, A., Bâ, C.T., Marchand, B. 2012, *Tissue Cell*, 44, 296.
20. Yoneva, A., Levron, C., Ash, A., Scholz, T. 2012, *J. Parasitol.*, 98, 423.
21. Yoneva, A., Levron, C., Nikolov, P.N., Mizinska, Y., Mariaux, J., Georgiev, B.B. 2012, *Parasitol. Res.*, 111, 135.
22. Yoneva, A., Levron, C., Oros, M., Orosová, M., Scholz, T. 2012, *Folia Parasitol.*, 59, 179.
23. Yoneva, A., Kuchta, R., Scholz, T. 2013, *Zool. Anz.*, 252, 486.
24. Cielocha, J.J., Yoneva, A., Cantino, M.E., Daniels, S., Jensen, K. 2013, *Invert. Biol.*, 132, 315.
25. Levron, C., Yoneva, A., Kalbe, M. 2013, *Acta Zool. (Stockh.)*, 94, 240.
26. Miquel, J., Świderski, Z. 2013, *C. R. Biologies*, 336, 65.
27. Miquel, J., Khallaayoune, K., Azzouz-Maache, S., Pétavy, A.-F. 2015, *Parasitol. Res.*, 114, 201.
28. Global Cestode Database. http://tapeworms.uconn.edu/
29. Miquel, J., Świderski, Z., Młocicki, D., Marchand, B. 2004, *Parasitol. Res.*, 94, 460.
30. Miquel, J., Torres, J., Foronda, P., Feliu, C. 2010, *Acta Zool. (Stockh.)*, 91, 212.
31. Marigo, A. M., Bâ, C. T., Miquel, J. 2011, *Acta Zool. (Stockh.)*, 92, 116.
32. Miquel, J., Eira, C., Świderski, Z., Conn, D. B. 2007, *J. Parasitol.*, 93, 545.
33. Miquel, J., Foronda, P., Torres, J., Świderski, Z., Feliu, C. 2009, *Parasitol. Res.*, 104, 1477.
34. Reynolds, E. S. 1963, *J. Cell Biol.*, 17, 208.
35. Miquel, J., Feliu, C., Marchand, B. 1999, *Int. J. Parasitol.*, 29, 499.
36. Miquel, J., Marchand, B. 1998, *J. Parasitol.*, 84, 1128.
37. Bâ, C. T., Marchand, B. 1994, *Int. J. Parasitol.*, 24, 225.
38. Miquel, J., Świderski, Z., Młocicki, D., Eira, C., Marchand, B. 2005, *Acta Parasitol.*, 50, 132.
39. Bâ, C. T., Marchand, B. 1992, *Ann. Parasitol. Hum. Comp.*, 67, 111.
40. Li, H.-Y., Brennan, J. P., Halton, D. W. 2003, *Acta Zool. Sin.*, 49, 370.
41. MacKinnon, B. M., Burt, M. D. B. 1984, *Can. J. Zool.*, 62, 1059.
42. Eira, C., Miquel, J., Vingada, J., Torres, J. 2006, *J. Parasitol.*, 92, 708.
43. Miquel, J., Marchand, B. 1998, *Parasitol. Res.*, 84, 239.
44. Bâ, A., Bâ, C. T., Marchand, B. 2000, *J. Submicrosc. Cytol. Pathol.*, 32, 137.
45. Bâ, C. T., Marchand, B. 1994, *Can. J. Zool.*, 72, 1633.
46. Świderski, Z. 1984, *Proc. Electron Microsc. Soc. South Africa*, 129.
47. Bâ, C. T., Marchand, B. 1994, *Acta Zool. (Stockh.)*, 75, 167.
48. Świderski, Z., Subilia, L. 1985, *Proc. Electron Microsc. Soc. South Africa*, 185.

49. Bâ, C. T., Marchand, B. 1994, *Acta Zool. (Stockh.)*, 75, 161.
50. Vijayalakshmi, V., Ramalingam, K. 2006, *J. Paras. Dis.*, 30, 134.
51. Bâ, C. T., Marchand, B. 1992, *J. Submicrosc. Cytol. Pathol.*, 24, 29.
52. Bâ, C. T., Marchand, B., Mattei, X. 1991, *J. Submicrosc. Cytol. Pathol.*, 23, 605.
53. Miquel, J., Bâ, C. T., Marchand, B. 1998, *Int. J. Parasitol.*, 28, 1453.
54. Miquel, J., Świderski, Z., Marchand, B. 2005, *Acta Parasitol.*, 50, 65.
55. Yoneva, A., Georgieva, K., Mizinska, Y., Georgiev, B. B., Stoitsova, S. R. 2006, *Acta Parasitol.*, 51, 200.
56. Yoneva, A., Georgieva, K., Mizinska, Y., Nikolov, P. N., Georgiev, B. B., Stoitsova, S. R. 2010, *Acta Zool. (Stockh.)*, 91, 184.
57. Yoneva, A., Georgieva, K., Nikolov, P. N., Mizinska, Y., Georgiev, B. B., Stoitsova, S. R. 2009, *Folia Parasitol.*, 56, 275.
58. Miquel, J., Świderski, Z., Foronda, P., Torres, J., Feliu, C. 2009, *Acta Parasitol.*, 54, 230.
59. Hidalgo, C., Miquel, J., Torres, J., Marchand, B. 2000, *J. Helminthol.*, 74, 73.
60. Miquel, J., Bâ, C. T., Marchand, B. 1997, *J. Submicrosc. Cytol. Pathol.*, 29, 521.
61. Bâ, C. T., Marchand, B. 1994, *Parasite*, 1, 51.
62. Bâ, C. T., Bâ, A., Marchand, B. 2005, *Acta Parasitol.*, 50, 208.
63. Bâ, C. T., Bâ, A., Marchand, B. 2005, *Parasitol. Res.*, 97, 173.
64. Polyakova-Krusteva, O., Vassilev, I. 1973, *Bull. Central Helminthol. Lab. (Sofia)*, 16, 153.
65. Bâ, C. T., Marchand, B. 1994, *Int. J. Parasitol.*, 24, 237.
66. Taeleb, A. A., Gamil, I. S. 2011, *Acta Parasitol. Glob.*, 2, 11.
67. Yoneva, A., Miquel, J., Świderski, Z., Georgieva, K., Mizinska, Y., Georgiev, B. B. 2006, *Acta Parasitol.*, 51, 264.
68. Świderski, Z., Salamatin, R. V., Tkach, V. V. 2000, *Vest. Zool.*, 34, 3.
69. Świderski, Z., Salamatin, R. V., Kornyushin, V. V. 2002, *Proc. 12th Conf. Ukrainian Soc. Parasitol.*, 132.
70. Miquel, J., Marchand, B. 1997, *Parasitol. Res.*, 83, 349.
71. Ndiaye, P. I., Agostini, S., Miquel, J., Marchand, B. 2003, *Parasitol. Res.*, 91, 175.
72. Yoneva, A., Świderski, Z., Georgieva, K., Nikolov, P. N., Mizinska, Y., Georgiev, B. B. 2008, *Parasitol. Res.*, 103, 1397.
73. Świderski, Z., Chomicz, L. 1994, *Proc. 13th Int. Cong. Electron Microsc.*, 707.
74. Bâ, C. T., Marchand, B. 1993, *J. Submicrosc. Cytol. Pathol.*, 25, 233.
75. Chomicz, L., Świderski, Z. 1992, *Proc. 5th Asia-Pacific Electron Microsc. Conf.*, 324.
76. Chomicz, L., Świderski, Z. 1992, *Proc. 5th Asia-Pacific Electron Microsc. Conf.*, 330.
77. Bâ, A., Bâ, C. T., Marchand, B. 2002, *Acta Parasitol.*, 47, 131.
78. Rosario, B. 1964, *J. Ultrastruct. Res.*, 11, 412.
79. Kelsoe, G. H., Ubelaker, J. E., Allison, V. F. 1977, *Z. Parasitenkd.*, 54, 175.
80. Robinson, J. M., Bogitsh, B. J. 1978, *Z. Parasitenkd.*, 56, 81.
81. Miquel, J., Ndiaye, P. I., Feliu, C. 2007, *Rev. Ibér. Parasitol.*, 67, 27.
82. Świderski, Z. P., Tkach, V. V. 1996, *Proc. Sixth Asia-Pacific Conf. Electron Microsc.*, 507.

83. Bâ, C. T., Marchand, B. 1998, *Microsc. Res. Tech*., 42, 218.
84. Bâ, C. T., Marchand, B. 1992, *Mol. Reprod. Dev.*, 33, 39.
85. Bâ, C. T., Marchand, B. 1996, *Invert. Reprod. Dev.*, 29, 243.
86. Jones, M. K. 1989, *Int. J. Parasitol.*, 19, 919.
87. Jones, M. K. 1994, *Acta Zool. (Stockh.)*, 75, 269.
88. Mokhtar-Maamouri, F., Azzouz-Draoui, N. 1990, *Ann. Parasitol. Hum. Comp.*, 65, 221.
89. Willms, K., Robert, L., Jiménez, J. A., Everhart, M., Kuhn, R. E. 2004, *Parasitol. Res.*, 93, 262.
90. Willms, K., Robert, L. 2007, *Parasitol. Res.*, 101, 967.
91. Miquel, J., Hidalgo, C., Feliu, C., Marchand, B. 2000, *Invert. Reprod. Dev.*, 38, 43.
92. Ndiaye, P. I., Miquel, J., Marchand, B. 2003, *Parasitol. Res.*, 89, 34.
93. Tian, X., Yuan, L., Huo, X., Han, X., Li, Y., Xu, M., Lu, M., Dai, J., Dong, L. 1998, *Chin. J. Parasitol. Paras. Dis.*, 16, 269.
94. Tian, X., Yuan, L., Li, Y., Huo, X., Han, X., Xu, M., Lu, M., Dai, J., Dong, L. 1998, *Chin. J. Parasitol. Paras. Dis.*, 16, 209.
95. Bâ, A., Bâ, C. T., Quilichini, Y., Dieng, T., Marchand, B. 2011, *Parasitol. Res.*, 108, 831.
96. Willms, K., Caro, J. A., Robert, L. 2003, *Parasitol. Res.*, 90, 479.
97. Morseth, D. J. 1969, *Exp. Parasitol.*, 24, 47.
98. Barrett, N. J., Smyth, J. D. 1983, *Parasitology*, 87, li.
99. Shi, D. Z., Liu, D. S., Wang, S. K., Craig, P. S. 1994, *Chin. J. Parasit. Dis. Contr.*, 7, 40.

Research Signpost
37/661 (2), Fort P.O.
Trivandrum-695 023
Kerala, India

Recent Advances in Pharmaceutical Sciences V, 2015: 117-132 ISBN: 978-81-308-0561-0
Editors: Diego Muñoz-Torrero, M. Pilar Vinardell and Javier Palazón

8. Dietary spray-dried animal plasma alleviates mucosal inflammation in experimental models

Anna Pérez-Bosque and Miquel Moretó
Grup de Fisiologia i Nutrició Experimental, Departament de Fisiologia, Facultat de Farmàcia
Institut de Recerca en Nutrició i Seguretat Alimentària, Universitat de Barcelona, Spain

Abstract. The intestinal and bronchoalveolar mucosae contribute to homeostasis by preventing the entrance of biological and chemical agents that could alter the stability of the system. In this review, we summarise the main effects of dietary supplementation with spray-dried plasma (SDP), a complex mixture of biologically active functional components, on two models of acute inflammation; a murine model of intestinal inflammation, based on the administration of *S. aureus* enterotoxin B (SEB), and a model of acute lung inflammation, using mice challenged with lipopolysaccharide from *E. coli* (LPS). Oral SDP modulates the immune response of the intestinal mucosa and restores the barrier function of the epithelium, preventing most of the effects of SEB on defensin expression, tight-junction permeability and mucosal cytokine production. In the lung, SDP supplementation partially prevents the LPS-induced release of pro-inflammatory cytokines, an effect that involves the participation of the common mucosal immune system. In both models, the effects of SDP are mediated by an increased T-reg response and enhanced release of anti-inflammatory cytokines that contribute to mucosal homeostasis.

Correspondence/Reprint request: Dr. Anna Pérez-Bosque, Department of Physiology, University of Barcelona Spain. E-mail: anna.perez@ub.edu

Introduction

Spray-dried plasma (SDP) is a protein-rich product obtained from the industrial fractionation of blood from porcine and bovine animals slaughtered for human consumption. Blood is collected with an anticoagulant, centrifuged to separate blood cells and spray-dried using high pressure and a temperature over 80ºC for a very short period of time. With this procedure, proteins are not denaturalised and their biological activity is mostly preserved [1].

At the end of the last century, SDP was initially proposed as a protein source for piglets [2]. Since then, many studies have demonstrated that SDP improves piglet and calf performance, and today it is widely used as an alternative to the use of antibiotics as growth promoters [3]. Numerous studies have shown that feeding SDP of either bovine or porcine origin reduces mortality and morbidity in various animal species challenged with pathogenic bacteria (*E. coli*, *Salmonella*), viruses (rotavirus, coronavirus, white spot syndrome virus) or protozoa (*C. parvum*) [4;5;6].

In addition, a greater efficacy of SDP has been described in younger pigs which have a less mature immune system [7], or in pigs kept under less hygienic conditions [8].

1. Effects of SDP on acute intestinal inflammation

The gastrointestinal tract provides a protective interface between the internal milieu and the permanent challenge resulting from microorganisms and antigens derived from food present in the lumen. The intestinal mucosa regulates the penetration of luminal antigens and the generation of immunologic responses in the gut, and dysregulation of these barrier mechanisms causes intestinal inflammation [9].

Since the host's immune responses can be modulated by diet [10], the dietary approach offers a therapeutic potential in conditions associated with gut barrier dysfunction and inflammatory response.

1.1. Intestinal barrier

A key function of the intestinal epithelium is to serve as a selective barrier allowing the uptake of nutrients while excluding toxins and microorganisms. Mucosal permeability mainly depends on the capacity of tight-junctions to efficiently seal the apical poles of epithelial cells. The

space between cells is occupied by interlocking proteins such as claudins, occludin or E-cadherin that bind scaffolding proteins such as ZO-1 and β-catenin which, in turn, link them to the cellular cytoskeleton [11]. An acute change of the intestinal barrier function contributes to disease pathogenesis, especially when the intestine is challenged by luminal antigens. Several bacterial products, such as Clostridium and Vibrio toxins, change the localisation of several tight-junction proteins [12] or reduce the number of strands in the tight-junction [13].

Staphylococcal enterotoxin B (SEB) reduced the expression of β-catenin in a rodent model of intestinal inflammation [14] and SDP supplementation prevented this effect (**Figure 1A**). Moreover, SEB treatment significantly increased the flux of 4 kD FITC-dextran (FD4, a fluorescent tracer of paracellular permeability) across the intestinal wall and SDP supplementation prevented this effect (**Figure 1B**). The effects of SEB on intestinal permeability were similar to those described in SEB-injected mice (15). β-catenin expression was negatively correlated with FD4 flux, suggesting that the increases in dextran flux are paralleled by a reduction in β-catenin expression (**Figure 1C**). These results indicate that the increase in FD4 flux induced by SEB treatment is associated with a reduction in the tightness of the epithelial junction complex and that SDP dietary supplementation resulted in complete recovery. The effects of SDP supplementation in reducing a toxin-induced increase in mucosal permeability may prevent the passage of microbial and food antigens to the interstitial space, thereby avoiding local inflammation [16].

Enterotoxins can also have indirect effects by inducing the release of pro-inflammatory cytokines such as IFN-γ and TNF-α. Both cytokines increase epithelial permeability by reducing the expression of β-catenin [17]. SEB also stimulates the secretion of IFN-γ and TNF-α from lymphocytes [18;19], which can disassemble tight-junction protein complexes [20] or reduce their expression [21;22], thus enhancing paracellular permeability of microvascular endothelial cells.

Mucosal homeostasis is also protected by mucosal defensins secreted by both Paneth cells and enterocytes. These are antimicrobial peptides that regulate the composition and number of luminal colonising microbes present in the small intestine, and they play an important role in reducing pathogen concentration in the intestinal lumen. Studies in humans indicate that reduced Paneth cell defensin expression may be a key pathogenic factor in ileal Crohn's disease, because it changes the profile of the colonising microbiota [23].

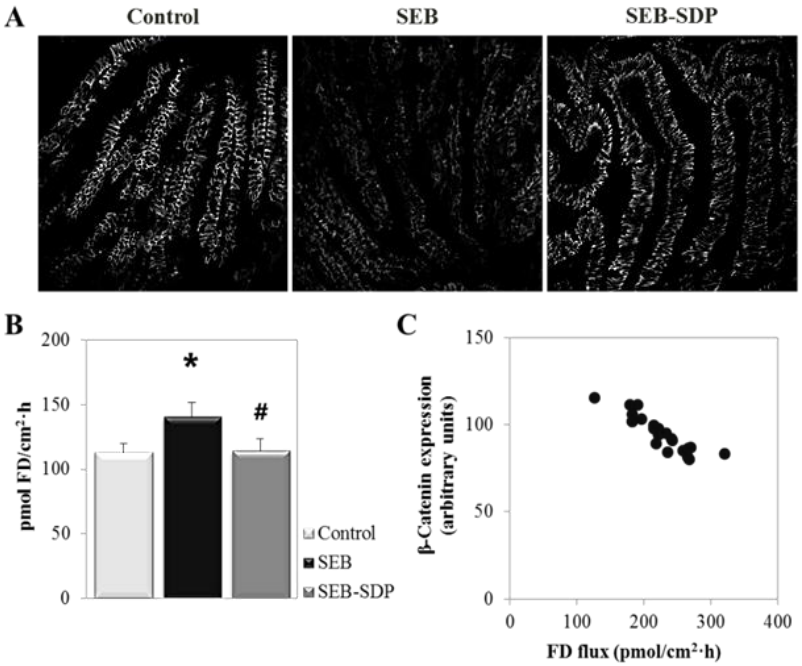

Figure 1. SDP effects on intestinal barrier function in acute inflammation (with permission from Pérez-Bosque et al., 2006)**.** Panel A shows representative images of β-catenin immunohistochemical localisation in jejunum from Control, SEB and SEB-SDP rats. Panel B shows the FITC-dextran (FD) flux across the intestinal wall of rat jejunum measured in an Ussing chamber. Results are expressed as means ± SEM (7-10 animals). Symbols indicate significant differences $P<0.05$; *SEB group vs Control group, #SEB-SDP group vs SEB group. Panel C shows the correlation between β-catenin expression and FD flux ($P<0.001$).

In rats, SEB reduces the expression of cryptdin 4 and β-defensin-1 (**Figure 2**). Since cryptdin 4 has the ability to block IL-1β release from LPS-activated monocytes [24], decreased expression of this defensin would result in increased intestinal IL-1β production, rendering the intestine more susceptible to SEB-induced damage and contributing to pathogenesis of inflammatory bowel diseases. β-defensin-1 is constitutively expressed by enterocytes, and when its expression is reduced, there is increased proliferation of several major components of the intestinal microbiota, including *Candida albicans*, *Bacteroides fragilis*, *Enterococcus faecalis* and *Escherichia coli* [25]. SDP restored the physiological production of mucosal

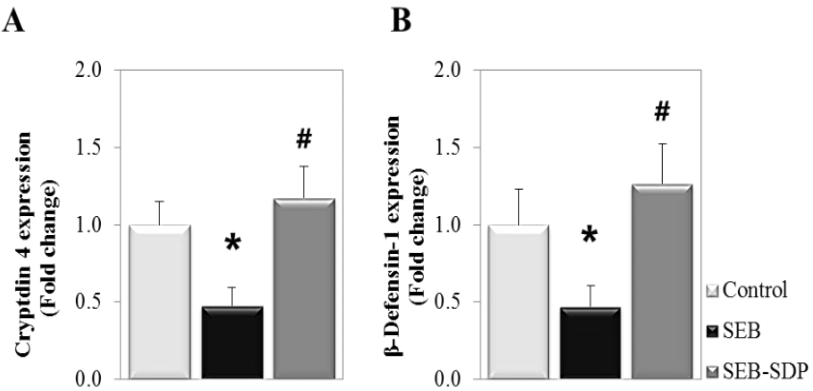

Figure 2. Effects of SDP supplementation on cryptdin 4 (A) and β-defensin 1 (B) expression in acute inflammation. Expression determined by real time PCR. Data are the mean ± SEM of 7-8 rats. Symbols indicate significant differences P<0.05; *SEB group vs Control group, #SEB-SDP group vs SEB group.

defensins, indicating that plasma protein supplementation may contribute to maintenance of intestinal immune homeostasis by maintaining the production of natural innate antibacterial agents, as well as by regulating the production of pro-inflammatory cytokines. The possible relationship between the current effects of SDP on defensin expression, and previous observations showing that dietary plasma proteins induce changes in the microbiota profile associated with a higher resistance to dysbiosis [26], should be further explored.

1.2. Intestinal immune response

Gut-associated lymphoid tissue (GALT) accounts for up to 80% of the mucosal immune system and is distributed along the intestine. It contains a broad network of secondary lymphoid organs, as well as a large number of lymphocytes, including several intestine-specific subpopulations [27]. Upon activation, the intestinal immune system coordinates a strong inflammatory response against invasive pathogenic bacteria (thus promoting protection) while providing inhibitory mechanisms to prevent an excessive response against commensal bacteria (thus promoting tolerance). However, if the immune system is stimulated and the response is not controlled, tissue may be damaged [18].

SEB administration induces a recruitment of neutrophils [28] and eosinophils [29]. The dietary inclusion of SDP does not modify the SEB-induced effects on neutrophil infiltration, but does reduce eosinophil infiltration and the degree of cell degranulation. The SEB challenge also increases the activation of intestinal T-helper lymphocytes present in Peyer's patches (PP), in mucosal *lamina propria* and in the intraepithelial compartment [28;30]. Furthermore, dietary supplementation with SDP prevents the SEB-induced activation of T-helper lymphocytes in all the above mentioned intestinal compartments (**Figure 3A**). SDP reduces the expression of mucosal pro-inflammatory cytokines [19], which is paralleled by a reduction in intestinal activated T cells (**Figure 3B**), consistent with the fact that activated T-helper lymphocytes release pro-inflammatory cytokines to amplify the immune response [31]. Bosi et al. [32] observed that pigs challenged with *E. coli* K88 and fed SDP had a lower intestinal expression of pro-inflammatory cytokines. The effect of SDP on the mucosal cytokine profile reduces mucosal inflammation and prevents changes in mucosal permeability and tight-junctional protein expression following SEB administration [14].

The inducible regulatory T cell (T-reg) population is another component of the mucosal immune system that maintains immunological unresponsiveness to self-antigens and suppresses excessive immune responses that can be deleterious to the host [33]. T-reg cells mediate peripheral T cell tolerance to antigens derived from dietary origin or from the commensal flora. In addition, after antigenic stimulation, T-reg lymphocytes can specifically inhibit the immune response of activated T-helper cells [34], through the expression of characteristic cytokines such as transforming growth factor-β and IL-10, distinct from either Th1 or Th2 cells.

SDP supplementation increased IL-10 production in SEB-challenged rats at both intestinal (Peyer's patches and intestinal mucosa) and systemic levels [19]. Dietary supplementation with plasma proteins increases the mucosal expression of IL-10, which suggests the involvement of this anti-inflammatory cytokine in regulating the production of pro-inflammatory cytokines (**Figure 3C**). This SDP effect on IL-10 contributes to intestinal homeostasis, since this cytokine is involved in the control of the intestinal pathology caused by T cell and innate immune cell activation. In view of the role of IL-10 in the amelioration of intestinal inflammation [35], it is worth noting that SDP can also increase mucosal IL-10 in absence of any challenge.

The observation that the effects of SEB on the release of systemic pro-inflammatory cytokines are small is in agreement with previous results in the spleen [28] and indicates that SEB has little effect on the peripheral immune system. However, the increase in IL-10 concentration in serum is highly correlated to a reduction in the TNF-α concentration (**Figure 3D**).

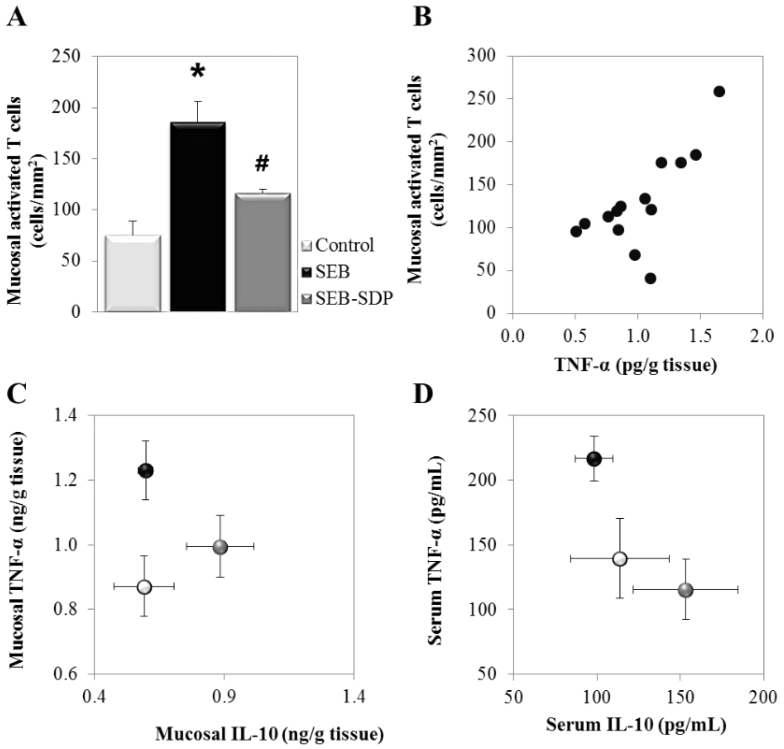

Figure 3. SDP effects on mucosal immune response in acute intestinal inflammation (with permission from Pérez-Bosque et al., 2008)**.** *Panel A* shows activated T lymphocytes in the intestinal lamina propria. Activated T cells were immunolocalised with specific antibodies on jejunal slides from Control, SEB and SEB-SDP rats. Results are expressed as means ± SEM (5-6 animals). Symbols indicate significant differences P<0.05; *SEB group vs Control group, #SEB-SDP group vs SEB group. *Panel B* shows the correlation between the number of activated T cells in the intestinal lamina propria and TNF-α mucosal concentration. The correlation coefficient was R^2=0.6971 (P<0.001). The correlation of TNF-α and IL-10 concentration in the intestinal mucosa and in serum is shown in panels C and D, respectively.

2. Effects of SDP on acute lung inflammation

The observation that SDP not only modulates GALT homeostasis [29] but also affects lymphoid tissue populations in peripheral tissues such as the spleen [36;28] and lung [37] has led to the hypothesis that plasma supplements may also modulate the immune response in non-intestinal mucosal tissues. This hypothesis is supported by the existence of the common mucosal immune system that connects the lymphoid tissue of the gut to the other mucosal areas, that is, nasopharyngeal, bronchoalveolar and genitourinary mucosae [38].

2.1. Common mucosal immune system

The respiratory and gastrointestinal tracts share some structural similarities. Both have an extensive luminal surface area, which is protected from commensal bacteria, pathogens and foreign antigens by a selective epithelial barrier [39] and an overlying mucus-gel layer [40]. These epithelial surfaces cover a mucosa-associated lymphoid tissue composed of resident lymphocytes. This lymphoid tissue regulates antigen sampling, lymphocyte trafficking and mucosal host defence [38]. Together with the genitourinary tract, they represent the main sites of intersection between the environment and the host.

An additional feature of mucosal barrier tissues is their contact with beneficial microbiota. Therefore, these tissues must protect the host from pathogenic challenges while at the same time maintaining a *peaceful coexistence* with the resident microbiota [41].

There is much evidence suggesting that the mucosal immune system is a system-wide organ. Studies have demonstrated that stimulation in one compartment of the mucosal immune system can lead to changes in distal areas. For example, intranasal immunisation results in vaginal protection against genital infection with herpes simplex virus type 2 [42]. Furthermore, the use of antibiotics in neonates has been associated with a greater risk of developing asthma [43], which suggests that alterations in the gut microflora can have an effect on the lungs. Collectively, such studies suggest that the mucosal immune system is actually a large interconnected network with individual components efficiently sharing information [44].

2.2. Pro-inflammatory immune response

In a mouse model of acute lung inflammation induced by inhalation of LPS, the pulmonary response is characterised by leukocyte migration

accompanied by a massive release of pro-inflammatory cytokines and chemokines (**Figure 4A**), which recruit monocytes and neutrophils into the lung airway and into the lung tissue [45]. Dietary inclusion of SDP reduces the innate immune response to LPS inhalation. The reduction in leukocyte numbers in bronchoalveolar lavage fluid (BALF) and lung tissue, the lower concentration of pro-inflammatory cytokines and chemokines in BALF and the lower iNOS expression in lung tissue all suggest a dietary-dependent reduction in the chemical mediators responsible for acute lung injury.

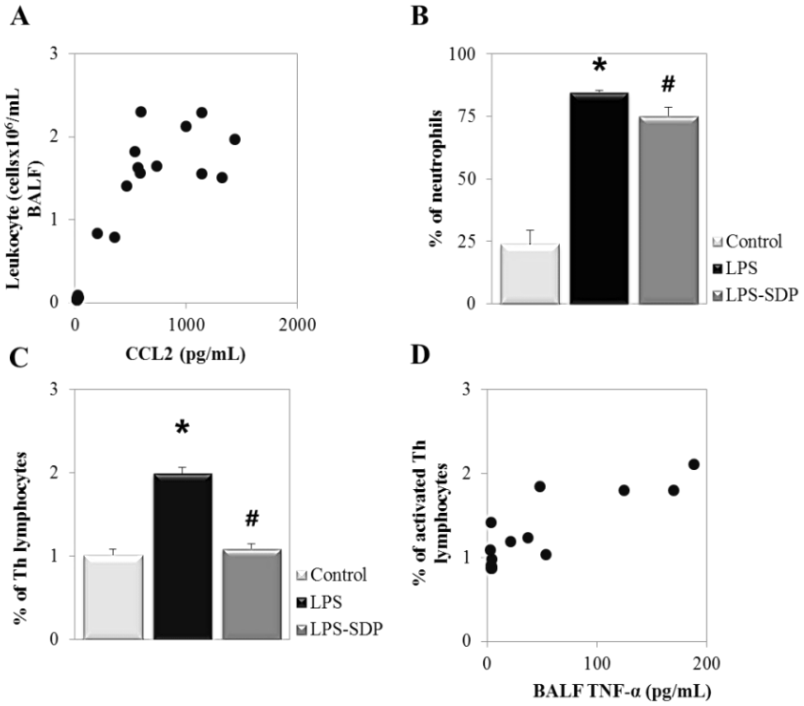

Figure 4. SDP effects on mucosal pro-inflammatory immune response in acute lung inflammation (with permission from Maijò et al., 2012a,b)**.** *Panel A* shows the correlation between leukocyte recruitment into lung airway and chemokine CCL2 concentration in bronchoalveolar lavage fluid (BALF). *Panel B and panel C* show the percentage of activated neutrophils (B) and activated Th lymphocytes (C) in the lung airway. Results are expressed as means ± SEM (5-6 animals). Symbols indicate significant differences P<0.05; *LPS group vs Control group, #LPS-SDP group vs SEB group. *Panel D* shows the correlation between the number of activated Th lymphocytes in BALF and IL-2 BALF concentration.

The LPS challenge increased the percentage of neutrophils by 70% [45]. The primary function of neutrophils is to contain and kill invading microbial pathogens [46]. In BALF and lung tissue, LPS increased the proportion of activated neutrophils (**Figure 4B**) and of activated monocytes [45], as a consequence of the release of large amounts of chemokines. SDP supplementation reduces the percentage of activated neutrophils and monocytes in the lung airway. The effects of SDP on the response of the innate immune system present in the lung are relevant because this system plays an important role in mediating defence against pathogens, detecting tissue damage and regulating tissue health and integrity [47]. Therefore, the lower cell migration and diminished activation of inflammatory cells in pulmonary tissue may reduce potential damage in respiratory epithelium and vascular endothelium associated with the inflammatory response.

LPS challenge also promotes the activation of Th lymphocytes at both local (lung tissue; **Figure 4C**) and systemic (blood) levels. These effects are accompanied by enhanced release of IL-2 in the lung (**Figure 4D**); this cytokine (almost exclusively produced by activated Th cells) promotes proliferation of lymphocytes, macrophages and NK cells [48]. SDP supplementation also reduces the percentage of activated Th lymphocytes and prevents the release of IL-2. This effect is consistent with the anti-inflammatory response previously described for plasma supplements [19].

2.3. Regulatory response during acute lung inflammation

The LPS challenge does not modify the percentage of T-reg cells (**Figure 5A**); however, dietary SDP inclusion increases the percentage of these cells and also reduces the T-activated:T-reg cell ratio (**Figure 5B**). T-reg cells reduce inflammation by counteracting the effects of other Th cells and contribute to suppression of innate and adaptive immune responses [49;50].

SDP promotes IL-10 production in the lung of inflamed mice, and the increases in the concentration of this cytokine are paralleled by increases in the percentage of T-reg cells (**Figure 5C**). Other studies carried out using a LPS model of acute lung inflammation in rats have demonstrated that treatment with IL-10 after endotoxin instillation protects against acute lung injury, possibly by suppressing pulmonary infiltration of activated neutrophils [51]. In the LPS-induced lung inflammation model, as in the

SEB model of intestinal inflammation, it has been shown that the dietary modulation of intestinal inflammation is mediated by an increase in mucosal IL-10 expression, which reduces the release of pro-inflammatory cytokines [19;52] (**Figure 5D**).

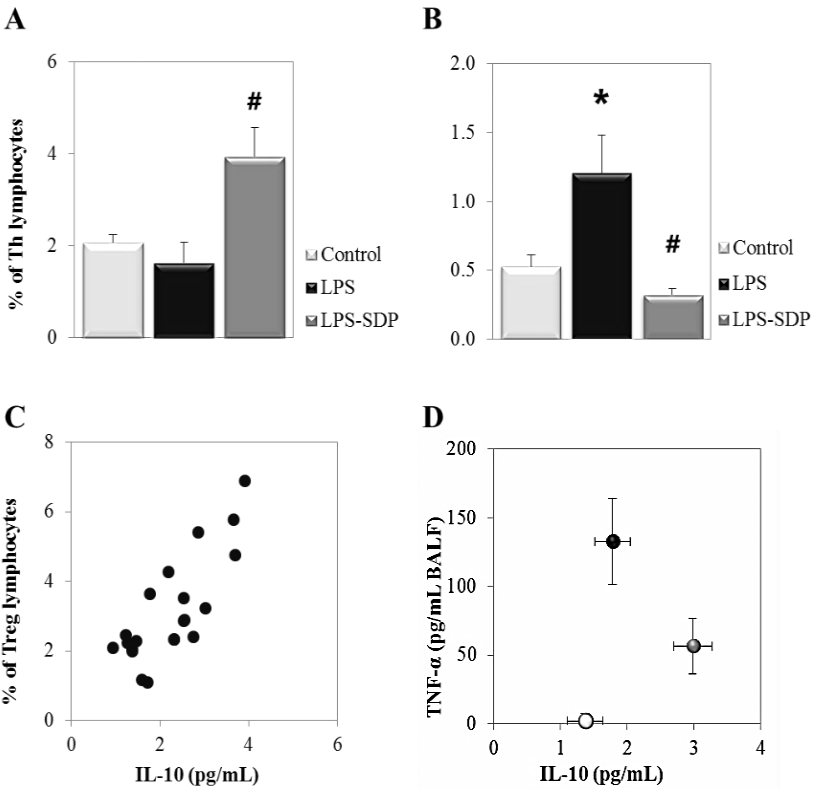

Figure 5. SDP effects on mucosal anti-inflammatory immune response in acute lung inflammation (with permission from Maijò et al., 2012b)**.** *Panel A and panel B* show the percentage of the regulatory T lymphocytes (T-reg) (A) and the ratio between activated Th lymphocytes and T-reg cells (B) in the lung airway. Results are expressed as means ± SEM (5-6 animals). Symbols indicate significant differences P<0.05; *LPS group vs Control group, #LPS-SDP group vs SEB group. *Panel C* shows the correlation between T-reg into lung airway and the concentration of the anti-inflammatory cytokine IL-10 in bronchoalveolar lavage fluid (BALF). *Panel D* shows TNF-α and IL-10 concentrations in BALF.

3. Mode of action of SDP

SDP is a highly complex mixture of functional peptides and proteins such as immunoglobulins and growth factors, with a high proportion of albumin [53]. As summarised by Petschow et al. [54], plasma supplements contribute to homeostasis by neutralising endotoxin in the intestinal lumen, promoting a stable microbiota, maintaining the gut barrier function and preserving the immune balance both in intestinal and peripheral tissues.

The mechanism by which oral plasma supplements modulate peripheral inflammation is not completely understood. However, there is increasing evidence that signals initiated in the intestinal lumen of different origin (dietary functional components, changes in the microflora, the presence of microbial cell wall components and even bacterial secreted products) can interact with the intestinal mucosa and have the capacity to regulate immune responses outside the gastrointestinal tract [55]. Plasma supplements ameliorate the inflammatory response by increasing the number of T-regs in the inflamed colon as well as by enhancing IL-10 release [56]. Therefore, there is evidence indicating that plasma supplements modulate the abundance of T-regs in the intestine (the inductor site) and stimulated blood and lung T-regs in the lung model (the effector site), both interconnected by the common mucosal system [55].

The mechanism of action of SDP is probably not unique. SDP contains a high proportion of immunoglobulins that can bind a variety of potential antigens in the lumen, preventing their attachment to the mucosa [32]. This is the mechanism claimed to explain the beneficial effects of SDP in the prevention of viral gastroenteritis in children [57], and in the reduction of diarrhoea in pigs [58] and in acquired immune deficiency syndrome patients infected with *C. parvum* [59]. However, it must be considered that over 250 peptides have been identified in plasma [53] and most of them will retain some biological function after spray-drying [1]. SDP may contain a fraction of natural antibodies that will contribute to immune homeostasis, enhancing anti-inflammatory IL-10 production, as suggested by Petschow et al. [60]. The presence of bioactive peptides in SDP may also cause changes in the intestinal microbiota profile. For example, SDP can inhibit the growth of pathogenic bacteria [61;58].

Animal plasma supplementation can also change the microbiota profile. Ovine Ig may alter the intestinal environment through a specific enrichment of Lactobacillus strains and depletion of enterobacteria [62], although

studies in piglets have yielded conflicting results [6;63]. In rats, the analysis of caecal microbiota showed that animals fed porcine SDP presented increased richness of the intestinal ecosystem [26]. Finally, it is worth noting that animal plasma supplements contain growth factors, cytokines and biologically active compounds that may also directly interact with mucosal receptors present both in enterocytes and ib dendritic cells, or that can reach the subepithelial compartment across the Peyer's patch M cells, as happens with food-derived peptides [64]. This is a largely unexplored area that deserves further attention.

4. Conclusions

Supplements prepared from animal plasma of porcine, bovine or ovine origin have been shown to contribute to gut homeostasis and act at luminal and mucosal levels. The main targets are the regulation of the intestinal barrier and the gut-associated immune system, which connects and modulates other mucosal areas, promoting the proliferation of regulatory lymphocytes and the expression of anti-inflammatory cytokines which presumably mediate most of its beneficial physiological effects. The mechanism by which plasma supplements initiate the regulatory responses is probably not unique but involves luminal mechanisms, with changes in the microbiota profile, direct or indirect interaction with enterocytes or with immune intestinal cells, and steps connecting the gut-associated phenomena with peripheral mucosal areas also exposed to the external environment. A better insight into the mechanisms implicated and a deeper knowledge of the specific plasma components involved are necessary to gain acceptance of these products.

Acknowledgements

The authors are grateful to APC Europe S.A. (Granollers, Spain), APC Inc. (Ankeny, IO, USA) for providing the spray-dried plasma supplement and for financial support. This research was also funded by the Ministerio de Economia y Competitividad (TRA2009-0317) and by the Generalitat de Catalunya (SGR2005-00632 and SGR2009-0047). The support of Dr. Lluïsa Miró in the preparation of the manuscript is also acknowledged.

References

1. Borg, B.S., Campbell, J.M., Russell, L.E., Rodríguez, C., Ródenas, J. 2002, *Am. Assoc. Swine Vet.*, 33, 97.
2. Gatnau, R., Zimmerman, D.R. 1990. *J. Anim. Sci.*, 68 (Suppl. 1), 374 (Abstr).

3. Torrallardona, D. 2010. *Asian-Aust. J. Anim. Sci.*, 23, 131.
4. Bikker, P., van Dijk, A.J., Dirkzwager, A., Fledderus, J., Ubbink-Blanksma, M., Beynen, A.C. 2004. *Livest. Prod. Sci.*, 86, 201.
5. Quigley, J.D. III, Drew, M.D. 2000. *Food Agr. Immunol.*, 12, 311.
6. Torrallardona, D., Conde, R., Badiola, J.I., Polo, J. 2007. *Livest. Sci.*, 108, 303.
7. Remus, A., Andretta, I., Kipper, M., Lehnen, C.R., Klein, C.C., Lovatto, P.A., Hauschild L. 2013. *Livest. Sci.*, 155, 294.
8. Coffey, R.D., Cromwell, G.L. 2001, *Pigs News Inform.*, 22, 39N.
9. O'Farrelly, C. 1998, *Gut*, 42, 603.
10. Isolauri, E., Sütas, Y., Kankaanpää, P., Arvilommi, H., Salminen, S. 2001. *Am. J. Clin. Nutr.*, 73, 444S.
11. Barrett, K.E. 2008. *Adv. Physiol. Educ.*, 32, 25.
12. Chen, M.L., Pothoulakis, C., LaMont, J.T. 2002. *J. Biol. Chem.*, 277, 4247.
13. Sonoda, N., Furuse, M., Sasaki, H., Yonemura, S., Katahira, J., Horiguchi, Y., Tsukita, S. 1999. J. *Cell Biol.*, 147, 195.
14. Pérez-Bosque, A., Amat, C., Polo, J., Campbell, J., Crenshaw, J., Russell, L., Moretó, M. 2006. *J. Nutr.*, 136, 2838.
15. Lu, J., Philpott, D.J., Saunders, P.R., Perdue, M.H., Yang, P.C., McKay, D.M. 1998. *J .Pharmacol. Exp. Ther.*, 287, 128.
16. Santos, J., Yang, P.C., Söderholm, J.D., Benjamin, M., Perdue, M.H. 2001. *Gut*, 48, 630.
17. Capaldo, C.T., Beeman, N., Hilgarth, R.S., Nava, P., Louis, N.A., Naschberger, E., Stürzl, M., Parkos, C.A., Nusrat, A. 2012. *Mucosal Immunol.*, 5, 681.
18. McKay, D.M, Benjamin, M.A., Lu, J. 1998. *Am. J. Physiol.*, 275, G29.
19. Pérez-Bosque, A., Miró, L., Polo, J., Russell, L., Campbell, J., Weaver, E., Crenshaw, J., Moretó, M. 2010. *J. Nutr.*, 140, 25.
20. Nusrat, A., Turner, J.R., Madara, J.L. 2000. *Am. J. Physiol.*, 279, G851.
21. Tsukita, S., Furuse, M., Itoh, M. 2002. The tight junction. In: Cell adhesion. Berkeley MC, Ed. Oxford University Press, New York, pp: 369-395.
22. Bruewer, M., Luegering, A., Kucharzik, T., Parkos, C.A., Madara, J.L., Hopkins, A.M., Nusrat, A. 2003. *J. Immunol.*, 171, 6164.
23. Salzman, N.H., Underwood, M.A., Bevins, C.L. 2007. *Semin. Immunol.* 19, 70.
24. Shi, J., Aono, S., Lu, W., Ouellette, A.J., Hu, X., Ji, Y., Wang, L., Lenz, S., van Ginkel, F.W., Liles, M., Dykstra, C., Morrison, E.E., Elson, C.O. 2007. *J. Immunol.*, 179, 1245.
25. Peyrin-Biroulet, L., Beisner, J., Wang, G., Nuding, S., Oommen, S.T., Kelly, D., Parmentier-Decrucq, E., Dessein, R., Merour, E., Chavatte, P., Grandjean, T., Bressenot, A., Desreumaux, P., Colombel, J.F., Desvergne, B., Stange, E.F., Wehkamp, J., Chamaillard, M. 2010. *Proc. Natl. Acad. Sci. U S A.*, 107, 8772.
26. Martin-Orúe SM, Pérez-Bosque A, Gómez de Segura A, Moretó, M. 2008. Gut Microbiome Meeting, Clermont-Ferrand, France, 2008. [Abstract]
27. Mayer, L. 2005. *Immunol. Rev.*, 206, 5.
28. Pérez-Bosque, A., Pelegrí, C., Vicario, M., Castell, M., Russell, L., Campbell, J.M., Quigley, J.D. 3rd, Polo, J., Amat, C., Moretó, M. 2004. *J. Nutr.*, 134, 2667.
29. Moretó, M., Pérez-Bosque, A. (2009). *J. Anim. Sci.* 87, E92.

30. Pérez-Bosque, A., Miró, L., Polo, J., Russell, L., Campbell, J., Weaver, E., Crenshaw, J., Moretó, M. 2008. *J. Nutr.*, 138, 533.
31. Mowat, A.M. 2003. *Nat. Rev. Immunol.*, 3, 331.
32. Bosi, P., Casini, L., Finamore, A., Cremokolini, C., Merialdi, G., Trevisi, P., Nobili, F., Mengheri, E. 2004. *J. Anim. Sci.*, 82, 1764.
33. Sakaguchi, S., Yamaguchi, T., Nomura, T., Ono, M. 2008. *Cell*, 133, 775.
34. Shevach, E.M. 2011. *Adv. Immunol.*, 112, 137.
35. Stoffels, B., Schmidt, J., Nakao, A., Nazir, A., Chanthaphavong, R.S., Bauer, A.J. 2009. *Gut*, 58, 648.
36. Touchette, K.J., Carroll, J.A., Allee, G.L., Matteri, R.L., Dyer, C.J., Beausang, L.A., Zannelli, M.E. 2002. *J. Anim. Sci*., 80, 494.
37. Campbell, J.M., Quigley, J.D. III, Russell, L.E., Koehnk, L. D. 2004. *J. Appl. Poult. Sci. Res.*, 13, 388.
38. Kiyono, H., Fukuyama, S. 2004. *Nat. Rev. Immunol.*, 4, 699.
39. Kominsky, D.J., Keely, S., MacManus, C.F., Glover, L.E., Scully, M., Collins, C.B., Bowers, B.E., Campbell, E.L., Colgan, S.P. 2011. *J. Immunol.*, 186, 6505.
40. Keely, S., Rawlinson, L.A., Haddleton, D.M., Brayden, D.J. 2008. *Pharm. Res.*, 25, 1193.
41. Belkaid, Y., Artis, D. 2013. *Eur. J. Immunol.*, 43, 3096.
42. Gallichan, W.S., Woolstencroft, R.N., Guarasci, T., McCluskie, M.J., Davis, H.L., Rosenthal, K.L. 2001. *J. Immunol.*, 166, 3451.
43. Sobko, T., Schiött, J., Ehlin, A., Lundberg, J., Montgomery, S., Norman, M. 2010. *Paediatr. Perinat. Epidemiol.*, 24, 88.
44. Gill, N., Wlodarska, M., Finlay, B.B. 2010. *Nat. Immunol.*, 11, 558.
45. Maijó, M. (a), Miró, L., Polo, J., Campbell, J., Russell, L., Crenshaw, J., Weaver, E., Moretó, M., Pérez-Bosque, A. 2012. *Br. J. Nutr.*, 107, 867.
46. Nathan, C. 2006. *Nat. Rev. Immunol.*, 6, 173.
47. Chaudhuri, N., Sabroe, I. 2008. *Paediatr. Respir. Rev.*, 9, 236.
48. Gaffen, S.L., Liu, K.D. 2004. *Cytokine*, 28, 109.
49. Sakaguchi, S., Powrie, F. 2007. *Science*, 317, 627.
50. Shevach, E.M., DiPaolo, R.A., Andersson, J., Zhao, D.M., Stephens, G.L., Thornton, A.M. 2006. *Immunol Rev.*, 212, 60.
51. Wu, C.L., Lin, L.Y., Yang, J.S., Chan, M.C., Hsueh, C.M. 2009. *Respirolog*,. 14, 511.
52. Maijó, M. (b), Miró, L., Polo, J., Campbell, J., Russell, L., Crenshaw, J., Weaver, E., Moretó, M., Pérez-Bosque, A. 2012. *J Nutr.* 2012 Feb;142(2):264-70.
53. Anderson, N.L., Anderson, N.G. 2002. *Mol. Cell Proteomics*, 1, 845.
54. Petschow, B.W., Blikslager, A.T., Weaver, E.M., Campbell, J.M., Polo, J., Shaw, A.L., Burnett, B.P., Klein, G.L., Rhoads, J.M. 2014. *World J. Gastroenterol.*, 20, 11713.
55. Forsythe, P. 2011.*Chest*, 139, 901.
56. Moretó, M., Miró, L., Maijó, M., Polo, J., Weaver, E., Crenshaw, J., Russell, L., Campbell, J., Pérez-Bosque, A. 2010. *Gastroenterol.*, 138, S743 (Abstract).
57. Guarino, A., Canani, R.B., Russo, S., Albano, F., Canani, M.B., Ruggeri. F.M., Donelli, G., Rubino, A. 1994. *Pediatrics*, 93, 12.

58. Lallès, J.P., Bosi, P., Janczyk, P., Koopmans, S.J., Torrallardona, D. 2009. *Animal*, 3, 1625.
59. Greenberg, P.D. & Cello, J.P. 1996. *J. Acquir. Immune. Defic. Syndr. Hum. Retrovirol.*, 13, 348.
60. Petschow, B.W., Burnett, B., Shaw, A.L., Weaver, E.M., Klein, G.L. 2014. *Clin. Exp. Gastroenterol.*, 24, 181.
61. Champagne, C.P., Raymond, Y., Pouliot, Y., Gauthier, S.F., Lessard, M. 2014. *Can. J. Microbiol.*, 60, 287.
62. Balan, P., Han, K.S., Lawley, B., Moughan, P.J. 2013. J. *Anim. Sci.*, 91, 3724.
63. Torrallardona, D., Conde, M.R., Badiola, I., Polo, J., Brufau, J. 2003. *J. Anim. Sci.*, 81, 1220.
64. Martínez-Augustin O., Rivero-Gutiérrez, B., Mascaraque, C., Sánchez de Medina, F. 2014 *Int. Mol. Sci*., 15, 22857.

Research Signpost
37/661 (2), Fort P.O.
Trivandrum-695 023
Kerala, India

Recent Advances in Pharmaceutical Sciences V, 2015: 133-148 ISBN: 978-81-308-0561-0
Editors: Diego Muñoz-Torrero, M. Pilar Vinardell and Javier Palazón

9. Alanine aminotransferase: A target to improve utilisation of dietary nutrients in aquaculture

Isidoro Metón[1], María C. Salgado[1], Ida G. Anemaet[1], Juan D. González[1]
Felipe Fernández[2] and Isabel V. Baanante[1]
[1]Departament de Bioquímica i Biologia Molecular (Farmàcia), Facultat de Farmàcia, Universitat de Barcelona, Joan XXIII 27, 08028 Barcelona, Spain; [2]Departament d'Ecologia, Facultat de Biologia, Universitat de Barcelona, Diagonal 645, 08028 Barcelona, Spain

Abstract. Alanine aminotransferase (ALT) is a sensitive marker of dietary protein utilisation in fish. Three ALT isoforms (cALT1, cALT2 and mALT) encoded by two genes have been isolated from gilthead sea bream (*Sparus aurata*). Molecular characterization of ALT isozymes and gene promoters suggest involvement of cALT1 and mALT in postprandial use of dietary amino acids, while cALT2 seems associated to hepatic gluconeogenesis. Inhibition of hepatic cytosolic ALT activity stimulates pyruvate kinase and decreases the renewal rate of alanine in *S. aurata*. These findings point to ALT as a target to spare protein and improve catabolism of dietary carbohydrates in cultured fish.

Introduction

Feeds supplied to fish in culture typically represent the largest variable cost in aquaculture producers' budget. Nowadays an important concern in

Correspondence/Reprint request: Dr. Isidoro Metón, Departament de Bioquímica i Biologia Molecular (Farmàcia), Universitat de Barcelona, Joan XXIII 27, 08028 Barcelona, Spain. E-mail: imeton@ub.edu

aquaculture is to reduce the amount of dietary protein and to increase the content of cheaper nutrients to replace fishmeal [1]. In addition, since a large quantity of wild-caught fish is used as a source of fishmeal for aquafeeds, a reduction in the amount of protein supplied with the diet to fish in culture will alleviate pressure and dependence on marine fisheries, which are often overexploited [2–4]. Moreover, an excess of protein in the diet of farmed fish enhances amino acid degradation and eutrophication of local waters as a result of increased excretion of ammonia and organic compounds [5,6].

Most fish species produced by aquaculture, such as gilthead sea bream (*Sparus aurata*), turbot and sea bass, are carnivorous ectothermic species and efforts to partially substitute dietary protein by other nutrients are limited by the metabolic features of these animals. Carnivorous fish present low capacity to metabolise dietary carbohydrates [7–9]. The metabolism of carnivorous fish is adapted to a preferential use of dietary amino acids as the main source for metabolic energy production.

Alanine aminotransferase (ALT; EC 2.6.1.2), also known as glutamate pyruvate transaminase, plays a major role in amino acid metabolism and gluconeogenesis by catalysing the reversible transamination between L-alanine and α-ketoglutarate to form pyruvate and L-glutamate. Therefore, ALT constitutes an important link between amino acids, carbohydrates and energy metabolism (Fig. 1).

ALT is a homodimer formed by two subunits of 50 kDa. Each subunit binds a molecule of the coenzyme pyridoxal-5-phosphate (PLP), which is necessary for enzyme activity. In mammals, the hepatic activity of ALT is regulated by hormonal and nutritional status, and its expression levels increase in rats fed with high protein diets, during starvation, after treatment with cortisol or β-adrenergic agonists, and in diabetic animals [10,11]. ALT and aspartate aminotransferase (AST) are quantitatively the most important aminotransferases in the fish liver [12]. Nevertheless, ALT activity is more sensitive to changes in the nutritional status than AST in *S. aurata* and other fish species.

In the present review we will address current knowledge of the nutritional regulation of ALT expression in fish and its potential use as a biotechnological target to enhance carbohydrate catabolism for energy purposes, and preserve dietary amino acids for growth in order to spare protein and improve the sustainability of aquaculture.

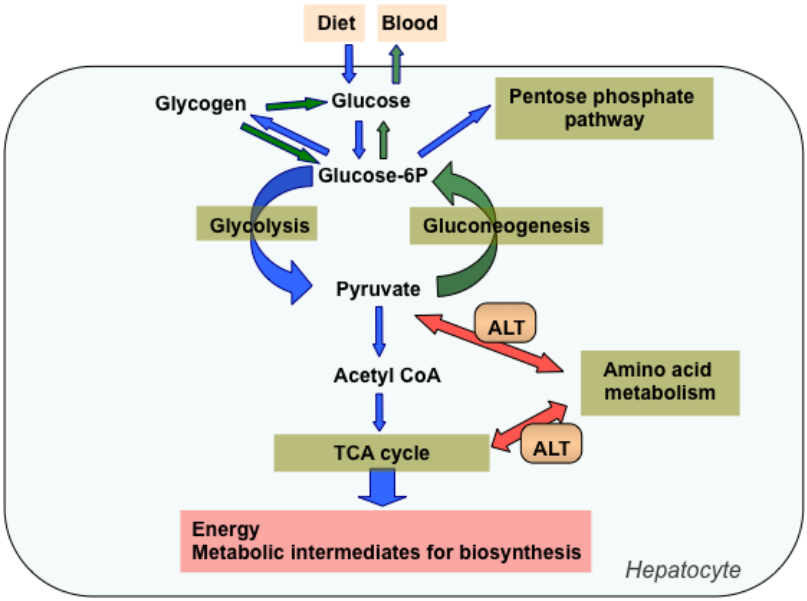

Figure 1. Role of ALT in the hepatic metabolism.

1. Hepatic ALT activity as a marker of dietary protein utilisation in fish

Partial substitution of dietary protein by carbohydrates promotes a metabolic adaptation that involves stimulation of key enzymes in glycolysis and pentose phosphate pathway in the liver of *S. aurata* [13–17]. Furthermore, supply of high protein/low carbohydrate diets increased ALT activity, while AST remained unaffected (Fig. 2A) [13,17]. Similar results were reported for Atlantic salmon [18] and rainbow trout [19,20]. This finding argues for a central role of ALT in the metabolic adaptation to changes in dietary nutrient composition. The increase in liver ALT activity in fish fed high protein diets may contribute to an efficient use of dietary amino acids either for growth or as a substrate for gluconeogenesis.

Hepatic ALT activity decreases in *S. aurata* following long-term starvation, whereas AST activity shows a slight tendency to increase [13]. The effect of starvation on ALT and AST activities in other fishes is variable and does not follow a clear pattern among different species.

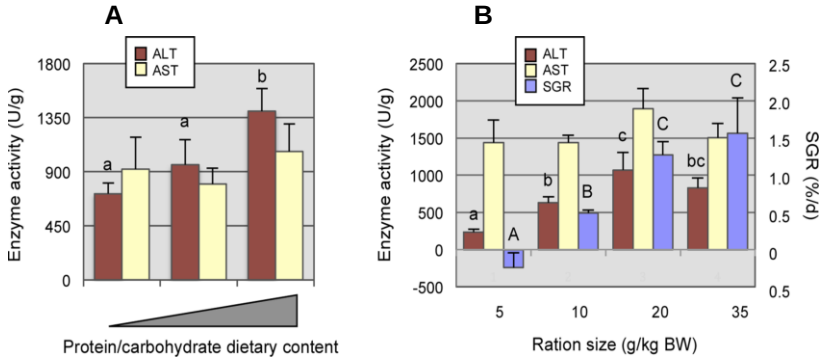

Figure 2. Nutritional regulation of ALT activity in the liver of *S. aurata*. (A) Effect of protein/carbohydrate dietary content on ALT and AST activity. Different letters indicate significant differences for ALT activity (lower-case letters) among diets. No significant differences were found for AST [17]. (B) Effect of ration size on somatic growth rate (SGR, expressed as weight gain percentage per day) and the hepatic activity of ALT and AST in *S. aurata*. Different letters indicate significant differences for ALT activity (lower-case letters) and SGR (upper-case letters) among ration sizes. No significant differences were found for AST [13].

Feeding *Sparus aurata* with different energy levels showed that liver ALT enzyme activity correlates with ration size and somatic growth rate. In contrast, regardless of the ration size no significant differences in AST activity were observed (Fig. 2B) [13].

2. Molecular cloning, subcellular localization, and kinetic properties of *Sparus aurata* ALT isozymes

Biochemical studies on rat and human ALT suggested the presence of soluble isoforms of ALT in cytosol and mitochondria [21–24]. The fact that K_m for alanine of rat mitochondrial ALT is one order of magnitude lower than the value of cytoplasmic ALT, led to the assumption that pyruvate formation from alanine is a major function of mitochondrial ALT [25]. However, later reexamination of the subject indicated that a considerable part of alanine-derived pyruvate originates in cytoplasm and that contribution of rat mitochondrial ALT activity during gluconeogenesis is negligible compared with that of the cytoplasmic enzyme [26]. In addition, presence of several cytosolic ALT and mitochondrial ALT isozymes have been demonstrated in mammalian tissues [27–30]. The metabolic function of

each ALT isoform in the cell and the molecular mechanism that generates ALT isoforms in mammals remain unknown.

Similarly as in mammals, distribution of ALT activity in liver extracts from *S. aurata* showed that more than 85 % of total ALT activity localizes to the cytosol, whereas mitochondrial ALT corresponds to about 14% of total ALT activity [31]. Three ALT isozymes were isolated from *S. aurata* tissues, named cALT1, cALT2 and mALT [31,32]. Alternative splicing of cALT gene generates cALT1 and cALT2, while a separate gene encodes mALT. Compared to cALT1 messenger, cALT2 mRNA contains an extra exon with an upstream translational start site that results in the inclusion of 23 amino acid residues at the N-terminus of the protein [32]. Considering that polyasparagine and polyglutamine regions are involved in protein-protein interaction through the formation of a polar zipper of hydrogen bonds between the side chains [33], presence of an asparagine-rich region in cALT2 suggests regulation of the enzyme activity by aggregation or interaction with effector proteins. In this regard, aggregation of ALT molecules gives rise to active oligomers during the purification of the rat liver enzyme [34].

The primary structure of *S. aurata* mALT protein shares an identity of 77 and 74 % with cALT1 and cALT2, respectively. Alignment of peptide sequences of piscine cALTs and mALT with mammalian ALT1 and ALT2 shows an identity of 66-71 %. The overall similarity with mammalian ALTs suggests a high degree of conservation of structure and reaction mechanism in vertebrate evolution. In the rat liver cytosolic ALT, Lys^{313} resides in the active site and participates in binding to the coenzyme PLP [35,36]. This residue is conserved in *S. aurata* ALTs and corresponds to Lys^{309}, Lys^{332} and Lys^{372}, in cALT1, cALT2 and mALT, respectively.

Subcellular localization of *S. aurata* ALT isoforms was examined by means of confocal fluorescence microscopy and immunodetection after expression of enhanced green fluorescent protein (GFP)-fusion proteins in transiently transfected eukaryotic cells. Both cALT1 and cALT2 show a diffuse distribution in the cell, indicating that both isoforms mostly exhibit cytosolic localization. A minor part of the two proteins is also present in vesicle-like structures [31,32].

Consistent with the physicochemical properties of a mitochondrial targeting signal presequence [37–40], the N-terminus of mALT comprises twelve positively charged, seventeen hydroxylated, and many hydrophobic residues within the first 70 amino acids. Indeed, fusion of GFP to the C-terminus of mALT (mALT-GFP) leads to colocalization of the fusion protein with mitochondrial markers. On the contrary, fusion of GFP to

mALT N-terminus or to the C-terminus of a mALT mutant lacking the N-terminal end blocks entry of the protein into mitochondria, and confirms presence of a mitochondrial targeting signal at the N-terminus of mALT. Immunodetection of CHO cells transfected with mALT-GFP revealed that although the protein is mostly found in the mitochondrial fraction, it is also detected in cytosol, although to a lesser extend and with higher molecular weight [31]. This finding argues for mALT import and processing into mitochondria according to the presequence import pathway, where basic N-terminal presequences are directed into mitochondria through interaction with translocases of the outer and inner membranes [41–43].

Expression of cALT1 in *S. aurata* is mainly found in liver, brain, skeletal muscle, intestine and kidney. No expression of cALT1 is detected in heart, gill or spleen. In contrast, maximal expression of cALT2 occurs in these three organs. Moderate cALT2 expression is observed in intestine, kidney and liver, whereas low cALT2 mRNA levels are detected in brain and skeletal muscle. mALT is ubiquitously expressed, with the higher levels in kidney, followed by liver, and intestine [32,44].

The occurrence of various ALT isozymes in tissues such as the liver supports the notion that ALT isoforms may play different roles in the cell. To unravel the molecular functions of *S. aurata* ALT proteins, kinetic characterisation of ALT isozymes was performed after expression of fish enzymes in *Saccharomyces cerevisiae* (Table 1) [32,44]. Kinetic properties of ALT isoforms were determined considering catalysis of the reaction in the direction of L-glutamate formation (forward reaction) and the direction of L-alanine formation (reverse reaction). Analysis of the forward/reverse ALT activity ratio and the fact that the reverse reaction mechanism of cALT2 followed a ping-pong bireactant system with, in contrast to cALT1, strong double substrate inhibition suggest that cALT2 preferentially converts L-alanine to pyruvate. Mutagenesis analysis demonstrated that residues 3-13 of cALT2 are essential for the reaction direction preference exhibited by this enzyme [32].

Taking into consideration that cALT1 and cALT2 expression in *S. aurata* is found in tissues that can undergo both glycolysis and gluconeogenesis, such as liver, kidney and intestine, it is conceivable that in these particular tissues cALT2 expression can be more restricted to metabolic conditions that favour gluconeogenesis. In contrast, cALT1 prevails during the fed state, which is characterised by elevated glycolysis and deviation of excess pyruvate to form L-alanine and provide 2-oxoglutarate to replenish the citric acid cycle in a metabolic situation where intermediates of this pathway can be used for biosynthetic purposes.

Table 1. Kinetic parameters of *S. aurata* cALT1, cALT2 and mALT [32,44].

	cALT1	cALT2	mALT
Forward reaction			
K_m^{Ala} (mM)	1.8	2.2	2.2
$K_m^{2\text{-Oxo}}$ (mM)	0.05	0.05	0.21
V_{max} (mmol/min/g)	57	14697	403
V_{max} / K_m^{Ala}	0.03	6.65	0.18
V_{max} / $K_m^{2\text{-Oxo}}$	1.18	288	1.89
Reverse reaction			
K_m^{Glu} (mM)	15.9	4.5	11.3
K_m^{Pyr} (mM)	0.69	0.15	0.32
V_{max} (mmol/min/g)	11.6	20.9	534
V_{max} / K_m^{Glu}	0.001	0.005	0.047
V_{max} / K_m^{Pyr}	0.02	0.14	1.68
K_i^{Glu} (mM)		34.9	
K_i^{Pyr} (mM)		36.5	

cALT2 was the only cALT isoform detected in non-gluconeogenic tissues such as heart, gill and spleen. This may be associated with the higher regulatory and kinetic versatility exhibited by this enzyme [32]. The metabolic function of cALT2 in these tissues seems to differ from the role exerted in liver, kidney or intestine, and might be related with processes such as amino acid interconversion and deamination.

Kinetic characterisation of *S. aurata* mALT indicates that this enzyme preferentially catalyzes the reaction in the pyruvate-forming direction [44].

3. Nutritional and hormonal regulation of cALT1, cALT2 and mALT expression

To analyse the functional role of ALT isozymes in intermediary metabolism, the effect of nutritional status and hormonal regulation was addressed on the expression of cALT1, cALT2 and mALT in *S. aurata*. Long-term starvation increases cALT2 mRNA levels and reduces cALT1 expression in liver of *S. aurata* [32]. Up-regulation of cALT2 expression in starved fish is consistent with preference of cALT2 in catalysing the production of pyruvate from L-alanine in a metabolic condition with decreased levels of hepatic pyruvate [45]. Indeed, alanine is the main amino acid released by skeletal muscle and taken up by the liver in starvation [46].

Food intake participates in short-term modulation of hepatic cALT1 and cALT2 expression. Consistent with the expression pattern in starved fish, cALT2 mRNA abundance decreased to minimum levels after a postprandial period of 4-8 hours. In contrast, the hepatic expression of cALT1 reached maximal values 2-8 hours following food intake. Likewise, administration of glucose and insulin to *S. aurata* significantly decreased cALT2 mRNA 6 hours after treatment, while cALT1 mRNA levels remained unaffected. Considering together kinetic data and nutritional regulation of cALTs expression, these observations point to up-regulation of cALT2 in conditions associated with increased gluconeogenesis, whereas cALT1 seems more involved in postprandial utilisation of dietary nutrients [32].

Similarly as for cALT1, starvation decreased mALT mRNA levels in liver and kidney of *S. aurata* [44,47]. Analysis of mALT expression in liver of fed *S. aurata* indicated a tendency to increase at postprandial time 6 hours [47]. Possibly, in the fed state cooperation of cALT1 and mALT allows addressing of dietary amino acids into the mitochondria to provide substrates for energy purposes. The fact that feeding *S. aurata* with high protein diets increases hepatic cALT1 expression while does not affect mALT [47,48], suggests that mALT is more involved in energy production from amino acids to maintain basal metabolism, whereas cALT1 would metabolise excess of dietary amino acids in the cytosol.

In mammals, type 2 diabetes leads to increased gluconeogenesis in the liver [49–51], and among the amino acids, alanine is the most effective gluconeogenic precursor [52]. Consistent with up-regulation of cALT2 expression in gluconeogenic conditions in liver, the diabetogenic action of streptozotocin (STZ), a glucosamine-nitrosourea derivative that causes β cell necrosis and that is widely used to generate diabetic animal models [53–55], leads to a marked increase in the hepatic expression of cALT2 in *S. aurata*, whereas cALT1 and mALT mRNA levels show a tendency to decrease [32,47]. The requirement for gluconeogenic substrates may be critical to enhance hepatic cALT2 expression in STZ-induced diabetic *S. aurata*.

4. Transcriptional control of *Sparus aurata* cALT and mALT gene promoters

To gain insight into the transcriptional regulation of ALT genes in fish, the promoter regions of cALT and mALT from *S. aurata* were isolated and characterised. The cALT and mALT promoters were the first ALT gene promoters reported for animals others than humans [44,56].

The *S. aurata* cALT promoter contains an initiator (Inr)-like element that overlaps the transcription start site. Sequential 5' deletions of promoter reporter constructs and analysis of transcriptional activity in sea bass larvae-derived SBL cells, allowed to conclude that the promoter region within 89 bp upstream from the transcriptional start constitutes the core functional promoter of this gene. Transient transfection experiments and EMSA analysis demonstrated that p300, a transcriptional coactivator that modulate the activity of a wide array of transcription factors [57,58], confers an activating signal on the cALT promoter by forming part of a complex that binds to a response element located at position -73 to -60 bp upstream from the transcription start site [56]. Recruitment of proteins with histone acetyltransferase activity, such as p300, to the Inr element of cALT promoter may provide an open DNA configuration that makes the site of transcriptional initiation more accessible to other transcription factors and the basal transcriptional machinery. In this regard, targeting of p300 to the Inr element might enable the recruitment of TFIID to the cALT promoter, as suggested for other TATA-less Inr-containing promoters [59,60].

Apart from acetylating histones, p300 acetylates several transcription factors in a regulated manner [61]. Transfection experiments in SBL cells showed that an acetyltransferase-deficient mutant of p300 failed to induce *S. aurata* cALT promoter activity, indicating that acetyltransferase activity of p300 is essential for p300-mediated transcriptional activation of cALT [56]. Thus, p300 may induce cALT promoter activity by acetylating histones and transcription factors. Indeed, EMSA assays and site-directed mutagenesis revealed that c-Myb transactivates *S. aurata* cALT promoter by binding to a c-Myb box at position -52 to -35 bp upstream from the transcriptional start. c-Myb-dependent transactivation of cALT occurred irrespective of the p300 response element [56]. However, since p300-mediated acetylation increases DNA binding activity of c-Myb and replacement of acetylated residues (lysines) in c-Myb by arginine dramatically decreases the transactivating capacity of c-Myb [62,63], p300-mediated acetylation of c-Myb possibly enhances binding of c-Myb to the *S. aurata* cALT promoter (Fig. 3).

Given that conditions associated with increased gluconeogenesis, such as starvation and treatment with STZ, result in a marked increase of cALT2 mRNA levels in the liver of *S. aurata*, cALT2 up-regulation can be responsible for serum increase of ALT activity under conditions associated with insulin resistance and development of type-2 diabetes [32]. In agreement with cALT2 expression, mRNA abundance of p300 and c-Myb increased in starved *S. aurata* and decreased in fish liver after the administration of insulin [56].

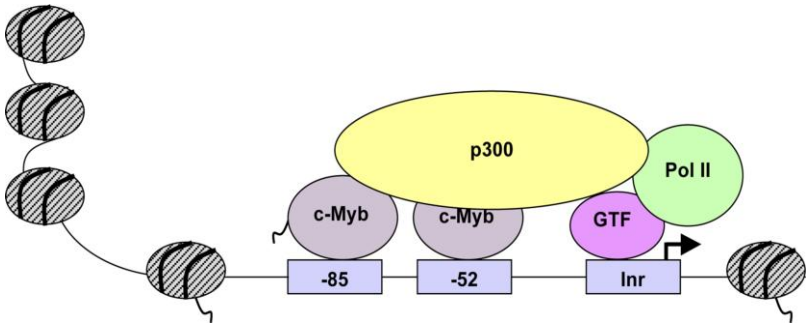

Figure 3. Coactivator p300 and c-Myb transactivate the *S. aurata* cALT promoter. Schematic representation of the cALT promoter region, with the DNA wrapped around nucleosomes forming histones (depicted in a grey circle). By acetylating the histone tails and transcription factors, i.e. c-Myb, p300 can make the DNA more accessible to other regulatory proteins. In addition, p300 can form a physical bridge between transcription factors and the general transcription factors and RNA polymerase II (Pol II). Inr, initiator element. GTF, General Transcription Factors. Acetylation is represented by the symbol`ㄣ . Figure adapted from [64].

Functionality of the promoter region of *S. aurata* mALT was assayed in human kidney-derived HEK293 cells transfected with fusion constructs containing sequencial 5'-deletions of the isolated fragment. The promoter region within 49 bp upstream from the transcription start site constitutes the core functional promoter for mALT gene. HNF4α transactivates the *S. aurata* mALT gene promoter by binding to a response element located at position -63 to -39 bp upstream from the transcriptional start [44]. Tissue distribution of *S. aurata* HNF4α expression, mainly in kidney, liver and intestine, correlates well with that observed for mALT [44].

There is increasing evidence suggesting a major role for HNF4α in the kidney [65–67], and involvement of this transcription factor in transactivation of genes involved in amino acid metabolism such as tyrosine aminotransferase and ornithine aminotransferase [68,69]. In the fish kidney, dietary amino acids are used as substrates for oxidation and gluconeogenesis [70]. Under gluconeogenic conditions, such as starvation and STZ-treatment, down-regulation of HNF4α expression correlates with decreased mALT mRNA levels in kidney of *S. aurata*, which suggest a central role of HNF4α in the transcriptional regulation of mALT. Expression of mALT in this tissue might be mainly involved in the oxidation of amino acids for energetic purposes rather than for providing gluconeogenic substrates [44].

5. Effect of ALT inhibition on the intermediary metabolism of *Sparus aurata*

Bearing in mind the central role of ALT linking amino acids, carbohydrates and energy metabolism, ALT was considered a candidate gene target to spare protein and improve the metabolic utilisation of dietary carbohydrates. To test this hypothesis, the metabolic effect of inhibiting cytosolic ALT activity on intermediary metabolism was addressed in *S. aurata* using amino-oxyacetate (AOA), an inhibitor of PLP-dependent transaminases [71]. Although *in vitro* AOA inhibits ALT activity in cytosolic and mitochondrial fractions isolated from liver of *S. aurata*, AOA only affects cytosolic ALT activity *in vivo*, which suggests that AOA does not enter mitochondria and thus cannot inhibit mALT [72]. Consequently, the effect of AOA *in vivo* may be restricted to cytosolic ALT activity and, during the fed state, essentially to cALT1, the cALT isoform mainly involved in postprandial utilisation of dietary nutrients [32]. Considering that mALT activity accounts for as less as about 14 % of total ALT activity in the liver of fed *S. aurata* [31], the use of AOA *in vivo* appeared to be suitable to specifically inhibit ALT activity of cytosolic fractions.

Dietary AOA supplementation to *S. aurata* for 30 days causes a significant inhibition on ALT activity, without affecting ALT protein levels and irrespective of nutrient composition of the diet. The most remarkable effects of AOA-dependent ALT inhibition on the intermediary metabolism is a significant increase in pyruvate kinase (PK) activity, a key enzyme in glycolysis, without affecting the gluconeogenic fructose-1,6-bisphosphatase activity nor glycemia [44].

It was reported that glutamate behaves as an inhibitor of PK activity, while alanine is a strong allosteric inhibitor of hepatic PK [73]. Taking into account that dietary AOA supplementation decreased glutamate and alanine levels in the liver of *S. aurata*, increased PK activity in the liver after long-term exposure to AOA may result from: i) low glutamate levels and the consequent loss of the glutamate-dependent PK inhibition; and ii) reduction of alanine concentration as a consequence of ALT inhibition. ^{1}H NMR studies showed that inclusion of AOA to the diet also decreased hepatic glycogen. Moreover, ^{2}H NMR analysis indicated decreased ^{2}H-enrichment level of alanine methyl hydrogens in the liver of fish exposed to AOA irrespective of the composition of the diet [72].

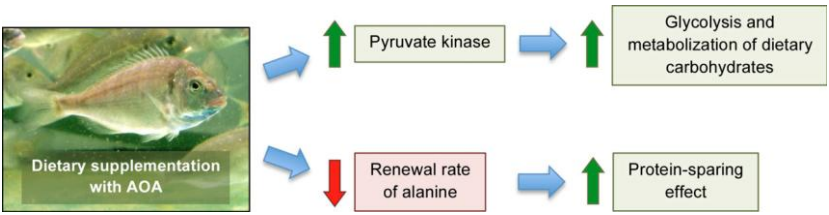

Figure 4. Effect of dietary amino-oxyacetate supplementation on the intermediary metabolism of *S. aurata*.

Altogether, these results suggest that AOA-dependent inhibition of cytosolic ALT activity in the liver stimulates glycolysis and decreases the renewal rate of alanine, which in turn may improve metabolism of dietary carbohydrates and spare protein (Fig. 4).

6. Conclusion

Molecular characterisation of *S. aurata* ALT isozymes including cloning and subcellular localisation of ALT isoforms, nutritional and hormonal regulation of ALT expression, enzyme kinetics, and transcriptional regulation of cALT and mALT gene promoters led to hypothesize that inhibition of cytosolic ALT activity could be useful to improve the use of dietary carbohydrates and spare protein in aquaculture. Preliminary studies showed that AOA-dependent inhibition of cALT activity gave rise to promising results including stimulation of PK activity and decreased renewal rate of alanine in the liver. To perform a more robust protein-sparing effect in order to promote an important increase in the use of dietary carbohydrates for energy production and preserve dietary amino acids for growth in cultured fish, strategies to apply in future studies should consider: i) use of interference RNA (iRNA) to specifically down-regulate the expression of cALT messengers; ii) explore the impact of post-translational mechanisms that may control ALT activity, such as protein-protein interactions; and iii) increase genomic and transcriptomic information available for *S. aurata* and other fish species with commercial interest to identify other candidate genes to perform a multifactorial action to improve the utilisation of dietary nutrients in fish farming.

Acknowledgements

This work was supported by grants BIO2006-01857 (MCYT, Spain), BIO2009-07589 (MCI, Spain) and AGL2012-33305 (MEC, Spain, co-funded by the European Regional Development Fund, ERDF, EC).

References

1. Naylor, R.L., Hardy, R.W., Bureau, D.P., Chiu, A., Elliott, M., Farrell, A.P., Forster, I., Gatlin, D.M., Goldburg, R.J., et al., 2009, *Proc. Natl. Acad. Sci. U. S. A.*, 106, 15103.
2. Naylor, R.L., Goldburg, R.J., Primavera, J.H., Kautsky, N., Beveridge, M.C., Clay, J., Folke, C., Lubchenco, J., Mooney, H., et al., 2000, *Nature*, 405, 1017.
3. Bostock, J., McAndrew, B., Richards, R., Jauncey, K., Telfer, T., Lorenzen, K., Little, D., Ross, L., Handisyde, N., et al., 2010, *Philos. Trans. R. Soc. Lond. B. Biol. Sci.*, 365, 2897.
4. Troell, M., Naylor, R.L., Metian, M., Beveridge, M., Tyedmers, P.H., Folke, C., Arrow, K.J., Barrett, S., Crepin, A.-S., et al., 2014, *Proc. Natl. Acad. Sci.*, 111, 13257.
5. Cole, D.W., Cole, R., Gaydos, S.J., Gray, J., Hyland, G., Jacques, M.L., Powell-Dunford, N., Sawhney, C., Au, W.W., 2009, *Int. J. Hyg. Environ. Health*, 212, 369.
6. Martinez-Porchas, M., Martinez-Cordova, L.R., 2012, *ScientificWorldJournal.*, 2012, 389623.
7. Wright Jr., J.R., O'Hali, W., Yang, H., Han, X.X., Bonen, A., 1998, *Gen. Comp. Endocrinol.*, 111, 20.
8. Moon, T.W., 2001, *Comp. Biochem. Physiol. B Biochem. Mol. Biol.*, 129, 243.
9. Polakof, S., Panserat, S., Soengas, J.L., Moon, T.W., 2012, *J. Comp. Physiol. B.*, 182, 1015.
10. Rosen, F., Harding, H.R., Milholland, R.J., Nichol, C.A., 1963, *J. Biol. Chem.*, 238, 3725.
11. Begum, N.A., Datta, A.G., 1992, *Mol. Cell Biochem.*, 113, 93.
12. Cowey, C.B., Walton, M.J., Intermediary metabolism, in: J.E. Halver (Ed.), Fish Nutr., Academic Press, San Diego, CA., 1989: pp. 260–321.
13. Metón, I., Mediavilla, D., Caseras, A., Cantó, E., Fernández, F., Baanante, I.V., 1999, *Br. J. Nutr.*, 82, 223.
14. Metón, I., Caseras, A., Fernández, F., Baanante, I.V., 2000, *Biochim. Biophys. Acta*, 1491, 220.
15. Caseras, A., Metón, I., Vives, C., Egea, M., Fernández, F., Baanante, I.V., 2002, *Br. J. Nutr.*, 88, 607.
16. Metón, I., Fernández, F., Baanante, I.V., 2003, *Aquaculture*, 225, 99.

17. Fernández, F., Miquel, A.G., Cordoba, M., Varas, M., Metón, I., Caseras, A., Baanante, I.V., 2007, *J. Exp. Mar. Bio. Ecol.*, 343, 1.
18. Fynn-Aikins, K., Hughes, S.G., Vandenberg, G.W., 1995, *Comp. Biochem. Physiol. Part A Physiol.*, 111, 163.
19. Lupiánez, J.A., Sánchez-Lozano, M.J., García-Rejón, L., De la Higuera, M., 1989, *Aquaculture*, 79, 91.
20. Sanchez-Muros, M.J., Garcia-Rejon, L., Garcia-Salguero, L., de la Higuera, M., Lupianez, J.A., 1998, *Int. J. Biochem. Cell Biol.*, 30, 55.
21. Swick, R.W., Barnstein, P.L., Stange, J.L., 1965, *J. Biol. Chem.*, 240, 3334.
22. Hopper, S., Segal, H.L., 1964, *Arch. Biochem. Biophys.*, 105, 501.
23. Gubern, G., Imperial, S., Busquets, M., Cortés, A., 1990, *Biochem. Soc. Trans.*, 18, 1288.
24. Sakagishi, Y., 1995, *Nihon Rinsho.*, 53, 1146.
25. DeRosa, G., Swick, R.W., 1975, *J. Biol. Chem.*, 250, 7961.
26. Lenartowicz, E., Wojtczak, A.B., 1988, *Arch. Biochem. Biophys.*, 260, 309.
27. Matsuzawa, T., Kobayashi, T., Ogawa, H., Kasahara, M., 1997, *Biochim. Biophys. Acta*, 1340, 115.
28. Yang, R.Z., Blaileanu, G., Hansen, B.C., Shuldiner, A.R., Gong, D.W., 2002, *Genomics*, 79, 445.
29. Lindblom, P., Rafter, I., Copley, C., Andersson, U., Hedberg, J.J., Berg, A.L., Samuelsson, A., Hellmold, H., Cotgreave, I., et al., 2007, *Arch. Biochem. Biophys.*, 466, 66.
30. Vedavathi, M., Girish, K.S., Kumar, M.K., 2004, *Mol. Cell Biochem.*, 267, 13.
31. Metón, I., Egea, M., Fernández, F., Eraso, M.C., Baanante, I.V., 2004, *FEBS Lett.*, 566, 251.
32. Anemaet, I.G., Metón, I., Salgado, M.C., Fernández, F., Baanante, I.V., 2008, *Int. J. Biochem. Cell Biol.*, 40, 2833.
33. Perutz, M.F., Pope, B.J., Owen, D., Wanker, E.E., Scherzinger, E., 2002, *Proc. Natl. Acad. Sci. U. S. A.*, 99, 5596.
34. Gatehouse, P.W., Hopper, S., Schatz, L., Segal, H.L., 1967, *J. Biol. Chem.*, 242, 2319.
35. Ishiguro, M., Takio, K., Suzuki, M., Oyama, R., Matsuzawa, T., Titani, K., 1991, *Biochemistry*, 30, 10451.
36. Ishiguro, M., Suzuki, M., Takio, K., Matsuzawa, T., Titani, K., 1991, *Biochemistry*, 30, 6048.
37. Abe, Y., Shodai, T., Muto, T., Mihara, K., Torii, H., Nishikawa, S., Endo, T., Kohda, D., 2000, *Cell*, 100, 551.
38. Truscott, K.N., Brandner, K., Pfanner, N., 2003, *Curr. Biol.*, 13, R326.
39. Mossmann, D., Meisinger, C., Vögtle, F.-N., 2012, *Biochim. Biophys. Acta*, 1819, 1098.
40. Schulz, C., Schendzielorz, A., Rehling, P., 2015, *Trends Cell Biol.*, 25, 265.
41. Neupert, W., Herrmann, J.M., 2007, *Annu. Rev. Biochem.*, 76, 723.

42. Chacinska, A., Koehler, C.M., Milenkovic, D., Lithgow, T., Pfanner, N., 2009, *Cell*, 138, 628.
43. Harbauer, A.B., Zahedi, R.P., Sickmann, A., Pfanner, N., Meisinger, C., 2014, *Cell Metab.*, 19, 357.
44. Salgado, M.C., Metón, I., Anemaet, I.G., González, J.D., Fernández, F., Baanante, I.V., 2012, *Mar. Biotechnol.*, 14, 46.
45. Veech, R.L., Veloso, D., Mehlman, M.A., 1973, *J. Nutr.*, 103, 267.
46. Felig, P., 1975, *Annu. Rev. Biochem.*, 44, 933.
47. Salgado, M.C., 2011, Control transcripcional i caracterització molecular de l'alanina aminotransferasa mitocondrial en l'orada (Sparus aurata), Ph. D. Thesis, Universitat de Barcelona, Barcelona, Spain.
48. González, J.D., 2012, Alanina aminotransferasa en Sparus aurata: control de la expresión génica mediante RNAi y de la actividad enzimática por aminooxiacetato, Ph. D. Thesis, Universitat de Barcelona, Barcelona, Spain.
49. Rosen, F., Roberts, N.R., Nichol, C.A., 1959, *J. Biol. Chem.*, 234, 476.
50. Zawadzki, J.K., Wolfe, R.R., Mott, D.M., Lillioja, S., Howard, B. V, Bogardus, C., 1988, *Diabetes*, 37, 154.
51. Schindhelm, R.K., Diamant, M., Dekker, J.M., Tushuizen, M.E., Teerlink, T., Heine, R.J., 2006, *Diabetes Metab. Res. Rev.*, 22, 437.
52. Yamamoto, H., Aikawa, T., Matsutaka, H., Okuda, T., Ishikawa, E., 1974, *Am. J. Physiol.*, 226, 1428.
53. Junod, A., Lambert, A.E., Stauffacher, W., Renold, A.E., 1969, *J. Clin. Invest.*, 48, 2129.
54. Like, A.A., Rossini, A.A., 1976, *Science*, 193, 415.
55. Wilson, G.L., Leiter, E.H., 1990, *Curr. Top Microbiol. Immunol.*, 156, 27.
56. Anemaet, I.G., González, J.D., Salgado, M.C., Giralt, M., Fernández, F., Baanante, I.V., Metón, I., 2010, *J. Mol. Endocrinol.*, 45, 119.
57. Shiama, N., 1997, *Trends Cell Biol.*, 7, 230.
58. Wang, F., Marshall, C.B., Ikura, M., 2013, *Cell. Mol. Life Sci.*, 70, 3989.
59. Abraham, S.E., Lobo, S., Yaciuk, P., Wang, H.G., Moran, E., 1993, *Oncogene*, 8, 1639.
60. Swope, D.L., Mueller, C.L., Chrivia, J.C., 1996, *J. Biol. Chem.*, 271, 28138.
61. Gayther, S.A., Batley, S.J., Linger, L., Bannister, A., Thorpe, K., Chin, S.F., Daigo, Y., Russell, P., Wilson, A., et al., 2000, *Nat. Genet.*, 24, 300.
62. Tomita, A., Towatari, M., Tsuzuki, S., Hayakawa, F., Kosugi, H., Tamai, K., Miyazaki, T., Kinoshita, T., Saito, H., 2000, *Oncogene*, 19, 444.
63. Sano, Y., Ishii, S., 2001, *J. Biol. Chem.*, 276, 3674.
64. Anemaet, I.G., 2008, Molecular characterization of cytosolic alanine aminotransferase gene expression in gilthead sea bream (Sparus aurata), Ph. D. Thesis, University of Barcelona, Barcelona, Spain.
65. Mohlke, K.L., Boehnke, M., 2005, *Curr. Diab. Rep.*, 5, 149.
66. MacDonald, M.J., Longacre, M.J., Langberg, E.-C., Tibell, A., Kendrick, M.A., Fukao, T., Ostenson, C.-G., 2009, *Diabetologia*, 52, 1087.

67. Niehof, M., Borlak, J., 2008, *Diabetes*, 57, 1069.
68. Kimura, A., Nishiyori, A., Murakami, T., Tsukamoto, T., Hata, S., Osumi, T., Okamura, R., Mori, M., Takiguchi, M., 1993, *J. Biol. Chem.*, 268, 11125.
69. Inoue, Y., Hayhurst, G.P., Inoue, J., Mori, M., Gonzalez, F.J., 2002, *J. Biol. Chem.*, 277, 25257.
70. Jürss, K., Bastrop, R., Metabolic Biochemistry, Elsevier, 1995.
71. John, R.A., Charteris, A., 1978, *Biochem. J.*, 171, 771.
72. González, J.D., Caballero, A., Viegas, I., Metón, I., Jones, J.G., Barra, J., Fernández, F., Baanante, I.V., 2012, *Br. J. Nutr.*, 107, 1747.
73. Fenton, A.W., Hutchinson, M., 2009, *Arch. Biochem. Biophys.*, 484, 16.

Research Signpost
37/661 (2), Fort P.O.
Trivandrum-695 023
Kerala, India

Recent Advances in Pharmaceutical Sciences V, 2015: 149-165 ISBN: 978-81-308-0561-0
Editors: Diego Muñoz-Torrero, M. Pilar Vinardell and Javier Palazón

10. Production of bacterial oxylipins by *Pseudomonas aeruginosa* 42A2

Ignacio Martin Arjol[1], Montserrat Busquets[2] and Àngels Manresa[1]
[1]Department of Sanitary Microbiology and Parasitology, Faculty of Pharmacy, University of Barcelona, 08028 Spain; [2]Department of Biochemistry and Molecular Biology, Faculty of Biology, University of Barcelona, 08028 Spain

Abstract. Oxylipins are a family of natural compounds that are reported to perform a variety of biological functions. Besides the biological properties of such compounds, interest in hydroxy fatty acids is increasing, due to the industrial applications of these renewable compounds as a starting material for resins, emulsifiers, plastics or polyesters. Hydroxy fatty acids are used as thickeners in a new generation of emulsifiers and lubricants, to reach new levels of performance. When grown in submerged culture with oleic or linoleic acid, Pseudomonas aeruginosa 42A2 produced several oxylipins. In this study, oxylipin production and its applications are examined.

Introduction

The main sources of hydroxy fatty acids (HFAs) are plants and a great variety of seed oils, particularly castor oil. In fact, HFAs are ubiquitous compounds in nature, as they are found in animals, fungi and bacteria. Classical

Correspondence/Reprint request: Dr. A. Manresa, Department of Sanitary Microbiology and Parasitology, Faculty of Pharmacy, University of Barcelona, Avinguda Joan XXIII s/n, 08028 Barcelona, Spain
E-mail: amanresa@ub.edu

oleochemistry occurs mainly at the ester functionality of the triglycerides. Whereas most native oils contain unsaturated fatty acids, as Biermann and collaborators stated, only a few reactions across the double bond of unsaturated FA are currently applied [1]. Numerous synthetic problems remain unsolved, and solutions must be found. As described in the literature, a great number of prokaryotes may be used for biotransformation processes. Microorganisms contain a wide range of enzymes for biotransformation, e.g. lipases, lipoxygenases, oxidases, epoxidases, P450 monooxigenases, that have enormous potential to develop new biotechnological processes with unsaturated fatty acids, making it possible to obtain a new brand of products with unexplored properties. *Candida* sp. or *Bacillus* sp. are reported to produce diacids (ω-unsaturated fatty acids), which are important compounds for polyester or polyamide synthesis [1], and epoxy fatty acids, which are used as PVC stabilizers or as starting materials to produce polyether polyols and are also found in reactions produced by the *Gaeumannomyces graminis* fungus [2]. The oxidation of unsaturated fatty acids is now focused on epoxidation, hydroxylation and double bond cleavage, to be used in fine chemistry and for further polymerization [1].

Microbial transformation is a powerful strategy to develop new lipid products. Lipases are the most common enzymes used in oleochemical processes. These enzymes do not require cofactors for catalysis, and show stereo-, regio- and chemoselectivity, high activity and stability. Most of them, e.g. those from *Pseudomonas cepacia*, *Candida antarctica*, *Rhizomucor miehei* or *Rhizopus delemar*, are commercially available. Recently, an increasing number of microorganisms producing HFAs have been reported as an efficient tool to convert inexpensive unsaturated fatty acids into value-added compounds [3]. Oxidative enzymes belonging to the P450 superfamily have been involved in α-hydroxylation or in the fatty acid synthase and β-hydroxylation systems in the case of β-HFAs; cytochrome P450 monooxygenases from different microorganisms, e.g. *Bacillus* or *Pseudomonas*, can produce ω-HFAs; and bacterial monooxygenases have been heterologously expressed [3]. Mid-position hydroxylation on saturated HFAs has been reported by Wallent [4] and Volkov [5]. Unsaturated HFAs have also been reported; the resulting product might be mono- or poly-HFAs [3]. The enzymes involved in these reactions are lipoxygenases and diol synthases [6, 7].

In nature, oxylipins have different functions. They act as signalling molecules and biological mediators, and they facilitate the plasticity of cell

membranes, the mobilization of lipids [8] and the generation of HFAs that are involved in cellular communication and the antibiosis effect. Although in minute amounts, polyesters of HFAs have been detected in oily seeds and in animal organisms, where they play the role of natural lubricants [9, 10].

The antimicrobial activity of such compounds and the functionality of the HFAs have attracted attention, leading to the generation of new polyesters, called estolides, which form a new class of green emulsifiers and lubricants. In this study, the production of hydroxy fatty acid derived from oleic acid (OA) and linoleic acid (LA) is described, as well as the applications of these compounds.

1. Microbial conversion of oleic acid

Since the first report of the microbial conversion of OA to 10-hydroxystearic acid by a *Pseudomonas* [4], scarce information has been published about the hydroxylation of OA whilst maintaining the unsaturated alkyl-chain. Heinz and co-workers reported that *Torulopsis* sp. produced 17-hydroxyoleic acid [11], and Soda and collaborators described the conversion of OA into ricinoleic acid (RA) by *Bacillus pumilus* [12]. Other uncommon HFAs have been described, such as 15-, 16-, 17-hydroxy-9*Z*-octadecenoic acid by *B. pumilus* [13] or 3-hydroxy-9*Z*-octadecenoic acid by *Alcaligenes* sp. 5-18 [14].

Although 7*S*,10*S*-dihydroxy-8*E*-octadecenoic acid ((7*S*,10*S*)-DiHOME) produced by *Pseudomonas aeruginosa* 42A2 was the first dihydroxylated derivative from OA to be described [15], the accumulation of HFAs has also been reported for several *P. aeruginosa* strains [16]. *Pseudomonas* 42A2 NCIMB 40045 is a gram negative bacterium with a versatile metabolism, which is the reason for its ubiquitous characteristic of being associated with other free-living soil microorganisms. It has the ability to transform long-chain unsaturated fatty acids into oxylipins.

1.1. Batch production

P. aeruginosa 42A2 accumulates several oxidized fatty acids, namely 10*S*-hydroperoxy-8*E*-octadecenoic acid ((10*S*)-HPOME), 10*S*-hydroxy-8*E*-octadecenoic acid ((10*S*)-HOME) and 7*S*,10*S*-dihydroxy-8*E*-octadecenoic acid (7S,10S- DiHOME), when it is incubated with OA as a single substrate in a minimal mineral medium (Fig. 1).

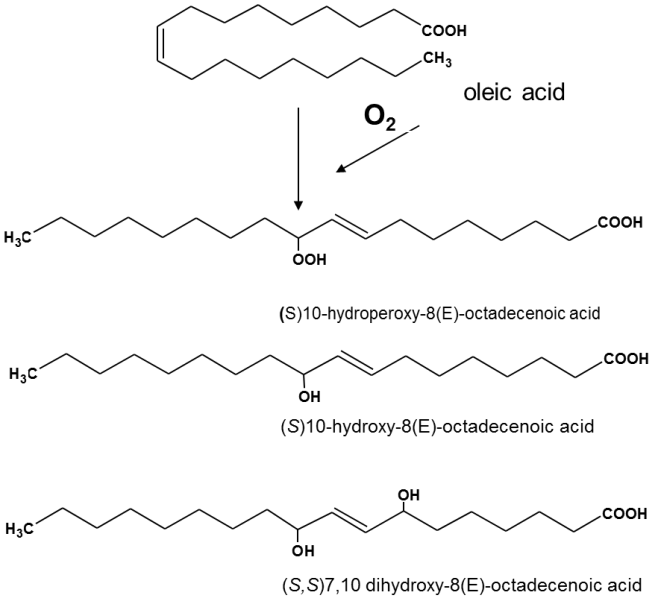

Figure 1. Products obtained from the conversion of OA by *P. aeruginosa* 42A2.

Although (10*S*)-HOME was first identified as the precursor of (7*S*,10*S*)-DiHOME [17], Martinez and co-workers suggest that the precursor of (7*S*,10*S*)-DiHOME is (10*S*)-HPOME, and that (10*S*)-HOME is a by-product obtained from the spontaneous reduction of (10*S*)-HPOME [6]. Subsequently, the two enzymes involved in the reaction were identified and the genomic structure of the diol synthase operon was elucidated. Thus, OA is transformed into (10*S*)-HPOME in a first enzymatic reaction, in order to produce (10*S*)-HOME spontaneously, and (7*S*,10*S*)-DiHOME is generated in a second enzymatic reaction. All of this enzymatic system is located in the periplasm of *P. aeruginosa* 42A2 [18].

Most microbial processes require air for cell growth. In some cases, foam accumulates during production, and can greatly disturb the process. To overcome foam formation in the production of (7*S*,10*S*)-DiHOME, which has surface activity properties, an innovative non-dispersive aeration system was designed. It is based on Higbie's penetration theory applied to a wetted-wall column. Hence, an innovative bioreactor was created for a foaming biotransformation [19].

The biotransformation kinetics were deduced by varying the substrate concentration from 10 to 20 $g \cdot L^{-1}$ to obtain different experimental data sets. The typical time course of the OA transformation (Fig. 2) indicated that (10*S*)-HPOME accumulation started soon after inoculation until the end of the exponential phase of cell growth. Most (7*S*,10*S*)-DiHOME and (10*S*)-HOME accumulation occurs during the stationary phase until the end of the process (30 h), which confirms the role of these compounds as secondary metabolites. A high conversion yield ($Y_{P/S}$) 0.9 was achieved and a cell yield ($Y_{P/X}$) of 3.2 was calculated. 10*S*-HPHOME was not detected at the end of the culture.

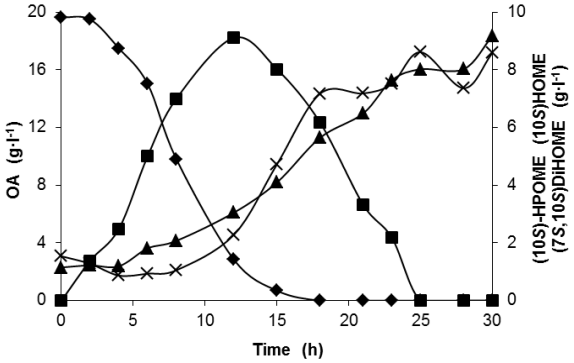

Figure 2. Kinetics of OA (♦) conversion by *P. aeruginosa* 42A2 (OA of 20 $g \cdot L^{-1}$) into (10*S*)-HPOME (■), (10*S*)-HOME (▲) and (7*S*,10*S*)-DiHOME (x).

As shown in Table 1, the volumetric productivity (P_V) that was calculated was substrate dependent. (10*S*)-HOME followed the same pattern as (10*S*)-HPOME, whereas the accumulation of (7*S*,10*S*)-DiHOME depended on the reaction of (10*S*)-HPOME with the hydroperoxy-diol synthase enzyme. Therefore, the production rate was proportional to the amount of (10*S*)-HPOME [18, 19].

Table 1. Effect of oleic acid concentration on volumetric productivity.

OA ($g \cdot L^{-1}$)	(10*S*)-HPOME ($g \cdot L^{-1} \cdot h^{-1}$)	(10*S*)-HOME ($g \cdot L^{-1} \cdot h^{-1}$)	(7*S*,10*S*)-DiHOME ($g \cdot L^{-1} \cdot h^{-1}$)
10	0.41	0.15	0.34
15	0.47	0.21	0.25
20	0.75	0.29	0.31

As expected, the experimental data fitted the mathematical model proposed by Monod, which corresponds to first-order reactions occurring during the biotransformation of OA into these oxidized compounds [19].

Due to the nature and functionality of the (10*S*)-HOME and (7*S*,10*S*)-DiHOME accumulated in the cultures, they might easily be further modified to form a new generation of polyesters named estolides (ESTs). ESTs are a class of polymeric secondary esters derived from addition across an unsaturated bond or with HFAs by a carboxyl moiety of another fatty acyl group.

2. Estolide production

Although in a minuscule amount, ESTs are present in nature in the epicuticular wax of some species of *Juniperus*, *Pinus* or *Coniferae*, and in the oil seeds of certain plants [20] or fungi [21]. ESTs are also found in the animal kingdom, in wool wax, beeswax [22], and in human meibomian gland secretion [23]. Furthermore, ESTs have been found in cultures of *Pseudomonas aeruginosa* 42A2 when cultivated with OA as substrate [24].

Yamaguchi and collaborators reported for the first time the esterification of castor oil in a two-step enzymatic reaction to obtain ESTs with a high yield [25]. This led to a new generation of environmentally friendly emulsifiers for a wide range of applications in the food industry. Particularly important are the RA ESTs, which are used as intermediates in the enzymatic production of polyglycerol polyricinoleate (E-476), as reported by Bodalo and co-workers [26, 27].

Two types of ESTs were synthesized from (10*S*)-HOME and (7*S*,10*S*)-DiHOME, using the thermostable commercial lipases Novozym 435 (lipase B from *Candida antarctica*), Lipozyme RM IM (*Rhizomucor miehei* lipase), and Lipozyme TL IM (*Thermomyces lanuginosus* lipase). Enzymatic reactions were carried out at 80 ºC under vacuum conditions to reduce the viscosity of HFAs monomers [28]. As shown in Fig. 3, the time course of the reaction using Novozym 435 (N435) offered the best performance with both HFAs. However, Lipozyme RM IM (L RM IM) behaved in a similar way to N435 when the substrate was (10*S*)-HOME. In contrast, Lipozyme TL IM (L TL IM) registered yields that were slightly lower than N435 in the polymerization of (7*S*,10*S*)-DiHOME.

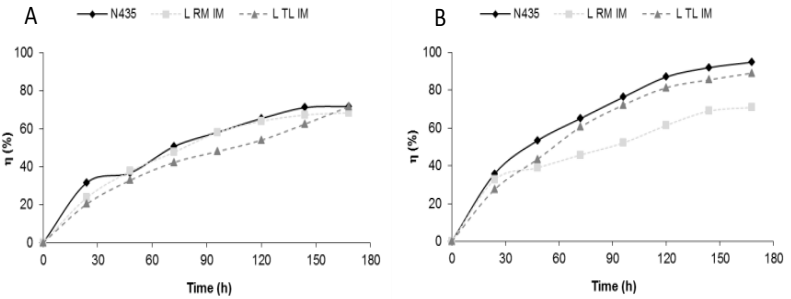

Figure 3. EST enzymatic production with 12% (w/w) of the corresponding lipase at 80 ºC for 168 h under vacuum conditions. A: (10*S*)-HOME; B: (7*S*,10*S*)-DiHOME.

Borgdorf and Warwel classified lipases according to their ratio competitive factor (RCF) [29]. This factor describes the selectivity of one single lipase toward two substrates with the same leaving group, and to two acyl groups.

Table 2. Reaction yield (%) in estolide formation from the oxylipin produced by *P. aeruginosa* 42A2 from oleic acid.

Lipase	RCF (%)	(10*S*)-HOME (%)	(7*S*,10*S*)-DiHOME (%)
Novozym 435	0.7	71.7	94.7
Lipozyme RM IM	1.3	68.4	70.8
Lipozyme TL IM	_	71.6	88.9

Although the lipase RCF should be taken into account, no relationship with the reaction yield was observed (Table 2). Bodalo and co-workers found that *sn*-1,3 selective lipases are unable to attack secondary alcohols [30]. However, the *sn*-1,3 specific lipases Lipozyme RM IM and Lipozyme TL IM had significant reaction yields with both substrates. The non-specific lipase Novozym 435 was the best catalyst with the highest reaction yields (71.7% and 94.7%), which indicates the importance of the nature of the lipase and the substrate.

There are no reports in the literature on EST synthesis from *trans*-HFA monomers. However, Aguieiras and partners used these enzymes in the production of mono-ESTs from OA and methyl ricinoleate, and achieved a

reaction yield of 33% after 48 h at 80 ºC using 6% enzyme (w/w) [31]. This reaction was also studied by Horchani and collaborators using the immobilized lipase of *Staphylococcus xylosus*. A 65% reaction yield was achieved after 55 h at 55 ºC [32].

Liquid chromatography coupled to MS has been found to be a time-consuming technique, especially the optimization of mass spectrometer potentials to obtain a low amount of fragmentation in the mass spectra of large molecules. In contrast, MALDI-TOF analyses carried out with a proper matrix and stabilization cation, e.g. Li^{+7} or Na^{+23}, is a fast technique with low fragment mass spectra, which means that the method could elucidate the number of oligomers synthesized. Finally, nuclear magnetic resonance (NMR) is a good complementary structural technique to MALDI-TOF, which provides characteristic chemical shifts to identify *trans*-ESTs. *trans*-EST structural characterization was carried out by MALDI-TOF mass spectrometry and NMR. MALDI-TOF analyses were carried out using a 2,5-dihydroxybenzoic acid (DBH) matrix saturated with acetonitrile [33]. ESTs from (10*S*)-HOME (M) are presented in Fig. 4A.

Some ions stand out from the rest, which means that the oligomers that are produced can be identified easier and faster. The following ions were detected *m/z* 601.5, $[2M\text{-}H_2O+Na^{23}]^+$; 881.7, $[3M\text{-}2H_2O+Na^{23}]^+$; 1162.0, $[4M\text{-}3H_2O+Na^{23}]^+$ and 1442.2, $[5M\text{-}4H_2O+Na^{23}]^+$. Hence, up to oligomers of five monomeric units of (10*S*)-HOME were synthesized. However, more ions were detected when (7*S*,10*S*)-DiHOME (M') was the substrate used (Fig. 4B): *m/z* 633.5, $[2M'\text{-}H_2O+Na^{23}]^+$; 929.7, $[3M'\text{-}2H_2O+Na^{23}]^+$; 1226.0, $[4M'\text{-}3H_2O+Na^{23}]^+$; 1522.3, $[5M'\text{-}4H_2O+Na^{23}]^+$; 1819.5, $[6M'\text{-}5H_2O+Na^{23}]^+$; 2115.7, $[7M'\text{-}6H_2O+Na^{23}]^+$; and in the enlarged region of the spectra the following ions were observed 2412.0, $[8M'\text{-}7H_2O+Na^{23}]^+$; and, 2709.2, $[9M'\text{-}8H_2O+Na^{23}]^+$. In this situation, up to oligomers of nine monomeric units of (7*S*,10*S*)-DiHOME were produced, as expected from the reaction yields presented in Table 2.

Furthermore, NMR spectroscopy was used to confirm the results observed in the MALDI-TOF analysis. Certain chemical shifts are decisive in order to identify *trans*-ESTs. In ^1H NMR spectra, these are the signals 2.28 ppm and 5.20 ppm, which correspond to the methylene protons (position 2) and to the methine proton (position 10) that are both adjacent to an ester group, respectively.

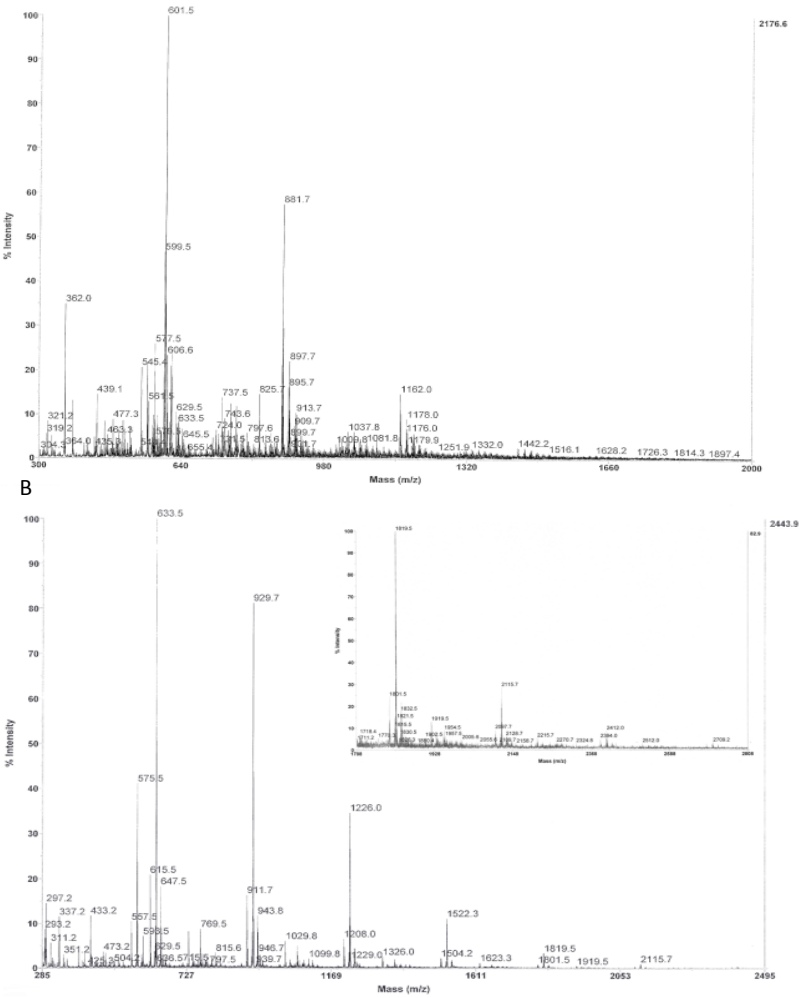

Figure 4. MALDI-TOF mass spectra with a DHB matrix saturated in acetonitrile. ESTs produced with Novozym 435 at 80 ºC under vacuum conditions for 168 h. A: (10*S*)-HOME ESTs; B: (7*S*,10*S*)-DiHOME ESTs.

An average number of monomers present in a sample could be calculated by integrating the methylene proton signal of 2.28 ppm. For ^{13}C

NMR spectra the determining signals are 74.50 ppm (position 10) and 173.17 ppm (position 1), which represent the presence of a tertiary carbon and an ester carbonyl, respectively. Fig. 5 represents the structure of ESTs of three monomeric units.

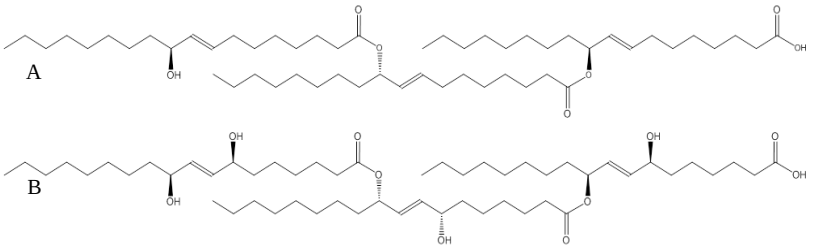

Figure 5. ESTs derived from (10*S*)-HOME (A) and (7*S*,10*S*)-DiHOME (B).

Finally, some physicochemical properties were determined for the produced ESTs: the Arrhenius relationship between viscosity and temperature (A and E_a), the glass transition temperature (T_g), and decomposition enthalpies (ΔHi).

According to mass spectrometry analysis, the ESTs analysed were considered as oligomers and not strictly polymers, due to their low polymerization degree. Such simple molecules were determined as Newtonian fluids, because their viscosity remained constant over different shear rates. A dynamic or absolute viscosity (η) determination was run over three different temperatures (20, 40 and 60 ºC) when possible, to calculate the pre-exponential factor (A) and activation energy (E_a) of the Arrhenius-type relationship [34]. This equation describes the dependence of viscosity on temperature, where A can be considered as the infinite-temperature viscosity value and E_a indicates the sensitivity of a substance to temperature [35].

$$\eta = A \cdot \exp\left(-{}^{E_a}/_{R \cdot T}\right)$$

Physicochemical analyses results are listed in Table 3. The parameters include A and E_a, density (ρ), kinematic viscosity at 40 ºC, reaction yield (η) and oligomer number (ON), which is the maximum number of oligomers synthesized.

Table 3. Viscosity and characterization parameters from ESTs.

Sample	$A \cdot 10^{-10}$ (Pa·s)	E_a (kJ·mol^{-1})	ρ (g·mL^{-1})	ν (cSt)	η (%)	ON (–)
(10*S*)-HOME	9.47	49.9	0.96	205	–	1
(7*S*,10*S*)-DiHOME	n.d.	n.d.	0.99	n.d.	–	1
(10*S*)-HOME N435	3.48	55.1	0.97	608	71.7	6
(10*S*)-HOME RM IM	5.79	53.6	0.97	495	68.4	6
(10*S*)-HOME TL IM	24.2	49.3	0.97	402	71.6	6
(7*S*,10*S*)-DiHOME N435	3.62	59.1	1.00	2510	94.7	9
(7*S*,10*S*)-DiHOME RM IM	0.14	67.7	1.02	3235	70.8	9
(7*S*,10*S*)-DiHOME TL IM	1.06	62.7	1.00	3000	88.9	10

As can be seen, the viscosity parameters for the (10*S*)-HOME ESTs are lower than those for (7*S*,10*S*)-DiHOME ESTs. The same is true for ON values. (7*S*,10*S*)-DiHOME ESTs were produced in higher yields; thus, their ON values were higher. In addition, the melting point of (7*S*,10*S*)-DiHOME was 56 ºC, due to the hydrogen bond interaction of the two hydroxyl groups. Hence, (7*S*,10*S*)-DiHOME EST viscosity parameters had higher values.

Table 4. EST calorimetric parameters.

Sample	T_g (ºC)	T_{onset1} (ºC)	ΔH_1 (J·g^{-1})	T_{onset2} (ºC)	ΔH_2 (J·g^{-1})	T_{onset3} (ºC)	ΔH_3 (J·g^{-1})	Residue (%)
(10*S*)-HOME	-60	119	-7.08	196	47.33	315	-161.3	0.35
(7*S*,10*S*)-DiHOME	-49	185	37.79	277	-56.16	366	147.3	1.23
(10*S*)-HOME N435	-63	–	–	213	33.97	323	-174.1	2.27
(10*S*)-HOME RM IM	-64	–	–	217	35.73	322	-174.0	1.57
(10*S*)-HOME TL IM	-66	–	–	218	27.64	338	-252.9	1.73
(7*S*,10*S*)-DiHOME N435	-50	187	34.37	295	-30.18	362	-118.9	1.37
(7*S*,10*S*)-DiHOME RM IM	-49	200	28.22	302	-36.23	370	-105.5	1.12
(7*S*,10*S*)-DiHOME TL IM	-50	201	18.97	300	-37.07	364	-133.5	2.74

Finally, thermal analysis, DSC (differential scanning calorimetry) and TGA (thermal gravimetric analysis) were used to characterize the new polyesters. Thermal parameters are listed in Table 4. T_g could be calculated for synthesized polyesters and even for both HFAs, indicating that these compounds lacked a crystal structure. EST T_g values were practically the

same as their corresponding substrates, which confirmed the simplicity of these molecules. Furthermore, onset temperatures and decomposition enthalpy values were maintained. These two points suggest that the oligomers produced had a larger quantity of dimers and trimers than higher polymerized oligomers.

3. Microbial conversion of linoleic acid

Due to the limited natural HFAs supply, research has focused on engineering castor oil production and developing new engineered microorganisms for RA production [36] and new processes for the microbial transformation of unsaturated fatty acids into HFAs [3, 37, 38]. The occurrence of lipoxygenase [39] and diol synthase activity [6, 18] in *P. aeruginosa* reinforces the versatile metabolic activity of this bacteria to produce diverse polyol oxylipins. When cultivated in submerged culture with linoleic acid as a substrate, *P. aeruginosa* 42A2 accumulated HFAs in the culture, with different degrees of hydroxylation [40].

Several oxylipins have been characterized from LA acid to date, due to the activity of bacterial lipoxygenases. Oxidized LA derivatives are hydroperoxides (9*S*)- and (13*S*)-HPODE (9*S*-hydroperoxide-10*E*,12*Z*-octadecadienoic and 13*S*-hydroperoxide-9*Z*,11*E*-octadecadienoic acids, respectively). These hydroperoxides can spontaneously transform into their corresponding hydroxides ((9*S*)-/(13*S*)-HODE), epoxyalcohols or even keto fatty acids; these last two by the action of hematin [41]. Recently, 10-hydroxy-12,15(*Z*,*Z*)-octadecenoic acid produced by a rec-enzyme from *Stenotrophomonas maltophilia* was characterized [42].

Scarce information has been reported on the bacterial production of dihydroxyl fatty acid. Besides 9,10-hydroxystearic acid, only (7*S*,10*S*)-DiHOME [15, 16] and 9,12-dihydroxy-10*E*-eicosenoic acid have been described [43]. Several trihydroxy-fatty acids have been reported so far from the bacterial transformation of RA into 7,10,12-trihydroxy-8*E*-octadecenoic acid [44] and from LA 9,10,13-trihydroxy-11*E*-octadecenoic ((9,10,13)-TriHOME) and 9,12,13-trihydroxy-10*E*-octadecenoic ((9,12,13)-TriHOME) [40]. A unique strain of *Bacillus* has been reported to accumulate 12,13,17-trihydroxy-9*Z*-octadecenoic acid [45].

When a complex substrate of fatty acids (60% LA, 40% OA, palmitic, stearic and linolenic acid) was supplied into the culture of *P. aeruginosa* 42A2, a mixture of compounds was found. The organic extract from the culture media contained several oxylipins (Table 5). Liquid chromatography coupled to tandem mass spectrometry (LC-MS/MS) was used to allow the

direct analysis of products and combine the resolution of LC with the detection specificity of MS/MS. This is a direct, fast method for detecting and resolving the structure of the products accumulated in the culture without the formation of derivatives.

Table 5. Fragment ions detected in the organic extract.

Product	Fragment ions (*m/z*)
(10*S*)-HOME	297 $[M-H]^-$; 279 $[M-H-H_2O]^-$; 154.9 indicating –OH at C10
(9*S*)-HODE	295 $[M-H]^-$; 277 $[M-H-H_2O]^-$; 171 indicating –OH at C9
(13*S*)-HODE	295 $[M-H]^-$; 277 $[M-H-H_2O]^-$; 195 indicating –OH at C13
(9,10,13)-TriHOME	329 $[M-H]^-$; 311.2 $[M-H-H_2O]^-$; 293 $[M-H-2H_2O]^-$; 127 indicating –OH at C9 and C10
(9,12,13)-TriHOME	329 $[M-H]^-$; 311.2 $[M-H-H_2O]^-$; 293 $[M-H-2H_2O]^-$; 129 indicating –OH at C12 and C13

In this case, isomers (9,10,13)-TriHOME and (9,12,13)-TriHOME are present in the ratio 3:1, which differs from that reported by Kim and partners (1:1) from the *P. aeruginosa* strain PR3 [46]. Due to the difficulty of separating these isomers, a multiple reaction monitoring (MRM) analysis was undertaken, in which the acquisition mode was based on the injection of the sample containing the ion to be studied, *m/z* 329, into the first quadrupole (Q1), fragmentation in the collision cell (Q2), and scanning of the product ions in the third quadrupole (Q3). The result is an MS/MS spectrum free of interferences where the most appropriate product ions are selected in the third quadrupole (Q3), *m/z* 127 and 129, to perform relative quantification and confirmation. Thus, it was seen (Fig. 6) that for ((9,10,13)-TriHOME) the characteristic transition was *m/z* 329–127, and for the other isomer, ((9,12,13)- TriHOME), the characteristic transition was *m/z* 329–129.

TriHOME compounds belong to a class of oxylipins with antifungal activity similar to those isolated from a variety of rice plant (9,12,13-trihydroxy-10*E*,15-octadecadienoic and 9,12,13-trihydroxy-10*E*-octadecanoic acids) suffering from black rot disease [47, 48] and involved in the defensive mechanism of plants [49, 50]. The presence of lipoxygenases in environmental bacteria [39] and diol synthase enzymes [18] suggests the involvement of the microbiota in the interaction with eukaryote organisms.

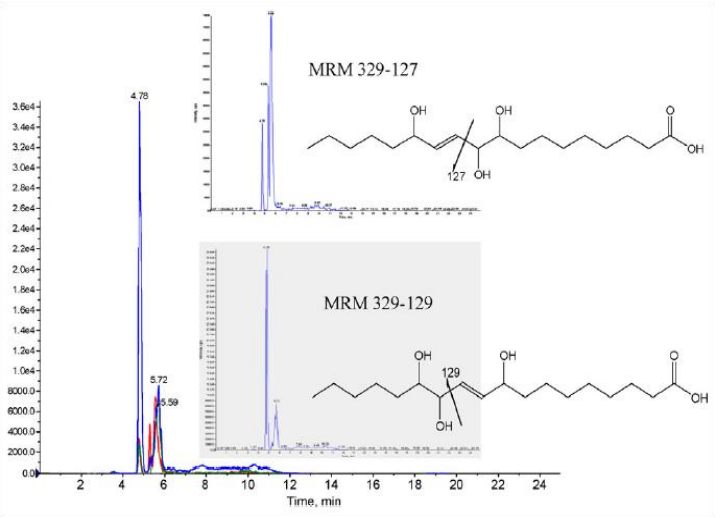

Figure 6. MRM analysis of trihydroxylated isomers derived from LA.

Although the mechanism of action of oxylipins is not yet understood, it has been suggested that the inhibition of growth may be due to the chemical or physical properties of oxylipins, rather than the interactions with specific cellular targets [50]. The oxylipins derived from OA, (10*S*)-HOME and (7*S*,10*S*)-DiHOME, could inhibit the growth of phytopathogenic fungal strains such as *Colletotrichum gloeosporioides*, *Fusarium oxysporum* and *Drechslera teres* and produce an antibacterial effect against *Escherichia coli* and *Micrococcus luteus* (MIC 64 $\mu g \cdot mL^{-1}$); *Staphylococcus aureus* (MIC 32 and 8 $\mu g \cdot mL^{-1}$ (10*S*)-HOME and (7*S*,10*S*)-DiHOME, respectively) and *Bacillus subtilis* (MIC 32 and 128 $\mu g \cdot mL^{-1}$ (10*S*)-HOME and (7*S*,10*S*)-DiHOME, respectively) [51].

It was found that the oxylipins derived from LA cultures, those described in Table 5, were able to inhibit bacterial growth (Table 6), similarly to those described (9,10,13-TriHOME and 9,12,13-TriHOME) from the mildew fungus in barley, *Blumeria graminis*, which reduced infection by up to 42% when applied *in vivo* [52], or 10-hydroxy-8-octadecenoic and 10-hydroxy-8,12-octadecenoic acids, which were found in the stomata of timothy grass after being infected with *Epichloe typhina* [53].

Table 6. Minimal inhibitory concentration of the HFAs described in Table 5.

Microorganism	MIC ($mg \cdot ml^{-1}$)
Bacillus subtilis ATCC 6333	64
Enterococcus hirae ATCC 10541	32
Micrococcus luteus ATCC 9341	64
Arthroderma uncinatum ATCC 15082	32
Aspergillus brasiliensis ATCC 14404	140
Aspergillus repens IMI 016114	140
Macrophomina phaseolina IMI 48561	32
Penicillium chrysogenum ATCC 9480	140
Penicillium funiculosum CECT 2914	32
Tricophyton mentagrophytes ATCC 18748	64
Verticillium dahliae 49507/A	32

4. Conclusion

The transformation of unsaturated fatty acids by *P. aeruginosa* 42A2 produced several oxylipins with different degrees of hydroxylation. Further polymerization of oxylipins obtained from OA renders a new family of ESTs with properties of Newtonian fluids similar to natural lubricants. New oxylipins were produced from LA with biological properties against phytopathogenic fungal strains.

Acknowledgements

This work was supported by the Ministerio de Economía y Competitividad (project HBP2006-0027, CTQ2014-59632-R and CTQ2010-21183-C02-01), Spain; by the Comissió Interdepartamental de Recerca i Tecnologia (CIRIT) project 2009SGR00327 and 2014SGR534; and, finally, by the IV Pla de Recerca de Catalunya (Generalitat de Catalunya) grant 2009SGR819. I. Martin-Arjol was a grateful recipient of an APIF fellowship from the University of Barcelona.

References

1. Biermann, U., Bornscheuer, U., Meier, M. A. R., Metzger, J. O., Schäfer, H. J. 2011, *Angew. Chem. Int. Ed.*, 50, 3854.
2. Hörnsten, L., Su, C., Osbourn, A. E., Garosi, P., Hellman, U., Wernstedt, C., Oliw, E. H. 1999, *J. Biol. Chem.*, 274, 28219.
3. Cao, Y., Zhang, X. 2013, *Appl. Microbiol. Biotechnol.*, 97, 3323.

4. Wallen, L. L., Benedict, R. G., Jackson, R. W. 1962, *Arch. Biochem. Biophys.*, 99, 249.
5. Volkov, A., Liavonchanka, A., Kamneva, O., Fiedler, T., Goebel, C., Kreikemeyer, B., Feussner, I. 2010, *J. Biol. Chem.*, 285, 10353.
6. Martinez, E., Hamberg, M., Busquets, M., Diaz, P., Manresa, A., Oliw, E. H. 2010, *J. Biol. Chem.*, 285, 9339.
7. Joo, Y.-C., Oh, D.-K. 2012, *Biotechnol. Adv.*, 30, 1524.
8. Brash, A. R. 1999, *J. Biol. Chem.*, 274, 23679.
9. Martin-Arjol, I., Busquets, M., Manresa, A. 2013, *Process Biochemistry*, 48, 224.
10. Cermak, S. C., Isbell, T. A., Evangelista, R. L., Johnson, B. L. 2011, *Industrial Crops and Products*, 33, 132.
11. Heinz, E., Tulloch, A. P., Spencer, J. F. T. 1970, *BBA-Lipid Lipid Met.*, 202, 49.
12. Soda, K. 1988, *Proc. - World Conf. Biotechnol. Fats Oils Ind.*,178.
13. Lanser, A. C., Plattner, R. D., Bagby, M. O. 1992, *J. Am. Oil Chem. Soc.*, 69, 363.
14. Esaki, N., Ito, S., Blank, W., Soda, K. 1994, *J. Ferment. Bioeng.*, 77, 148.
15. Mercade, E., Robert, M., Espuny, M. J., Bosch, M. P., Manresa, M. A., Parra, J. L., Guinea, J. 1988, *J. Am. Oil Chem. Soc.*, 65, 1915.
16. Hou, C. T., Bagby, M. O., Plattner, R. D., Koritala, S. 1991, *J. Am. Oil Chem. Soc.*, 68, 99.
17. Hou, C. T., Bagby, M. O. 1992, *J. Ind. Microbiol.*, 9, 103.
18. Estupiñan, M., Diaz, P., Manresa, A. 2014, *Biochim. Biophys. Acta*, 1842, 1360.
19. Martin-Arjol, I., Llorens, J. L., Manresa, A. 2014, *Appl. Microbiol. Biotechnol.*, 98, 9609.
20. Brieskorn, C. H. 1978, *Fette, Seifen, Anstrichmittel*, 80, 15.
21. Zhang, H., Olson, D. J. H., Van, D., Purves, R. W., Smith, M. A. 2012, *Industrial Crops and Products*, 37, 186.
22. Noble, W. R., Eisner, A., Scanlan, J. T. 1960, *J. Am. Oil Chem. Soc.*, 37, 14.
23. Wojtowicz, J. C., Uchiyama, E., Pascuale, M. A. D., Aronowicz, J. D., McCulley, J. P. 2008, *Vision Pan-America*, VII, 48.
24. Peláez, M., Orellana, C., Marqués, A., Busquets, M., Guerrero, A., Manresa, A. 2003, *J. Am. Oil Chem. Soc.*, 80, 859.
25. Yamaguchi, C., Akita, M., Asaoka, S., Osada, F. 1989, *Japanese Kokai Tokkyo Koho*, JP 01016591 A 19890120.
26. Ortega-Requena, S., Bódalo-Santoyo, A., Bastida-Rodríguez, J., Máximo-Martín, M. F., Montiel-Morte, M. C., Gómez-Gómez, M. 2014, *Biochem. Eng. J.*, 84, 91.
27. Manresa-Presas, A., Bódalo-Santoyo, A., Gómez-Carrasco, J. L., Gómez-Gómez, E., Bastida-Rodríguez, J., Máximo-Martín, M. F., Hidalgo-Montesinos, A. M., Montiel-Morte, M. C. 2008, *Oficina Española de Patentes y Marcas*, ES 2300197 A1.
28. Martin-Arjol, I. 2014, *Universitat de Barcelona*, Barcelona, Doctoral Thesis.
29. Borgdorf, R., Warwel, S. 1999, *Appl. Microbiol. Biotechnol.*, 51, 480.

30. Bódalo, A., Bastida, J., Máximo, M. F., Montiel, M. C., Gómez, M., Murcia, M. D. 2008, *Biochem. Eng. J.*, 39, 450.
31. Aguieiras, E. C. G., Veloso, C. O., Bevilaqua, J. V., Rosas, D. O., da Silva, M. A. P., Langone, M. A. P. 2011, *Enzyme Res.*, 1.
32. Horchani, H., Bouaziz, A., Gargouri, Y., Sayari, A. 2012, *J. Mol. Catal. B: Enzym.*, 75, 35.
33. Price, N. P. J., Manitchotpisit, P., Vermillion, K. E., Bowmanc, M. J., Leathers, T. D. 2013, *Carbohyd. Res.*, 370, 24.
34. García-Zapateiro, L. A., Franco, J. M., Valencia, C., Delgado, M. A., Gallegos, C., Ruiz-Méndez, M. V. 2013, *Grasas y Aceites*, 64, 497.
35. Giap, S. G. E. 2010, *J. Phys. Sci*., 21, 29.
36. Beopoulos, A., Verbeke, J., Bordes, F., Guicherd, M., Bressy, M., Marty, A., Nicaud, J. M. 2014, *Appl. Microbiol. Biotechnol.*, 98, 251.
37. Kaneshiro, T., Kuo, T. M., Hou, C. T. 2002, *Lipid Biotechnology*, *CRC Press*, Cap 31.
38. Metzger, J. O., Bornscheuer, U. 2006, *Appl. Biochem. Biotechnol*, 71, 13.
39. Hansen, J., Garreta, A., Benincasa, M., Fusté, M. C., Busquets, M., Manresa, A. 2013, *Appl. Microbiol. Biotechnol.*, 97, 4737.
40. Martin-Arjol, I., Bassas-Galia, M., Bermudo, E., Garcia, F., Manresa, A. 2010, *Chem. Phys. Lipids*, 163, 341.
41. Oliw, E. H., Garscha, U., Nilsson, T., Cristea, M. 2006, *Anal. Biochem.*, 354, 111.
42. Oh, H.-J., Shin, K.-C., Oh, D.-K. 2013, *Biotechnol. Lett.*, 35, 1487.
43. Back, K.-Y., Sohn, H.-R., Hou, C. T., Kim, H.-R. 2011, *J. Agr. Food Chem.*, 59, 9652.
44. Kuo, T. M., Kim, H., Hou, C. T. 2001, *Curr. Microbiol.*, 43, 198.
45. Gardner, H. W., Hou, C. T., Weisleder, D., Brown, W. 2000, *Lipids*, 35, 1055.
46. H. Kim, H. W. G. a. C. T. H. 2000, *J. Ind. Microbiol. Biotechnol.*, 25, 109.
47. Kato, T., Yamaguchi, Y., Uyehara, T., Yokoyama, T. 1983, *Tetrahedron Lett.*, 24, 4715.
48. Masui, H., Kondoa, T., Kojima, M. 1989, *Phytochemistry*, 28, 2613.
49. Bleé, E. 1995, *INFORM*, 6, 852.
50. Prost, I., Dhondt, S., Rothe, G., Vicente, J., Rodriguez, M. J., Kift, N., Carbonne, F., Griffiths, G., Esquerré-Tugayé, M. T., Rosahl, S., Castresana, C., Hamberg, M., Fournier, J. 2005, *Plant Physiol.*, 139, 1902.
51. Culleré, J. 2002, *Universitat de Barcelona*, Barcelona, Doctoral Thesis.
52. Cowley, T., Walters, D. 2005, *Pest Management Science*, 61, 572.
53. Koshino, H., Togiya, S., Yoshihara, T., Sakamura, S., Shimanuki, T., Sato, T., Tajimi, A. 1987, *Tetrahedron Lett.*, 28, 73.

Research Signpost
37/661 (2), Fort P.O.
Trivandrum-695 023
Kerala, India

Recent Advances in Pharmaceutical Sciences V, 2015: 167-186 ISBN: 978-81-308-0561-0
Editors: Diego Muñoz-Torrero, M. Pilar Vinardell and Javier Palazón

11. Inflammation and metabolic dysregulation in diabetic cardiomyopathy

Xavier Palomer, Emma Barroso and Manuel Vázquez Carrera
Department of Pharmacology and Therapeutic Chemistry, Faculty of Pharmacy, University of Barcelona, CIBERDEM (CIBER de Diabetes y Enfermedades Metabólicas Asociadas) and IBUB (Institute of Biomedicine of the University of Barcelona), Diagonal 643, Barcelona E-08028, Spain

Abstract. Diabetic cardiomyopathy is characterized by structural and functional alterations in the heart muscle of people with diabetes that finally lead to heart failure. Metabolic disturbances characterized by increased lipid oxidation, intramyocardial triglyceride accumulation and reduced glucose utilization have all been involved in the pathogenesis of diabetic cardiomyopathy. On the other hand, evidences arisen in the recent years point to a potential link between chronic low-grade inflammation in the heart and metabolic dysregulation. Interestingly, the progression of heart failure and cardiac hypertrophy usually entails the activation of pro-inflammatory pathways. Therefore, in this chapter we summarize novel insights into the crosstalk between inflammatory processes and metabolic dysregulation in the failing heart during diabetes.

Introduction

The human heart produces, and immediately hydrolyzes, approx. 30 kg of ATP every day to carry out the mighty job of pumping more than 7,000 L/day

Correspondence/Reprint request: Dr. Xavier Palomer Tarridas and Dr. Manuel Vázquez Carrera, Department of Pharmacology and Therapeutic Chemistry, Faculty of Pharmacy, University of Barcelona. Diagonal 643, E-08028, Barcelona. Spain. E-mail: mvazquezcarrera@ub.edu, xpalomer@ub.edu

of blood. Therefore, it is not surprising that any abnormality that deregulates its proper working may become life-threatening. In fact, heart disease is the major cause of death for both men and women in developed countries and, according to the World Health Organization, by 2020 it is expected to be the leading cause of death throughout the world. Heart disease is often grouped with metabolic disorders because it is frequently a consequence of uncorrected type 2 diabetes and obesity-related dyslipidemia. Insulin resistance, which is a hallmark of type 2 diabetes, is a risk factor of heart failure, the leading cause of death in type 2 diabetic patients. Diabetic cardiomyopathy, which refers to structural and functional alterations in the heart muscle of people with diabetes that finally lead to heart failure, is related to disturbances in myocardial energy metabolism. Diabetic cardiomyopathy is only said to exist if heart failure is not accompanied by coronary artery disease or hypertension that may account for the heart muscle disorder.

An increasing body of evidence suggests a potential link between chronic low-grade inflammation and metabolic disorders that are associated with abnormal cytokine production and increased levels of saturated fatty acids, such as insulin resistance, type 2 diabetes and obesity. The progression of heart disease usually entails a local rise in pro-inflammatory cytokines, including interleukin (IL)-6, monocyte chemoattractant protein-1 (MCP-1) and tumour necrosis factor-α (TNF-α) [1]. These molecules exert several autocrine and paracrine effects in cardiac cells via downstream activation of the transcription factor nuclear factor (NF)-κB, which may contribute to states that are associated with myocardial inflammation, for example heart failure and dilated cardiomyopathy. However, the underlying mechanisms linking inflammation, heart failure and dilated cardiomyopathy are complex, since they are coupled to systemic metabolic abnormalities and changes in cardiomyocyte phenotype. In this review we summarize recent insights into the crosstalk between inflammatory processes and metabolic dysregulation in the failing heart during diabetes.

1. Metabolic regulation in the healthy heart

Free fatty acids are the preferred energy substrate in the adult heart, supplying about 70% of total ATP [2]. However, since the human heart requires a constant supply of fuel, other substrates such as glucose (20%) or lactate (10%) may provide additional fuel sources in diverse physiological and nutritional circumstances. Glucose uptake is mostly

regulated by glucose transporters (GLUTs), of which GLUT4 is the most abundant in cardiac cells (Fig. 1) [3]. Once inside the cytosol, glucose is phosphorylated into glucose-6-phosphate, which can either be stored as glycogen or converted into pyruvate, the end product of glycolysis. Then, pyruvate enters the mitochondria where it undergoes oxidative decarboxylation by the pyruvate-dehydrogenase complex (PDC), which catalyses the rate-limiting step of glucose oxidation. Specific PDC kinases (PDKs) are responsible for the phosphorylation-induced inactivation of PDC. As such, PDK4, the most expressed PDK isoform in the heart, decreases glucose oxidation while allowing increased fatty acid β-oxidation. With regard to the fatty acids, they cross the cardiomyocyte cell membrane through passive diffusion or by specific transport proteins, including fatty acid translocase (FAT/CD36), fatty acid binding protein (FABP) and fatty acid transport protein 1 (FATP1). In the cytoplasm, fatty acids are acylated, and either enter the mitochondria by the action of carnitine palmitoyl transferase 1 (CPT-1) or are incorporated into the intracellular lipid pool in the form of triglycerides. In the mitochondrial matrix, fatty acids are oxidized by the β-oxidation pathway to form acetyl-CoA. At this point, pathways for glucose and fatty acid oxidation merge, since acetyl-CoA, which is produced from both pathways, enters the tricarboxylic acid (TCA) cycle. Finally, reduced flavin adenine dinucleotide ($FADH_2$) and nicotinamide adenine dinucleotide (NADH) generated through β-oxidation and the TCA cycle, respectively, carry electrons to the electron transport chain, thus driving ATP synthesis by oxidative phosphorylation.

Under physiological conditions, glucose utilization is reduced in the heart by increased fatty acid oxidation via the Randle cycle. After a high carbohydrate supply, insulin activates the protein kinase B (PKB)/Akt signalling pathway and subsequent translocation of GLUT4 from intracellular vesicles towards the sarcolemma, the cell membrane of cardiac cells. As such, insulin promotes glucose uptake and utilization, thereby reducing myocardial oxygen consumption and increasing cardiac efficiency [4]. Insulin also enhances the uptake of fatty acids, but instead of being oxidized, they are stored in the intracellular pool of lipids. The AMP-activated protein kinase (AMPK) is another important regulator of cardiac energy homeostasis. Conditions leading to energy depletion, for instance the failing heart or increased ATP demand, lead to AMPK activation, which switches off energy-consuming pathways and stimulates ATP-producing pathways such as fatty acid β-oxidation and glycolysis.

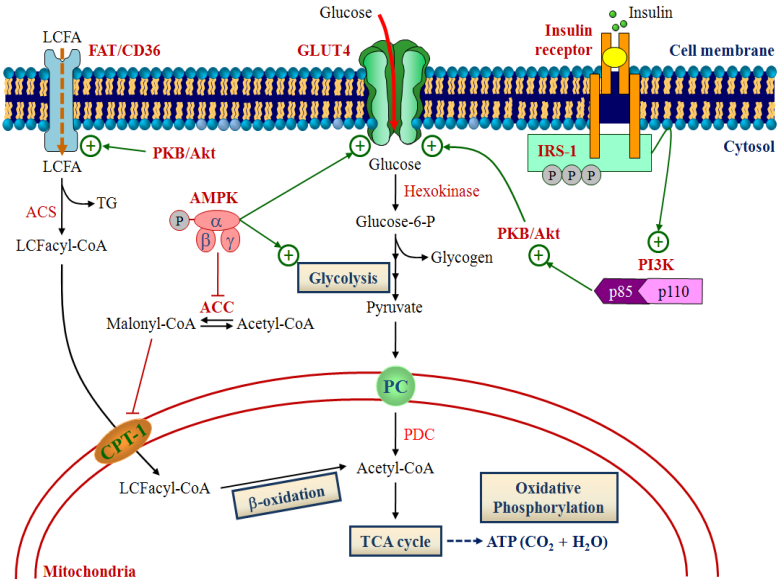

Figure 1. Metabolic regulation in the normal heart. Glucose, after uptake by specific transporters (GLUT4), is phosphorylated and can either be stored as glycogen or converted into pyruvate (glycolysis). In the mitochondria, pyruvate undergoes oxidative decarboxylation by the pyruvate-dehydrogenase complex (PDC). Long-chain fatty acids (LCFA) that enter into the cytoplasm by passive diffusion or specific transporters (FAT/CD36) are acylated by acyl-CoA synthetase (ACS), and either enter the mitochondria (carnitine palmitoyl transferase 1, CPT-1), or are incorporated into triglycerides (TG). In the mitochondrial matrix, fatty acids undergo β-oxidation to form acetyl-CoA. The acetyl-CoA formed during glucose or fatty acid oxidation enters the tricarboxylic acid (TCA) cycle and finally generates ATP through oxidative phosphorylation. Initiation of the insulin receptor substrate 1 (IRS-1) cascade by insulin induces the phosphatidylinositol 3 kinase (PI3K), which activates the protein kinase B (PKB)/Akt. AMPK promotes myocardial GLUT4 activity and stimulates glycolytic enzymes, while it induces CPT-1 activity through acetyl-CoA carboxylase (ACC) phosphorylation-mediated inhibition.

Cardiac metabolism is mostly regulated at the transcriptional level by the peroxisome proliferator-activated receptor (PPAR) transcription factor family, which consists of three isoforms, PPARα (or NR1C1), PPARβ/δ

(NR1C2) and PPARγ (NR1C3). The PPAR family of ligand-activated nuclear receptors require heterodimerization with another nuclear receptor, the 9-*cis*-retinoic acid receptor (RXR or NR2B), in order to be activated. Heterodimerization is then followed by coactivator recruitment and subsequent binding to DNA specific sequences called PPAR-response elements (PPRE), located within the promoter regions of PPAR target genes. Notable among the PPAR target genes with identified PPREs are those coding for lipid and glucose homeostasis. PPARα and PPARβ/δ are the predominant isoforms in the heart, where they share some overlapping functions [5]. Transgenic mice with constitutive overexpression of PPARβ/δ in the heart show increased myocardial glucose utilization, do not accumulate myocardial lipids and display normal cardiac function [6]. Another study has reported that constitutive cardiac overexpression of PPARβ/δ in adult mice results in elevated myocardial oxidative metabolism, while myocardial glycogen content and the activity of the PDC and AMPK are markedly reduced, overall resulting in improved cardiac function [7]. In agreement with this, cardiomyocyte-restricted PPARβ/δ deficiency in mice leads to cardiac pathological development [8]. The best-characterized coactivator of PPARs is the cardiac-enriched PPARγ coactivator-1 (PGC-1)α, which regulates the expression of several genes involved in the electron transport chain, mitochondrial biogenesis, fatty acid β-oxidation and glucose oxidative metabolism, including *PDK4*. *PDK4* gene expression is known to be controlled by a plethora of different transcription factors. Some of them are coactivated by PGC-1α: PPARs, oestrogen-related receptors (ERRs) and the forkhead transcription factor (FOXO1 or FKHR); but others acting in a PGC-1α-independent manner: E2F1, LXR (liver X receptor) or RXR (retinoid X receptor).

2. Metabolic remodelling in the development of diabetic cardiomyopathy

The heart has the capacity to adapt to various pathophysiological conditions by adjusting its relative metabolism of carbohydrates and fatty acids. The loss of this metabolic flexibility is associated with pathological cardiac hypertrophy and heart failure. During diabetes, the occurrence of insulin resistance in the myocardium, together with increased rates of systemic lipolysis, means that the heart relies almost exclusively on mitochondrial fatty acid β-oxidation as the sole fuel source [6]. Reduced

myocardial glucose uptake and utilization owing to altered insulin signalling may account for the loss of this capacity to switch between glucose and fatty acids in insulin-resistant and insulin-deficient forms of diabetes. Despite the higher fatty oxidation rate that occurs in the diabetic heart, myocardial lipid accumulation is a feature of this disease. The heart is not a major site of lipid storage, but fatty acids can be stored as triacylglycerols and phospholipids within the cardiomyocyte, particularly when they are abundant, as occurs with diabetes or obesity. If this accumulation persists over time, the heart will begin to accumulate toxic lipid intermediates linked to the development of insulin resistance and lipotoxic cardiomyopathy. In fact, there is a strong correlation between intracardiac lipid accumulation and heart failure in humans [9].

Metabolic dysregulation occurring in the heart of obese and diabetic patients often involves derangements in the activity of both PPARs and PGC-1α. The expression and activity of PPARα and PGC-1α are increased in the early stages of insulin resistance in the heart [10], thus promoting excessive utilization of fatty acids instead of glucose, and driving diabetic cardiomyopathy [6]. In contrast, in overt diabetes the expression and activity of PPARα and PGC-1α are reduced, inducing mitochondrial dysfunction and cardiac hypertrophy [11]. Some debate exists about the role of PGC-1α during diabetes, since it has been reported to be down-regulated in the myocardial tissue of streptozotocin-induced diabetic rats, a fact which is accompanied by a reduction in left ventricular function [12], but also activated in streptozotocin-induced mice [13]. PPARβ/δ also plays an important role in diabetic cardiomyopathy. It has been demonstrated that deletion of the *PPARβ/δ* gene in the heart results in cardiac dysfunction, cardiac hypertrophy and myocardial lipid accumulation [14]. Diabetic cardiomyopathy induced with streptozotocin in rats is associated with ventricular hypertrophy, intramyocardial lipid accumulation and a marked decrease in cardiac PPARβ/δ protein levels [15]. Furthermore, PPARβ/δ protein levels are reduced in neonatal rat cardiomyocytes and rat H9c2 cardiomyoblasts exposed to hyperglycaemia [15].

Transgenic mice with cardiac-specific overexpression of PDK4, and thus with chronic suppression of glucose oxidation, exhibit an insulin-resistant profile characterized by low glucose oxidation rates and high fatty acid catabolism [16]. This shift in the substrate preference constrains metabolic flexibility and predisposes to cardiomyocyte fibrosis and cardiomyopathy. Interestingly, transgenic PDK4 mice are protected against

high-fat diet-induced myocyte lipid accumulation, probably owing to their increased capacity for mitochondrial fatty acid oxidation. This is related to the activation of AMPK and its known target, PGC-1α, and the increased capacity for uncoupled mitochondrial respiration.

3. The role of NF-κB-induced inflammation in diabetic cardiomyopathy

Under various pathological stimuli, the human myocardium secretes a number of pro-inflammatory cytokines and chemokines, which exert several pleiotropic effects in cardiac cells. Sustained increases in their levels may contribute to states that are associated with myocardial inflammation (i.e. heart failure and dilated cardiomyopathy) [17]. Pro-inflammatory cytokine expression is under the control of the ubiquitous and inducible transcription factor NF-κB, which is itself activated in congestive heart failure and cardiac hypertrophy [18]. Several exogenous and endogenous stimuli may induce NF-κB transcriptional activity, notably the pro-inflammatory cytokines themselves, hyperglycaemia, elevated free fatty acid levels in plasma, reactive oxygen species, angiotensin II, endothelin 1, lipoproteins and anoxia.

In mammals, NF-κB consists of five members: p65 (RelA), RelB, c-Rel, NF-κB1 (p50 and its precursor p105) and NF-κB2 (p52 and its precursor p100), which form either homodimers or heterodimers. The most abundant form of the NF-κB family is the p65/p50 heterodimer, which is often used synonymously for NF-κB. In resting cells, NF-κB is present in the cytoplasm as an inactive heterodimer bound to an inhibitor protein subunit, IκB. After stimulation, the canonical or classical pathway of NF-κB signalling involves the activation of the IκB kinase (IKK) complex, which specifically phosphorylates IκB. Phosphorylation of IκB induces its subsequent proteasome-mediated degradation, thus releasing the NF-κB heterodimer, which then translocates to the nucleus and binds to specific promoter sequences on its target genes to begin the transcription machinery. Furthermore, the p50/p65 heterodimer may undergo a series of post-translational modifications including phosphorylation, acetylation and methylation, which allow finely-tuned regulation of transcriptional activity.

The main cardiac responses to diabetes are oxidative stress, inflammation, endothelial dysfunction, cardiac fibrosis, hypertrophy and

apoptosis, in all of which NF-κB may participate. Cardiac inflammation is an early and notable response to diabetes and is actively involved in the development of heart failure during diabetic cardiomyopathy [19]. Several pro-inflammatory cytokines that have elevated levels in circulation in obese and diabetic patients, such TNF-α and IL-6, are involved in the physiopathological process that relates obesity and insulin resistance in the heart [2].

4. Crosstalk between inflammation and metabolism in the diseased heart

4.1. PPARβ/δ activation blocks lipid-induced inflammation in the heart

In the heart, excess dietary fat may result in myocardial insulin resistance, and is related to a range of direct effects, including inflammation, hypertrophy, fibrosis and contractile dysfunction. PPARs are capable of limiting myocardial inflammation independently of binding to DNA, through a mechanism termed trans-repression. Several mechanisms have been proposed to explain these anti-inflammatory effects, for example the physical interaction between PPARs and NF-κB, thereby resulting in a functional cross-inhibition of their transcriptional activity. In the heart of mice fed a high-fat diet or in human cardiac AC16 cells, treatment with the saturated fatty acid palmitate induced the expression of *TNF-α*, *MCP-1* and *IL-6*, together with the activity of NF-κB (Fig. 2A) [20]. Interestingly, the PPARβ/δ agonist GW501516 abrogated this pro-inflammatory profile. Similarly, NF-κB-dependent inflammation was induced in the heart of PPARβ/δ knockout mice, a fact which is consistent with the anti-inflammatory activity of PPARβ/δ [20]. This latter study reported that PPARβ/δ activation by GW501516 strongly enhanced the physical interaction between the p65 subunit of NF-κB and PPARβ/δ (Fig. 2B), thereby suggesting that this mechanism may also interfere with NF-κB trans-activation capacity in the heart. Furthermore, addition of GSK0660 partially blocked the enhanced interaction between p65 and PPARβ/δ in AC16 cells, thus linking this physical interaction with PPARβ/δ availability in the nucleus and its subsequent activity. Likewise, PPARβ/δ activation with its agonists L-165041 or GW0742 inhibits phenylephrine- and lipopolysaccharide-induced NF-κB activation in cultured neonatal rat cardiomyocytes and H9c2 cells through enhanced physical interaction between p65 and PPARβ/δ [21,22]. Other studies also

demonstrate that PPARβ/δ activation by ligand administration or adenoviral overexpression in cultured cardiac myocytes suppresses the NF-κB signalling pathway and displays potent anti-inflammatory effects [13,23].

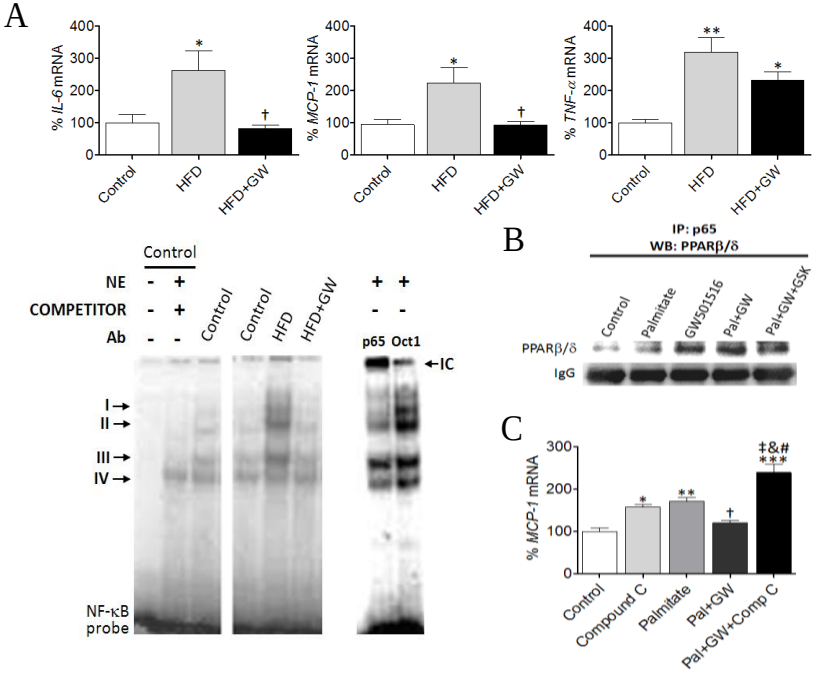

Figure 2. The PPARβ/δ agonist GW501516 (GW) prevents inflammation in the heart of mice fed a high-fat diet (HFD). (A) mRNA levels assessed by real-time RT-PCR (*upper panel*) and electrophoretic mobility shift assay showing NF-κB activity (*lower panel*, Ab, antibody; NE, nuclear extract; IC, immunocomplex). *P<0.05, **P<0.01 vs. Control; †P<0.05 vs. HFD. (B) Co-immunoprecipitation of nuclear protein extracts obtained from AC16 cells treated with palmitate (Pal), GW501516 (GW) and GSK0660 (GSK). (C) *MCP-1* mRNA levels assessed by real-time RT-PCR in AC16 cells treated with palmitate, GW501516 and compound C (Comp C). *P<0.05, **P<0.01 vs. Control; †P<0.05, ‡P<0.01 vs. Palmitate; &P<0.001 vs. Pal+GW.

"Reprinted from Álvarez-Guardia et al., Biochimica et Biophysica Acta (BBA) - Molecular and Cell Biology of Lipids, 1811:59-67, Copyright © (2011), with permission from Elsevier Limited".

It has been reported that GW501516 is able to regulate lipid and glucose metabolism in human skeletal muscle by AMPK-dependent, but PPARβ/δ-independent, mechanisms [21]. Since activation of AMPK may block NF-κB signalling pathway through the blockade of IKK activity [22], it might be feasible that GW501516 was blocking lipid-induced inflammatory pathways in cardiac cells through AMPK-dependent mechanisms. An experiment in which the AMPK inhibitor compound C was added before GW501516 and palmitate confirmed the anti-inflammatory role of this kinase in human cardiac AC16 cells (Fig. 2C). These results are relevant, especially taking into account that PPARβ/δ has been postulated as a potential target in the treatment of obesity and the insulin resistance state. Since chronic low-grade inflammation plays a significant role in cardiac hypertrophy and heart failure, and GW501516 has been shown to ameliorate metabolic disturbances in heart caused by high-fat diets, it is tempting to speculate that PPARβ/δ might serve as a therapeutic target to prevent cardiac disease in metabolic disorders.

4.2. The role of the PPAR/PGC-1α/PDK4 axis in the crosstalk between inflammatory processes and metabolism

Cardiac *PGC-1α* expression, along with its target transcription factors PPARs and ERRα, are all reduced in animal models of heart failure [23,13] and in pathological forms of cardiac hypertrophy [24,25], suggesting that this decrease may be responsible for an energetic failure that can eventually lead to cardiac dysfunction. Likewise, PGC-1α knockout mice exhibit lower cardiac power and increased reliance on glucose oxidation [26]. Exposure of human cardiac AC16 cells to TNF-α inhibited the expression of *PGC-1α*, a fact which resulted in a reduction in *PDK4* expression and subsequent increase in the glucose oxidation rate (Fig. 3A) [27]. It is worth mentioning that all these changes were abrogated with parthenolide, thus demonstrating the involvement of the NF-κB pathway [28]. In consonance with this, transgenic mice with constitutive and specific overexpression of TNF-α in the heart, a well-characterized model of cytokine-induced cardiomyopathy, displayed reduced *PGC-1α* and *PDK4* expression in the heart, and this was accompanied an increase in glucose utilization. In a similar way, phenylephrine and LPS down-regulate the expression of *PGC-1α* and *PDK4* in rat neonatal cardiomyocytes, resulting in an increase in glucose utilization and a decrease in fatty acid oxidation, a phenotype which resembles that observed during cardiac hypertrophy [28,29]. Interestingly,

the PPARβ/δ agonist L-165041 prevented the reduction in *PDK4* expression induced by both phenylephrine and LPS [22]. Overall data suggest the hypothesis that the NF-κB-mediated inhibition of PGC-1α accounts for the shift towards increased glycolysis during cardiac hypertrophy and heart failure.

An appealing question arose about the specific molecular mechanisms by which *PGC-1α* was down-regulated after NF-κB activation in cardiac cells. Co-immunoprecipitation studies not only demonstrated that the p65 subunit of NF-κB interacted with PGC-1α in the basal state, but also this

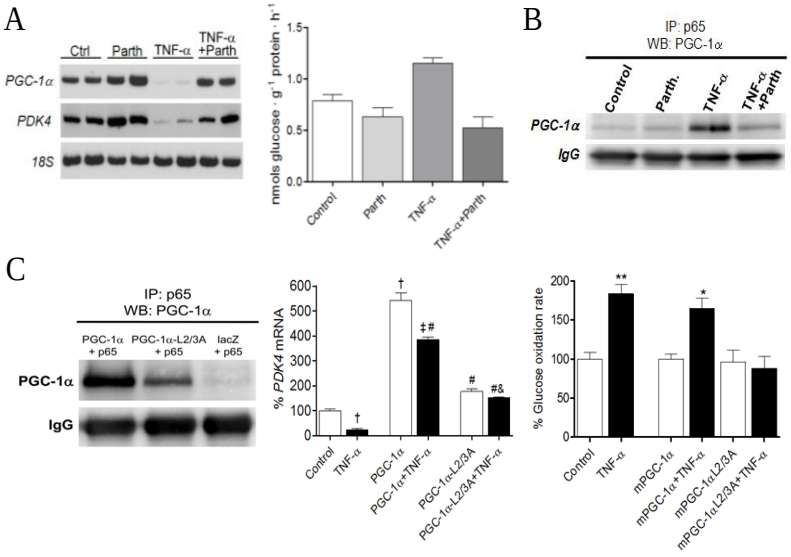

Figure 3. The p65 subunit of NF-κB binds to PGC-1α in cardiac cells. (A) *PGC-1α* and *PDK4* expression determined by RT-PCR and [U-^{14}C]-glucose oxidation rate in AC16 cells treated with TNF-α and the NF-κB inhibitor parthenolide (Parth). (B) Co-immunoprecipitation of nuclear protein extracts obtained from AC16 cells treated with TNF-α and/or parthenolide. (C) Co-immunoprecipitation (*left panel*) of nuclear protein extracts obtained from AC16 cells transfected with PGC-1α, PGC-1αL2/3A or lacZ (Control); analysis of *PDK4* gene expression determined by RT-PCR (*middle panel*, † P<0.01 vs. Control; ‡ P<0.01 vs. PGC-1α; # P<0.01 vs. TNF-α; & P<0.001 vs. PGC-1α+TNF-α); and [U-^{14}C]-glucose oxidation rate expressed as a percentage with respect to control cells (*right panel*, *P < 0.05, **P < 0.01 vs. Control).

binding was increased after stimulation of NF-κB activity, and owing to p65 accumulation in the nucleus (Fig. 3B) [30]. Modulation of the PGC-1α protein levels by means of overexpression or gene silencing demonstrated that the main factor limiting the degree of association between p65 and PGC-1α is the amount of p65 present in the nucleus.

PGC-1α binds nuclear receptors through three leucine-rich LXXLL motifs (named L1, L2 and L3), which are located within the N-terminus of the coactivator, and it is widely recognized that PGC-1α associates with other co-regulators via these LXXLL motifs [31]. Given that NF-κB also requires the binding to specific LXXLL motifs located within the sequence of specific coactivators to drive gene expression [32], we investigated whether these motifs were responsible of the modulation of PGC-1α activity by p65. On the basis of co-immunoprecipitation studies, and using a mutated form of PGC-1α, we reported that the L2 and L3 motifs play a crucial role in p65 binding (Fig. 3C) [30]. Therefore, in cardiac cells, the increased physical interaction between p65 and the L2/L3 motifs of PGC-1α after NF-κB activation might reduce *PGC-1α* expression, thereby leading to a reduction in *PDK4* expression and the subsequent increase in glucose oxidation observed during the pro-inflammatory state (Fig. 3C) [30].

4.3. PPAR-independent mechanisms in the regulation of PDK4 during inflammation

Other mechanisms might also account for the down-regulation of PGC-1α after NF-κB activation. For instance, NF-κB activation may indirectly stimulate PKB/Akt [30] and, since PGC-1α contains a consensus binding site for PKB/Akt phosphorylation that reduces its stability, it may result in a diminution in its transcriptional activity [33]. PKB/Akt also has the capacity to phosphorylate the FOXO1 transcription factors [34], thereby inducing their ubiquitination-dependent degradation and eventually leading to a decrease in the expression of their target genes (i.e. *PGC-1α*) [35].

We have also recently proposed a novel mechanism by which the inflammatory processes driven by NF-κB can down-regulate *PDK4* through inhibition of the E2F1 transcription factor in a PPAR- and ERRα-independent manner. E2F1 is known for its major role in regulating the G1/S phase transition during cell cycle progress, hence acting as a critical regulator of cell survival and proliferation [36]. However, it has also been demonstrated that it may regulate *PDK4* expression through specific sites

located within the promoter of the gene that encodes for the latter [37]. Protein co-immunoprecipitation analyses revealed that *PDK4* downregulation entailed enhanced physical interaction between the p65 subunit of NF-κB and E2F1 (Fig. 4A) [38]. The association between p65 and E2F1 has already been established in human [39] and murine fibroblasts [40]. Chromatin immunoprecipitation analyses demonstrated that p65 translocation into the nucleus prevented the recruitment of E2F1 to the *PDK4* promoter and its subsequent E2F1-dependent gene transcription in human cardiac cells (Fig. 4B), thus influencing glucose oxidation (Fig. 4C). Interestingly, the NF-κB inhibitor parthenolide prevented the inhibition of E2F1.

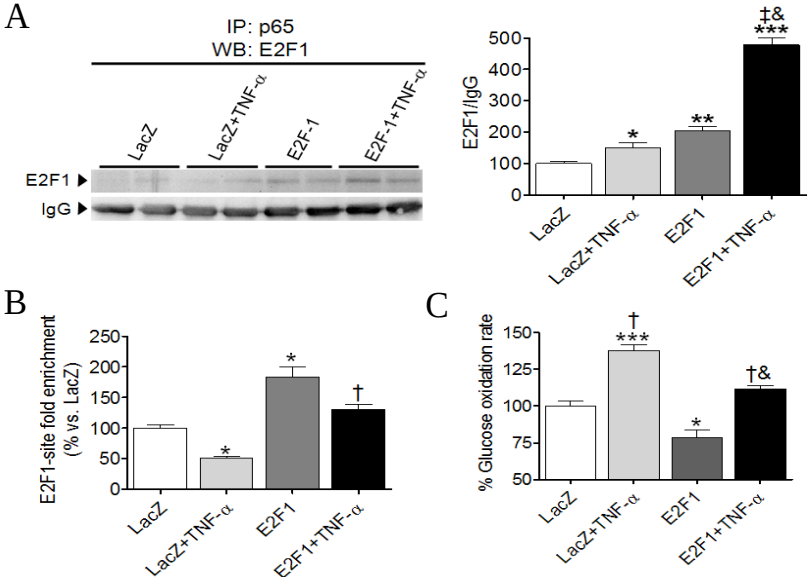

Figure 4. The interplay between NF-κB and E2F1 regulates metabolism in cardiac cells. (A) Co-immunoprecipitation of nuclear protein extracts obtained from AC16 cells treated with or without TNF-α and transfected with LacZ- or E2F1-carrying plasmids. (B) Chromatin immunoprecipitation demonstrating the E2F1-site fold enrichment at the PDK4 promoter and (C) [U-^{14}C]-glucose oxidation rate in AC16 cells overexpressing the human LacZ-control or the E2F1 genes incubated with TNF-α. *P<0.05, **P<0.01, ***P<0.001 vs. LacZ; †P<0.01 vs. E2F1; &P<0.01 vs. LacZ+TNF-α.

Based on these findings, we envision a model for the regulation of *PDK4* expression and cardiac cell metabolism by NF-κB and E2F1, in which NF-κB might serve as a molecular switch that regulates E2F1-dependent *PDK4* gene transcription. As inappropriate PDK4 activity would have catastrophic consequences in high-metabolic-rate organs, the basal repression of E2F1-dependent *PDK4* expression by NF-κB might be crucial for normal cardiac function. Since E2F1 plays an important role in cardiac myocyte growth and is also involved in metabolism regulation through *PDK4* modulation, targeting this transcription factor could provide us with an effective therapy for treating detrimental left ventricular hypertrophy leading to heart failure.

There are several other pathways that may account for the interplay between inflammation and metabolic responses in the heart. For instance, the heart of obese mice fed a high-fat diet display a reduction in glucose metabolism, GLUT and AMPK activity, which is accompanied by macrophage infiltration and enhanced inflammation [41]. A similar profile is observed after IL-6 administration in mice, whereby this cytokine suppresses the glucose metabolism and induces insulin resistance owing to AMPK activity and IRS-1 inhibition [42]. In accordance with this, AMPK activation diminishes NF-κB signalling, attenuates cardiac hypertrophy and improves cardiac function in rats subjected to trans-aortic constriction or in rat neonatal cardiomyocytes induced with angiotensin II [42].

Enhanced saturated free fatty acid (e.g. palmitate) levels up-regulate the lipid intermediates ceramides and diacylglycerol (DAG), the latter being a powerful activator of protein kinase C (PKC)θ. Likewise, hyperglycaemia activates the glycolytic pathway and increases the production of the PKC/DAG pathway [43]. PKC activation may provoke insulin resistance by means of IRS-1 inhibition and inflammation through NF-κB induction [44]. On the other hand, ceramides are lipotoxic molecules that modulate cellular energy metabolism and are enhanced in several models of lipotoxic cardiomyopathy. They are necessary and sufficient intermediates linking saturated fats to the inhibition of insulin signalling and enhanced inflammation [45]. In transgenic mice prone to dilated cardiomyopathy owing to ceramide accumulation in the heart, there is an up-regulation of fatty acid oxidation while glucose oxidation is down-regulated [46]. This has been related to the ceramide-dependent increase in the expression of genes such as *PDK4*, and the fatty acid transporters *FAT/CD36*, *FATP1 or ACS* [46].

Finally, recent studies have revealed an important link between sirtuin 1 (SIRT1), energy metabolism and inflammation [46]. The main reason for this link is perhaps that besides its ability to inhibit NF-κB activity, SIRT1 may associate with and deacetylate PGC-1α, leading to enhanced transcriptional activity of the latter. A paradigmatic example of this is given by the overexpression of SIRT1 in transgenic mice fed a high-fat diet, which show lower lipid-induced inflammation along with better glucose tolerance [47]. This study reported that the beneficial effects of SIRT1 were due both to the induction of the antioxidant proteins via stimulation of PGC-1α, and lower activation of pro-inflammatory cytokines, owing to NF-κB activity down-modulation. Similarly, SIRT1 inhibition in primary myotubes down-regulates PGC-1α and its target mitochondrial transcriptional regulators, ERRα and mtTFA, along with the expression levels of mitochondrial and fatty acid utilization genes [48]. On the other hand, both the activation of SIRT1 with resveratrol and overexpression of SIRT1 reduced phenylephrine-induced hypertrophy and the down-regulation of fatty acid oxidation genes in neonatal rat cardiac myocyte [49]. According to a study by Planavila *et al*. [50], SIRT1 overexpression led to enhanced PPARα binding to the p65 subunit of NF-κB and subsequent p65-deacetylation, thus blocking NF-κB activity. Consistent with this, isoproterenol-induced cardiac hypertrophy, metabolic dysregulation and inflammation were prevented by resveratrol in wild-type mice, but not in PPARα-null mice. Moreover, SIRT1 overexpression led to deacetylation of PGC-1α [50] and phosphorylation-induced AMPK activation [50]. In fact, besides the PPAR/PGC-1α pathway, SIRT1 modulates the activity of a number of proteins involved in cardiac metabolic homeostasis. For instance, it has been reported an important role of SIRT1 in regulating the ERR transcriptional pathway during the progression of heart failure, thus promoting mitochondrial dysfunction [51].

5. Conclusion

Free fatty acids are the preferred energy substrate in the adult heart, although other substrates such as glucose or lactate may provide additional fuel sources in diverse circumstances. At the transcriptional level, cardiac metabolism is mostly regulated by the PPAR/PGC-1α/PDK4 axis. The PGC-1α co-activates PPARα, PPARβ/δ and ERRα to regulate the

expression of genes involved in the electron transport chain, mitochondrial biogenesis, fatty acid β-oxidation and glucose oxidative metabolism. One of its key target genes, *PDK4*, may promote insulin resistance through the inhibition of efficient glucose utilization. During diabetes, and owing to the insulin resistance and the dysregulation in the activity of both PPARs and PGC-1α, the myocardium relies almost exclusively on mitochondrial fatty acid β-oxidation as the main fuel source. As a consequence, one of the hallmarks of diabetic cardiomyopathy is myocardial lipid accumulation, which is related to the development of lipotoxic cardiomyopathy. During diabetic cardiomyopathy, the excess of fatty acid oxidation in mitochondria induces the formation of reactive oxygen species and the accumulation of lipid intermediates, promoting NF-κB activation and, as a result, contributing to cardiac inflammation and subsequent development of heart failure.

In this review, we report that PPAR activation is capable of limiting myocardial inflammation by means of trans-repression through several mechanisms, including the physical interaction between PPARs and pro-inflammatory NF-κB. Notably, PPARα and PPARβ/δ activation might prevent metabolic disturbances occurring during diabetic cardiomyopathy, while inhibiting inflammatory processes in the heart. This is relevant, especially taking into account that PPARs have been postulated as potential targets in the treatment of obesity and the insulin resistance state. On the other hand, several studies point to PGC-1α as a potential contributor to cardiac dysfunction and heart failure in metabolic disorders with an inflammatory background. Here, we have described several well-known and new mechanisms by which PGC-1α activity is modulated after NF-κB induction, for instance the sequestration of PGC-1α protein by p65, the PKB/Akt-mediated phosphorylation of PGC-1α, or FOXO inhibition (Fig. 5). PGC-1α down-regulation often results in diminished *PDK4* expression, a crucial step in determining the rates of glucose and fatty acid oxidation in the heart. However, other mechanisms may account for PDK4 down-regulation, including the inhibition of E2F1.

In summary, an increasing body of evidence suggests a potential link between chronic inflammation and metabolic disturbances in the heart. Gaining more insight into the mechanisms by which cardiac inflammatory processes may deregulate metabolic homeostasis in the heart may assist in devising new therapeutic strategies to restore cardiac function during insulin resistance and diabetes.

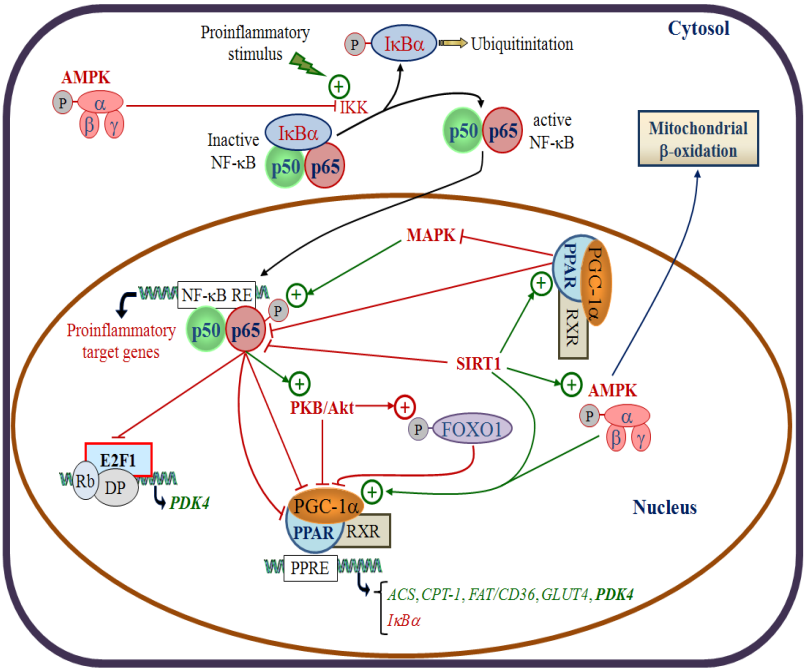

Figure 5. Crosstalk between inflammation and metabolism in the diseased heart. PPAR activation is capable of limiting myocardial NF-κB activity through several mechanisms, such as its physical interaction with the p65 subunit of NF-κB, or the inhibition of MAPK phosphorylation. PPARα is also capable of inhibiting NF-κB activity by inducing *IκBα* expression. After NF-κB activation, the increased physical interaction between p65 and PGC-1α reduces the transcriptional activity of the latter, thus diminishing its target gene expression (*ACS*, *CPT-1*, *FAT/CD36*, *GLUT4*, and *PDK4*). NF-κB may also down-regulate PDK4 through inhibition of the E2F1 transcription factor. SIRT1 down-regulates NF-κB activity through p65 deacetylation and enhances the activities of PGC-1α and AMPK. AMPK also diminishes NF-κB signalling due to IKK inhibition and the subsequent lowering of IkBα degradation. NF-κB activation may also indirectly stimulate PKB/Akt, which catalyzes the phosphorylation-mediated inhibition of PGC-1α, and also has the capacity to phosphorylate FOXO1, thereby inducing its degradation and finally leading to a decrease in the expression of *PGC-1α*.

"Reprinted from Palomer et al., International Journal of Cardiology, 168:3160-3172, Copyright © (2013), with permission from Elsevier Limited".

Acknowledgements

This study was supported by funds from the Ministerio de Economía y Competitividad of the Spanish Government [SAF2012-30708]. CIBER de Diabetes y Enfermedades Metabólicas Asociadas (CIBERDEM) is an initiative of the Instituto de Salud Carlos III (ISCIII) - Ministerio de Economía y Competitividad.

References

1. Haugen, E., Chen, J., Wikstrom, J., Gronros, J., Gan, L.M., Fu, L.X. 2007, *Int J Cardiol*, 115, 24.
2. Gray, S. and Kim, J.K. 2011, *Trends Endocrinol Metab*, 22, 394.
3. Coort, S.L., Bonen, A., van der Vusse, G.J., Glatz, J.F.C., Luiken, J.J. 2007, *Mol Cell Biochem*, 299, 5.
4. Iliadis, F., Kadoglou, N., Didangelos, T. 2011, *Diabetes Res Clin Pract*, 93 Suppl 1, S86.
5. Gilde, A.J., van der Lee, K.A., Willemsen, P.H., Chinetti, G., van der Leij, F.R., van der Vusse, G.J., Staels, B., van Bilsen, M. 2003, *Circ Res*, 92, 518.
6. Burkart, E.M., Sambandam, N., Han, X., Gross, R.W., Courtois, M., Gierasch, C.M., Shoghi, K., Welch, M.J., Kelly, D.P. 2007, *J Clin Invest*, 117, 3930.
7. Liu, J., Wang, P., Luo, J., Huang, Y., He, L., Yang, H., Li, Q., Wu, S., Zhelyabovska, O., Yang, Q. 2011, *Hypertension*, 57, 223.
8. Liu, J., Wang, P., He, L., Li, Y., Luo, J., Cheng, L., Qin, Q., Brako, L.A., Lo, W.K., Lewis, W., Yang, Q. 2011, *PPAR Res*, 2011, 372854.
9. Pagano, C., Calcagno, A., Granzotto, M., Calabrese, F., Thiene, G., Federspil, G., Vettor, R. 2008, *Nutr Metab Cardiovasc Dis*, 18, 189.
10. Duncan, J.G., Bharadwaj, K.G., Fong, J.L., Mitra, R., Sambandam, N., Courtois, M.R., Lavine, K.J., Goldberg, I.J., Kelly, D.P. 2010, *Circulation*, 121, 426.
11. Duncan, J.G. and Finck, B.N. 2008, *PPAR Res*, 2008, 253817.
12. Chang, L.T., Sun, C.K., Wang, C.Y., Youssef, A.A., Wu, C.J., Chua, S., Yip, H.K. 2006, *Int Heart J*, 47, 901.
13. Finck, B.N. 2007, *Cardiovasc Res*, 73, 269.
14. Cheng, L., Ding, G., Qin, Q., Huang, Y., Lewis, W., He, N., Evans, R.M., Schneider, M.D., Brako, F.A., Xiao, Y., Chen, Y.E., Yang, Q. 2004, *Nat Med*, 10, 1245.
15. Yu, B.C., Chang, C.K., Ou, H.Y., Cheng, K.C., Cheng, J.T. 2008, *Cardiovasc Res*, 80, 78.
16. Zhao, G., Jeoung, N.H., Burgess, S.C., Rosaaen-Stowe, K.A., Inagaki, T., Latif, S., Shelton, J.M., McAnally, J., Bassel-Duby, R., Harris, R.A., Richardson, J.A., Kliewer, S.A. 2008, *Am J Physiol Heart Circ Physiol*, 294, H936.
17. Turner, N.A., Mughal, R.S., Warburton, P., O'regan, D.J., Ball, S.G., Porter, K.E. 2007, *Cardiovasc Res*, 76, 81.

18. Gupta, S., Young, D., Maitra, R.K., Gupta, A., Popovic, Z.B., Yong, S.L., Mahajan, A., Wang, Q., Sen, S. 2008, *J Mol Biol*, 375, 637.
19. Lorenzo, O., Picatoste, B., Ares-Carrasco, S., Ramirez, E., Egido, J., Tunon, J. 2011, *Mediators Inflamm*, 2011, 652097.
20. Álvarez-Guardia, D., Palomer, X., Coll, T., Serrano, L., Rodriguez-Calvo, R., Davidson, M.M., Merlos, M., El, K., I, Michalik, L., Wahli, W., Vazquez-Carrera, M. 2011, *Biochim Biophys Acta*, 1811, 59.
21. Planavila, A., Rodríguez-Calvo, R., Jove, M., Michalik, L., Wahli, W., Laguna, J.C., Vázquez-Carrera, M. 2005, *Cardiovasc Res*, 65, 832.
22. Planavila, A., Laguna, J.C., Vázquez-Carrera, M. 2005, *J Biol Chem*, 280, 17464.
23. Ding, G., Cheng, L., Qin, Q., Frontin, S., Yang, Q. 2006, *J Mol Cell Cardiol*, 40, 821.
24. Ventura-Clapier, R., Garnier, A., Veksler, V. 2008, *Cardiovasc Res*, 79, 208.
25. Lin, J., Handschin, C., Spiegelman, B.M. 2005, *Cell Metab*, 1, 361.
26. Finck, B.N. and Kelly, D.P. 2007, *Circulation*, 115, 2540.
27. Lehman, J.J., Boudina, S., Banke, N.H., Sambandam, N., Han, X., Young, D.M., Leone, T.C., Gross, R.W., Lewandowski, E.D., Abel, E.D., Kelly, D.P. 2008, *Am J Physiol Heart Circ Physiol*, 295, H185.
28. Palomer, X., Álvarez-Guardia, D., Rodriguez-Calvo, R., Coll, T., Laguna, J.C., Davidson, M.M., Chan, T.O., Feldman, A.M., Vazquez-Carrera, M. 2009, *Cardiovasc Res*, 81, 703.
29. Li, Y.Y., Chen, D., Watkins, S.C., Feldman, A.M. 2001, *Circulation*, 104, 2492.
30. Álvarez-Guardia, D., Palomer, X., Coll, T., Davidson, M.M., Chan, T.O., Feldman, A.M., Laguna, J.C., Vazquez-Carrera, M. 2010, *Cardiovasc Res*, 87, 449.
31. Sano, M., Tokudome, S., Shimizu, N., Yoshikawa, N., Ogawa, C., Shirakawa, K., Endo, J., Katayama, T., Yuasa, S., Ieda, M., Makino, S., Hattori, F., Tanaka, H., Fukuda, K. 2007, *J Biol Chem*, 282, 25970.
32. Soyal, S., Krempler, F., Oberkofler, H., Patsch, W. 2006, *Diabetologia*, 49, 1477.
33. Meng, F., Liu, L., Chin, P.C., D'Mello, S.R. 2002, *J Biol Chem*, 277, 29674.
34. Li, X., Monks, B., Ge, Q., Birnbaum, M.J. 2007, *Nature*, 447, 1012.
35. Asada, S., Daitoku, H., Matsuzaki, H., Saito, T., Sudo, T., Mukai, H., Iwashita, S., Kako, K., Kishi, T., Kasuya, Y., Fukamizu, A. 2007, *Cell Signal*, 19, 519.
36. Yang, J., Williams, R.S., Kelly, D.P. 2009, *Mol Cell Biol*, 29, 4091.
37. Vara, D., Bicknell, K.A., Coxon, C.H., Brooks, G. 2003, *J Biol Chem*, 278, 21388.
38. Hsieh, M.C., Das, D., Sambandam, N., Zhang, M.Q., Nahle, Z. 2008, *J Biol Chem*, 283, 27410.
39. Palomer, X., Álvarez-Guardia, D., Davidson, M.M., Chan, T.O., Feldman, A.M., Vazquez-Carrera, M. 2011, *PLoS One*, 6, e19724.
40. Araki, K., Kawauchi, K., Tanaka, N. 2008, *Oncogene*, 27, 5696.
41. Tanaka, H., Matsumura, I., Ezoe, S., Satoh, Y., Sakamaki, T., Albanese, C., Machii, T., Pestell, R.G., Kanakura, Y. 2002, *Mol Cell*, 9, 1017.

42. Ko, H.J., Zhang, Z., Jung, D.Y., Jun, J.Y., Ma, Z., Jones, K.E., Chan, S.Y., Kim, J.K. 2009, *Diabetes*, 58, 2536.
43. Li, H.L., Yin, R., Chen, D., Liu, D., Wang, D., Yang, Q., Dong, Y.G. 2007, *J Cell Biochem*, 100, 1086.
44. Koike, N., Takamura, T., Kaneko, S. 2007, *Life Sci*, 80, 1721.
45. Bruce, C.R., Hoy, A.J., Turner, N., Watt, M.J., Allen, T.L., Carpenter, K., Cooney, G.J., Febbraio, M.A., Kraegen, E.W. 2009, *Diabetes*, 58, 550.
46. Park, T.S., Hu, Y., Noh, H.L., Drosatos, K., Okajima, K., Buchanan, J., Tuinei, J., Homma, S., Jiang, X.C., Abel, E.D., Goldberg, I.J. 2008, *J Lipid Res*, 49, 2101.
47. Rodgers, J.T., Lerin, C., Gerhart-Hines, Z., Puigserver, P. 2008, *FEBS Lett*, 582, 46.
48. Pfluger, P.T., Herranz, D., Velasco-Miguel, S., Serrano, M., Tschop, M.H. 2008, *Proc Natl Acad Sci U S A*, 105, 9793.
49. Gerhart-Hines, Z., Rodgers, J.T., Bare, O., Lerin, C., Kim, S.H., Mostoslavsky, R., Alt, F.W., Wu, Z., Puigserver, P. 2007, *EMBO J*, 26, 1913.
50. Planavila, A., Iglesias, R., Giralt, M., Villarroya, F. 2011, *Cardiovasc Res*, 90, 276.
51. Chan, A.Y., Dolinsky, V.W., Soltys, C.L., Viollet, B., Baksh, S., Light, P.E., Dyck, J.R. 2008, *J Biol Chem*, 283, 24194.

Cover image by Roser Estelrich and Joan Estelrich